

Science! true daughter of Old Time thou art!
Who alterest all things with thy peering eyes.
Why preyest thou thus upon the poet's heart,
Vulture, whose wings are dull realities?
How should he love thee? or how deem thee wise,
Who wouldst not leave him in his wandering
To seek for treasure in the jewelled skies,
Albeit he soared with an undaunted wing?
Hast thou not dragged Diana from her car?
And driven the Hamadryad from the wood
To seek a shelter in some happier star?
Hast thou not torn the Naiad from her flood,
The Elfin from the green grass, and from me
The summer dream beneath the tamarind tree?
– Edgar Allan Poe, "Sonnet – to Science"

"What makes the desert beautiful," said the little
prince, "is that somewhere it hides a well..."
– Antoine de Saint-Exupéry, *Le Petit Prince*

University of Alberta

**Poxviral Manipulation of Bcl-2 Proteins: Fowlpox Virus FPV039
and Deerpox Virus DPV022 Inhibit Apoptosis by Neutralising Bak
and Bax, while Noxa Contributes to Vaccinia Virus-induced
Apoptosis**

by

Logan Elliott Banadyga

A thesis submitted to the Faculty of Graduate Studies and Research
in partial fulfillment of the requirements for the degree of

Doctor of Philosophy

in

Virology

Medical Microbiology and Immunology

©Logan Elliott Banadyga

Spring 2011

Edmonton, Alberta

Permission is hereby granted to the University of Alberta Libraries to reproduce single copies of this thesis and to lend or sell such copies for private, scholarly or scientific research purposes only. Where the thesis is converted to, or otherwise made available in digital form, the University of Alberta will advise potential users of the thesis of these terms.

The author reserves all other publication and other rights in association with the copyright in the thesis and, except as herein before provided, neither the thesis nor any substantial portion thereof may be printed or otherwise reproduced in any material form whatsoever without the author's prior written permission.

To my mom and my dad,
for keeping the deposit on my mobile crane operating
business.

ABSTRACT

Poxviruses are renowned for encoding proteins that modulate virtually every aspect of the host immune system. One effective barrier against virus infection is apoptosis, a form of programmed cell death. Apoptosis is controlled at the mitochondria by pro- and anti-apoptotic members of the highly conserved Bcl-2 family of proteins, and two members in particular, Bak and Bax, are absolutely critical to the induction of cell death. Although poxviruses encode an array of effective inhibitors of apoptosis, only members of the *Avipoxvirus* genus, of which fowlpox virus is the prototypical member, encode proteins with obvious, albeit limited, sequence identity to cellular Bcl-2 proteins. Fowlpox virus, the prototypical avipoxvirus, encodes FPV039, a protein that possesses two of the four highly conserved Bcl-2 homology (BH) domains that characterise the Bcl-2 family. Here we demonstrate that, like cellular Bcl-2 proteins, FPV039 localised to the mitochondria where it prevented apoptosis induced by a variety of cytotoxic stimuli, including virus infection itself. FPV039 inhibited apoptosis induced by Bak and Bax through an interaction with Bak and activated Bax. FPV039 also interacted with a discrete subset of BH3-only proteins, the upstream activators of Bak and Bax, to prevent Bax activation in the first place. Additionally, we have characterised the function and mechanism of action of a novel deerpox virus protein, DPV022. Intriguingly, DPV022 lacks obvious homology to cellular Bcl-2 proteins but shares limited regions of amino acid identity with two other poxviral inhibitors of apoptosis, vaccinia virus F1L and myxoma virus M11L, which are themselves unrelated. Here we demonstrate that DPV022 localised to the mitochondria where it interacted directly with Bak and Bax to inhibit apoptosis, even in the absence all cellular anti-apoptotic Bcl-2 proteins. We have also embarked on a preliminary analysis of the apical events

that initially trigger apoptosis during infection with vaccinia virus, the prototypical poxvirus. Accordingly, we demonstrate that the BH3-only protein Noxa contributed to the vaccinia virus-induced apoptotic response, possibly through an involvement with dsRNA. Together, this study represents a comprehensive analysis of the ways in which poxviruses manipulate the cellular Bcl-2 family of proteins, the arbiters of cell death.

ACKNOWLEDGEMENTS

It is not possible to do Science without the help of others. Thankfully, for the last six and a half years, I've been surrounded by the most helpful friends, colleagues, and mentors I could ask for.

To Michele: thanks for taking a chance on the kid from Saskatchewan. In your lab, I learned how to do good science, how to talk good science, and how to write good science. Whatever success I may encounter down whatever path Science takes me, know that it was you got me going in the right direction. I am proud to have had you as a supervisor, and I am happy, now, to count you among my colleagues and friends.

Thank you Drs. Jim Smiley and Shairaz Baksh for serving on my committee. I could not have asked for more sagacious scientists to see me through graduate school. Likewise, thanks to Drs. Ing Swie Goping and Joanna Shisler for serving on my thesis examine committee.

When I think of the "Barry Lab" it will always be comprised of the five people who were there the day I showed up as a summer student. Thank you Dr. Shawn Wasilenko, Dr. John Taylor, Dr. Tara Stewart, Dr. Brianne Couturier, and David Bond. You five taught me everything I know. Thanks also to the many Barry Lab members who came after me and left before me, in particular Kate Garcia-Fagan and Dr. Kirstin Veugelers, who became great friends. And then there are those I leave behind. Thanks to all of the current members of the lab for putting up with me and supporting me as I tried to finish up, especially Kristin Burles (BFFITL) and John Thibault. Also, thanks to the two undegraduate project students I supervised, Jenna Gerig and Sing-Chi Lam, who contributed materially to this thesis.

I've relied on a lot of people for technical assistance throughout my tenure as a grad student, but the inexhaustible help provided by Gerry Barron, with the confocal microscope at the Cross Cancer Centre, and Kris Ellestad, with qRT-PCR in the Powers Lab, was invaluable to me. Thank you both.

Nothing would happen behind the scenes if it weren't for Mary Pat Gibson, Tabitha Vasquez, Debbie Doudiet, and Anne Giles. Thanks for your hard work. Thanks for entertaining my erratic ideas.

I've been lucky enough to make many friends in the Department of Medical Microbiology, and I thank all of you for the many good times we've shared. In particular, thanks to Nikki McFarlane, my old IMINSA buddy and a fantastic friend. Also, thanks to Wendy Magee and Chad Irwin for your friendship and perspective from the other pox lab.

A simple "thanks" will never be enough for Logan Sibley and Amy Congdon-Sibley, but it's the best I can do on this page. I do not deserve to have friends as good as you. And I do not know how I would have made it through graduate studies with my sanity intact if I didn't have your shoulders to cry on, lean on, and stand on. Thank you.

A bijillion points for both Steph Campbell and Nick Van Buuren. We have been stuck with each other since day one, and our friendship is among the most important things I'll take with me from the lab. It's difficult to describe just how much I've valued having you two in my life... but there is one word that comes close to summing it all up: heckyeah!

Finally, although my parents, Perry and Cindy, may not understand every word beyond this page, I know they appreciate each of them. Mom and Dad, you are the reason for my success. Your support and encouragement and love (and strict bedtimes and strict work ethic!) have, above all else, made the most important contribution to this thesis. You're the best parents and I love you.

TABLE OF CONTENTS

	Page
Chapter 1 Introduction	1
1.1. Poxviruses	2
1.1.1. The family <i>Poxviridae</i>	2
1.1.1.1. The orthopoxviruses	4
1.1.1.2. The avipoxviruses	5
1.1.1.3. The cervidpoxviruses	6
1.1.2. Poxvirus morphology and genetics	6
1.1.3. Poxvirus dissemination	8
1.1.4. Poxviruses evade the immune system	11
1.2. Apoptosis	11
1.2.1. Apoptosis: a form of programmed cell death	11
1.2.2. Caspases demolish the cell	12
1.2.3. The intrinsic and extrinsic apoptotic pathways	14
1.2.4. Mitochondria and the release of cytochrome c	17
1.2.5. The Bcl-2 family of proteins regulates apoptosis	18
1.2.5.1. The pro-apoptotic multi-domain Bcl-2 proteins	23
1.2.5.2. The anti-apoptotic multi-domain Bcl-2 proteins	24
1.2.5.3. The BH3-only proteins	25
1.2.5.4. Bcl-2 proteins are evolutionarily conserved	26
1.2.6. The activation of Bak and Bax	26
1.2.6.1. The indirect and direct models of Bak and Bax activation	28
1.2.6.2. The embedded together model of Bak and Bax activation	33
1.2.6.3. A unified picture of Bak and Bax activation?	34
1.2.6.4. The alternative regulation and function of Bcl-2 family proteins	38
1.2.7. The permeabilisation of the mitochondrial outer membrane	40
1.2.8. The experimental dissection of apoptosis	41
1.3. Viruses inhibit apoptosis	42
1.3.1. Viral Bcl-2-like proteins inhibit apoptosis	43
1.3.1.1. Epstein-Barr virus BHRF1 and BALF1	44
1.3.1.2. Adenovirus E1B 19K	46
1.3.1.3. Cytomegalovirus vMIA, m38.5, and m41.1	47
1.3.1.4. Kaposi's sarcoma herpesvirus KSBcl-2	49
1.3.1.5. African swine fever virus A179L	49
1.3.2. Poxviral Bcl-2-like proteins inhibit apoptosis	50
1.3.2.1. Myxoma virus M11L	50
1.3.2.2. Vaccinia virus F1L	53
1.3.2.3. Orf virus and ORFV125	54
1.3.2.4. N1L and other vaccinia virus vBcl-2 proteins	54
1.3.2.5. Fowlpox virus and FPV039	55
1.3.2.6. Deerpox virus and DPV022	55
1.4. Viruses induce apoptosis	56
1.4.1. Noxa contributes to virus-induced apoptosis	56
1.4.2. The cellular response to double-stranded RNA	60
1.4.3. Vaccinia virus E3L	61

1.5.	Thesis objectives	63
Chapter 2	Materials and methods	65
2.1.	Cell lines	66
2.2.	DNA methodology and cloning	68
2.2.1.	Plasmids	68
2.2.2.	Polymerase chain reaction	68
2.2.3.	Agarose gel electrophoresis and gel extractions	71
2.2.4.	DNA ligation	71
2.2.5.	Restriction endonuclease digestion	72
2.2.6.	Bacterial transformation	72
2.2.7.	Plasmid preparation	72
2.2.8.	DNA sequencing and computer analyses	73
2.2.9.	Cloning methods	73
2.2.9.1.	FPV039	73
2.2.9.2.	DPV022	75
2.2.9.3.	N1L, Puma, Bcl-x _L , Mcl-1, Bid, and tBid	77
2.3.	Transfections	77
2.4.	Viruses and their manipulation	78
2.4.1.	Viruses	78
2.4.2.	Virus infection protocol	80
2.4.3.	Generation of recombinant vaccinia viruses	80
2.4.4.	Plaque purification	81
2.4.5.	Preparation of virus chromosomal DNA	83
2.4.6.	Preparation of virus stocks	83
2.4.7.	Quantification of virus	84
2.5.	Protein methodology	84
2.5.1.	Antibodies	84
2.5.2.	Immunoprecipitations	84
2.5.3.	Acetone precipitation	86
2.5.4.	SDS poly-acrylamide gel electrophoresis	86
2.5.5.	Semi-dry transfer	87
2.5.6.	Western blotting	87
2.5.7.	Sequence analyses	87
2.6.	Assays	88
2.6.1.	Immunoprecipitations to detect interaction	88
2.6.1.1.	FPV039 and Bak	88
2.6.1.2.	FPV039 and Bax	88
2.6.1.3.	FPV039 and BH3-only proteins	89
2.6.1.4.	DPV022 and Bak and Bax	89
2.6.2.	Confocal microscopy to assess sub-cellular localisation	90
2.6.2.1.	Live-cell confocal microscopy to assess localisation of FPV039 and DPV022	90
2.6.2.2.	Fixed-cell confocal microscopy to assess localisation of dsRNA, I3L, and Noxa	90
2.6.3.	Measurement of mitochondrial membrane potential	91
2.6.4.	Measurement of Bak and Bax activation	93

2.6.4.1.	Measurement of Bak and Bax N-terminus exposure by flow cytometry	93
2.6.4.2.	Measurement of Bax N-terminus exposure by fixed-cell confocal microscopy	94
2.6.4.3.	Measurement of Bax N-terminus exposure by immunoprecipitation	94
2.6.4.4.	Assessment of Bax oligomerisation by cross-linking	94
2.6.5.	Assessment of apoptosis by PARP and caspase-3 cleavage	95
2.6.6.	Quantification of dsRNA by flow cytometry	95
2.6.7.	Analysis of Noxa expression levels	96
2.6.7.1.	Assessment of Noxa protein levels	96
2.6.7.2.	Assessment of Noxa mRNA levels	96
2.6.8.	Colony formation assay	98
2.6.9.	Yeast colony assay	98
Chapter 3	Fowlpox virus encodes a Bcl-2 homologue that protects cells from apoptotic death through interaction with the pro-apoptotic protein Bak	100
3.1.	Brief introduction	101
3.2.	Results	101
3.2.1.	Fowlpox virus encodes a Bcl-2 homologue	101
3.2.2.	FPV039 is a tail-anchored protein that localises to the mitochondria	103
3.2.3.	FPV039 inhibits TNF α -induced loss of mitochondrial membrane potential	107
3.2.4.	FPV039 interacts with the pro-apoptotic protein Bak and inhibits Bak-induced apoptosis	109
3.2.5.	FPV039 interacts with endogenous Bak during vaccinia virus infection	113
3.2.6.	FPV039 inhibits apoptosis induced by virus infection	117
3.2.7.	FPV039 inhibits the activation-associated conformational change of Bak	119
Chapter 4	The fowlpox virus Bcl-2 homologue, FPV039, interacts with activated Bax and a discrete subset of BH3-only proteins to inhibit apoptosis	122
4.1.	Brief introduction	123
4.2.	Results	123
4.2.1.	FPV039 inhibits apoptosis induced by Bax	123
4.2.2.	FPV039 inhibits the conformational activation of Bax	125
4.2.3.	FPV039 inhibits Bax oligomerisation	130
4.2.4.	FPV039 interacts with Bax	132
4.2.5.	FPV039 interacts with endogenous activated Bax	134
4.2.6.	FPV039 inhibits apoptosis induced by BH3-only proteins	138
4.2.7.	FPV039 interacts with a subset of BH3-only proteins	138
Chapter 5	Deerpox virus encodes an inhibitor of apoptosis that regulates Bak and Bax	143
5.1.	Brief introduction	144
5.2.	Results	144

5.2.1.	DPV022 shares sequence homology with F1L and M11L but not Bcl-2 family proteins	144
5.2.2.	DPV022 localises to the mitochondria and inhibits apoptosis	146
5.2.3.	DPV022 interacts with Bak and inhibits Bak-induced apoptosis	148
5.2.4.	DPV022 interacts with Bax and inhibits Bax-induced apoptosis	152
5.2.5.	DPV022 replaces the cellular anti-apoptotic Bcl-2 proteins	160
5.2.6.	DPV022 interacts with endogenous Bak and Bax during virus infection	162
5.2.7.	DPV022 inhibits the conformational activation of Bak and Bax during virus infection	162
Chapter 6	The role of E3L, double-stranded RNA, and Noxa in the apoptotic response to vaccinia virus infection	168
6.1.	Brief introduction	169
6.2.	Results	170
6.2.1.	Vaccinia virus devoid of E3L induces apoptosis even in the presence of F1L	170
6.2.2.	Increased levels of dsRNA are detected upon infection with VVΔE3L	172
6.2.3.	dsRNA produced during VVΔE3L infection localises around virus factories	175
6.2.4.	The BH3-only protein Noxa is upregulated during vaccinia virus infection	177
6.2.5.	The BH3-only protein Noxa also localises to VVΔE3L virus factories	179
6.2.6.	Noxa contributes to vaccinia virus-induced apoptosis	182
Chapter 7	Discussion	186
7.1.	Poxviruses inhibit apoptosis	187
7.1.1.	FPV039 and the vBcl-2-like proteins	187
7.1.2.	FPV039 inhibits apoptosis	191
7.1.3.	DPV022 inhibits apoptosis	200
7.1.4.	The evolution of poxviral vBcl-2 proteins	203
7.1.5.	Of chickens and deer	207
7.1.6.	More than meets the eye?	208
7.1.7.	To infinity and beyond	209
7.2.	Vaccinia virus induces apoptosis	210
7.3.	Summary	217
	References	220
	Appendix A	251
A.1.	A unified model of Bak/Bax activation	252

LIST OF TABLES

	Page
Table 2.1. Cell Lines Used	67
Table 2.2. Plasmids Used	69/70
Table 2.3. Oligonucleotides Used for Cloning	74
Table 2.4. Viruses Used	79
Table 2.5. Antibodies Used	85
Table 2.6. Oligonucleotides Used for Quantitative Real-time PCR	97

LIST OF FIGURES

	Page
Chapter 1 Introduction	
Figure 1.1. The family <i>Poxviridae</i>	3
Figure 1.2. Poxvirus structure and genome	7
Figure 1.3. The vaccinia virus replication cycle	9
Figure 1.4. The apoptotic caspases	13
Figure 1.5. The extrinsic apoptotic pathway	15
Figure 1.6. The intrinsic apoptotic pathway	16
Figure 1.7. The Bcl-2 family of proteins	20
Figure 1.8. The BH domain sequences	21
Figure 1.9. The structure of Bcl-2 proteins	22
Figure 1.10. Proposed models describing Bak/Bax activation	29
Figure 1.11. BH3-only proteins inhibit the anti-apoptotic Bcl-2 family members	30
Figure 1.12. BH3-only proteins directly activate Bak and Bax	32
Figure 1.13. The regulation of apoptosis by Bcl-2 family proteins	35
Figure 1.14. Bcl-2 protein interactions	36
Figure 1.15. Viral Bcl-2 proteins	45
Figure 1.16. Poxviral vBcl-2 orthologues	51
Figure 1.17. The structure of M11L and F1L	52
Figure 1.18. Noxa and E3L	58
Chapter 2 Materials and methods	
Figure 2.1. FPV039 and DPV022 constructs generated	76
Figure 2.2. Generation of recombinant vaccinia viruses	82
Chapter 3 Fowlpox virus encodes a Bcl-2 homologue that protects cells from apoptotic death through interaction with the pro-apoptotic protein Bak	
Figure 3.1. Alignment of FPV039 with human Bcl-2	102
Figure 3.2. FPV039 localises to the mitochondria in mammalian cells	104
Figure 3.3. FPV039 localises to the mitochondria in chicken cells	106
Figure 3.4. FPV039 inhibits TNF α -induced apoptosis	108
Figure 3.5. FPV039 interacts with the pro-apoptotic protein Bak	110
Figure 3.6. FPV039 inhibits Bak-induced apoptosis	112
Figure 3.7. FPV039 interacts with endogenous Bak during vaccinia virus infection	114
Figure 3.8. FPV039 interacts with endogenous Bak in chicken cells	116
Figure 3.9. FPV039 inhibits virus-induced apoptosis	118
Figure 3.10. FPV039 inhibits the conformational activation of Bak	120
Chapter 4 The fowlpox virus Bcl-2 homologue, FPV039, interacts with activated Bax and a discrete subset of BH3-only proteins to inhibit apoptosis	
Figure 4.1. FPV039 inhibits Bax-induced apoptosis	124
Figure 4.2. FPV039 inhibits Bax activity	126
Figure 4.3. FPV039 inhibits Bax activity	128
Figure 4.4. FPV039 inhibits the conformational activation of Bax	129
Figure 4.5. FPV039 inhibits Bax oligomerisation	131

Figure 4.6.	FPV039 interacts with Bax	133
Figure 4.7.	FPV039 interacts with Bax in the absence of Bak	135
Figure 4.8.	FPV039 interacts with endogenous active Bax during vaccinia virus infection	137
Figure 4.9.	FPV039 inhibits apoptosis induced by BH3-only proteins	139
Figure 4.10.	FPV039 interacts with Bim _L	141
Figure 4.11.	FPV039 interacts with a subset of BH3-only proteins	142
Chapter 5	Deerpox virus encodes an inhibitor of apoptosis that regulates Bak and Bax	
Figure 5.1.	DPV022 shares regions of sequence homology with F1L and M11L but not cellular Bcl-2 proteins	145
Figure 5.2.	DPV022 localises to the mitochondria	147
Figure 5.3.	DPV022 inhibits TNF α -induced apoptosis	149
Figure 5.4.	DPV022 interacts with Bak in the absence of all other Bcl-2 family proteins	151
Figure 5.5.	DPV022 interacts with ectopically expressed Bak	153
Figure 5.6.	DPV022 inhibits Bak-induced apoptosis	154
Figure 5.7.	DPV022 interacts with Bax in the absence of all other Bcl-2 family proteins	155
Figure 5.8.	DPV022 interacts with ectopically expressed Bax	157
Figure 5.9.	DPV022 inhibits Bax-induced apoptosis	158
Figure 5.10.	DPV022 inhibits Bax oligomerisation	159
Figure 5.11.	DPV022 can replace the endogenous anti-apoptotic Bcl-2 proteins	161
Figure 5.12.	DPV022 interacts with endogenous Bak and Bax during virus infection	163
Figure 5.13.	DPV022 inhibits the conformational activation of Bak	164
Figure 5.14.	DPV022 inhibits the conformational activation of Bax	166
Chapter 6	The role of E3L, double-stranded RNA, and Noxa in the apoptotic response to vaccinia virus infection	
Figure 6.1.	Vaccinia virus devoid of F1L or E3L, but not wild-type vaccinia virus, induce apoptosis	171
Figure 6.2.	Increased levels of dsRNA are detected upon VV Δ E3L infection	174
Figure 6.3.	dsRNA localises around VV Δ E3L virus factories	176
Figure 6.4.	The BH3-only protein Noxa is upregulated during VVCop infection	178
Figure 6.5.	Noxa is upregulated during VV Δ E3L infection	180
Figure 6.6.	Endogenous Noxa localises to VV Δ E3L virus factories	181
Figure 6.7.	Ectopically expressed Myc-Noxa localises to VV Δ E3L virus factories	183
Figure 6.8.	Noxa-deficient cells undergo reduced apoptosis during VV Δ E3L infection	184
Chapter 7	Discussion	
Figure 7.1.	FPV039 inhibits apoptosis	193
Figure 7.2.	The inhibition of Bak and Bax activity by vBcl-2 proteins	194
Figure 7.3.	The evolutionary relationship of poxviral vBcl-2 proteins	204
Figure 7.4.	Working hypothesis for the role of Noxa during VV Δ E3L	212

Figure 7.4.	Working hypothesis for the role of Noxa during VV Δ E3L infection	212
Figure 7.5.	Noxa contributes to vaccinia virus-induced apoptosis	218
Appendix A		
Figure A.1.	A unified model of Bak/Bax activation	252

LIST OF ABBREVIATIONS AND SYMBOLS

ACTB – β -actin
AIF – apoptosis-inducing factor
AraC – cytosine arabinoside
ASFV – African swine fever virus
ATP – adenosine triphosphate
Bad – Bcl-2 antagonist of cell death
Bak – Bcl-2 antagonist/killer
Bax – Bcl-2-associated x protein
Bcl-2 – B-cell lymphoma/leukaemia 2
Bcl-x_L – Bcl-2-like protein x large isoform
Bcl-x_S – Bcl-2-like protein x small isoform
Bcl-w – Bcl-2-like protein w
Bcl-2A1 – Bcl-2-like protein A1
BGMK – Buffalo green monkey kidney
BH – Bcl-2 homology
Bid – BH3-interaction domain death agonist
Bik – Bcl-2-interacting killer
Bim – Bcl-2-interacting mediator of cell death
Bim_{EL} – Bim extra-long isoform
Bim_L – Bim long isoform
Bim_S – Bim short isoform
Bmf – Bcl-2 modifying factor
BMH – 1,6-bismaleimidoheptane
BMK – baby mouse kidney
bp – base pairs
CHAPS – 3-[3-cholamidopropyl)-dimethylammonio]-1-propanesulfonate
cBcl-2 – cellular Bcl-2 protein
CrmA – cytokine response modifier A
CTL – cytotoxic T-lymphocyte
 $\Delta\psi_M$ – mitochondrial membrane potential
Da – Dalton
DAPI – 4'6-diamino-2-phenylindole
DMEM – Dulbecco's modified Eagle medium
DMF – dimethylformamide
DMSO – dimethylsulfoxide
DNA – deoxyribonucleic acid
dsDNA – double-stranded deoxyribonucleic acid
dsRNA – double-stranded ribonucleic acid
DTT – dithiothreitol
EBV – Epstein-Barr virus
ECL – enhanced chemiluminescence
EDTA – ethylenediaminetetraacetic acid
EGFP – enhanced green fluorescent protein
EMCV – encephalomyocarditis virus
ER – endoplasmic reticulum
EV – enveloped virus
FACS – fluorescence activated cell sorting
FADD – FAS-associated death domain
FAS – apoptosis-stimulating fragment

FASL – apoptosis-stimulating fragment ligand
g – gram
GAPDH – glyceraldehyde-3 phosphate dehydrogenase
GDP – guanosine diphosphate
GTP – guanosine triphosphate
h – hour
HA – haemagglutinin
HCMV – human cytomegalovirus
hpi – hours post-infection
Hrk – harakiri
HRP – horseradish peroxidase
HSV-1 – herpes simplex virus 1
IAP – inhibitor of apoptosis
IFN – interferon
IP – immunoprecipitation
IPTG – isopropyl β -D-1 thiogalactopyranoside
IRF – interferon regulatory factor
IV – immature virus
k – kilo-
KSHV – Kaposi's sarcoma herpesvirus
l – litre
LB – Luria-Bertani broth
LMH – chicken leghorn male hepatocellular carcinoma
LMP – low melting point
Mcl-1 – myeloid cell leukaemia sequence 1
Mcl-1s – Mcl-1 short isoform
MCMV – murine cytomegalovirus
 μ – micro-
m – milli-
M – molar
MAC – mitochondrial apoptosis-induced channel
MOAP-1 – modulator of apoptosis 1
MCMV – murine cytomegalovirus
MEF – mouse embryo fibroblasts
min – minute
MOI – multiplicity of infection
MOM – mitochondrial outer membrane
MOMP – mitochondrial outer membrane permeabilisation
mRNA – messenger ribonucleic acid
MV – mature virus
MV – measles virus
MVA – modified vaccinia virus Ankara
n – nano-
NF- κ B – nuclear factor kappa B
NK – natural killer cell
NTP – nucleoside triphosphate
OAS – 2'-5' oligoadenylate synthetase
ORF – open reading frame
PAGE – polyacrylamide gel electrophoresis
PARP – poly (ADP-ribose) polymerase
PBS – phosphate-buffered saline

PCR – polymerase chain reaction
PFU – plaque forming units
PKR – dsRNA-dependent protein kinase
PTPC – permeability transition pore complex
Puma – p53-upregulated modulator of apoptosis
PVDF – polyvinylidene fluoride
RNA – ribonucleic acid
RT-PCR – real-time polymerase chain reaction
s – second
SDS – sodium dodecyl sulfate
SMAC – second mitochondrial-derived activator of caspases
SSC – sodium chloride sodium citrate
STS – staurosporine
SV – sendai virus
TAE – tris acetate EDTA
TBST – tris-buffered saline plus Tween 20
TK – thymidine kinase
TLR – toll-like receptor
TM – transmembrane
TMRE – tetraethylrhodamine ethyl ester
TNF – tumour necrosis factor
TNFR – tumour necrosis factor receptor
TRADD – TNFR-associated death domain
vBcl-2 – virus Bcl-2-like protein
VDAC – voltage dependent anion channel
VSV – vesicular stomatitis virus
VV – vaccinia virus
WB – Western blot
WT – wild-type
WV – wrapped virus
x g – times gravity
X-gal – 5-bromo-4-chloro-3-indolyl- β -D-galactopyranoside
XIAP – x-linked inhibitor of apoptosis
zVAD.fmk – carbobenzoxy-valyl-alanyl-aspartyl-[O-methyl]- fluoromethylketone

CHAPTER ONE

INTRODUCTION

1.1. POXVIRUSES

Poxviruses comprise a large and extensive family of double-stranded DNA viruses, distinctive for their ability to replicate exclusively and almost independently in the cytoplasm of infected cells (97, 316). Such an autonomous replication cycle requires that poxviruses encode their own proteins for copying their genome and transcribing their genes, and this requirement, in part, explains the large poxviral genome sizes (316). The remainder of the poxvirus genome is dedicated to encoding proteins that modulate host-pathogen interactions, something at which all poxviruses excel. Thus, the study of poxviruses and how they manipulate cells has historically contributed much to our understanding of basic virology, genetics, and immune defence mechanisms. Undoubtedly, the continued use of poxviruses as biochemical tools to dissect cellular pathways will prove invaluable in our attempts to explain the mysteries of biology.

1.1.1. The family *Poxviridae*. Members of the *Poxviridae* family exist throughout the world and infect a wide variety of animals: those that infect insects are classified under the sub-family *Entomopoxvirinae*, whereas those that infect vertebrate hosts are classified under the *Chordopoxvirinae* sub-family (Fig. 1.1) (97, 316). Chordopoxviruses are by far the best studied of all poxviruses and are further sub-divided into nine genera: *Capripoxvirus*, *Suipoxvirus*, *Cervidpoxvirus*, *Leporipoxvirus*, *Yatapoxvirus*, *Orthopoxvirus*, *Molluscipoxvirus*, *Parapoxvirus*, and *Avipoxvirus*. Despite the vast ranks within the poxvirus family, only variola virus, an orthopoxvirus, and molluscum contagiosum virus, a molluscipoxvirus, are sole human pathogens (97). Nevertheless, several poxviruses, including monkeypox virus, Orf virus, and cowpox virus, are zoonoses, capable of infecting and causing disease in humans when transferred

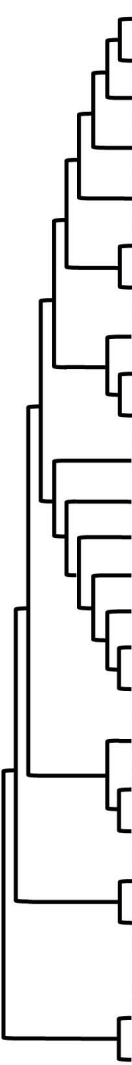
	Species	Genus	Sub-family
	Lumpy skin disease virus	<i>Capripoxvirus</i>	<i>Chordopoxvirinae</i>
	Sheeppox virus*		
	Goatpox virus		
	Swinepox virus*	<i>Suipoxvirus</i>	
	Deerpox virus*	<i>Cervidpoxvirus</i>	
	Myxoma virus*	<i>Leporipoxvirus</i>	
	Shope fibroma virus		
	Yaba monkey tumor virus*	<i>Yatapoxvirus</i>	
	Yaba-like disease virus		
	Tanapox virus		
	Cowpox virus	<i>Orthopoxvirus</i>	
	Ectromelia virus		
	Vaccinia virus*		
	Monkeypox virus		
	Variola virus		
	Camelpox virus		
	Taterapox virus		
	Molluscum contagiosum virus*	<i>Molluscipoxvirus</i>	
	Orf virus*	<i>Parapoxvirus</i>	
	Bovine papular stomatitis virus		
	Fowlpox virus*	<i>Avipoxvirus</i>	
	Canarypox virus		
<i>Melontha melontha</i> *	<i>Entomopoxvirus α</i>	<i>Entomopoxvirinae</i>	
<i>Melanoplus sanguinipes</i>	<i>Entomopoxvirus β</i>		
<i>Amsacta moorei</i> *			
<i>Chironimus luridus</i> *	<i>Entomopoxvirus γ</i>		

Figure 1.1. The family *Poxviridae*. The *Poxviridae* family is divided into two sub-families, the *Chordopoxvirinae*, comprised of nine genera, and the *Entomopoxvirinae*, comprised of three genera. Example poxvirus species are listed for each genus, and the prototypical member of each genus is marked with an asterisk (*). The phylogenetic tree to the left of the table illustrates the evolutionary relationship between poxviruses (adapted from ref. 208).

from their animal host (97). Several other poxviruses, including the leporipoxvirus myxoma virus, which infects rabbits, and the orthopoxvirus extromelia virus, which infects mice, do not infect humans but serve as useful laboratory model systems (97, 316). The poxvirus genera and type species most relevant to this study are discussed in more detail below.

1.1.1.1. The orthopoxviruses. The most infamous of all poxviruses, and one of the most infamous viruses known to mankind, is variola virus, the causative agent of smallpox (134). This highly infectious disease has plagued human civilisations throughout the world for well over 4000 years, causing a disfiguring “pockmarked” rash and killing, in some cases, between 30 and 40% of afflicted people (97). However, due to a massive vaccination campaign mounted by the World Health Organisation (WHO) in the 1960s and 1970s, the planet has been free of smallpox for over 30 years, with the last natural case of smallpox occurring in 1977 (134, 402). To this day, smallpox is the only human infectious disease to have been completely eliminated, and its eradication stands as one of humankind’s most spectacular achievements (134).

The eradication of smallpox owes a lot to the work of Edward Jenner, an English physician now regarded as the father of modern vaccination (402). In 1796, Jenner observed that infection with cowpox virus, which causes a mild, self-limiting rash in humans, protected from subsequent infection with variola virus (218). We now know that cowpox, an orthopoxvirus, is antigenically related to variola virus and that vaccination with cowpox induces cross-protective immunity against other orthopoxviruses, including variola. Jenner originally coined the term “vaccination” from the Latin word “*vacca*” for cow in reference to

the specific inoculation of cowpox virus to prevent smallpox. In tribute to Jenner, however, Louis Pasteur later repurposed the term to refer to any immunisation.

At some point in the 200-year propagation of the smallpox vaccine, a novel poxvirus, distinct from cowpox and all others, arose as the predominant virus used for vaccination. “Vaccinia” virus, as it was named, became the virus used by the WHO to eradicate smallpox and, to this day, is still used as the vaccinating agent against smallpox (97, 134). Although the ultimate origins of this virus are unknown, vaccinia virus (VV) is the best and most studied of all poxviruses. As a result, VV, which is easy to maintain in the laboratory and amenable to genetic manipulation, now serves as a robust and commonly used model system for investigating virus biology and host-pathogen interactions (318). The fact that, like all poxviruses, VV encodes numerous proteins that interfere with the host immune system, make VV especially useful in dissecting immune pathways (220, 390).

1.1.1.2. The avipoxviruses. The genus *Avipoxvirus* includes a variety of species that all infect birds (97, 435). Phylogenetic analyses suggest that avipoxviruses are the most evolutionarily divergent of the chordopoxviruses, reflecting the fact that avipoxviruses are the only chordopoxviruses that infect non-mammalian animals (164, 269, 305). Indeed, one distinguishing feature of the avipoxviruses is their large genome size. Fowlpox virus, the proto-typical avipoxvirus, and canarypox virus, a closely related virus, have genomes of 288 kbp and 365 kbp, respectively, making them the largest among all poxviruses (4, 438). In addition to the complement of genes shared with other chordopoxviruses, the avipoxviruses encode numerous novel proteins as well as

proteins predicted to function as host-range factors or immune modulators (4, 390, 438).

Fowlpox virus causes disease in chickens and turkeys, and outbreaks can result in significant economic loss for the poultry industry (97, 127, 320, 435). Disease caused by fowlpox infection can manifest in two forms (435). Cutaneous fowlpox, which has a low mortality rate, produces lesions on unfeathered areas, including the comb, wattle, beak area, and legs, and is probably spread mechanically by an arthropod vector. Diptheritic fowlpox results from respiratory transmission of the virus between infected birds and produces lesions on the oropharynx that eventually form a pseudomembrane and asphyxiate the animal. Healthy flocks do not typically succumb to fowlpox virus infection, but egg production is often reduced and, in flocks under stress, mortality can be as high as 50% (97, 320). Interestingly, avipoxviruses do not cause disease in mammals. Although fowlpox virus is unrestricted for entry into mammalian cells, only early genes are expressed and infection is eventually aborted (404). The expression of early genes (which has been reported to last up to fourteen days) coupled with the inability to productively infect mammalian cells, has therefore made avipoxviruses prime candidates in the development of live vaccine vectors and gene therapy tools (37, 399).

1.1.1.3. The cervidpoxviruses. Deerpox virus has been isolated on more than one occasion from skin lesions found on several, geographically isolated wild mule deer (*Odocoileus hemionus*) (313, 344, 467). Natural and experimental infection of mule deer with deerpox virus produces characteristic ulcers around the face, neck, and feet, and in most cases disease appears to be mild, at least in adult animals (38, 313, 344, 467). The genomes of two deerpox virus isolates

have been completely sequenced, and four others have been partially sequenced (2, 313). Not unexpectedly, deerpox virus encodes numerous proteins—many of them novel—that are predicted to interfere with the host immune system (2, 313). Deerpox virus is most closely related to the sui- and capripoxviruses; however, phylogenetic analyses suggest that deerpox virus is as distinct as other chordopoxvirus genera are from each other (2, 208). Accordingly, the International Committee on Taxonomy of Viruses (ICTV) has recently classified deerpox virus as the type species of the newest chordopoxvirus genus, *Cervidpoxvirus* (313).

1.1.2. Poxvirus morphology and genetics. All poxviruses are physically large viruses, with a complex and unique morphology (Fig. 1.2A) (86, 316). Orthopoxviruses, with dimensions of approximately 360 x 270 x 250 nm, are just visible by light microscopy and typically described as being barrel- or brick-shaped with a distinctively uneven surface. In general, the overall morphology and size of poxviruses is consistent throughout the *Chordopoxvirinae*, including the avi- and cervidpoxviruses. Two infectious forms of the virion exist: the mature virus (MV; also known as the intracellular mature virus, IMV) and the enveloped virus (EV; also known as the extracellular enveloped virus, EEV). The MV is the basic infectious unit, comprised of a single lipid bilayer that surrounds a dumbbell-shaped core, which, itself is flanked by heterogenous material referred to as lateral bodies (Fig. 1.2B). The EV differs from the MV in that it is surrounded by an additional lipid bilayer with different viral proteins incorporated, making EV and MV antigenically and functionally distinct.

The dsDNA genome is held within the core of the virion in a complex nucleoprotein structure (86, 316). The poxvirus genome is a single, linear,

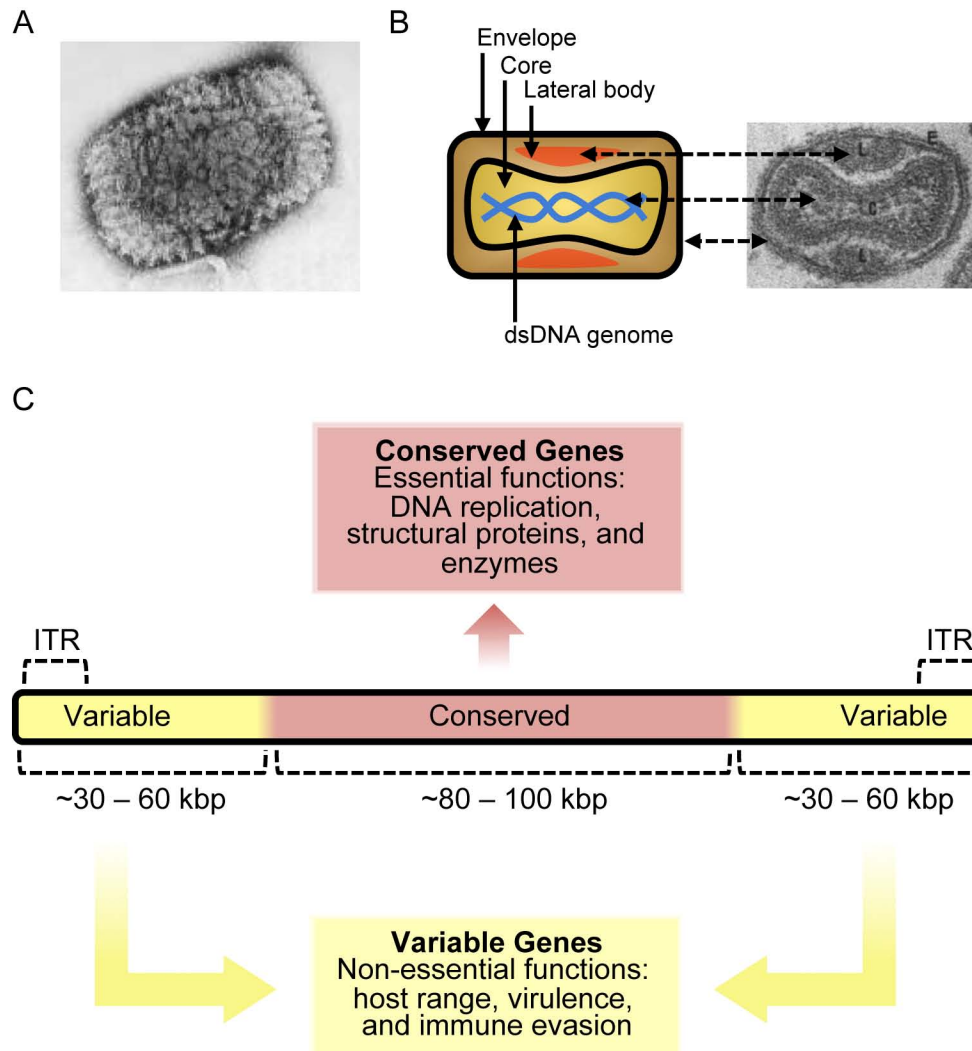


Figure 1.2. Poxvirus structure and genome. (A) An electron micrograph of a single VV virion (adapted from ref. 304). (B) A schematic representation of a VV virion cross-section is compared with an electron micrograph cross-section (adapted from ref. 316). The virion's envelope (E), core (C), and lateral bodies (L) are indicated on the schematic with solid arrows, and the same structures are highlighted in the electron micrograph with dashed arrows. The double-stranded DNA genome is also indicated with an arrow. (C) A schematic representation of the poxvirus genome (adapted from ref. 303). The linear, dsDNA genome possesses a central region conserved among poxviruses that encodes proteins essential to the viral replication cycle. The terminal regions of the genome are variable among different poxviruses and often encode immunomodulatory proteins. The ends of the genome are demarcated by inverted terminal repeat sequences and form covalently closed hairpins.

covalently closed molecule of dsDNA (Fig. 1.2C). For a virus, the genomes are relatively large, ranging in size from 130 to over 300 kilobase pairs (kbp), and contain on average around 200 open reading frames, about ninety of which are conserved among all chordopoxviruses (164, 439). The general organisation of the chordopoxvirus genome is remarkably similar between genera: highly conserved genes involved in virion structure and nucleic acid metabolism are found in the central 90 kbp and are required for viral replication, whereas genes involved in immune evasion or host-specific interactions are found near the termini and vary widely (164, 269, 439). Overall the gene order and spacing in the central region of the genome is similar in all chordopoxviruses except the avipoxviruses, which show several rearrangements and insertions (4, 305). All poxvirus genomes possess inverted terminal repeats that covalently connect the ends of the two DNA strands in a hairpin loop (316). Notably, the poxvirus genome is particularly amenable to homologous recombination, both naturally and experimentally, thus permitting simple genetic manipulation of VV in the laboratory (133, 316, 318).

1.1.3. Poxvirus dissemination. It is not surprising that a virus as complex as a poxvirus has an equally complex replication cycle (Fig. 1.3). Although many of the details surrounding poxvirus entry, genome replication, and dissemination are still a matter of debate, the overall process is generally well understood (86, 316, 368). The VV replication cycle begins with a fusion event between the MV membrane and the plasma membrane of the host cell, which results in the release of the core into the cytoplasm (317). In the case of EV, the additional membrane is disrupted upon attachment to the cell, permitting fusion between the MV membrane and the plasma membrane. The cellular receptors required

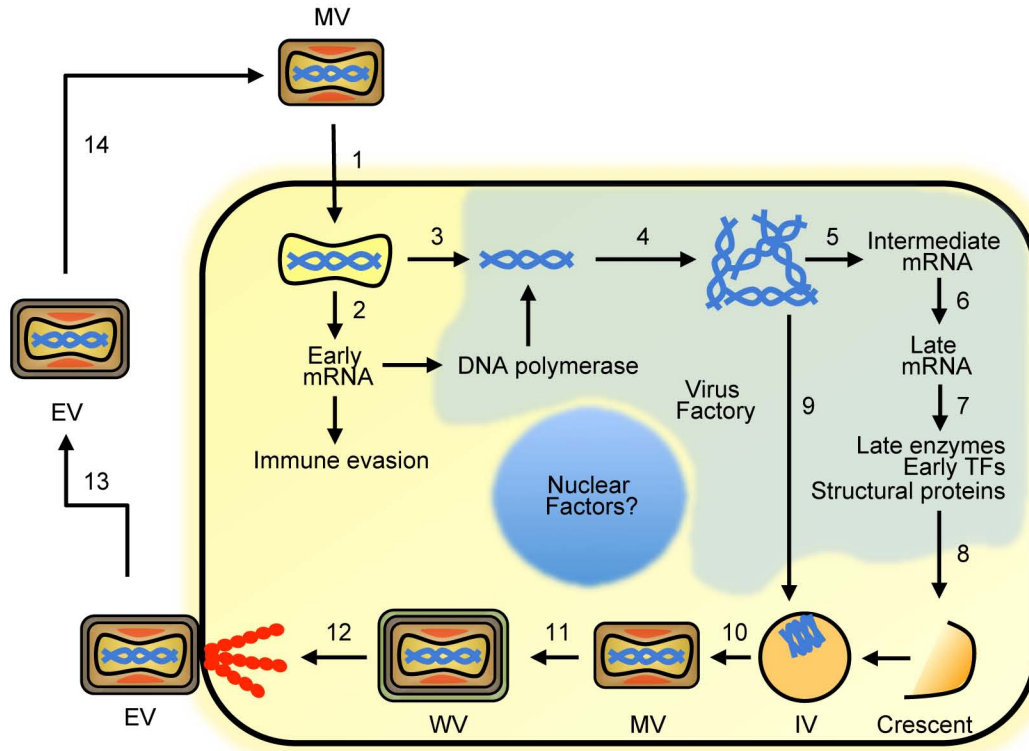


Figure 1.3. The vaccinia virus replication cycle. Mature virus (MV) binds an unknown receptor on the surface of the cell, and the MV membrane fuses with the plasma membrane or an endocytic vesicle to release the core into the cytoplasm (1). Early mRNA, encoding immune evasion proteins and enzymes necessary for DNA replication, is synthesised from the core (2). Uncoating of the DNA genome (3) precedes DNA replication mediated by the DNA polymerase and other early proteins (4). DNA replication takes place in peri-nuclear virus factories. Following DNA replication, intermediate mRNA is synthesised (5), followed by late mRNA (6), which encodes structural proteins and early transcription factors to be packaged in the virion (7). Assembly begins with the formation of a membrane crescent in the cytoplasm (8), which envelops the DNA genome (9) to form the immature virus (IV). Maturation of the IV results in the MV (10), the major infectious form of VV. MV constitutes the majority of virus produced during VV infection and remains in the cytoplasm until released during cell lysis. A minority of the MV obtains two additional membranes from trans-Golgi or endosomal cisternae to form the wrapped virus (WV), with a total of three membranes (11). WV fuses with the plasma membrane to lose one of its membranes and become enveloped virus (EV), with a total of two membranes (12). The majority of EV remains associated with the extracellular surface of the plasma membrane and polymerises actin in the cytoplasm beneath the virus to form an “actin tail” that propels EV to nearby uninfected cells (12). A minority of EV dissociates from the cell and can disseminate systemically (13). EV must shed its additional membrane before infecting another cell as an MV (14). Nuclear and cytoplasmic cellular factors may be involved in virus replication and assembly, although this remains unclear. (Adapted from ref. 316).

for entry are still unknown; however, the viral fusion machinery is shared among all poxviruses, suggesting an ancient and conserved mechanism of entry (392). Once the core is released into the cytoplasm, partial uncoating occurs and the transcription of early genes is initiated by the virus-associated DNA-dependent RNA polymerase and other proteins packaged in the core. The early proteins include enzymes required for DNA replication as well as proteins involved in immune modulation. Virus cores are then transported to the periphery of the nucleus where complete uncoating occurs and DNA replication can begin. The site of poxviral DNA replication and initial virus assembly is known as the “virus factory” and is visible as a discrete, DNA-rich structure under the microscope. Each infecting virion is capable of initiating the formation of an independent factory, although factories of a mixed origin are also observed (225). The initiation of DNA replication is required for intermediate gene transcription, the products of which are, in turn, required for late gene transcription. Late proteins include the structural components of the virion as well as the enzymes packaged into the virion core that are required to initiate the next round of replication. A crescent-shaped lipid bilayer encircles newly replicated genomic DNA to form the immature virus (IV). Proteolytic cleavage of core proteins produces the characteristic brick-shaped MV. MV is the most abundant form of virus produced during infection and accumulates in cytoplasmic occlusion bodies until released upon cell lysis. Interestingly, however, MV has recently been shown to induce the phosphatidylserine exposure and membrane blebbing typically associated with apoptosis to promote uptake of virions into uninfected cells by macropinocytosis (306, 307). A small proportion of MV is wrapped in two additional membranes derived from trans-Golgi or endosomal cisternae to form the so-called wrapped virus (WV). WV subsequently fuses with the plasma

membrane to lose one of the additional two membranes and become EV, which still has one more membrane than MV, and is important for dissemination of the virus *in vivo*. The majority of EV remains associated with the outside of the plasma membrane and is propelled to uninfected cells by an actin tail that polymerises in the cytoplasm beneath the EV (41, 190, 407). Only a minority of the EV is ever released from the surface of the cell.

1.1.4. Poxviruses evade the immune system. Because viruses are obligate intracellular parasites, they must contend with the host immune system in order to replicate and mount a productive infection (136). Poxviruses are renowned for interfering with both the innate and adaptive arms of the immune system, and much of the expansive poxviral genome is dedicated to encoding proteins that subvert host immune defences and modulate host-pathogen interactions (220, 390). Indeed, so great are their numbers and so varied their kind, that not a single common immunomodulatory gene can be found in all poxviruses, a fact that reflects a close association between each poxvirus and its host (220, 390). By interfering at almost every level of the immune response, poxviruses prevent the production of interferons, chemokines, and inflammatory cytokines, and they inhibit critical events in the immune response, including antigen presentation (390). Importantly, poxviruses are also masters of cell fate, and they encode numerous proteins that inhibit apoptosis, the ultimate outcome of many immune responses (26).

1.2. APOPTOSIS

1.2.1. Apoptosis: a form of programmed cell death. The Greek word “*apoptosis*” refers to the dropping or falling off of leaves or petals from a tree or

flower. In 1972, John Kerr and colleagues borrowed this term to describe a commonly observed but little recognised “mechanism of controlled cell deletion,” in reference to the discrete membrane-bound “blebs” shed from dying cells late during this process (231). As Kerr *et al.* predicted, today we recognise apoptosis as an intrinsic and highly structured mechanism of programmed cell death whose basic tenets are conserved throughout all metazoans (183, 231).

The field of apoptosis research has expanded profoundly since 1972, and we now have a complex, although not nearly complete, understanding of how cells master their own fate (183, 260). Mediated by an elaborate genetic programme, apoptosis comprises a series of signalling pathways that function to systematically dismantle unwanted cells in a precise and innocuous manner. Indeed, apoptosis was first identified based on the distinct biochemical and morphological changes with which it is associated. As apoptosis proceeds, the nucleus begins to fragment as the chromatin condenses and the DNA is degraded, the cytoskeleton is rearranged as the cell shrinks and detaches from its surroundings, and finally the eponymous membrane blebbing results in the complete dissolution of the apoptotic cell into so-called “apoptotic bodies.” The engulfment of these apoptotic bodies by nearby phagocytes results in the tidy removal of the apoptotic cell, typically in the absence of any cell leakage or inflammation (427). This process of “cell suicide” is required for proper development of all multi-cellular organisms, and it is responsible for maintaining tissue homeostasis and eliminating damaged or infected cells. The selective and purposeful dismantling of cells is so exquisitely regulated that any shift in the balance can be catastrophic: apoptotic dysfunction has been linked with the development of cancer and autoimmunity, while accelerated or unwanted apoptosis may lead to immunodeficiency or degenerative diseases (183, 260).

1.2.2. Caspases demolish the cell. Regardless of how apoptosis begins, it always ends with the activation of caspases (Fig. 1.4). Caspases, the molecules responsible for the physical demolition of the apoptotic cell, are a group of highly specific cysteinyl aspartate proteases that cleave their target proteins only after the aspartic acid residue in the tetrapeptide motif X-X-X-Asp (where X differs for each caspase) (427, 432). Caspases reside in the cell as inactive pro-enzymes and must undergo proteolytic processing to form the catalytically active enzyme, often a hetero-tetramer. A variety of cellular signalling cascades, including death receptor activation and the release of cytochrome c from the mitochondria (described in section 1.2.3.), result in the dimerisation and auto-activation of the “initiator” caspases-2, -8, -9, and -10. Once activated, the initiator caspases cleave and activate the “executioner” caspases-3, -6, and -7. The executioner caspases then go on to cleave hundreds of cellular proteins, making them responsible for the direct disassembly of the cell and the phenotypic changes classically associated with apoptosis (291, 427).

1.2.3. The intrinsic and extrinsic apoptotic pathways. The events that lead to the activation of caspases and the destruction of the cell by apoptosis can be broadly divided into two cellular signalling pathways: the extrinsic (or death receptor pathway) (Fig. 1.5) and the intrinsic (or mitochondrial) pathway (Fig. 1.6). The extrinsic pathway begins with a death receptor, such as tumour necrosis factor receptor (TNFR) or apoptosis stimulating fragment (FAS), binding to its cognate ligand, TNF α or FAS ligand (FASL), respectively (472). Subsequent trimerisation of FAS results in the association of its cytoplasmic “death domains” and the recruitment of the cytosolic adaptor protein FAS-associated death domain (FADD), which interacts with FAS via its own death

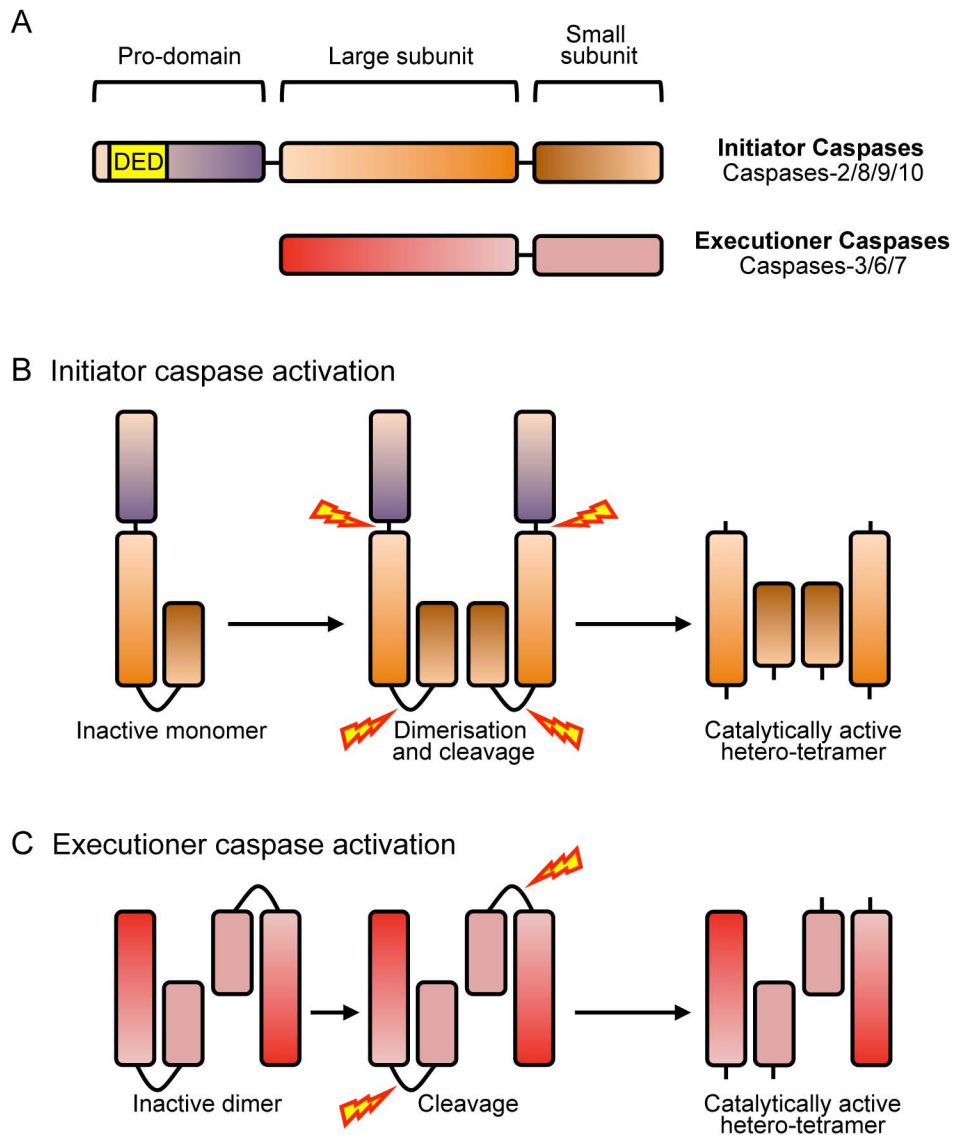


Figure 1.4. The apoptotic caspases. (A) The caspases involved in the apoptotic dismantling of the cell can be classified as either initiator caspases (caspases-2, -8, -9, -10) or executioner caspases (including caspases-3, -6, -7). Both types of caspases are comprised of a large and a small domain, and the initiator caspases have an additional regulatory pro-domain, which, in the case of caspase-8, contains the death effector domain (DED) responsible for interacting with FADD. (B) Initiator caspases are typically activated following dimerisation of the inactive monomers and auto-catalytic cleavage to form the catalytically active hetero-tetramer. (C) Executioner caspases are cleaved and activated by the initiator caspases to form the catalytically active hetero-tetramer. (Adapted from ref. 418).

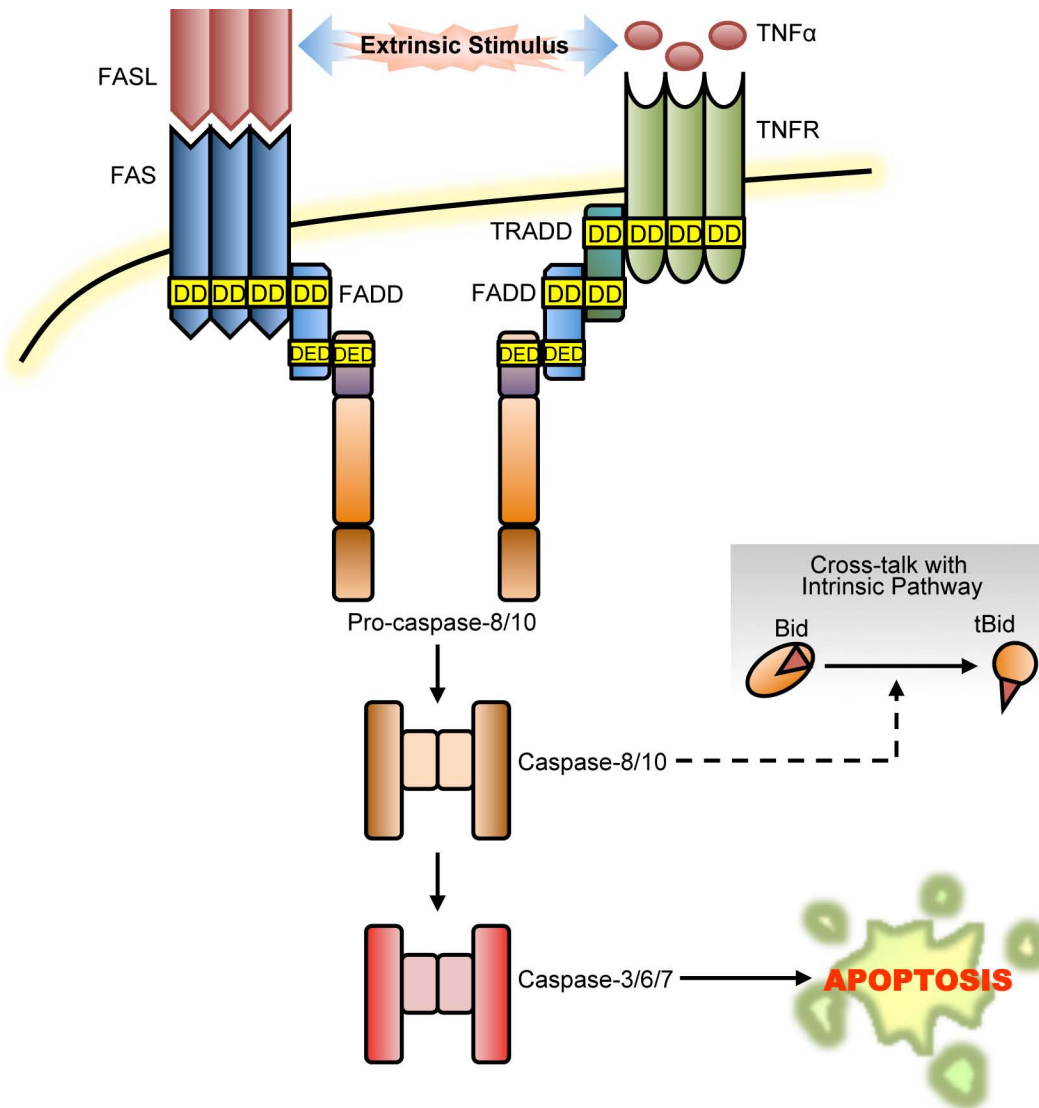


Figure 1.5. The extrinsic apoptotic pathway. The extrinsic apoptotic pathway begins with the trimerisation of a death receptor, such as FAS or TNFR, upon binding its cognate ligand, FASL or TNF α . The adaptor proteins TRADD and/or FADD recruit the initiator caspases pro-caspase-8 or -10, which become auto-catalytically activated and go on to cleave and activate the effector caspases-3,-6, and -7. Caspases-3/6/7 cleave a variety of substrates and commit the cell to death. The extrinsic pathway bisects the intrinsic pathway with the caspase-8-mediated cleavage of the BH3-only protein Bid, which, once cleaved into its active form, tBid, can induce Bak and Bax activation (see Fig. 1.6).

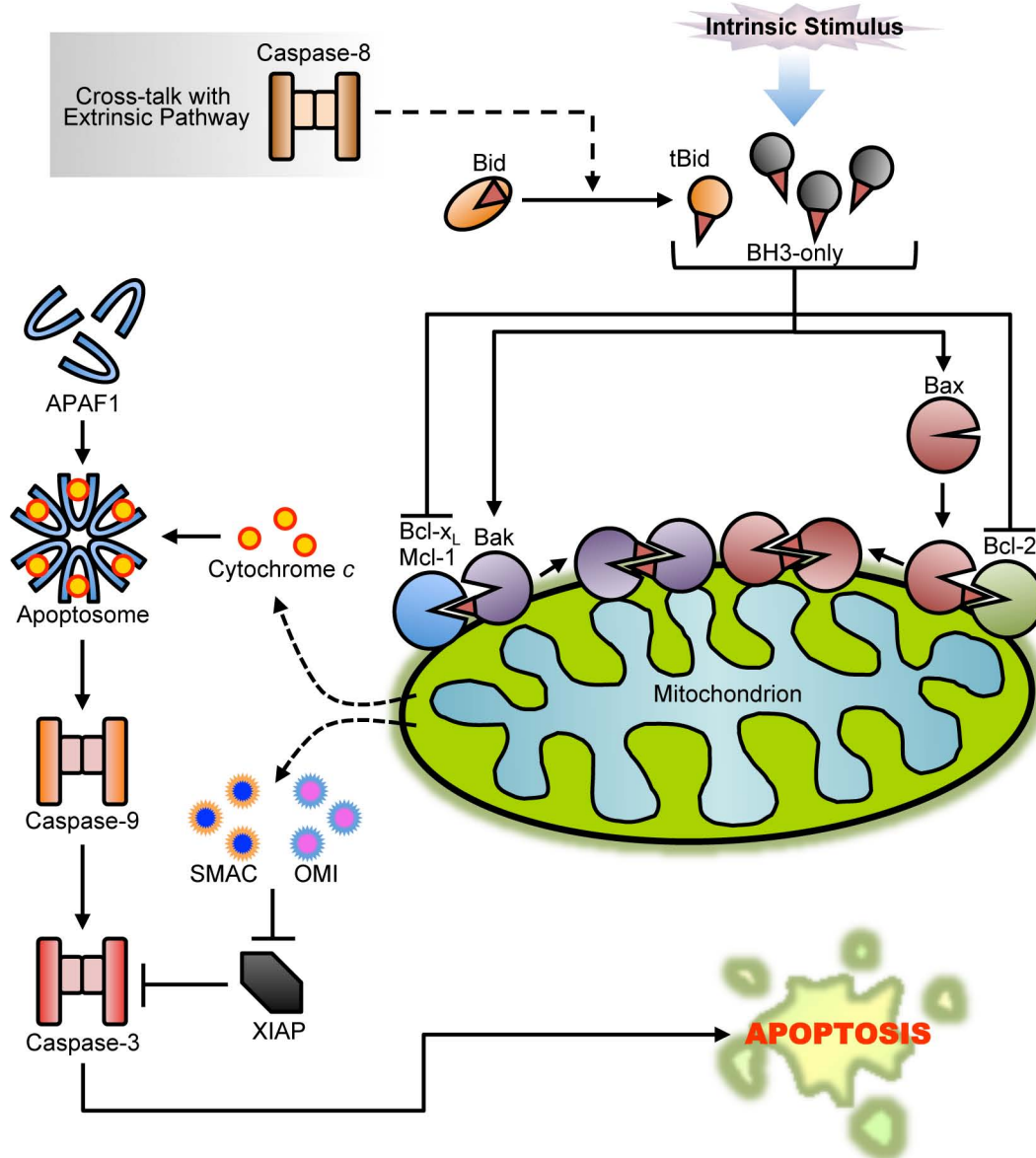


Figure 1.6. The intrinsic apoptotic pathway. The intrinsic apoptotic pathway begins with an intracellular stress that activates one or more of the BH3-only proteins. Once activated, BH3-only proteins inhibit the anti-apoptotic Bcl-2 family members and/or directly activate Bak and Bax. Following activation, Bak and Bax form homo-oligomers that destabilise the mitochondrial outer membrane and result in the release of cytochrome c, as well as SMAC and OMI. Cytochrome c complexes with APAF1 to form the apoptosome, which activates the initiator caspase-9. Caspase-9 goes on to cleave and activate caspase-3. SMAC and OMI promote the activation of caspase-3 and apoptosis by inhibiting the activity of XIAP, a cytoplasmic protein that inhibits caspase-3 activation. The intrinsic pathway is bisected by the extrinsic pathway with the caspase-8-mediated cleavage of the BH3-only protein Bid, which, once cleaved into its active form, tBid, can induce Bak and Bax activation (see Fig. 1.5).

domains (70, 204). Trimerisation of TNFR1 results in the initial recruitment of an additional adaptor protein, TNFR-associated death domain (TRADD), followed by the subsequent recruitment of FADD (71, 195, 196, 445). In addition to the death domain, FADD also possesses a “death effector domain” that interacts with a similar domain in the initiator caspases pro-caspase-8 or -10 (45). The recruitment of multiple pro-caspase-8/10 molecules to the death receptor complex results in caspase-8/10 auto-activation (321), and activated caspase-8/10 goes on to cleave effector caspases-3 and -7, which carry out the dismantling of the cell. Importantly, because activation of the TNFR receptor by TNF α also activates a pro-survival signalling pathway mediated by NF- κ B, protein synthesis must be inhibited for TNF α to effectively induce apoptosis (442).

On the other hand, the intrinsic apoptotic pathway is initiated following some sort of intracellular stress and requires the involvement of the mitochondria. The highly conserved Bcl-2 family of proteins is responsible for detecting these cellular stresses and subsequently liberating cytochrome *c* and other caspase-activating molecules from the mitochondria (75, 418, 483). A comprehensive review of the intrinsic pathway comprises the remainder of section 1.2.

Notably, cross-talk exists between the extrinsic and intrinsic pathways (Fig. 1.5 & 1.6). Besides cleaving and activating effector caspases, caspase-8 also cleaves the Bcl-2 family protein Bid (see section 1.2.5.3.) (275, 290). This cleaved form of Bid, known as truncated Bid (tBid), becomes myristoylated at its newly exposed N-terminus, resulting in its localisation to the mitochondria (491). At the mitochondria, tBid interacts with other Bcl-2 proteins to facilitate the release of cytochrome *c*, which then results in the activation of caspases.

1.2.4. Mitochondria and the release of cytochrome c. Mitochondria are typically thought of as the energy producing organelles of the cell, but they also play a critical role in the induction of apoptosis via the intrinsic pathway. Within the intermembrane space of the mitochondria is sequestered a pool of apoptogenic molecules that, when released into the cytoplasm, activate caspases and commit the cell to death (340). The release of these molecules occurs when the integrity of the mitochondrial outer membrane (MOM) is disrupted in a process known as mitochondrial outer membrane permeabilisation (MOMP) (418). MOMP is tightly regulated by the Bcl-2 family of proteins and is described, in detail, in section 1.2.7.

The most important apoptogenic molecule sequestered by the mitochondria is cytochrome *c*, a 15 kDa protein that, in healthy cells, forms part of the electron transport chain (340). Upon MOMP, however, cytochrome *c* is released from the intermembrane space of the mitochondria and into the cytosol, where it activates a signalling cascade that results in caspase activation (Fig. 1.6) (284). Cytochrome *c* binds to apoptotic protease-activating factor 1 (APAF1) and promotes a conformational change in APAF1 that results in its oligomerisation and the ATP-dependent assembly of a heptameric complex known as the “apoptosome” (238, 278). The apoptosome recruits the initiator pro-caspase-9 to the complex and assists in its auto-activation (278). Once activated, caspase-9 cleaves and activates the executioner caspases-3 and -7, thereby committing the cell to death (278). Cytochrome *c* is absolutely required for the activation of caspases following MOMP, and cells without cytochrome *c* do not undergo intrinsic apoptosis (276).

The induction of apoptosis by cytochrome *c* release can be effectively inhibited by the X-linked inhibitor of apoptosis (XIAP), a cytosolic protein that

inhibits caspases by binding to the active forms of caspases-9, -3, and -7 and directly inhibiting their activity (106, 124). Therefore, to counteract XIAP, two additional proteins are released from the mitochondrial intermembrane space upon MOMP. Second mitochondrial-derived activator of caspase (SMAC, also known as Diablo) and OMI (also known as HtrA2) bind to XIAP and prevent its ability to inactivate caspases (118, 181, 417, 448) (Fig. 1.6).

Importantly, the requirement for SMAC and OMI to antagonise XIAP discriminates between so-called type I and type II cells (221). Type I cells undergo apoptosis after the activation of the extrinsic death pathway, alone, and do not require the involvement of the intrinsic death pathway and MOMP. Conversely, type II cells, such as the HeLa cells used in this study, are unable to die solely by death receptor ligation. Type II cells require the caspase-8-mediated cleavage of Bid and the subsequent activation of the intrinsic pathway to release SMAC and OMI and overcome XIAP inhibition of caspases (472).

At least two other molecules, apoptosis-inducing factor (AIF) and endonuclease G, are also released from the intermembrane space upon MOMP, and both may contribute to caspase-independent cell death by mediating DNA cleavage (277, 415).

1.2.5. The Bcl-2 family of proteins regulates apoptosis. The integrity of the MOM and the release of cytochrome *c* is tightly regulated by the highly conserved B-cell lymphoma/leukaemia-2 (Bcl-2) family of proteins. The founding and prototypic member of this family, Bcl-2, was discovered over twenty years ago when the *Bcl-2* gene was found at the t(14;18) chromosomal translocation breakpoint in B-cell follicular lymphomas (20, 79, 347, 436, 437). The translocation of *Bcl-2* placed the gene under the control of the immunoglobulin

heavy chain gene promoter and enhancer on chromosome 14, resulting in Bcl-2 over-expression (394). The subsequent and novel discovery that Bcl-2 inhibited cell death—instead of promoting cellular proliferation—fundamentally changed the way oncogenesis was viewed (192, 302, 332, 446). Since then, the ranks of the Bcl-2 family have expanded dramatically to include both pro- and anti-apoptotic members that not only influence the development of cancer, but also play a critical role in almost all cellular apoptotic programmes, including the defence against pathogens.

Bcl-2 family members, whether pro-apoptotic or anti-apoptotic, are united by the presence of at least one of four highly conserved Bcl-2 homology (BH) domains (Fig. 1.7 & 1.8) (75, 483). The pro-apoptotic multi-domain proteins Bak and Bax possess BH domains 1-3, while the BH3-only proteins, a second subset of pro-apoptotic Bcl-2 proteins, possess, as their name implies, only a BH3 domain. Conversely, the anti-apoptotic multi-domain members of the Bcl-2 family, including Bcl-2 and Bcl-x_L, possess all four BH domains (Fig. 1.7). Many Bcl-2 family members, including all multi-domain proteins, also possess a hydrophobic C-terminal transmembrane (TM) domain that is required for their activity and responsible for targeting these proteins to the cytoplasmic face of many different intracellular membranes, such as the MOM (47, 281, 382).

Interestingly, structural analyses of several multi-domain Bcl-2 family members reveal strikingly similar α -helical structures for both the anti- and pro-apoptotic proteins (78, 99, 103, 191, 301, 314, 319, 351, 352, 416) (Fig. 1.9). Two predominantly hydrophobic α -helices (helix 5 and helix 6) form the core of all multi-domain Bcl-2 proteins, and these helices are surrounded by another six or seven amphipathic α -helices, depending on the protein. Certain α -helices comprise all or part of a BH domain, with helix 1 and 2 comprising the BH4 and

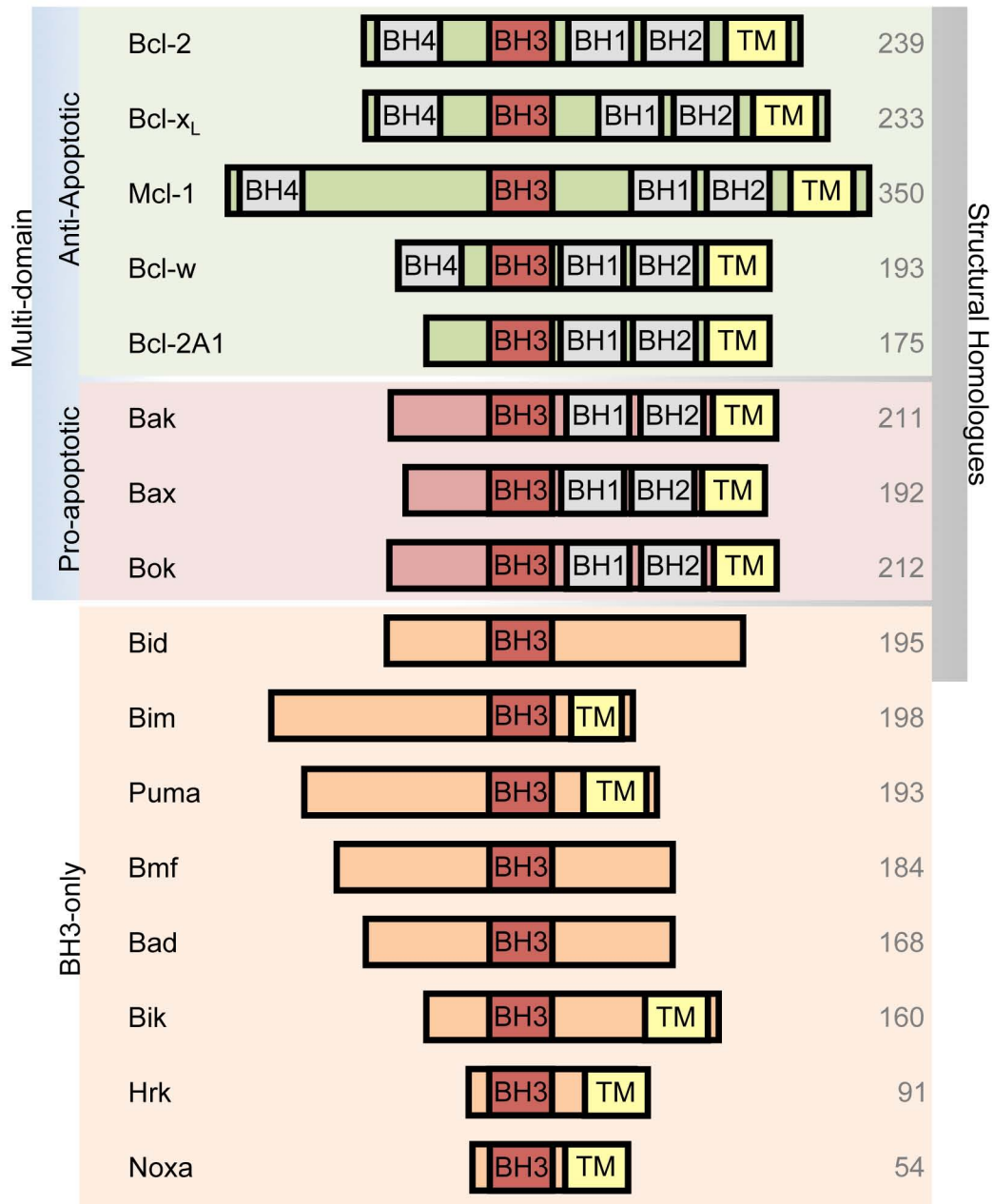


Figure 1.7. The Bcl-2 family of proteins. The Bcl-2 family can be divided into multi-domain anti-apoptotic members, multi-domain pro-apoptotic members, and BH3-only members. All members of the family are united by the presence of at least one Bcl-2 homology (BH) domain, and most members possess a C-terminal transmembrane (TM) tail. All of the multi-domain members and the BH3-only protein Bid are structurally homologous, whereas the remainder of the BH3-only proteins share only their BH3 domain in common with the Bcl-2 family (352). The number of amino acids of each protein is given to the right.

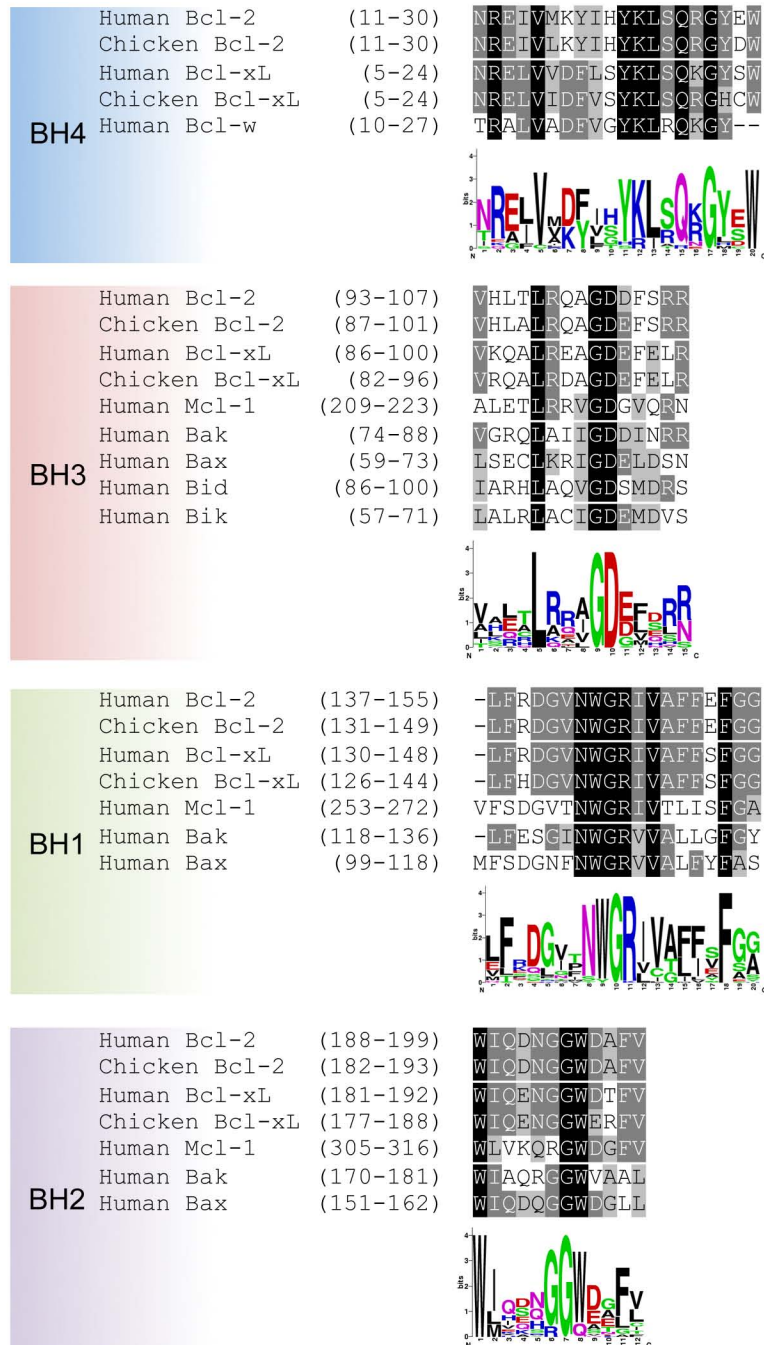


Figure 1.8. The BH domain sequences. BH domains are highly conserved among cellular Bcl-2 family members, as depicted in this alignment of BH domains from various human and chicken Bcl-2 proteins. Identical amino acids are highlighted in black and highly conserved amino acids are highlighted in dark grey. Amino acids similar to those that are highly conserved are highlighted in light grey with black text (AlignX). Sequence logos graphically depicting the conservation of each domain were obtained from PROSITE, where the height of each letter is proportional to the frequency with which it occurs in multiple aligned domains. The BH4, 3, 1, and 2 logos were generated from 19, 30, 44, and 47 hits, respectively, from the UniProtKB/Swiss-Prot database.

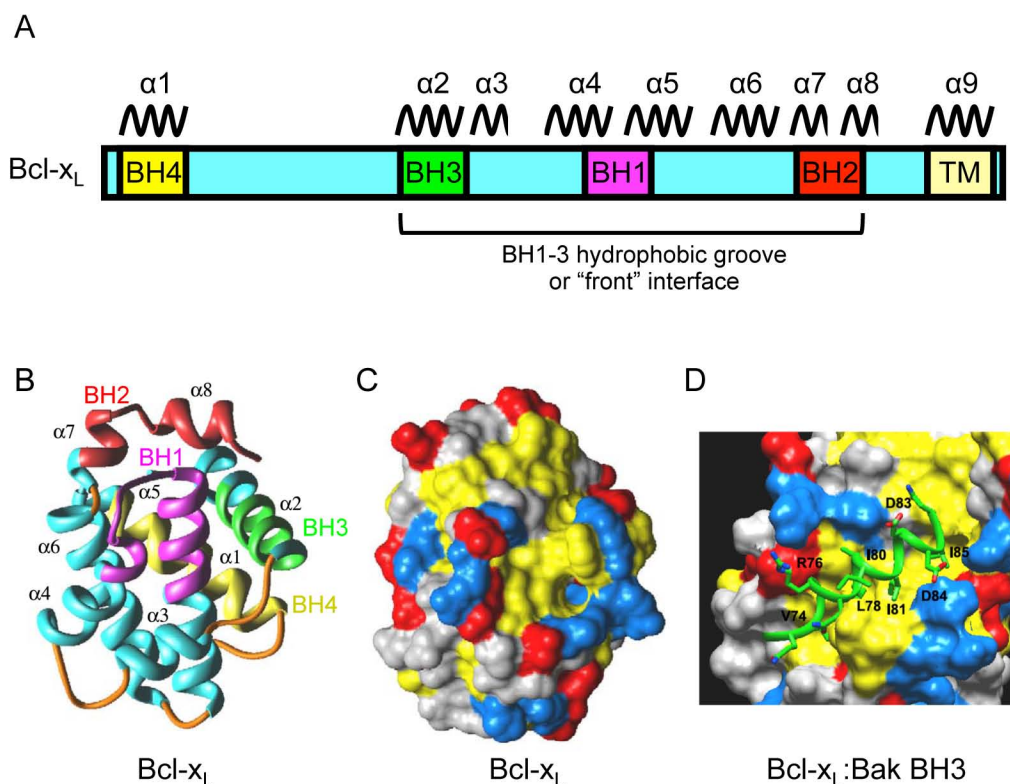


Figure 1.9. The structure of Bcl-2 proteins. (A) The 9 α -helices that comprise the Bcl- x_L protein structure are shown relative to the location of the Bcl-2 homology (BH) domains. The hydrophobic binding groove created by BH domains 1-3 is indicated. The structure of Bcl- x_L is representative of the other multi-domain Bcl-2 proteins (adapted from ref. 107). (B) A ribbon diagram depicting the structure of Bcl- x_L . All α -helices are indicated, with the exception of the transmembrane (TM) helix 9. The BH domains are colour coded to correspond with the diagram in (A) (adapted from ref. 352). (C) A surface representation of Bcl- x_L with leucine, valine, isoleucine, phenylalanine, tyrosine, tryptophan, methionine, and alanine coloured yellow; arginine, lysine, and histidine coloured blue; aspartic acid and glutamic acid coloured red; and all other amino acids coloured grey. The BH1-3 groove is comprised mainly of hydrophobic (yellow) residues (adapted from ref. 352). (D) A surface representation of the Bcl- x_L hydrophobic groove bound to a 16 amino acid peptide comprising the Bak BH3 domain (colour coded as in (C)). The Bak BH3 peptide binds as an amphipathic α -helix stabilised by hydrophobic contacts with Bcl- x_L (adapted from ref. 352).

BH3 domains, respectively; helices 4 and 5 comprising the BH1 domain; and helices 7 and 8 comprising the BH2 domain. A ninth helix forms the hydrophobic TM domain (Fig. 1.9A & B). The helices that make up BH domains 1-3 form a hydrophobic groove capable of binding the amphipathic BH3 α -helix of other Bcl-2 family members with high affinity, thus forming the basis for the homo- and heterotypic interactions that characterise the Bcl-2 family (Fig. 1.9C & D) (352). Indeed, the highly conserved BH domains, especially BH domains 1-3, are essential to the regulation of apoptosis by Bcl-2 family members (174, 482, 488). However, the realisation that several viruses encode structural, but not sequence, homologues of anti-apoptotic Bcl-2 proteins suggests that the overall structure of Bcl-2 proteins may be more functionally relevant than the presence of highly conserved BH domains (117, 251, 252). Ultimately, it is probably the structure of the Bcl-2 family of proteins, rather than the sequence, *per se*, that determines the co-operative and antagonistic interactions that occur among the members of this family and regulate the fate of the cell.

1.2.5.1. The pro-apoptotic multi-domain Bcl-2 proteins. The two most important members of the Bcl-2 family are arguably the pro-apoptotic multi-domain proteins Bcl-2 antagonist or killer (Bak) (76, 131) and Bcl-2-associated X protein (Bax) (338), which are required for the induction of apoptosis (483). In healthy cells, Bak is constitutively localised to the MOM and ER membranes by a C-terminal hydrophobic TM domain (163). Conversely, Bax exists as an inactive monomer in the cytoplasm or loosely bound to the MOM with its TM domain (helix 9) buried in the hydrophobic groove formed by BH domains 1-3 (416). Upon receipt of an apoptotic stimulus, Bax becomes activated and undergoes a conformational change that results in the extrusion of the TM domain, re-

localisation to the MOM, and insertion of the TM domain into the MOM to adopt a topology similar to that of Bak (156, 199, 200, 474). Additional conformational changes in both Bak and Bax result in their homo-oligomerisation, and these oligomers are thought to facilitate MOMP and allow the release of cytochrome *c* (10, 11, 126, 162, 163, 310, 311, 458). Mice deficient in either Bak or Bax, but not both, show limited developmental defects, and cells deficient in either protein are still able to undergo MOMP (282, 459, 502). However, mice lacking both Bak and Bax suffer severe developmental abnormalities and most die perinatally, while cells deficient in both of these proteins do not undergo MOMP or cytochrome *c* release and fail to die by numerous apoptotic stimuli (282, 459, 502). Together these data demonstrate that Bak and Bax are absolutely required for apoptosis by the intrinsic pathway, and they suggest that Bak and Bax may function redundantly. Another pro-apoptotic multi-domain protein, Bok (also known as Mtd), has also been identified, although its activity and relevance are not well characterised and appear to be limited to the ovaries, testes, and uterus (142, 197, 212).

1.2.5.2. The anti-apoptotic multi-domain Bcl-2 proteins. Bak and Bax are held in check, in part, by the anti-apoptotic multi-domain Bcl-2 proteins, of which Bcl-2, Bcl-2-like protein x large isoform (Bcl-x_L) (44), and myeloid cell leukaemia sequence 1 (Mcl-1) (247) are the best described. Similar to Bak, Bcl-2 is constitutively localised to the ER, nuclear membrane, and MOM by a C-terminal TM domain, whereas Mcl-1 localises predominantly to the MOM (5, 283, 327, 480). Bcl-x_L, on the other hand, is predominantly cytosolic in healthy cells, with its TM domain sequestered within the BH1-3 groove (219). Upon apoptotic stimulus, Bcl-x_L becomes activated, resulting in the exposure of the TM domain

and re-localisation to the MOM (199). At the mitochondria and upon the induction of apoptosis, Bcl-2 and Bcl-x_L undergo additional conformational changes and, along with Mcl-1, inhibit apoptosis by interacting with and inactivating Bak, Bax, and the BH3-only proteins (75, 483). Interestingly, the anti-apoptotic multi-domain protein, Bcl-w, exists in the cytoplasm of healthy cells; however, its anti-apoptotic activity is negatively correlated with its integration into the MOM upon induction of apoptosis (147, 473). Nonetheless, the activity of Bcl-w, as well as Bcl-2A1 (also known as A1 and Bfl-1) (77, 280), Bcl-B (229), and Boo/Diva (213, 405), the only other anti-apoptotic, multi-domain Bcl-2 proteins described to date, remains relatively poorly characterised.

1.2.5.3. The BH3-only proteins. Both the pro- and anti-apoptotic multi-domain Bcl-2 proteins are regulated by the third subset of Bcl-2 family proteins, the BH3-only proteins (287). Although there have been numerous and varied proteins identified with a BH3 domain, only eight of them are typically considered to be among the “core” BH3-only proteins directly involved in the induction of apoptosis: BH3-interacting domain death agonist (Bid) (452), Bcl-2-interacting mediator of cell death (Bim) (198, 333), Bcl-2 antagonist of cell death (Bad) (479), Bcl-2-interacting killer (Bik) (49, 173), Bcl-2 modifying factor (Bmf) (359), Noxa (also known as PMAIP1) (334), p53-upregulated modulator of apoptosis (Puma) (169, 323, 484), and harakiri (Hrk) (209, 211). With the exception of Bid, which is structurally homologous to the multi-domain Bcl-2 proteins (78, 301), BH3-only proteins are diverse and related to each other and other Bcl-2 proteins only through the conserved BH3 domain (287).

BH3-only proteins reside in the cytoplasm of healthy cells until they are activated, either transcriptionally or post-translationally, by a variety of stimuli to

induce apoptosis (75). For example, Bim is upregulated in response to growth factor deprivation (112), whereas Puma is upregulated in a p53-dependent manner in response to DNA damage (169, 323, 484). Bad is activated post-translationally by phosphorylation in response to growth factor deprivation (490), whereas Bid is cleaved and activated by caspase-8 (275, 290). Importantly, Noxa is upregulated in response to infection by a number of viruses, and it can be post-translationally activated by dsRNA (for further discussion see section 1.4.1.) (157, 257, 413). Indeed, BH3-only proteins are responsive and highly attuned to a variety of cellular stresses, most of which we have yet to identify. Regardless, once activated, BH3-only proteins induce apoptosis by activating Bak and Bax or inhibiting the anti-apoptotic Bcl-2 proteins (146). The fact that each BH3-only protein interacts with only a specific subset of multi-domain pro- and anti-apoptotic Bcl-2 proteins plays a significant (and contentious) role in the activation of Bak and Bax (73).

1.2.5.4. Bcl-2 proteins are evolutionarily conserved. The Bcl-2 family of proteins is highly conserved, and orthologues have been identified in all metazoans analysed to date (12). In fact, the marine sponges *Geodia cydonium* and *Suberites domuncula* both encode proteins with obvious BH1 and BH2 domains, suggesting that the regulation of apoptosis by Bcl-2 family members is conserved even to the lowest metazoan phylum (464). Bcl-2-like genes have also been identified in fishes, including zebrafish and pufferfish; insects, including the fruitfly *Drosophila melanogaster*; and worms, such as the nematode *Caenorhabditis elegans* (12). In fact, Robert Horvitz shared the 2002 Nobel Prize in Physiology or Medicine for his part in the elucidation of the *C. elegans* apoptotic programme, which included the discovery of the anti-apoptotic Bcl-2

orthologue Ced-9 and the BH3-only orthologue EGL-1 (87, 184-186). Furthermore, the initial genome sequence of the chicken (*Gallus gallus*), the natural host of fowlpox virus, revealed the presence of numerous Bcl-2 orthologues, including Bcl-2- and Bcl-x_L-like proteins, a Bak-like protein, and several BH3-only proteins, of which Bmf and Bid have already been characterised (12, 88, 111, 154). The absence of a Bax-like gene in chickens is peculiar but may reflect the incompletely annotated state of the chicken genome (12). Additionally, several viruses have co-opted Bcl-2-like proteins to inhibit apoptosis during virus infection, and some of these are discussed in more detail in section 1.3. It is clear from their extraordinary evolutionary conservation among all multi-cellular organisms that the Bcl-2 proteins represent an ancient and important mechanism for regulating cell death.

1.2.6. The activation of Bak and Bax. Because Bak and Bax are the critical determinants of cell fate, understanding the molecular details that govern their activity is paramount to understanding apoptosis. Unfortunately, the events leading to the activation of Bak and Bax and, ultimately, the permeabilisation of the MOM are complex and have proven difficult to examine empirically. Although it has been known for several years that MOMP and the release of cytochrome *c* is associated with conformational changes in Bak and Bax and the subsequent homo-oligomerisation of both proteins (163, 200, 246, 324, 458), precisely how Bak and Bax are induced to undergo those conformational changes and how those changes lead to MOMP is not well understood. Moreover, our understanding of the interactions that occur among Bcl-2 family members is relatively detailed but often contradictory, making it difficult to demonstrate or infer the functional consequences of these interactions (73, 483). Indeed, a

thorough understanding of the mechanism behind Bak and Bax activation has been deemed the “holy grail” of apoptosis research, and the field is still anticipating its discovery (483).

Several models have been proposed to account for the regulation of apoptosis by Bak and Bax. Well over a decade ago, Korsmeyer and colleagues proposed the original “rheostat” model, suggesting that the ability of Bcl-2 to interact with and inhibit Bax (and therefore prevent apoptosis) was regulated by the relative amounts of each protein (245). Since then the situation has grown more complex. Many of the very early assessments of interaction between Bcl-2 proteins were confounded by the use of detergents that have subsequently been shown to artificially induce interactions between these proteins (200, 201), and the activation of Bax, in particular, is complicated by the finding that, in healthy cells, it exists as a largely cytosolic monomer, whereas Bcl-2 is tethered to intracellular membranes (200, 201). At least for the regulation of Bax, it is now accepted that Bax does not interact with anti-apoptotic Bcl-2 proteins, including Bcl-2, in healthy cells (115, 240). On the other hand, Bak, which is localised to the MOM, probably constitutively interacts with the anti-apoptotic Bcl-2 proteins Mcl-1 and Bcl-x_L until receipt of an apoptotic stimulus (94, 470). However, following such an apoptotic stimulus, conformational changes in several Bcl-2 family proteins, including Bak and Bax, may significantly alter their interaction partners. Additionally, the demonstration that BH3-only proteins control apoptosis by differentially interacting with Bak and Bax as well as the anti-apoptotic Bcl-2 family members has further confused our understanding of Bak and Bax activation (73).

1.2.6.1. The indirect and direct models of Bak and Bax activation. Recently, in light of the diversity of current data, two competing models have been postulated to explain the phenomenon of Bak and Bax activation. The “indirect activation” (also known as the “displacement” or “derepression”) model and the “direct activation” model both attempt to describe the events leading to Bak- and Bax-mediated MOMP based on contradictory evidence regarding the inherent activation state of Bak and Bax and the functional outcome of the interactions observed among Bcl-2 proteins (Fig. 1.10). It is well established that BH3-only proteins depend on the presence of Bak and Bax to induce apoptosis, suggesting that the pro-apoptotic activity of BH3-only proteins is functionally linked to Bak and Bax (502). It is also established that different BH3-only proteins interact with different anti-apoptotic Bcl-2 family members with varying degrees of affinity: Bim, tBid, and possibly Puma interact with all anti-apoptotic Bcl-2 proteins (Bcl-2, Bcl-x_L, Bcl-w, Bcl-2A1, and Mcl-1), whereas Bad and Bmf interact with Bcl-2, Bcl-x_L, and Bcl-w; Bik and Hrk interact with Bcl-x_L, Bcl-w, and Bcl-2A1; and Noxa interacts with only Bcl-2A1 and Mcl-1 (Fig. 1.11) (56, 64, 249, 271). Importantly, the interactions between these anti-apoptotic Bcl-2 proteins and BH3-only proteins correlate with an inhibition of apoptosis (56, 64, 69, 249, 271, 471). However, exactly how these interactions regulate the activation of Bak and Bax and the induction of apoptosis is a major point of contention between the indirect and direct models.

The indirect activation model proposes that BH3-only proteins indirectly promote apoptosis by interacting with anti-apoptotic Bcl-2 proteins to displace Bak and Bax, which, the model suggests, are inherently active and able to oligomerise and permeabilise the MOM upon their displacement (Fig. 1.10) (262, 469). Only when all anti-apoptotic Bcl-2 proteins are inhibited by BH3-only

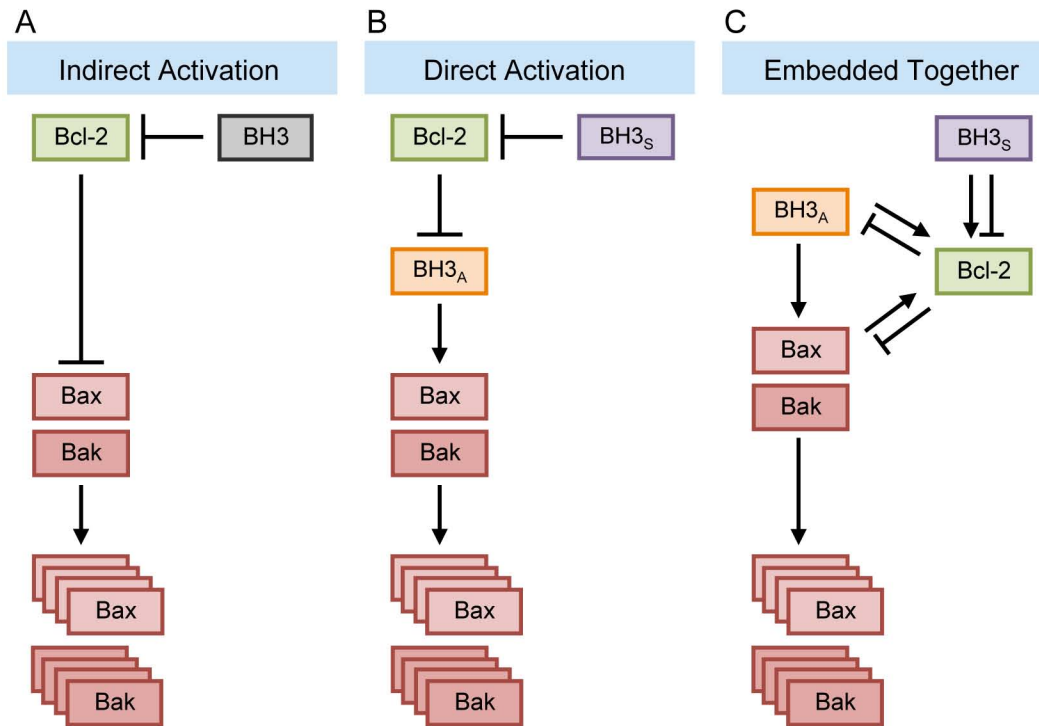


Figure 1.10. Proposed models describing Bak/Bax activation. (A) The indirect activation model proposes that BH3-only proteins bind to anti-apoptotic Bcl-2 family members and cause the release of Bak/Bax, which are then able to oligomerise and induce MOMP without any further activation. (B) The direct activation model divides BH3-only proteins into sensitiser (BH3_s) and activator (BH3_a) sub-classes. Sensitiser BH3-only proteins bind anti-apoptotic Bcl-2 family members and cause the release of activator BH3-only proteins, which are then able to bind and directly activate Bak/Bax. (C) The embedded together model emphasises the critical role that the MOM plays in the activation of Bcl-2 proteins and incorporates aspects of both the indirect and direct models. Like the direct model, sensitiser BH3-only proteins are proposed to bind anti-apoptotic Bcl-2 family members and cause the release of activator BH3-only proteins, which then activate Bak/Bax. Like the indirect model, anti-apoptotic Bcl-2 proteins are also capable of interacting with and inactivating Bak/Bax. Additionally, the BH3-only proteins and Bak/Bax are proposed to play a role in activating the anti-apoptotic Bcl-2 family members. (Note that “Bcl-2” is representative of all anti-apoptotic Bcl-2 proteins).

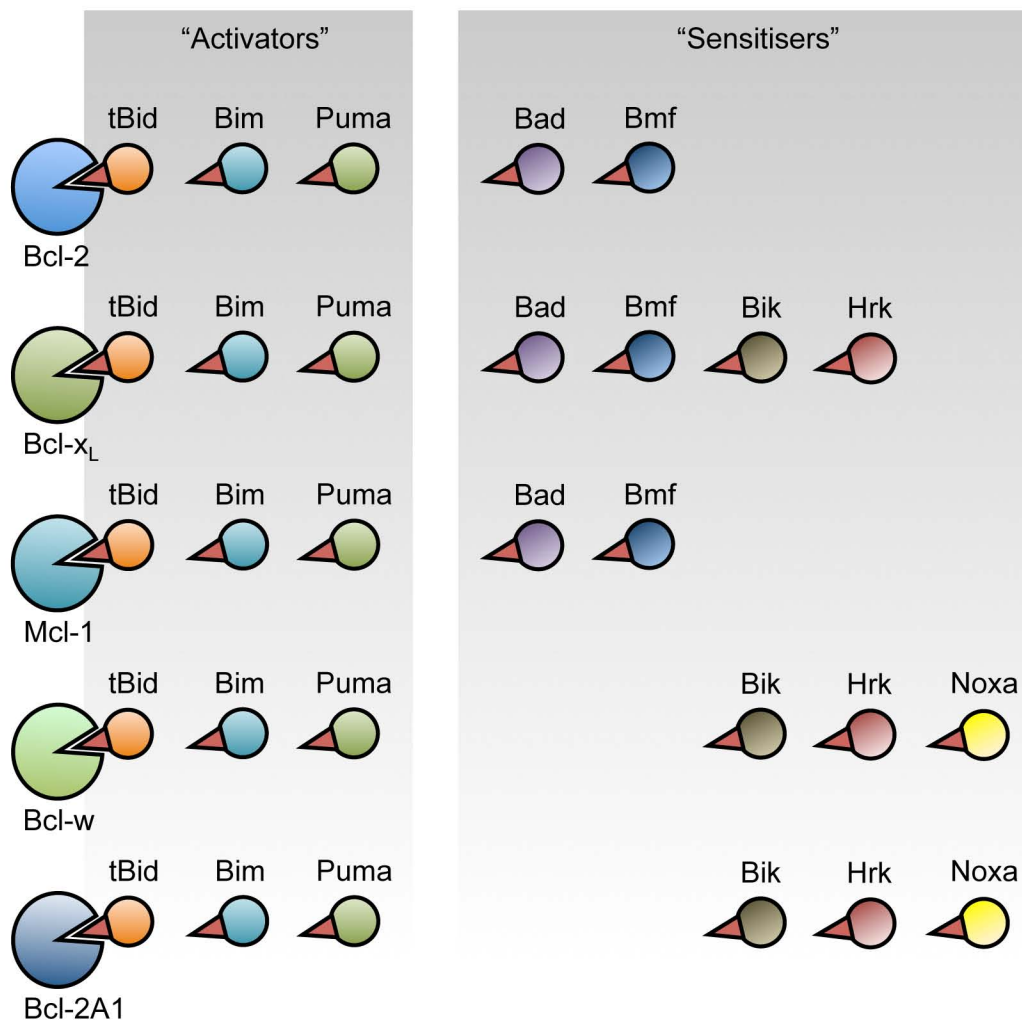


Figure 1.11. BH3-only proteins inhibit the anti-apoptotic Bcl-2 family members. BH3-only proteins possess a differential ability to interact with and inhibit the anti-apoptotic Bcl-2 proteins. Although the BH3-only proteins can be classified as "activators" or "sensitisers" based on their ability to interact with and activate Bak and Bax (see Fig. 1.12), this classification also correlates with their ability to neutralise the anti-apoptotic Bcl-2 proteins. The activator BH3-only proteins, tBid, Bim, and Puma, bind and neutralise all five anti-apoptotic Bcl-2 proteins, whereas the sensitizer BH3-only proteins each bind and neutralise a discrete subset. The indirect model of apoptosis proposes that BH3-only proteins function exclusively by binding and neutralising the anti-apoptotic Bcl-2 family members as depicted here.

proteins will Bak and Bax be free to induce apoptosis (441, 471). However, because the interactions between BH3-only proteins and anti-apoptotic Bcl-2 proteins vary, certain BH3-only proteins, such as Bim and tBid, which interact with all anti-apoptotic Bcl-2 proteins to displace Bak and Bax, are predicted to be more potent at inducing apoptosis than other BH3-only proteins, such as Noxa and Bad, which interact with only a subset of anti-apoptotic Bcl-2 proteins (Fig. 1.11). Thus, in certain cases, multiple BH3-only proteins may be required to release Bak and Bax from repression by all anti-apoptotic Bcl-2 proteins (470).

Conversely, the direct activation model asserts that Bak and Bax are inherently inactive, unbound by anti-apoptotic Bcl-2 proteins, and must be directly activated by certain BH3-only proteins before oligomerising and permeabilising the MOM (Fig. 1.10). This model divides BH3-only proteins into two functional groups: the activators and the sensitisers. Upon an apoptotic stimulus, the sensitiser BH3-only proteins, Bik, Hrk, Bad, Bmf, and Noxa, bind to the anti-apoptotic Bcl-2 proteins and, instead of displacing Bak and Bax, displace the activator BH3-only proteins, Bim, tBid, and Puma (Fig. 1.12) (236, 237, 289). The activator proteins are then free to bind and activate Bak and Bax (104, 236, 237, 250, 271, 289, 458). Unlike the interactions between BH3-only proteins and the anti-apoptotic Bcl-2 proteins, interactions between activator BH3-only proteins and Bak and Bax have been typically difficult to detect. This has led to the “hit-and-run” hypothesis, whereby activator BH3-only proteins are predicted to transiently interact with and, in so doing, activate Bak and Bax before dissociating and moving on to activate additional Bak and Bax molecules. Nonetheless, activating interactions between Bax and chemically stabilised Bim and Bid BH3 domains have been demonstrated (144, 449), and, more recently, full-length tBid, Bim, and Puma have been shown to bind Bak and Bax and drive

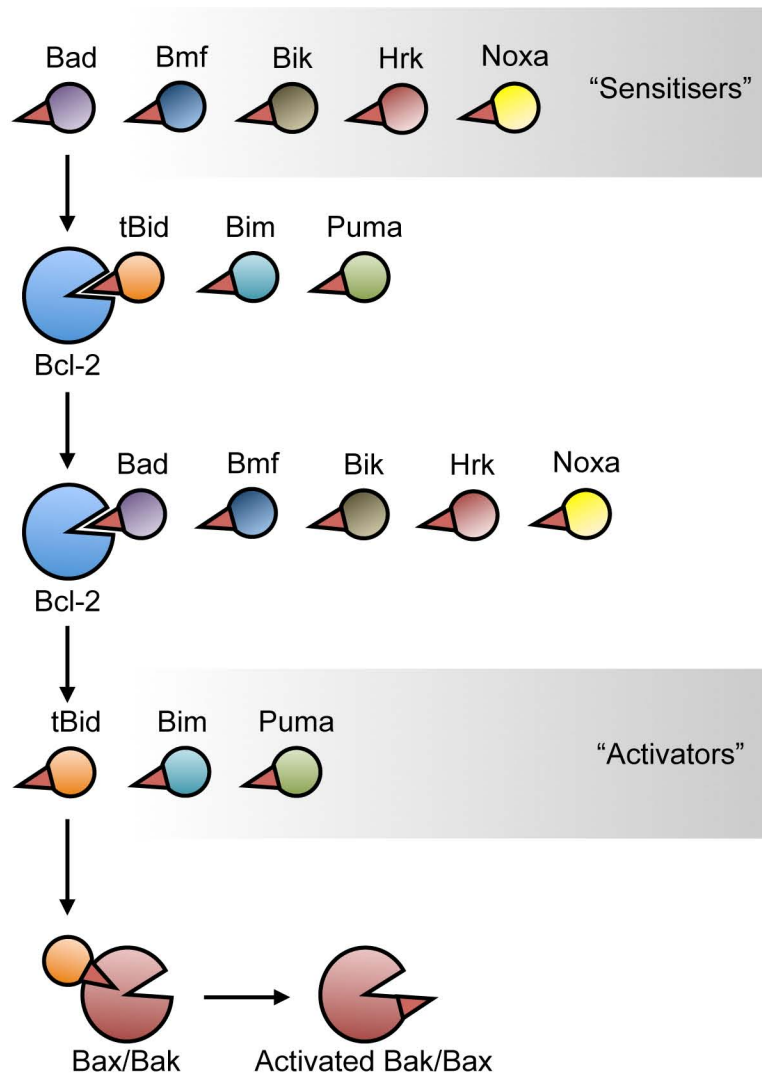


Fig. 1.12. BH3-only proteins directly activate Bak and Bax. BH3-only proteins can be classified as "activators" or "sensitisers" based on their ability to bind and activate Bak and Bax. The direct model of apoptosis proposes that sensitizer BH3-only proteins bind to the anti-apoptotic Bcl-2 proteins to displace the activator BH3-only proteins, tBid, Bim, and Puma. The activator BH3-only proteins would then be free to bind and activate Bak and Bax.

their homo-oligomerisation (237). More recent data has confused the distinction between activator and sensitiser proteins, suggesting that all BH3-only proteins can act as sensitisers to release other BH3-only proteins from repression by anti-apoptotic Bcl-2 family members and all BH3-only proteins can act, with varying degrees of potency, as direct activators (119, 249).

1.2.6.2. The embedded together model of Bak and Bax activation. Despite the abundance of data for both the indirect and direct models, neither sufficiently addresses the mechanism of Bak and Bax activation. In fact, it is likely that aspects of both the indirect and direct models are correct, or at least that aspects of both models hold true under different cellular circumstances (249, 308). In an effort to reconcile the indirect and direct models and incorporate experimental evidence not considered by either, David Andrews and colleagues proposed a third model for Bak and Bax activation known as the “embedded together” model (Fig. 1.10) (43, 262, 263). The embedded together model emphasises the critical role that membranes play in the structural conformations of Bcl-2 proteins and how these conformations influence the interactions that occur among Bcl-2 family members. In healthy cells, Bcl-2 is tethered to the ER and MOM solely by helix 9, which comprises the C-terminal transmembrane domain (65, 217). However, upon stimulation with tBid or the Bim BH3 peptide, Bcl-2 undergoes a major conformational change that results in the insertion of helices 5 and 6 into the membrane (115, 240). Similarly, after the insertion of its transmembrane domain (helix 9), but before homo-oligomerisation, Bax also undergoes a conformational change that results in the insertion of helices 5 and 6 into the MOM (8, 481). Interestingly, this conformational change in Bcl-2 to a so-called “multi-spanning monomer” is a pre-requisite for its ability to interact with a multi-spanning

monomer of Bax and inhibit Bax homo-oligomerisation (115). The embedded together model also integrates the indirect and direct models to postulate that the anti-apoptotic Bcl-2 proteins interact with and inhibit the activity of both BH3-only proteins and Bak and Bax. The model goes further to suggest that BH3-only proteins can both inhibit and activate the anti-apoptotic Bcl-2 proteins. Indeed, tBid has been shown to rapidly bind membranes where it then recruits and activates both Bax and Bcl-x_L (39, 289). Bcl-x_L binds to tBid to prevent the additional recruitment and activation of Bax, and it binds to tBid-activated Bax to prevent Bax homo-oligomerisation and apoptosis (39). Conversely, the BH3-only protein Bad binds Bcl-x_L to release tBid and allow tBid to activate Bax (289).

1.2.6.3. A unified picture of Bak and Bax activation? The precise molecular mechanisms that regulate Bak and Bax activation, and, therefore, the commitment to cell death, have yet to be completely elucidated. However, the last decade has nonetheless seen a tremendous increase in our basic understanding of the functional interactions, chronology, and kinetics that regulate the Bcl-2 family of proteins and govern cellular fate. We are at the point, now, where we can begin to describe the basic biochemical pathway that leads from an apoptotic signal through the activation of Bak and Bax to MOMP and the execution of the cell (Fig. 1.13).

Upon receipt of an apoptotic stimulus, BH3-only proteins, the sentinels of the cell, become transcriptionally or post-translationally activated (287). Once activated, the so-called activator BH3-only proteins, Bim, tBid, Puma, and perhaps others, bind to and activate Bax (Fig. 1.12) (104, 119, 236, 237, 249, 271). In the case of tBid, activation results in its rapid relocalisation to the MOM, from where it recruits and activates Bax, which is likely loosely associated with

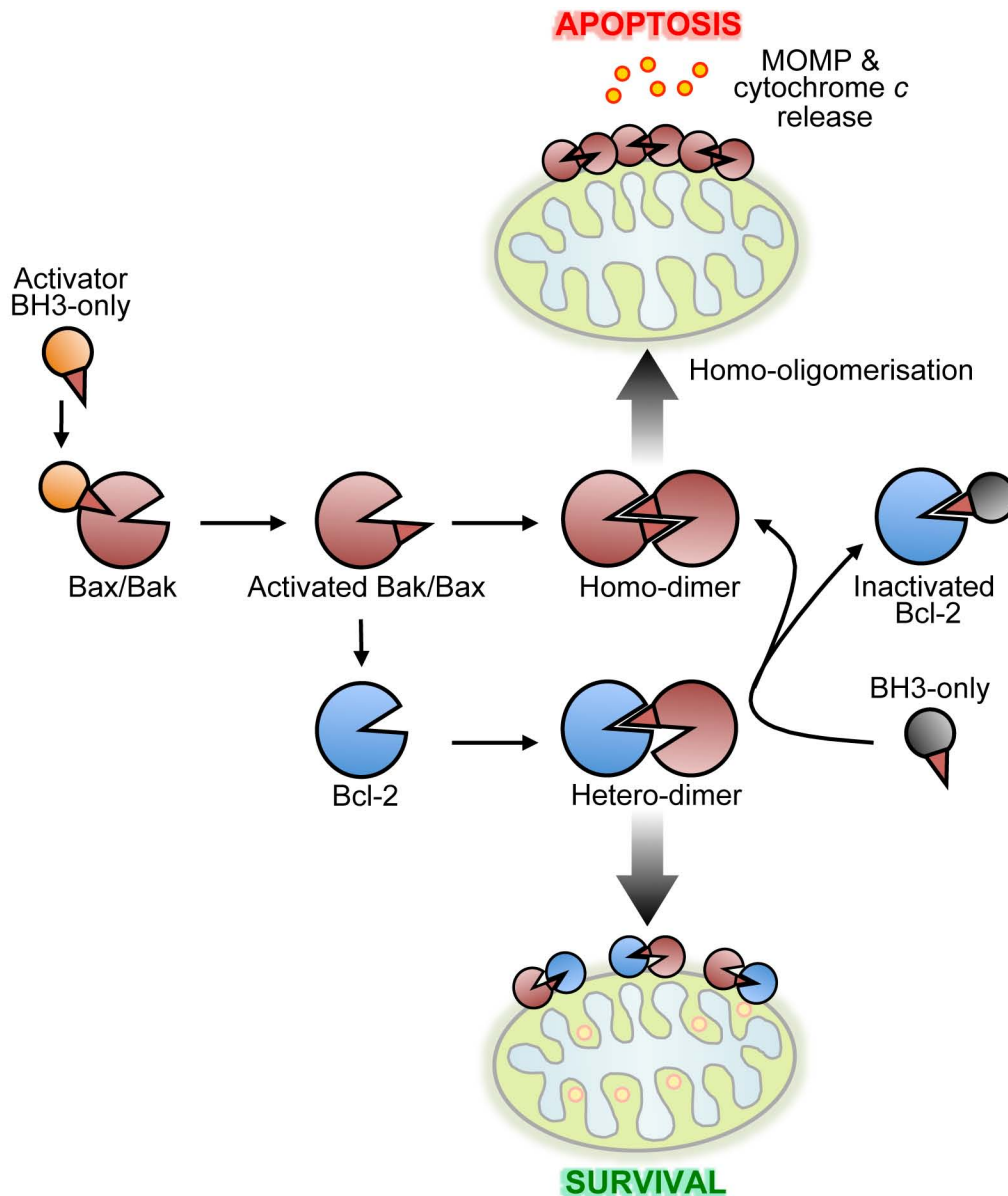


Fig. 1.13. The regulation of apoptosis by Bcl-2 family proteins. In healthy cells Bak and Bax reside as inactive monomers. Upon receipt of an apoptotic stimulus, activator BH3-only proteins interact with Bak/Bax at the rear interface (Fig. 1.12), inducing a series of conformational changes that result in Bak/Bax activation. Active Bak/Bax forms symmetric homo-dimers via the front interface that then interact with other dimers via the rear interface to nucleate the formation of Bak/Bax oligomers (Fig. 1.14), leading to mitochondrial outer membrane permeabilisation and apoptosis. Bcl-2 and other anti-apoptotic Bcl-2 family members interact with active Bak/Bax to form oligomerisation-incompetent hetero-dimers or trimers (Fig. 1.14), facilitating the survival of the cell. BH3-only proteins can also bind anti-apoptotic Bcl-2 proteins to release activator BH3-only proteins (as in Fig. 1.12), or they may bind anti-apoptotic Bcl-2 proteins to release Bak/Bax from repression and allow Bak/Bax homo-oligomerisation and apoptosis. The ability of anti-apoptotic Bcl-2 proteins to inactivate Bak/Bax depends largely on their sequestration of activator BH3-only proteins and active Bak/Bax.

the MOM (289). Whether Bim and Puma also rapidly relocate to the MOM before they activate Bax remains to be determined. Bim, tBid, and Puma bind via their BH3 domains to a recently characterised “rear” interface on Bax composed of helices 1 and 6 and the loop region between helices 1 and 2 (Fig. 1.14) (55, 96, 144, 160, 237). This binding initiates a conformational change in Bax that results in the extrusion of helix 9, the TM helix, from the hydrophobic BH1-3 groove, also referred to as the “front” interface (42, 144, 156, 199, 474, 497). Current evidence suggests that BH3-only binding to the rear interface of Bax is reversible and that once a BH3-only protein initiates a conformational change in Bax it can dissociate and continue to activate additional Bax monomers in a catalytic fashion (42, 497). Regardless, Bax helix 9 inserts into the MOM, and this insertion into the membrane is associated with a conformational change that exposes an N-terminal domain and a subsequent conformational change of Bax into a multi-spanning monomer (8, 440). Upon extrusion of helix 9 and integration into the membrane, the BH1-3 domains of the Bax front interface become exposed, allowing the now-accessible Bax BH3 domain to interact with the rear interface of another inactive Bax monomer and activate it, much like a BH3-only protein would, in an amplification process termed auto-activation (420, 497). Once two Bax molecules become activated, they interact with each other at their front interfaces to form a symmetrical dimer wherein the BH3 domain of one Bax fills the hydrophobic cleft created by the BH1-3 domains of the second Bax, and *vice versa* (Fig. 1.14) (42, 145, 237, 497). The formation of this front:front dimer is then proposed to alter the conformation of the rear interface and permit a rear:rear interaction with another Bax dimer (497). In this way, two Bax dimers generate a tetramer that can then propagate into an oligomer (497), and oligomerisation is both necessary and

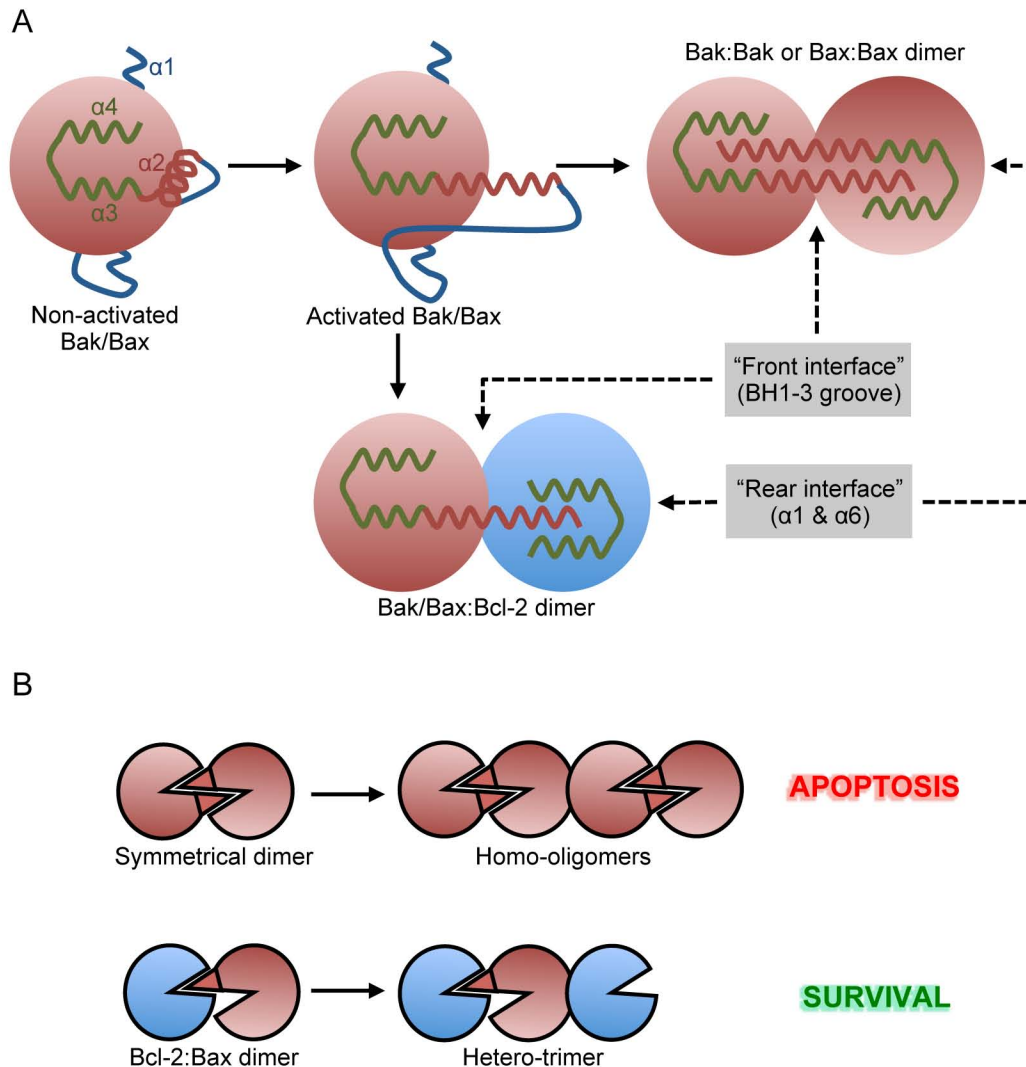


Figure 1.14. Bcl-2 protein interactions. (A) Upon the activation of Bak/Bax, the BH3 domain ($\alpha 2$) is extruded and the hydrophobic BH1-3 groove or "front interface" ($\alpha 4$ and $\alpha 3$) is exposed. Interaction between two activated Bak or two activated Bax monomers involves the reciprocal binding of the exposed BH3 domain of one Bak/Bax monomer in the BH1-3 groove of the other monomer and *vice versa* to form a symmetrical dimer. Interaction between Bak/Bax and an anti-apoptotic Bcl-2 protein is similar except that the anti-apoptotic Bcl-2 protein does not contribute its BH3 domain to binding the Bak/Bax hydrophobic groove. (B) Symmetrical Bak/Bax dimers interact with each other via the rear interface (comprised of $\alpha 1$ and $\alpha 6$) to nucleate the formation of homo-oligomers and induce MOMP. Anti-apoptotic Bcl-2 protein and Bak/Bax hetero-dimers may form hetero-trimers via the rear interface of Bcl-2 and Bak/Bax. Both hetero-dimers and -trimers are unable to oligomerise and serve to inactivate Bak/Bax, thereby preventing MOMP. (Adapted from ref. 109).

sufficient for Bax to induce apoptosis (Fig. 1.13) (10, 11, 145). Our understanding of Bax activation has been informed and confirmed by the experimental evidence for the activation of the closely related protein Bak. Intriguingly, the activation processes for both proteins is nearly identical. Bim, tBid, and Puma bind to a rear pocket on Bak to initiate a similar series of conformational changes that result in the formation of symmetrical Bak dimers that form tetramers via a rear:rear interaction and ultimately nucleate homo-oligomerisation (108, 109, 236, 237, 335). However, because Bak is constitutively integrated into the MOM by helix 9, its regulation is necessarily less complex and its killing kinetics quicker than Bax (237).

Anti-apoptotic Bcl-2 proteins inhibit apoptosis by directly interacting with Bak and Bax to prevent their homo-oligomerisation and by interacting with and sequestering BH3-only proteins (Fig. 1.13). Upon activation of Bcl-2 by certain BH3-only proteins and perhaps active Bax, Bcl-2 changes conformation to a multi-spanning monomer and becomes competent to interact with and inhibit the activity of activated Bax (115, 240). This interaction occurs both the canonical way, via the BH3 domain of Bax and the front interface (BH1-3 groove) of Bcl-2, and via a rear:rear interface involving helices 1 and 6 of both Bax and Bcl-2, in a manner analogous to the homo-dimerisation and tetramerisation of both Bax and Bak (Fig. 1.14) (113, 248). The resulting Bcl-2:Bax:Bcl-2 hetero-trimers cannot stably form higher-order oligomers, suggesting that Bcl-2 functions as a defective Bax-like protomer (113, 115). Moreover, Bcl-x_L appears to inhibit Bax activity by functioning as a dominant-negative Bax (39, 104). In cells undergoing apoptosis, Bcl-x_L competes with activated Bax for binding to tBid and both inactive and active Bax; as a result, Bcl-x_L prevents Bax from binding to membranes and oligomerising. Conversely, in healthy cells Bak interacts with Bcl-x_L and Mcl-1

(94, 470), and, during apoptosis, this interaction is displaced by the BH3-only proteins Noxa, Bim, and Bik, leaving Bak free to induce apoptosis (397, 470). The ability of Mcl-1 to inhibit Bak activity also appears to be regulated by ubiquitination, which, upon the induction of apoptosis, targets Mcl-1 for rapid proteasomal degradation (94, 328). Additionally, upon activation of Bak during apoptosis, Bak interacts with and is inhibited by Bcl-2, possibly in a manner analogous to Bcl-2 and Bax (375).

The regulation of Bak and Bax by the anti-apoptotic Bcl-2 proteins is further controlled by the BH3-only proteins. In some instances, so-called sensitiser BH3-only proteins can bind and inhibit the anti-apoptotic Bcl-2 proteins to release activator BH3-only proteins that can then provoke the activation of Bak and Bax (Fig. 1.12) (236, 289). As mentioned, BH3-only proteins also exert a pro-apoptotic effect by instigating the release of activated Bak and Bax from inhibitory interactions with anti-apoptotic Bcl-2 family members (Figs. 1.11 & 1.13) (249, 397, 470).

1.2.6.4. The alternative regulation and function of Bcl-2 family proteins.

Despite the advances in our understanding of Bak and Bax regulation, it is important to appreciate that the Bcl-2 family of proteins do not function in a vacuum. Many of the studies that have elucidated the basic pathway to Bak and Bax activation described above were performed using contrived systems involving isolated mitochondria, synthetic membranes, and only specific, often mutated, Bcl-2 proteins. Indeed, the activation of Bak and Bax is probably influenced by numerous proteins and other factors not related to the core Bcl-2 family of proteins discussed above. For example, the transcription factor p53, which lacks any discernible homology to Bcl-2 family proteins, may interact with

and activate both Bak and Bax (74, 272), whereas interferon regulatory factor 3 (IRF3), another transcription factor, has recently been shown to possess a degenerate BH3 domain and interact with Bax to activate it in response to virus infection (60). Another protein with a degenerate BH3 domain, MOAP-1, also appears to directly promote the activation of Bax following death receptor stimulation (21, 421, 422). Even non-protein factors such as heat and intracellular pH have been shown to directly activate Bak and Bax (233, 343). Conversely, some non-Bcl-2 family proteins may prevent the activation of Bak and Bax. Humanin, for example, interacts with and inactivates Bax (166), while the voltage dependent anion channel isoform 2 (VDAC2) has been shown to interact with Bak and sequester it to an inactive complex in the MOM (68, 261). Similarly, the regulation of the anti-apoptotic, multi-domain proteins is also complicated by other factors. Bcl-2 is subject to inhibitory phosphorylation (336, 478), and the protein levels of Mcl-1 are tightly regulated by ubiquitination involving the BH3 domain-containing E3 ligase Mule (498). The short isoforms of Mcl-1 and Bcl-x_L, known as Mcl-1s and Bcl-x_S, respectively, are pro-apoptotic but their relevance to cell death remains poorly understood (16, 44). Moreover, both Bcl-x_L and Bcl-2 can be converted to pro-apoptotic proteins via caspase-3 cleavage (30, 66, 81, 159), or, in the case of Bcl-2, binding to the nuclear receptor Nur77 (279), suggesting that the division between pro- and anti-apoptotic Bcl-2 family members is a fungible one. Finally, the Bcl-2 family and several Bcl-2-related proteins probably also influence the dynamics of mitochondrial morphology, ER-related signalling pathways, and autophagy, each of which are processes that may contribute to apoptosis (180, 274, 371). For example, mitochondrial fission and fusion appear to be regulated, at least in part, by Bak, Bax, Bcl-2, and Bcl-x_L, and mitochondrial fission may directly contribute

to MOMP (371). Indeed, although the minimal elements required for the induction of apoptosis by Bcl-2 family members are well characterised, we have yet to fully realise the sheer scope of the molecular mechanisms the cell uses to control its fate.

1.2.7. The permeabilisation of the mitochondrial outer membrane.

Regardless of how Bak and Bax become activated, it is clear that their activation and oligomerisation is a prerequisite for MOMP and the release of apoptogenic molecules, such as cytochrome *c*. Cells lacking both Bak and Bax are unable to release cytochrome *c* upon apoptotic insult, whereas cells deficient in one of the two proteins still demonstrate cytochrome *c* release, implicating both Bak and Bax as critical mediators of MOMP (459). In fact, the addition of Bax, alone, to isolated mitochondria is enough to elicit cytochrome *c* release (224). The homo-oligomerisation of Bak and Bax is also necessary, and perhaps sufficient, for membrane permeabilisation (145, 250), and Bak and Bax mutants that are unable to homo-oligomerise are also unable to facilitate the release of cytochrome *c* (10, 109). In addition to Bak and Bax, it has been suggested that the permeability transition pore complex (PTPC), a large voltage-dependent, high-conductance ion channel that connects the inner and outer mitochondrial membranes, might be responsible for cytochrome *c* release. However, the deletion of cyclophilin D, a critical component of the channel, has no effect on the induction of apoptosis (18, 322, 383). Likewise, the deletion of all three isoforms of VDAC, another component of the PTPC and proposed mediator of membrane permeabilisation, does not prevent cytochrome *c* release or caspase activation (19). Indeed, it is no longer disputed that MOMP depends on the activation and

homo-oligomerisation of Bak and Bax (418). The mechanism behind MOMP and the release of cytochrome *c* is, however, still a matter of debate.

Originally, the structural determination of Bcl-x_L and Bax revealed homology to the bacterial pore-forming toxins colicin and diphtheria toxin, leading to the hypothesis that Bcl-2 proteins could form pores in membranes by themselves (319, 416). In fact, Bax has been shown to form ion channels in membranes that are inhibited by Bcl-2, but the relevance of these channels, and similar ones formed by the anti-apoptotic proteins Bcl-2 and Bcl-x_L, is still unclear (9, 312, 381, 384). A much larger proteinaceous channel composed of oligomerised Bak or Bax and termed the mitochondrial apoptosis-induced channel (MAC) has been characterised more recently, and several studies support the notion that MAC is sufficient to release cytochrome *c* (101, 295, 346, 348). On the other hand, a number of investigations have shown that activated Bax destabilises and bends membranes to promote the formation of a lipid pore big enough to release cytochrome *c* and some of the much larger molecules that are released upon membrane permeabilisation (28, 29, 380, 428). Whether the permeabilisation of the MOM by Bak and Bax is achieved by the formation of a proteinaceous pore, a lipid pore, or a combination of both, remains to be satisfactorily determined. The size of Bak or Bax oligomers required to make up these pores is also contentious, complicated by the fact that Bak and Bax may continue to oligomerise even after MOMP and cytochrome *c* release (122, 325, 376, 499).

1.2.8. The experimental dissection of apoptosis. The induction of apoptosis and the activation of Bak and Bax can be achieved experimentally and measured using a variety of techniques, many of which are employed in this study. Two

common methods for examining the cellular apoptotic response include the measurement of mitochondrial membrane potential and the assessment of Bak and Bax conformation. The electron transport chain in the inner mitochondrial membrane generates a membrane potential ($\Delta\psi_M$) across the mitochondrial inner membrane by pumping H^+ ions into the intermembrane space. The resulting energy potential is then used to drive ATP synthesis. During apoptosis, however, the $\Delta\psi_M$ is lost concomitant with MOMP (447, 486, 487). Tetraethylrhodamine ethyl ester (TMRE) is a cationic fluorescent molecule that is selectively pumped across the mitochondrial inner membrane and accumulates in healthy, respiring mitochondria with an intact $\Delta\psi_M$ (125, 309). The loss of the $\Delta\psi_M$ upon MOMP therefore results in the concurrent loss of TMRE fluorescence, which can be measured and used as an indication of apoptosis. The activation states of Bak and Bax can also be assessed using the conformationally specific antibodies mouse anti-Bax6A7 and mouse anti-BakAb-1. Following Bax translocation to the MOM, a conformational change results in the exposure of the Bax N-terminus (helix 1) and an epitope comprised of Bax amino acids 14 to 23. This epitope is recognised by the monoclonal 6A7 antibody (200, 201, 353), and its detection is generally interpreted as a sign of Bax conformational activation and impending apoptosis (104, 200, 481). The monoclonal antibody Ab-1 is thought to detect a similar N-terminal conformational change in Bak upon its activation (162, 163), although more recent data suggests that Ab-1 may in fact be recognising a more global conformational change in Bak, rather than just the exposure of the Bak N-terminus (237). Importantly, the conformation of Bcl-2 family proteins, including Bak and Bax, is altered by non-ionic detergents such as TRITON X-100 and NP-40 into an artificially activated state that results in the exposure of the Bax 6A7 epitope and can result in artefactual dimerisation of Bcl-2 proteins (200, 201).

Conversely, the zwitterionic detergent CHAPS does not perturb the conformation of Bcl-2 family proteins and, for this reason, was used almost exclusively in the present study.

1.3. VIRUSES INHIBIT APOPTOSIS

Apoptosis is an important and powerful weapon in the multi-cellular organism's war against viruses, and it serves to protect the life of the organism at the expense of the life of a single cell in that organism. Because viruses are obligate intracellular parasites, they depend on healthy cells to complete their replication cycle and mount a productive infection. The selective destruction of an infected cell by apoptosis therefore halts infection by robbing the virus of the biochemical machinery it needs to replicate. In fact, so important is apoptosis to both the innate and adaptive immune system that many immune responses culminate in cellular suicide (433). Both the natural killer (NK) cells of the innate immune system and the cytotoxic T lymphocytes (CTL) of the adaptive immune system remove virally-infected cells by direct ligation of death receptors, such as Fas, on target cells or by the specific delivery of the protease granzyme B, which cleaves and activates caspases as well as the BH3-only protein Bid to induce apoptosis (24). Additionally, NK cells and CTLs, as well as other cells of the immune system, including dendritic cells and macrophages, produce cytotoxic cytokines, such as TNF α , to further promote apoptosis of infected cells. In contrast to the relatively slower cellular immune response to infection, apoptosis can also be rapidly initiated within the infected cell itself: a variety of pattern recognition receptors or other sensors of cell stress, including BH3-only proteins, detect a viral infection and activate numerous cellular signalling cascades, many of which result in the death of the infected cell (433).

Given that viruses require the cells they infect to remain alive, at least long enough for the virus to replicate, it is not surprising that numerous viruses have evolved mechanisms to inhibit cell death at almost every point. For example, poxviruses, including vaccinia, myxoma, and cowpox virus, encode soluble or membrane bound TNFR homologues that bind to TNF α and prevent it from activating cellular TNFRs (6, 202, 288, 387, 400). Alternatively, some poxviruses, such as molluscum contagiosum virus, and many herpesviruses, including Kaposi's sarcoma herpesvirus (KSHV) and herpesvirus saimiri, encode proteins with death effector domains that bind to the death effector domains in FADD and caspase-8 to prevent the activation of caspases upon death receptor ligation (36, 203, 398, 431). Several viruses also encode proteins that directly inhibit activated caspases. Perhaps the best-characterised example is the cowpox virus protein CrmA (and its VV orthologue SPI-2), which acts as a suicide substrate for caspases-1 and -8 as well as granzyme B (116, 232, 361, 363, 500). Similarly, inhibitors of apoptosis (IAP) encoded by baculoviruses were discovered to prevent virus-induced apoptosis by directly inhibiting caspases, and IAP homologues have since been identified in humans (XIAP) as well as other viruses, including African swine fever virus (ASFV) and the entomopoxvirus *Amsacta moorei* (40, 120, 330). Finally, because many apoptotic pathways converge upon the Bcl-2 family at the mitochondria, several viruses encode proteins that function to inhibit Bcl-2 protein activity and prevent apoptosis.

1.3.1. Viral Bcl-2-like proteins inhibit apoptosis. Mitochondria, and the Bcl-2 family of proteins that preside over them, play a critical role in regulating and inducing apoptosis. Many viruses therefore encode proteins that function analogously to cellular anti-apoptotic Bcl-2 proteins in their ability to inhibit the

activation of Bak and Bax and prevent MOMP. Some of these viral proteins possess sequence identity with cellular Bcl-2 (cBcl-2) proteins, especially in the BH1 and BH2 domains, whereas others share no discernible sequence homology with any known proteins (95, 176, 355). Intriguingly, however, almost all of these proteins have predicted or defined structural homology with the multi-domain members of the Bcl-2 family, suggesting that the overall alpha-helical structure of Bcl-2 proteins and their viral counterparts is critical to their function. Given the structural and functional similarities with cBcl-2 proteins, these virally-encoded inhibitors of intrinsic apoptosis can be collectively described as viral Bcl-2-like (vBcl-2) proteins, although whether they are the product of divergent evolution from an original cBcl-2 or convergent evolution towards Bcl-2-like function is unknown. Examples of vBcl-2 proteins from a variety of viruses are discussed below (Fig. 1.15).

1.3.1.1. Epstein-Barr virus BHRF1 and BALF1. When the cellular protein Bcl-2 was first discovered, it was noted to have amino acid sequence identity with a previously identified protein in Epstein-Barr virus (EBV), a gammaherpesvirus (80). The BamHI fragment H rightward open reading frame 1 (BHRF1) protein has since been shown to localise to the mitochondria (188) where it inhibits MOMP and cytochrome *c* release induced by a variety of stimuli, including death receptor ligation, DNA damaging agents, and γ irradiation (138, 140, 182, 228, 297, 424). BHRF1 is highly conserved in both sequence and function in geographically distinct EBV isolates and throughout primate EBV isolates, suggesting that its anti-apoptotic activity is critical to the replication cycle of EBV (234, 468). In fact, BHRF1 appears to be required immediately upon EBV

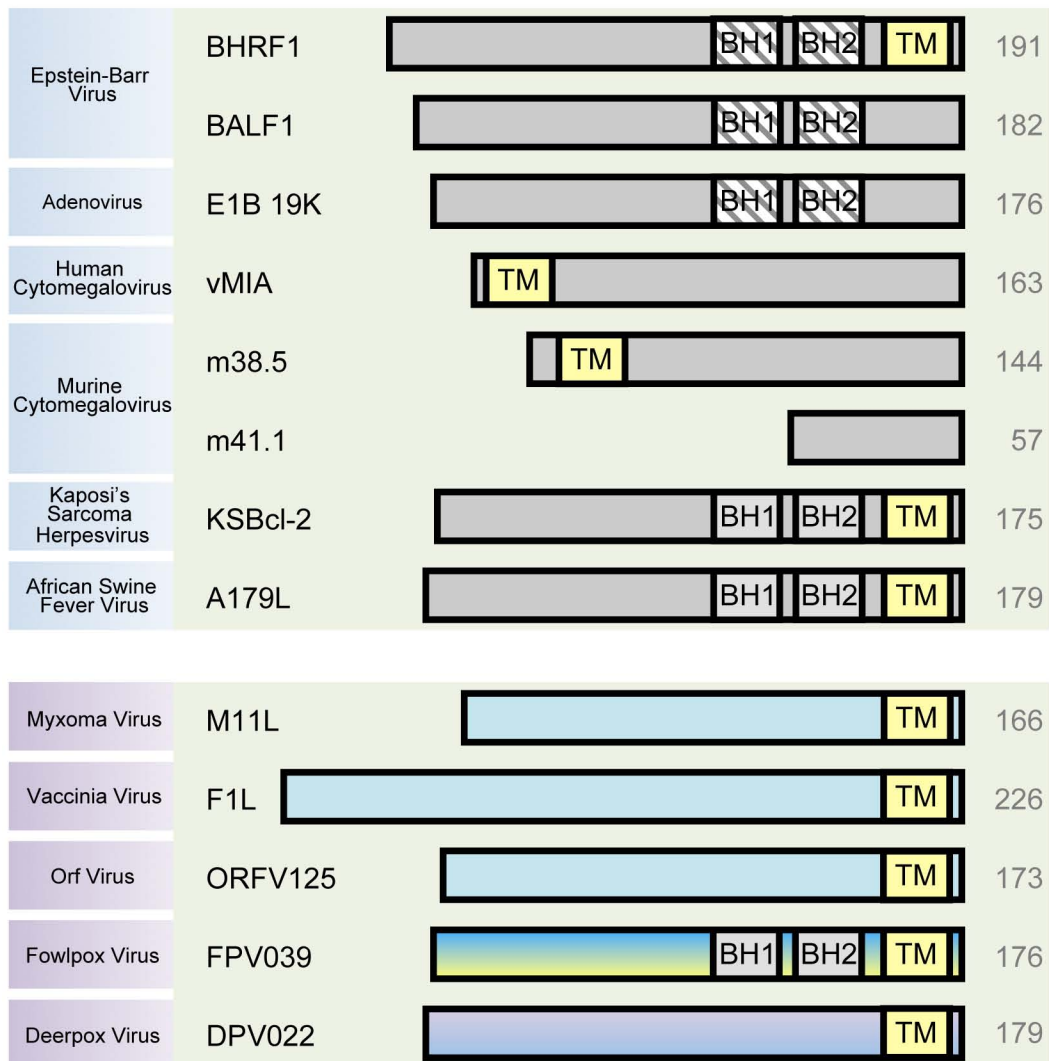


Figure 1.15. Viral Bcl-2 proteins. With the possible exception of m38.5 and m41.1, all viral inhibitors of intrinsic apoptosis possess predicted or defined structural homology with cellular Bcl-2 family proteins, making their designation as vBcl-2 proteins logical. The amino acid sequence of vBcl-2 proteins varies widely among different viruses. Some vBcl-2 proteins possess obvious Bcl-2 homology (BH) domains (indicated with a solid colour), others possess degenerate BH domains (indicated with a hatched pattern), and others share no sequence identity with cellular Bcl-2 proteins. BH-like domains predicted based on structural data are not indicated. Notably, FPV039 is the only poxviral vBcl-2 to share obvious sequence identity with the cellular Bcl-2 proteins. The number of amino acids of each protein is given to the right. TM, transmembrane.

infection to inhibit apoptosis and permit the establishment of latency, and BHRF1 may contribute to oncogenesis in EBV-associated tumours (7).

The structure of BHRF1 revealed an overall similarity to cBcl-2 proteins with the notable lack of a prominent hydrophobic groove, expected to be necessary for mediating interactions with Bcl-2 family members (206). Despite reports from Huang *et al.* that BHRF1 failed to interact with BH3 peptides derived from Bak, Bax, Bik, and Bad (206), other groups have since demonstrated that BHRF1 co-immunoprecipitates with Bak, Bid, Bim, and Puma (92, 105, 138, 430). No interaction between BHRF1 and Bax has been observed (92, 105, 138, 430), although BHRF1 nonetheless strongly inhibits the activation of both Bax and Bak (92). Interestingly, the ability of BHRF1 to interact with Bim, but not Bak, correlates with the anti-apoptotic activity of BHRF1—at least in the context of cytokine deprivation—suggesting that BHRF1 can inhibit Bax activation by targeting the upstream BH3-only proteins (105).

BALF1, another protein encoded by EBV, also shares regions of sequence identity with cBcl-2 proteins, with a degenerate BH1 and BH2 domain but no identifiable TM domain (294). Although BALF1 was initially shown to interact with both Bak and Bax and inhibit apoptosis (294), a contradictory study suggested that BALF1 was capable of neither and, in fact, functioned as a negative regulator of BHRF1 (34). Conversely, a more recent study suggests that BHRF1 and BALF1 are functionally redundant (7), further confusing the true function of BALF1.

1.3.1.2. Adenovirus E1B 19K. The 19 000-dalton E1B protein (E1B 19K) encoded by adenovirus is perhaps the best characterised vBcl-2, and its study has proven integral to the discovery of cBcl-2 family members. E1B 19K

possesses a degenerate BH1 domain, which is critical for its function, as well as a degenerate BH2 domain, and, like BHRF1, E1B 19K lacks an identifiable TM domain (63, 72, 463). Nonetheless, E1B 19K translocates to the mitochondria upon apoptotic stimulus and inhibits MOMP induced by a variety of stimuli, including adenovirus infection, itself (48, 93, 350, 362, 463). Furthermore, Bcl-2 can functionally replace E1B 19K during adenovirus infection, demonstrating that adenovirus requires the inhibition of apoptosis at the mitochondria for productive infection and that E1B 19K fulfils that requirement (72, 410).

Bak was originally discovered when it was pulled out of a yeast two-hybrid assay with E1B 19K as the bait (131). Since then, E1B 19K has been shown to inhibit Bak-induced apoptosis and prevent Bak oligomerisation, probably by interacting with an activated form of Bak possessing the conformationally altered N-terminus (92, 93). E1B 19K likely also functions as a replacement for Mcl-1, serving to bind the Bak that is released upon the ubiquitination and degradation of Mcl-1 during adenovirus infection (94). Similarly, the ability of E1B 19K to interact with Bax depends on a tBid-induced conformational change in Bax (350), indicating that, like its interaction with Bak, E1B 19K only interacts with a form of Bax possessing the exposed N-terminus (92). This interaction depends on the Bax BH3 domain (172), and it is enough to prevent Bax-induced apoptosis and Bax oligomerisation (171, 414). Bik, the inaugural BH3-only protein, was also discovered when it was identified as an E1B 19K interacting partner (173). Interestingly, Bik is a potent inhibitor of E1B 19K activity (173) and, along with Bim, is upregulated and activated in response to adenovirus infection (411), suggesting that these BH3-only proteins regulate E1B 19K and are involved in adenovirus-induced apoptosis.

1.3.1.3. Cytomegalovirus vMIA, m38.5, and m41.1. The betaherpesvirus human cytomegalovirus (HCMV) does not encode a protein with obvious sequence homology to cBcl-2 family members; however, HCMV was nevertheless shown to protect infected cells from apoptosis induced by co-infection with an adenovirus deficient for E1B 19K, implying the existence of an anti-apoptotic mechanism (501). The HCMV protein responsible for inhibiting apoptosis has since been identified and termed the viral mitochondrial inhibitor of apoptosis (vMIA) (153). As the name implies, vMIA localises to the mitochondria where it inhibits MOMP and cytochrome *c* release in response to a variety of toxic stimuli (153). Although vMIA was originally thought to be a unique protein, structural modelling predicts that vMIA folds similarly to Bcl-x_L and contains putative BH-like domains 1-3 (345). Unlike cBcl-2 proteins, however, the localisation of vMIA to the MOM depends on an N-terminal, not a C-terminal, mitochondrial targeting sequence (153, 179). Regardless, vMIA is required by HCMV to permit efficient virus replication that would otherwise be prevented by the initiation of apoptosis upon infection (364).

The mechanism of action for vMIA is unlike any other cBcl-2 or vBcl-2 protein identified to date. Upon vMIA expression, even in the absence of HCMV infection or other external apoptotic stimuli, vMIA recruits Bax from the cytoplasm to the mitochondria where it interacts with Bax and promotes Bax insertion into the MOM, conformational change, and oligomerisation into complexes containing vMIA (14, 356). Despite the apparent vMIA-promoted activation of Bax, cytochrome *c* is not released from the mitochondria and apoptosis does not occur (14, 356). Although the structure of vMIA is predicted to be similar to that of other cBcl-2 proteins, the interaction between vMIA and Bax appears not to require the BH1-3-like groove of vMIA and the BH3 domain of Bax (345).

Instead, vMIA and Bax have been predicted to interact via electrostatic interactions involving an alpha-helical region in vMIA between the putative BH1- and BH2-like domains and a stretch of amino acids in Bax between the BH3 and BH2 domains (345). Whether or not vMIA interacts with Bak remains the subject of controversy, an interaction between vMIA and Bak having been observed by one investigation (331) but not another (14).

vMIA homologues are probably encoded by every primate CMV, whereas homologues are absent from rodent CMVs, including murine CMV (MCMV) (299). Interestingly, however, the MCMV m38.5 protein, which is encoded at a genome position analogous to that of vMIA in HCMV, has recently been shown to localise to the mitochondria and inhibit apoptosis (298). Despite the absence of any sequence similarity between m38.5 and vMIA, m38.5 functions almost identically to vMIA by recruiting Bax to the mitochondria where it interacts with Bax and inhibits its activity after permitting its limited conformational activation (15, 223, 331). m38.5 is unable to interact with Bak or inhibit Bak-mediated apoptosis (15, 223, 331), yet infection with MCMV inhibits Bak-mediated apoptosis, signifying the presence of an additional anti-apoptotic factor (223). Indeed, the newly identified m41.1 protein has been shown to interact with Bak, but not Bax, and inhibit Bak oligomerisation and Bak-induced apoptosis (52). Thus, MCMV encodes two proteins that separately neutralise Bak and Bax and operate synergistically to inhibit apoptosis (52). Notably, vMIA, like m38.5, is unable to prevent Bak-induced apoptosis (14), suggesting that HCMV either encodes a protein analogous to m41.1 or that HCMV replication is restricted to cells in which Bax activity is dominant over Bak.

1.3.1.4. Kaposi's sarcoma herpesvirus KSBcl-2. The gammaherpesvirus Kaposi's sarcoma herpesvirus (KSHV) also encodes a vBcl-2 protein, designated KSBcl-2, with highly conserved BH1 and BH2 domains (67, 378). The solution structure of KSBcl-2 revealed an overall structure very similar to the cellular anti-apoptotic proteins Bcl-2 and Bcl-x_L (205). Although KSBcl-2 inhibits apoptosis in response to a variety of stimuli, including Bax and sindbis virus infection (67, 378), it does not hetero-dimerise with full-length Bak or Bax (67). Instead, KSBcl-2 interacts with a variety of different BH3-only proteins, including Bid, Bim, Noxa, Puma, Bik, Bmf, and Hrk (138), suggesting that interacting with and inhibiting BH3-only proteins might be an effective way to prevent the activation of Bak and Bax and inhibit apoptosis.

1.3.1.5. African swine fever virus A179L. The African swine fever virus (ASFV), a virus distantly related to poxviruses, encodes A179L, a vBcl-2 protein with very highly conserved BH1 and BH2 domains (3, 326). The ability of A179L to inhibit apoptosis is dependent on highly conserved residues within the BH1 domain (365), and may be mediated by interactions with Bak and Bax and/or the BH3-only proteins Bim, tBid, Puma, Bad, Hrk, Bmf, and Bik (141). However, relative to the other vBcl-2 proteins discussed here, the anti-apoptotic mechanism of A179L remains poorly characterised.

1.3.2. Poxviral Bcl-2-like proteins inhibit apoptosis. Poxviruses are renowned for encoding numerous proteins that interfere with almost every aspect of the immune response, including apoptosis (Fig. 1.15) (425). With the exception of molluscum contagiosum virus, a functional or putative vBcl-2 has been identified in every member of the *Chordopoxvirinae* family (Fig. 1.16).

Orthologues of the myxoma virus M11L protein are present in all members of the *Yata*-, *Capri*-, *Sui*-, and *Leporipoxvirus* genera, whereas orthologues of vaccinia virus F1L, Orf virus ORFV125, and fowlpox virus FPV039 are present in all members of the *Ortho*-, *Para*-, and *Avipoxvirus* genera, respectively. Interestingly, members of the genus *Cervidpoxvirus* appear to encode a protein with limited homology to both VV F1L and myxoma virus M11L. The almost universal distribution of vBcl-2 proteins among the poxvirus family implies that the inhibition of apoptosis at the mitochondria is critical to the replication cycle of all poxviruses.

1.3.2.1. Myxoma virus M11L. Disruption of the myxoma virus gene *M11L* results in the dramatic attenuation of myxoma virus in European rabbits (339). Interestingly, this attenuation was shown to correlate with an increased level of apoptosis *in vivo* in rabbit T lymphocytes infected with myxoma virus (292). M11L is now recognised as a potent vBcl-2 that localises to the MOM where it inhibits MOMP and cytochrome *c* release in response to numerous stimuli, including death receptor ligation and virus infection (128, 129, 409, 450). Other than a putative BH3-like domain and a C-terminal TM domain (128, 450), M11L shares very little sequence similarity with cBcl-2 family members. Despite this lack of primary sequence similarity, however, the overall structure of M11L has recently proven to be nearly identical to that of Bcl-2 (Fig. 1.17) (117, 251).

M11L likely inhibits apoptosis by directly neutralising the critical pro-apoptotic Bcl-2 proteins, Bak and Bax (251, 409, 450). M11L interacts constitutively with Bak and inhibits Bak-induced apoptosis (450). Similarly, M11L did not prevent the translocation of Bax to the MOM upon apoptotic insult, but once at the MOM, M11L interacted with Bax and prevented the exposure of the

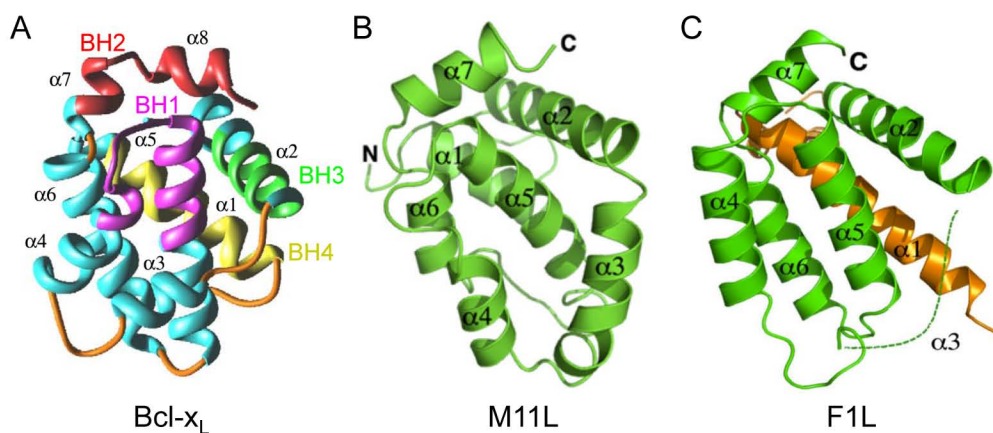


Figure 1.17. The structure of M11L and F1L. The cellular Bcl-x_L (A) adopts an α -helical structure typical of all multi-domain cellular Bcl-2 family proteins. Myxoma virus M11L (B) and vaccinia virus F1L (C) both fold like Bcl-2 family proteins, despite sharing no sequence identity with cellular Bcl-2 proteins. Interestingly, F1L was found to exist as a domain-swapped dimer, with helix one ($\alpha1$; coloured orange) being the swapped domain. The BH domains are labelled for Bcl-x_L, and all α -helices are indicated for each protein. (Adapted from refs. 251 & 252).

Bax N-terminus, a sign of Bax activation (409). M11L also interacts with the extra long isoform of Bim (Bim_{EL}); however, the relevance of this interaction is unknown considering that the anti-apoptotic activity of M11L correlates with its binding to Bak and Bax and not Bim_{EL} (251). Paradoxically, the short isoform of Bim (Bim_S) was shown in the same study to induce apoptosis even in the presence of M11L (251). Additionally, it is possible that the observed interaction between M11L and the peripheral benzodiazepine receptor, a component of the PTPC, also contributes to the anti-apoptotic activity of M11L, although the mechanism remains unclear (129).

1.3.2.2. Vaccinia virus F1L. VV strain Copenhagen, which is naturally devoid of the caspase inhibitor CrmA/SPI-2, still inhibits MOMP and cytochrome *c* release in response to a variety of apoptotic stimuli, prompting Wasilenko and colleagues to hypothesise the existence of an additional inhibitor of apoptosis encoded by VV (454). Indeed, the novel protein F1L was later identified as the factor responsible for inhibiting apoptosis at the mitochondria during VV infection (455). Like M11L and cBcl-2 proteins, F1L requires its C-terminal TM domain to localise to the mitochondria and inhibit apoptosis (406, 455); however, outside of the TM domain, F1L shares no obvious sequence identity with M11L or any cBcl-2 family member (455). Nonetheless, analysis of the hydrophobic amino acids present in F1L and cBcl-2 proteins resulted in the identification of highly divergent BH-like domains critical to the function of F1L (53). The crystal structure of F1L confirmed the presence of these BH-like domains and demonstrated that, like M11L, F1L adopted a Bcl-2-like fold (252). However, unlike any cBcl-2 or vBcl-2 structures determined to date, F1L is purported to

exist as a domain-swapped dimer, with helix 1 as the exchanged domain (Fig. 1.17) (252).

To effectively inhibit MOMP and cytochrome *c* release induced by virus infection and a variety of other cytotoxic stimuli, F1L neutralises the activity of both Bak and Bax (357, 426, 453, 455). Through a constitutive interaction with Bak, F1L prevents Bak oligomerisation and Bak-induced apoptosis (357, 453). Conversely, although F1L does not interact with Bax, it prevents Bax translocation to the mitochondria, conformational activation, and oligomerisation, probably by interacting with and inactivating Bim, a BH3-only protein and Bax activator (426). In fact, Bim as well as Bad and Noxa, have been suggested to contribute to VV-induced apoptosis, but the mechanism of their contribution is ill-defined (137, 358, 426). In addition to its inhibition of Bak and Bax, F1L has also been shown to prevent the induction of apoptosis at a step immediately downstream from MOMP by directly binding the initiator caspase-9 and inhibiting its activation (492). Interestingly, despite the ability of F1L to potently inhibit apoptosis—perhaps at two distinct stages—VV devoid of F1L shows no replication defect in tissue culture (453). Presumably the absence of F1L during *in vivo* infection would attenuate VV; however, this has yet to be determined.

1.3.2.3. Orf virus and ORFV125. The ability of Orf virus to inhibit UV-induced MOMP and cytochrome *c* release has been attributed to the viral protein ORFV125 (460, 461). ORFV125 is predicted to adopt a Bcl-2-like fold and may possess the structural equivalents of BH domains 1-4, as well as a C-terminal TM domain (460, 461). Importantly, mutations in the BH1-3-like domains and deletion of the TM domain abrogate the ability of ORFV125 to inhibit apoptosis (461). ORFV125 inhibits the activation-associated N-terminal conformational

change in both Bak and Bax, probably by interacting with a variety of BH3-only proteins, including Bim, Bik, Puma, Noxa, and Hrk, and by preferentially binding to active Bax (460, 461). Curiously, ORFV125 is the only poxviral vBcl-2 that does not interact with Bak (461).

1.3.2.4. N1L and other vaccinia virus vBcl-2 proteins. N1L is an important virulence factor encoded by VV (27). Although N1L was initially shown to inhibit NF- κ B signalling by interacting directly with components of the inhibitor of NF- κ B kinase (IKK) complex (114), recent data contradict this finding and suggest, instead, that N1L functions to inhibit apoptosis, possibly by interacting with Bax, Bid, or Bad (13, 89). Interestingly, the overall structure of N1L is similar to that of cBcl-2 proteins (13, 89), suggesting that F1L is not the only Bcl-2-like protein encoded by VV.

1.3.2.5. Fowlpox virus and FPV039. Genomic analyses revealed that members of the *Avipoxvirus* genus are the only poxviruses that encode proteins with significant amino acid sequence homology to cBcl-2 proteins (4, 438). Both fowlpox virus and canarypox virus encode proteins, FPV039 and CPV058, respectively, with obvious BH1 and BH2 domains as well as putative TM domains (4, 438). Unlike cBcl-2 family members, however, both proteins lack obvious BH3 and BH4 domains and are predicted to be relatively small in size. At the outset of this study, with no structural information available for any poxviral inhibitor of apoptosis, we became intrigued by the limited regions of amino acid homology between FPV039 and cBcl-2 proteins and the lack of BH3 and BH4 domains. Accordingly, we hypothesised that FPV039 would inhibit apoptosis. The major objective of this study was, therefore, to define the function of the

fowlpox virus protein FPV039 and characterise its mechanism of action (section 1.5.).

1.3.2.6. Deerpox virus and DPV022. Deerpox virus, the prototypical member of the newly defined *Cervidpoxvirus* genus, also encodes a putative vBcl-2 protein, DPV022 (2). Surprisingly, although DPV022 lacks obvious amino acid sequence identity with cBcl-2 proteins, DPV022 possesses limited regions of identity with both M11L and F1L, which share no sequence identity themselves. Based on this homology, we hypothesised that DPV022 would inhibit apoptosis, and the characterisation of DPV022 comprises the second objective of this study (section 1.5.).

1.4. VIRUSES INDUCE APOPTOSIS

That viruses should encode a variety of proteins to inhibit apoptosis implies that virus infection, itself, elicits a pro-apoptotic response from the infected host. Furthermore, because viruses encode vBcl-2 proteins to specifically inactivate the intrinsic apoptotic pathway, it follows that virus infection, itself, must specifically activate the intrinsic pathway. Indeed, many viruses, including vaccinia and myxoma virus, induce MOMP and cytochrome c release in the absence of their endogenous vBcl-2 proteins, F1L and M11L, respectively (292, 453). However, although the ability of viruses to inhibit apoptosis at the mitochondria is well documented, the viral and cellular signals that initially activate apoptosis in virus-infected cells remain unclear. Given that BH3-only proteins become translationally or post-transcriptionally activated in response to a variety of cellular stresses, it is likely that they play a role in sensing signals associated with viral infection and translating those signals to the

mitochondria to induce apoptosis. For example, the apoptotic response to adenovirus may be completely dependent on BH3-only proteins: both Bik and Bim are upregulated in response to adenovirus infection and inhibition of BH3-only proteins alone, not Bak and Bax, inhibited apoptosis (411). Furthermore, both Bim and Bad have been implicated in the apoptotic response to VV (358, 426). Indeed, the fact that many vBcl-2 proteins, including F1L, interact with BH3-only proteins to prevent the activation of Bak and/or Bax provides indirect evidence suggesting that BH3-only proteins are integral to virus-induced apoptosis (426).

1.4.1. Noxa contributes to virus-induced apoptosis. The gene encoding what we now refer to as the BH3-only protein Noxa was originally discovered in 1990 as a transcript upregulated by phorbol 12-myristate 13-acetate (PMA) in adult T-cell leukaemia (ATL) cells (189). The gene was originally named ATL-derived PMA-responsive gene (APR) and then renamed PMA-induced protein 1 (PMAIP1). It was not until 2000 that the gene was re-discovered and given the name Noxa, from the Latin for “damage” (334). Oda and colleagues identified Noxa as a novel member of the BH3-only subgroup of Bcl-2 family proteins in mouse embryonic fibroblasts, and they demonstrated that, upon x-ray irradiation, Noxa was upregulated and induced apoptosis in a p53-dependent manner (334). Indeed, Noxa, along with the other BH3-only protein Puma, appears to be the major regulator of apoptosis in response to DNA damage and p53 expression (334, 388, 396). However, Noxa can be upregulated in a p53-independent manner by other transcription factors, including E2F1 and, under hypoxic conditions, HIF1 α (187, 239). Noxa is also upregulated in certain cancerous cell lines, including melanoma and myeloma cells, by inhibition of the proteasome

with bortezomib, an anti-cancer drug known by the trade name Velcade (135, 360). Unexpectedly, upregulation of Noxa in these cells occurs not only at the protein level, as a result of impaired protein degradation, but also at the transcript level, in a c-Myc-dependent manner (329). Indeed, *bona fide* response elements for all four of these transcription factors—p53, E2F1, HIF1a, and c-Myc—can be found in the *Noxa* promoter (Fig. 1.18A).

Of all the BH3-only proteins directly involved in the induction of apoptosis, Noxa is the most restricted in its binding to anti-apoptotic Bcl-2 proteins, capable of binding only Mcl-1 and Bcl-2A1 (Fig. 1.11) (64). Whereas the functional consequences of the Noxa:Bcl-2A1 interaction have not been well studied, it is clear that the Noxa:Mcl-1 axis plays an important role during cell death, at least in response to specific stimuli, like DNA damage. Following an apoptotic stimulus, Noxa is thought to bind Mcl-1, displace Bak, and trigger the ubiquitination and proteasomal degradation of Mcl-1, presumably freeing Bak to oligomerise and induce apoptosis (94, 214, 328, 470). Likewise, binding of Noxa to Mcl-1 has also been shown to displace Bim, which would then be free to bind and activate Bak and/or Bax (170, 315). Additionally, Noxa, itself, may directly bind and activate Bax, suggesting that, at least in some cases, Noxa can act as a so-called “activator” BH3-only protein (119, 413). Nevertheless, despite the important contribution that Noxa makes to DNA damage- and p53-induced apoptosis, Noxa expression alone is relatively poor at inducing apoptosis when compared to other BH3-only proteins (64). The basis for Noxa’s weak pro-apoptotic activity is not well understood, although it may be affected by cell type, apoptotic stimulus, and the cellular complement of anti-apoptotic Bcl-2 proteins. Regardless, in order to function at all, Noxa depends on both a C-terminal mitochondrial targeting domain and the BH3-only domain (Fig. 1.18B) (334, 393).

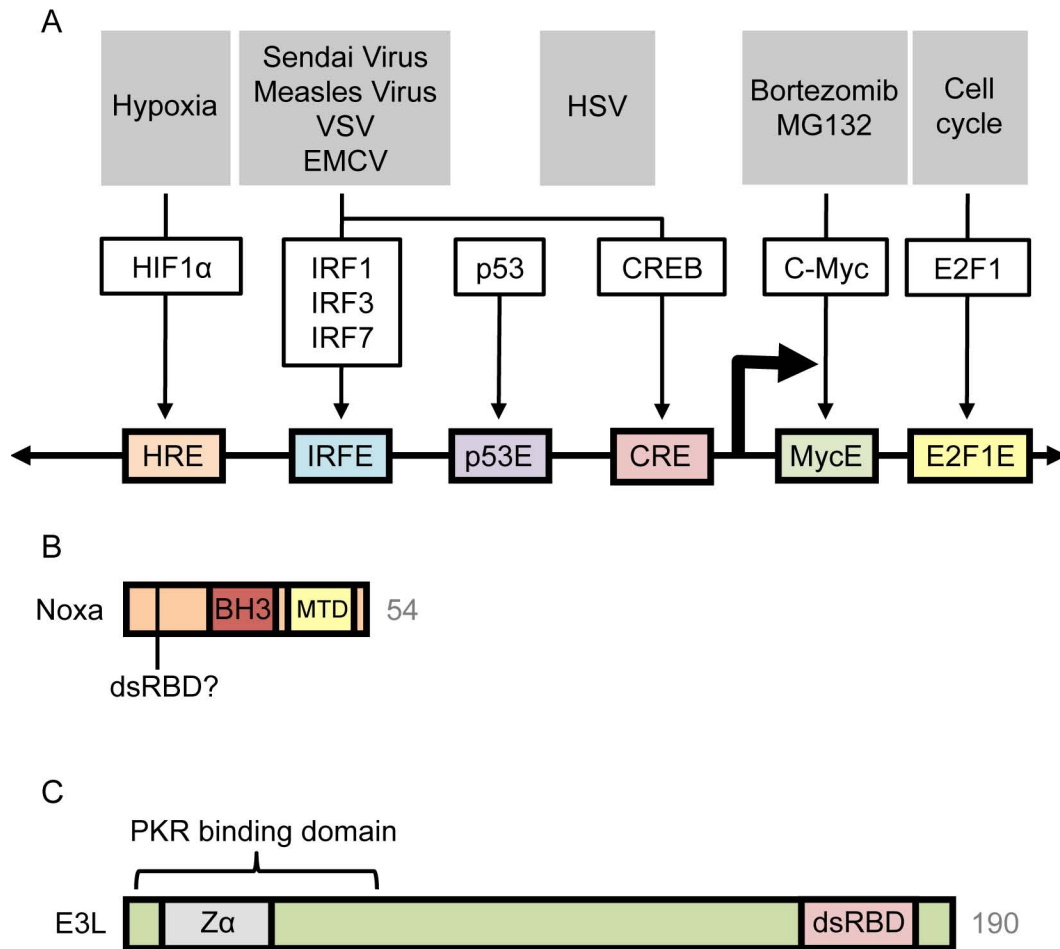


Figure 1.18. Noxa and E3L. (A) The Noxa promoter contains a hypoxia response element (HRE) activated by the transcription factor HIF1 α in response to hypoxia; an interferon regulatory factor (IRF) element (IRFE) activated by IRF1/3/7 and a cAMP-responsive element (CRE) activated by the cAMP-responsive element binding protein (CREB) in response to infection with sendai virus, measles virus, vesicular stomatitis virus, and encephalomyocarditis virus; a p53 response element (p53E) activated by p53 in response to a variety of stimuli, including DNA damage; a Myc element (MycE) activated by c-Myc in response to proteasome inhibition; and a E2F1 element (E2F1E) activated by E2F1 in response to cell-cycle inhibition. Infection with herpes simplex virus 1 results in Noxa upregulation via an unknown mechanism. (B) The 54 amino acid Noxa protein possesses a mitochondrial targeting domain (MTD) and a BH3 domain. A dsRNA binding domain (dsRBD) has been proposed to exist near the N-terminus of the protein. (C) The 190 amino acid E3L protein, encoded by VV, possesses a C-terminal dsRBD and an N-terminal Z-DNA binding domain (Z α). The N-terminus also facilitates a direct interaction with the cellular protein PKR.

It is also worth noting that, whereas murine and rat Noxa possess two BH3 domains, human and all other Noxa homologues described to date possess only one BH3 domain and are about half the size as murine Noxa (91, 334). The functional relevance, if any, of the two BH3 domains in rodent Noxa is unknown, and may simply be the result of a failed gene duplication event (91).

Intriguingly, recent evidence has demonstrated that Noxa may be critical for the apoptotic response to virus infection. Noxa is upregulated in a p53-independent manner following infection with encephalomyocarditis virus (EMCV), vesicular stomatitis virus (VSV), sendai virus (SV), measles virus (MV), and herpes simplex virus 1 (HSV-1), as well as treatment with double-stranded RNA (dsRNA), a by-product of virus replication (Fig. 1.18A) (157, 257, 413). VSV, SV, MV, and synthetic dsRNA have been shown to activate the transcription factors cAMP-responsive element binding protein (CREB) and interferon regulatory factor (IRF) 1, 3, and 7, which drive *Noxa* expression by binding to a cAMP-responsive element and an IRF response element, respectively, that are also present in the *Noxa* promoter (157, 257). In the case of SV, both CREB and IRF3 are activated by phosphorylation triggered by toll-like receptor (TLR) 3 signalling (257). EMCV may also upregulate *Noxa* in a similar manner, although the details remain untested (413). Conversely, the ability of HSV-1 to upregulate *Noxa* is not dependent on the response elements for p53, CREB, or IRF1, 3, and 7, implying the existence of yet another mechanism of *Noxa* upregulation (257). Importantly, Noxa is critical to the induction of apoptosis by infection with EMCV and VSV or treatment with dsRNA and interferon (157, 257, 413). Indeed, EMCV infection or dsRNA treatment promoted an interaction between Noxa and Bax, perhaps suggesting that a dsRNA-induced post-translational activation of Noxa

leads to its direct activation of Bax and the subsequent induction of apoptosis (413).

1.4.2. The cellular response to double-stranded RNA. dsRNA is an inevitable by-product of most viral replication strategies, and its recognition by the cell results in the activation of numerous cellular signalling pathways, including those that lead to apoptosis (227). Although poxviruses have a dsDNA genome, dsRNA is nonetheless produced late during VV infection as the result of overlapping convergent transcription (46, 83, 84, 121). Failure to terminate transcription during the synthesis of VV late genes results in the extension of mRNA transcripts (316). Complementary RNA sequences are consequently produced from oppositely transcribed genes, and these sequences can then hybridise to form dsRNA (84). Notably, because VV late gene synthesis depends on DNA replication, so too does the production of dsRNA (84).

The fact that dsRNA is almost exclusively associated with virus infection means that the cell is acutely sensitive to its presence and able to rapidly incite numerous immune responses to shut down viral infection (227). For example, TLR3 is a pattern recognition receptor that recognises extracellular dsRNA, thought to be present in endosomes containing engulfed apoptotic bodies (227). Conversely, a group of recently identified RNA helicases, including RIG-I and Mda5, recognise intracellular dsRNA in virus-infected cells (465). Signalling through both TLR3 and the RNA helicases converges upon the activation of the transcription factors IRF3, IRF7, and NF- κ B. Activation of these transcription factors promotes the increased production of Type I interferons (IFN α and IFN β) and a variety of inflammatory cytokines. In addition to activating the innate immune system and promoting the development of an adaptive immune

response, the type I interferons also upregulate a variety of proteins that help establish an overall anti-viral state within the cell (227, 465).

Two of the most important proteins upregulated by type I interferons are the dsRNA-dependent protein kinase (PKR) and the 2'-5' oligoadenylate synthetase (OAS), both of which are activated by dsRNA and, once activated, shut down virus infection (143, 193). Upon binding to dsRNA, OAS undergoes a conformational change that allows it to polymerise ATP by 2'-5' linkages instead of the typical 3'-5' linkages (177, 230). These 2'-5' linked As then activate the ribonuclease RNaseL, which goes on to cleave cellular and viral mRNAs, thereby inhibiting protein synthesis and the viral replication cycle (17, 82, 194, 466).

PKR, a serine-threonine kinase, also inhibits protein synthesis to stop virus infection, albeit by a different mechanism (369, 391). PKR binds to dsRNA via two dsRNA-binding motifs at its N-terminus and subsequently undergoes a series of conformational changes that result in the exposure of its kinase domain, homo-dimerisation, and, finally, auto-phosphorylation (110, 493). Once activated, PKR phosphorylates the alpha subunit of the eukaryotic translation initiation factor 2 (eIF-2) (130, 273). eIF-2 normally promotes the delivery of the Met-tRNA to the 40S ribosome to initiate protein synthesis, a process that is dependent on GDP to GTP exchange; however, upon phosphorylation, eIF-2 complexes with the GTP exchange factor eIF-2B and is inactivated (293, 412). In the absence of a functional eIF-2, cellular and viral translation is effectively stopped (23, 265, 267).

PKR is also involved in activating a variety of other signalling cascades, including those mediated by NF- κ B and the cellular apoptotic machinery. Activated PKR interacts with TRAF family proteins, upstream activators of NF- κ B, as well as the IKK complex to activate NF- κ B signalling, although the details of

this activation are currently unknown (149, 150). The ability of PKR to induce apoptosis is linked to the death-receptor adaptor protein FADD because inhibitors of FADD signalling blocks PKR-induced apoptosis (22, 148). However, over-expression of Bcl-2 or the ASFV-encoded vBcl-2, A179L, also block PKR-induced apoptosis, suggesting that the intrinsic apoptotic pathway might also be involved (51, 268). Interestingly, during VV infection, dsRNA has been reported to induce apoptosis in a PKR-dependent manner (235, 266).

1.4.3. Vaccinia virus E3L. VV has long been known to actively inhibit the interferon response in infected cells (341, 342), and it is now clear that VV affects this inhibition with numerous proteins that obstruct several aspects of the interferon signalling pathways (349). The inhibition of PKR activity was initially attributed to a VV “inhibitory factor” (366, 462) that was later identified as the VV-encoded dsRNA-binding protein E3L (Fig. 1.18C) (59, 456). E3L is thought to inhibit PKR activation in at least three ways: (1) by binding directly to dsRNA via a C-terminal dsRNA-binding domain and sequestering dsRNA from recognition by PKR, (2) by binding directly to PKR via an N-terminal domain and holding PKR in an inactive conformation, and (3) by interacting with both dsRNA and PKR to sequester the entire complex (58, 372, 395). E3L has also been shown to inhibit the activation of the transcription factors IRF3/7 and NF- κ B (102, 401, 476, 495) and the antiviral proteins OAS, ISG15, and ADAR (165, 285, 367). Additionally, E3L is purported to possess an N-terminal Z-DNA-binding domain with which it binds Z-DNA near the transcription start sites of cellular genes and activates their transcription, a function that is reportedly important for VV pathogenesis (Fig. 1.18C) (241, 242, 253, 258, 389). The importance of E3L to

VV infection is underscored by its high degree of conservation among the orthopoxviruses and its role as a host-range and virulence factor (32, 50).

Previous studies have shown that VV devoid of E3L induces apoptosis in a PKR-dependent manner, despite the presence of the vBcl-2 protein F1L (235, 266). However, a study by Fischer *et al.*, using the highly mutated modified vaccinia virus Ankara (MVA), demonstrated that MVA devoid of E3L induced apoptosis that was dependent on Noxa (137). Taken together, these results suggest a model whereby E3L binds and sequesters dsRNA preventing the upregulation and/or activation of Noxa, which would otherwise translate its apoptotic signal to Bax, and possibly Bak, at the mitochondria to contribute to cell death. It is unclear why F1L, which functions at the mitochondria to neutralise Bak and Bax, is unable to inhibit the induction of apoptosis by Noxa in this case. Thus, the third objective of this study was to investigate the role that dsRNA, Noxa, and E3L play in VV-induced apoptosis (section 1.5.)

1.5. THESIS OBJECTIVES

Apoptosis is a critical component of the host's anti-viral response. By committing suicide, an infected cell effectively halts viral replication and limits the spread of infection. It therefore comes as no surprise that viruses should need to inhibit apoptosis from occurring in the first place. Because mitochondria comprise a major junction in the cellular apoptotic response, many viruses, including poxviruses, have targeted the Bcl-2 family of proteins to inhibit cell death. Indeed, not only do viruses inhibit Bak and Bax activity, but they do so using proteins analogous to the cellular Bcl-2 proteins. By understanding how these viral Bcl-2 proteins interfere with their cellular counterparts and prevent apoptosis, we can shed light on both the regulation of cellular apoptosis and the

viral replication cycle. Conversely, the fact that viruses encode proteins to inhibit apoptosis implies that infection, itself, is an apoptotic stimuli. However, the viral signals that induce the activation of BH3-only proteins and, eventually, Bak and Bax, remain poorly understood. In an effort to better understand the regulation of cell death, we conducted a comprehensive study with the following objectives:

Objective 1: FPV039, encoded by fowlpox virus, and its orthologue in canarypox virus are the only poxviral proteins to possess obvious sequence identity with cellular Bcl-2 family proteins, with a BH1, BH2, and TM domain. Given this homology, we hypothesised that FPV039 would function to inhibit apoptosis by interfering with the Bak and Bax, and we sought to characterise its mechanism of action.

Objective 2: DPV022, encoded by deerpox virus, shares no sequence identity with cellular Bcl-2 proteins but it does share discrete regions of sequence identity with F1L and M11L, which themselves are unique. Given the intriguing relationship between DPV022, F1L, and M11L, we hypothesised that DPV022 would inhibit apoptosis, and we sought to characterise its mechanism of action.

Objective 3: The BH3-only protein Noxa is upregulated in response to infection by a variety of viruses, and it contributes to the induction of apoptosis in response to those viruses. Moreover, Noxa activation appears to be linked to the presence of dsRNA. We hypothesised that Noxa might also play a role during VV infection and we used a VV mutant devoid of E3L, the dsRNA-binding protein, to address the role that Noxa and dsRNA play in initiating apoptosis in response to VV infection.

CHAPTER TWO

MATERIALS AND METHODS

2.1. CELL LINES

All cell lines used in this study are listed in Table 2.1. HeLa, human embryonic kidney (HEK) 293T, CV-1, baby hamster kidney (BHK) cells, chicken leghorn male hepatocellular carcinoma (LMH) (226), wild-type (WT) baby mouse kidney (BMK), *Bak*^{-/-} BMK, and *Noxa*^{-/-} BMK cells were maintained at 37°C and 5% CO₂ in Dulbecco's modified Eagle medium supplemented with 10% heat-inactivated foetal bovine serum (HI-FBS; Invitrogen), 50 U/ml of penicillin (Invitrogen), 50 µg/ml of streptomycin (Invitrogen), and 200 µM L-glutamine (Invitrogen). HeLa, HEK 293T, CV-1, BHK, and LMH cells were obtained from the ATCC, and WT, *Bak*^{-/-}, and *Noxa*^{-/-} BMK cells were a gift from E. White (Rutgers University, Piscataway, NJ) (100). Buffalo green monkey kidney cells were obtained from Diagnostic Hybrids and maintained as described above in medium supplemented with 10% newborn calf serum (Invitrogen) instead of HI-FBS. HuTK^{-/-}-143B cells were obtained from the ATCC and maintained as described above in medium additionally supplemented with 25 µg/ml 5-bromodeoxyuridine (Sigma-Aldrich). Mouse embryo fibroblast (MEF) cells expressing pMIH empty vector or pMIH-Flag-DPV022 were made by retroviral infection as described previously (64, 470). Hygromycin resistant MEFs were cloned, and protein expression was confirmed by intracellular FACS analysis using an anti-Flag antibody. These MEFs were generated and used in the laboratory of D. Huang (Walter and Eliza Hall Institute, Parkville, Australia) to perform the experiment depicted in Fig. 5.11. WT, Bcl-2 over-expressing, and Bak- and Bax-deficient (*Bak*^{-/-}/*Bax*^{-/-}) Jurkat cells were maintained at 37°C and 5% CO₂ in Roswell Park Memorial Institute 1640 medium supplemented with 10% HI-FBS, 50 U/ml of penicillin, 50 µg/ml of streptomycin, 200 µM L-glutamine, and 100 µM β-mercaptoethanol (Sigma-Aldrich). WT Jurkats were obtained from

Table 2.1. Cell Lines Used

Cell Line	Tissue	Properties	Source
HeLa	Human cervical adenocarcinoma epithelial cells		ATCC
HEK 293T	Human embryonic kidney (HEK) fibroblasts	Transformed with SV40 T antigen	ATCC
HuTK ^{-/-} -143B	Human osteosarcoma cells	Lacks thymidine kinase gene	ATCC
Jurkat	T lymphocyte derived from acute T cell leukaemia	Wild-type	ATCC
Jurkat Bcl-2	T lymphocyte derived from acute T cell leukaemia	Over-expresses Bcl-2	(25)
Jurkat <i>Bak</i> ^{-/-} / <i>Bax</i> ^{-/-}	T lymphocyte derived from acute T cell leukaemia	Lacks <i>Bak</i> and <i>Bax</i> genes	(451)
BGMK	Buffalo African green monkey kidney (BGMK) fibroblasts		Diagnostic Hybrids
CV-1	African green monkey kidney fibroblasts		ATCC
LMH	Chicken Leghorn male hepatocellular carcinoma (LMH) epithelial cells		ATCC
BMK	Baby mouse kidney epithelial cells	Wild-type	(100)
<i>Bak</i> ^{-/-} BMK	Baby mouse kidney epithelial cells	Lacks <i>Bak</i> gene	(100)
<i>Noxa</i> ^{-/-} BMK	Baby mouse kidney epithelial cells	Lacks <i>Noxa</i> gene	(100)
BHK	Baby hamster kidney fibroblasts	Used for amplification of VVΔE3L	ATCC
MEF	Mouse embryo fibroblasts	Used for retroviral transduction of pMIH or pMIG vectors	D. Huang

the ATCC, Bcl-2 over-expressing Jurkats were generated as previously described (25), and *Bak*^{-/-}/*Bax*^{-/-} Jurkats were a gift from H. Rabinowich (University of Pittsburgh School of Medicine, Pittsburgh, PA) (451).

2.2. DNA METHODOLOGY AND CLONING

2.2.1. Plasmids. All plasmids used in this study are listed in Table 2.2. pGEM-T (Promega) was used for all TA cloning, and pEGFP-C1, -C2, or -C3 (Clontech) were used to generate all enhanced green fluorescent protein (EGFP)-fusion constructs. pEGFP-F1L and pSC66-Flag-F1L were generated as described previously (455). pMA-DPV022 was purchased from Geneart (Regensburg, Germany); pSC66 was provided by D. Burshtyn (University of Alberta, Edmonton, AB) (57); pSC66-Flag-DPV022 was generated from synthetic cDNA (Blue Heron Biotechnonology) and provided by D. Huang (Walter and Eliza Hall Institute, Parkville, Australia); pcDNA-HA-Bak, pcDNA3-HA-Bax, and pEGFP-M11L were provided by G. McFadden (University of Florida, Gainesville, FL) (128, 409, 450); pcDNA3-Flag-Bim_L and pcDNA3-Bmf-T7 were provided by R. Davis (University of Massachusetts Medical School, Boston, MA) (270); pEGFP-Bcl-2 was provided by C. Bleackley (University of Alberta, Edmonton, AB) (128); pcDNA3.1-Myc-Noxa was provided by D. Leaman (University of Toledo, Toledo, OH) (413); pcDNA3-Myc-Bik was provided by E. White (Rutgers University, Piscataway, NJ) (173); and pXJ40-HA-Bad was provided by S. Baksh (University of Alberta, Edmonton, AB). pGALL(TRP1), pGALL(TRP1)-Bcl-x_L, pGALL(TRP1)-DPV022, pGALL(TRP1)-Bak, pGALL(TRP1)-Bax, pMIH, pMIH-Flag-DPV022, pMIG, and pMIG-Bim_S2A were generated and used by the laboratory of D. Huang to perform certain experiments (Fig. 5.4, 5.7, 5.11). All other plasmids

Table 2.2. Plasmids Used

Plasmid	Description/Use	Source
pGEM-T	TA cloning vector	Promega
pEGFP-C1, -C2, -C3	CMV promoter; used to generate EGFP N-terminal fusion proteins	Clontech
pSC66	Synthetic poxviral early/late promoter; VV thymidine kinase sequence flanks <i>lacZ</i> , promoter, and multiple cloning site; used to generate VV recombinants	D. Burshtyn & (57)
pEGFP-FPV039(1-176)	Expresses wild-type FPV039 (fowlpox virus)	This study
pSC66-Flag-FPV039(1-176)	Used to generate recombinant VVΔF1L expressing Flag-tagged, wild-type FPV039	This study
pEGFP-FPV039(Δ41-54)	Expresses FPV039 lacking putative BH3 region	This study
pSC66-Flag-FPV039(Δ41-54)	Used to generate recombinant VVΔF1L expressing Flag-tagged FPV039(Δ41-54)	This study
pEGFP-FPV039(1-94)	Expresses FPV039 lacking C-terminal 82 amino acids	This study
pSC66-Flag-FPV039(1-94)	Used to generate recombinant VVΔF1L expressing Flag-tagged FPV039(1-94)	This study
pEGFP-FPV039(1-141)	Expresses FPV039 lacking C-terminal 35 amino acids	This study
pEGFP-FPV039(142-176)	Expresses only C-terminal 35 amino acids of FPV039	This study
pMA-DPV022	Codon optimised DPV022; used to clone pEGFP-DPV022 (deerpox virus)	Geneart
pEGFP-DPV022	Expresses wild-type DPV022	This study
pSC66-Flag-DPV022	Used to generate recombinant VVΔF1L expressing Flag-tagged DPV022	D. Huang
pEGFP-F1L	Expresses wild-type F1L (vaccinia virus)	(455)
pSC66-Flag-F1L	Used to generate recombinant VVCop expressing Flag-tagged F1L	(455)
pEGFP-M11L	Expresses wild-type M11L (myxoma virus)	(128)
pEGFP-N1L	Expresses wild-type N1L (vaccinia virus)	This study
pEGFP-Bcl-2	Expresses wild-type Bcl-2 (human)	(128)
pEGFP-Bcl-x _L	Expresses wild-type Bcl-x _L (human)	This study
pEGFP-Mcl-1	Expresses wild-type Mcl-1 (human)	This study
pcDNA3-HA-Bak	Expresses wild-type, HA-tagged Bak (human)	(450)
pcDNA3-HA-Bax	Expresses wild-type, HA-tagged Bax (human)	(409)
pcDNA3-Flag-Bim _L	Expresses wild-type, Flag-tagged Bim _L (human)	(270)
pcDNA3-Myc-Bik	Expresses wild-type, Myc-tagged Bik (human)	(173)
pcDNA3-Bmf-T7	Expresses wild-type, T7-tagged Bmf (human)	(270)
pXJ40-HA-Bad	Expresses wild-type, HA-tagged Bad (human)	S. Baksh
pcDNA3-HA-Puma	Expresses wild-type, HA-tagged Puma (human)	This study
pcDNA3.1-Myc-Noxa	Expresses wild-type, Myc-tagged Noxa (human)	(413)
pcDNA3-Bid-Flag	Expresses wild-type, full-length, Flag-tagged Bid (human)	This study
pcDNA3-tBid-Flag	Expresses wild-type, caspase-8-cleaved, Flag-tagged Bid (human)	This study

Table 2.2. Plasmids Used, *continued*

Plasmid	Description/Use	Source
pGALL(TRP1)	Backbone vector for transforming yeast; contains GALL promoter system for galactose-inducible gene expression	D. Huang
pGALL(TRP1)-Bcl-x _L	Expresses Bcl-x _L ; induced by galactose	D. Huang
pGALL(TRP1)-DPV022	Expresses DPV022; induced by galactose	D. Huang
pGALL(TRP1)-Bak	Expresses Bak; induced by galactose	D. Huang
pGALL(TRP1)-Bax	Expresses Bax; induced by galactose	D. Huang
pMIG	Retroviral expression vector comprised of a multiple cloning site and the EGFP gene separated by an IRES ^a to produce bicistronic mRNA	D. Huang
pMIH	Retroviral expression vector comprised of a multiple cloning site and the hygromycin resistance gene separated by an IRES ^a to produce bicistronic mRNA	D. Huang
pMIH-Flag-DPV022	Expresses a Flag-tagged DPV022 and the hygromycin resistance gene	D. Huang
pMIG-Bim _s 2A	Expresses Bim _s 2A and EGFP	D. Huang

^aIRES, internal ribosome entry site

were generated during this study, as described in section 2.2.9. All plasmids encode human proteins except those encoding viral proteins.

2.2.2. Polymerase chain reaction. Polymerase chain reactions (PCR) used to amplify DNA destined to be cloned into expression vectors were typically performed in 50 µl volumes containing 10 mM Tris-HCl (pH 8.85), 25 mM KCl, 5 mM $(\text{NH}_4)_2\text{SO}_4$, 2 mM MgSO_4 , 100 µM dNTPs, 250 nM of each primer, and 5 U of Pwo DNA polymerase (Roche). All other PCR was typically performed in 50 µl volumes containing 20 mM Tris-HCl (pH 8.4), 50 mM KCl, 2.5 mM MgCl_2 , 100 µM dNTPs, 250 nM of each primer, and 2.5 U of Taq (Invitrogen) DNA polymerase (Invitrogen). All of the primers used for cloning in this study are listed in Table 2.3. PCR reactions were carried out in a Techgene thermocycler (Techne) for 30 cycles comprised of a 95°C denaturing step for 30 s, a 55°C annealing step for 30 s, and a 72°C elongation step for 1 min per kilobase.

2.2.3. Agarose gel electrophoresis and gel extractions. DNA samples were mixed with sample loading buffer (5% glycerol; 0.4% (w/v) bromophenol blue; 0.4% (w/v) xylene cyanol; 10 mM EDTA, pH 7.5) and separated by electrophoresis at ~90 V through 1-2% (w/v) agarose gels prepared with agarose (Invitrogen) and 1xTAE buffer (40 mM Tris-acetate, 1mM EDTA). Gels were run in 1xTAE buffer. Gels were stained with 10 µg/ml ethidium bromide (Sigma-Aldrich) and visualised using the ImageQuant 300 and ImageQuant 300 Capture software (GE Healthcare).

A Qiaquick Gel Extraction Kit (Qiagen) was used to purify electrophoresed DNA. Briefly, bands were excised from the agarose gel and dissolved in 3 volumes (µg/µl) Buffer QG at 50°C for approximately 10 min. The

Table 2.3. Oligonucleotides Used for Cloning

Oligonucleotide	Sequence ^a	Sense ^b	RE ^c	Source
FPV039 1FWD	<u>AAGCTT</u> ATGGCTAGTAATATGAAA	+	HindIII	Qiagen
FPV039 REV176	<u>GGATCC</u> TTACATATAAAAGGAACATAT	-	BamHI	Qiagen
FPV039 REV141	<u>GGATCC</u> TTAATATATACGAATTCATTCC CAATA	-	BamHI	Qiagen
FPV039 142FWD	<u>GAATTCT</u> CAAAAACTATTCGTATATT	+	EcoRI	Qiagen
FPV039 REV40	TTCATTATAATTGGATATAGAATCTATTA CAAA	-	none	IDT
FPV039 55FWD	AATTATAATGAATTTGATATA	+	none	IDT
VV-FPV039 1FWD	<u>GTCGACATGGACTACAAAGACGATGAC</u> <u>GACAAGGCTAGTAGTAATATGAAA</u>	+	Sall	Qiagen
VV-FPV039 REV176	GCGGCCGCTTACATATAAAAGGAACAT AT	-	NotI	Qiagen
N1L FWD	<u>GGTACC</u> ATGAGGACTCTACTTATT	+	KpnI	IDT
N1L REV	<u>GGATCC</u> TTATTTTTTACCATATAGATC	-	BamHI	IDT
BCLXL FWD	<u>GAATTC</u> ATGTCTCAGAGCAACCGG	+	EcoRI	IDT
BCLXL REV	<u>GGATCC</u> TCATTTCGACTGAAGAG	-	BamHI	IDT
BID FWD	<u>AAGCTT</u> ATGGACTGTGAGGTCAAC	+	HindIII	IDT
BID REV	<u>GGATCC</u> TTACTTGTCTCATCGTCTTTG <u>TAGTCGTCCATCCCATTCTGGC</u>	-	BamHI	IDT
BID c8FWD	<u>AAGCTT</u> ATGGGCAACCGCAGCAGCCAC	+	HindIII	IDT

^aRestriction endonuclease sites are underlined and the Flag-tag sequence is highlighted in grey.

^bSense, +; antisense, -

^cIdentity of restriction endonuclease (RE) site underlined in "Sequence" column.

sample was transferred to a QIAquick DNA column, and, following washes, DNA was eluted by centrifugation (17 000 x g, 1 min) using 50 µL of Buffer EB (10 mM Tris-Cl, pH 8.5).

2.2.4. DNA ligation. Blunt-ended PCR products generated by Pwo DNA polymerase and destined for cloning into expression vectors were first subjected to an A-addition reaction (Qiagen) before ligation into the TA-cloning vector pGEM-T (Promega). Ligation of modified PCR products into pGEM-T was performed according to the manufacturer's instructions. Briefly, 50 ng of pGEM-T, 3 U of T4 DNA ligase, 5 µl of 2x Rapid Ligation Buffer (60 mM Tris-HCl, pH 7.8; 20 mM MgCl₂; 20 mM DTT; 2 mM ATP; 10% (v/v) polyethylene glycol), and 3 µl PCR product were mixed together and incubated at 4°C for 20 h. All other ligations were performed using T4 DNA ligase (New England Biolabs) according to the manufacturer's instructions. Briefly, 400 U of T4 DNA ligase and 1x Reaction Buffer (50 mM Tris-HCl, pH 7.5; 10 mM MgCl₂; 10 mM DTT; 1 mM ATP; 25 µg/ml BSA) were used to ligate vector and DNA insert ratios of 1:3, 1:6, and 1:9. Reactions were incubated at 4°C for 20 h. Ligations were transformed into *E. coli* strain DH5α as described in section 2.2.6.

2.2.5. Restriction endonuclease digestion. In general, restriction endonuclease digestions were performed in a total volume of 20 µl using 10-15 U of restriction enzyme (Invitrogen), the appropriate reaction buffer (Invitrogen), and 10 µg of RNase (Sigma-Aldrich). Digestions were allowed to proceed at 37°C for 1 h.

2.2.6. Bacterial transformation. Chemically competent *E. coli* strain DH5 α were prepared as described elsewhere (377), and transformed using a heat-shock procedure. Briefly, 50 μ l *E. coli* were incubated with DNA on ice for 30 min followed by a 1 min incubation at 42°C and a subsequent 2 min incubation on ice. Cells were then supplemented with 250 μ l SOC media and allowed to recover at 37°C for 1 h. Following recovery, cells were plated onto Luria-Bertani (LB) agar plates containing the appropriate antibiotic, either 100 μ g/ml ampicillin (Sigma-Aldrich) or 30 μ g/ml kanamycin (Sigma-Aldrich). *E. coli* transformed with pGEM-T were often plated onto LB agar plates containing 100 μ g/ml ampicillin, 80 μ g/ml X-gal, and 0.5 mM IPTG to allow for blue/white screening of recombinants.

2.2.7. Plasmid preparation. Plasmids used during cloning were isolated and prepared using the Alkaline Lysis with SDS Miniprep method (377). *E. coli* were grown in a 5 ml LB broth overnight culture with the appropriate antibiotic before 1.5 ml of culture was removed and pelleted. Bacterial cells were re-suspended in 100 μ l buffer containing 50 mM glucose, 25 mM Tris (pH 8.0), and 10 μ M EDTA before being lysed on ice in 200 μ l buffer containing 10 mM NaOH and 1% SDS. Membrane and proteins were precipitated on ice using 100 μ l buffer containing 3M KCH₃COO and 11.5% glacial acetic acid. Following centrifugation (9000 x g, 15 min), DNA was separated from the supernatant by extraction with an equal volume of phenol:chloroform (1:1). The aqueous phase was extracted again with an equal volume of chloroform, and DNA was precipitated in 2.5 volumes of 95% ethanol at 4°C for 10 min. DNA was pelleted by centrifugation (9000 x g, 10 min), and the pellet was re-suspended in dH₂O.

High quality preparations of plasmid DNA for transfections were obtained with a Maxi Prep Kit, used according to manufacturer's instructions (Qiagen). *E.*

coli cultures were typically grown in a 400 ml LB broth overnight culture with the appropriate antibiotic. However, in the case of bacteria transformed with a low-copy plasmid, such as pSC66, 400 ml LB broth cultures were permitted to grow for 7-8 h before being treated with 170 µg/ml chloramphenicol (Sigma-Aldrich) and grown for an additional 12-16 h.

DNA concentration was determined using a spectrophotometer (Eppendorf) to measure the optical density at 280 nm.

2.2.8. DNA sequencing and computer analyses. The Molecular Biology Sequencing Unit in the Department of Biology at the University of Alberta completed all DNA sequencing. Basic Local Alignment Search Tool (BLAST) programmes provided by the National Center for Biotechnology Information (NCBI) were used to analyse DNA sequence.

2.2.9. Cloning methods

2.2.9.1. FPV039. All FPV039 constructs were generated using the primers listed in Table 2.3. WT FPV039(1-176) was PCR amplified from fowlpox virus DNA (provided by C. Upton, University of Victoria, Victoria, BC) using the FPV039 1FWD and FPV039 REV176 primers. FPV039(1-94), which contains a stop codon (TAA) in place of the Tyr-95 immediately after the putative BH1 domain, was obtained fortuitously by PCR using the FPV039 1FWD and FPV039 REV176 primers. FPV039(1-141), missing the mitochondria targeting sequence, was generated via PCR using the FPV039 1FWD and FPV039 REV141 primers. FPV039(142-176), comprising only the mitochondria targeting sequence, was generated via PCR using the FPV039 142FWD and FPV039 REV176 primers. FPV039(Δ41-54), which lacks 14 internal amino acids, was generated by over-

lapping PCR. DNA encoding the N-terminal 40 amino acids of FPV039 was PCR amplified from pEGFP-FPV039(1-176) using the FPV039 1FWD primer and the internal reverse primer FPV039 REV40; DNA encoding the C-terminal 122 amino acids of FPV039 was PCR amplified from pEGFP-FPV039(1-176) using the internal forward primer FPV039 55FWD and the FPV039 REV176 primer. The resulting PCR products were combined, and an additional PCR was performed using the FPV039 1FWD and FPV039 REV176 primers. Flag-tagged versions of FPV039(1-176), Flag-FPV039(1-176); FPV039(1-94), Flag-FPV039(1-94); and FPV039(Δ 41-54), Flag-FPV039(Δ 41-54), were generated via PCR from pEGFP-FPV039(1-176), pEGFP-FPV039(1-94), or pEGFP-FPV039(Δ 41-54), respectively, using the VV-FPV039 1FWD and VV-FPV039 REV176 primers. All PCR products were cloned into the pGEM-T vector, and constructs were sequenced to ensure the absence of errors. FPV039(1-176), FPV039(1-94), FPV039(1-141), FPV039(142-176), and FPV039(Δ 41-54) were sub-cloned into pEGFP-C3 to generate versions of each FPV039 construct fused to EGFP at the N-terminus. Flag-FPV039(1-176), Flag-FPV039(1-94), and Flag-FPV039(Δ 41-54) were sub-cloned into the pSC66 vector for use in making recombinant VVs (section 2.4.3.). All FPV039 constructs are displayed diagrammatically in Figure 2.1.

2.2.9.2. DPV022. WT DPV022 from mule deer poxvirus strain W-848-83 was codon optimised to remove rare codons, polyA sites, and RNA instability motifs (Geneart). Codon optimisation increased the GC content of DPV022 from 25% to 53% in order to prolong mRNA half-life, and codon usage was adapted to the bias of *Homo sapiens*. Codon optimised DPV022 was synthesised with 5' EcoRI and 3' BamHI restriction sites in backbone vector pMA. Following restriction

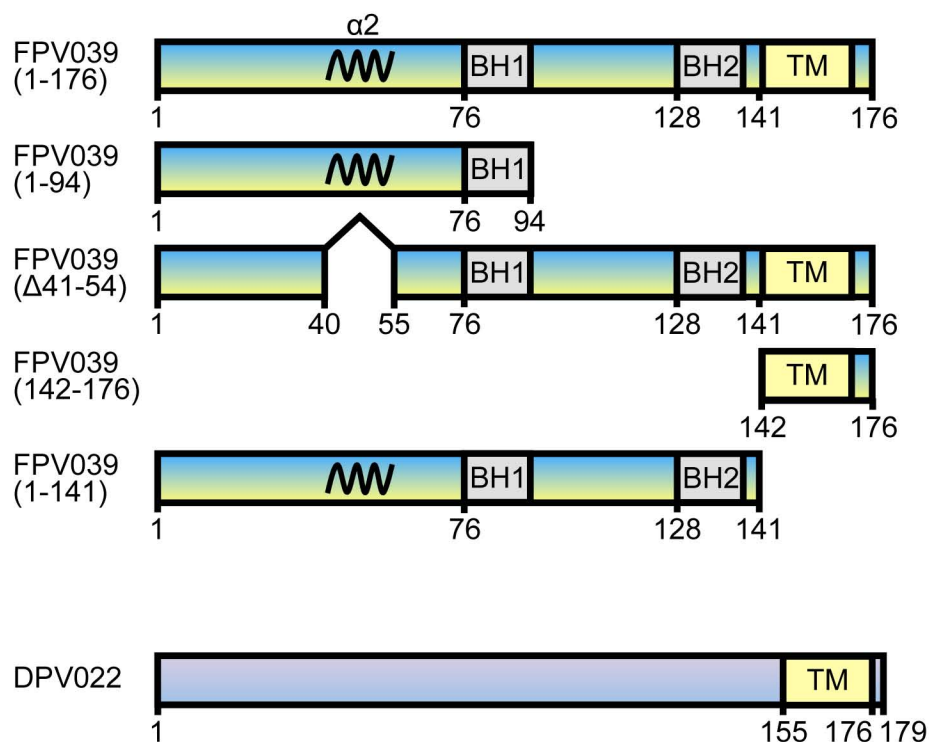


Figure 2.1. FPV039 and DPV022 constructs generated. A schematic representation of the wild-type FPV039 and mutant constructs as well as wild-type DPV022. All constructs were sub-cloned into the pEGFP vector, which places an EGFP tag at the N-terminus of the protein. FPV039(1-176), FPV039(1-94), FPV039($\Delta 41-54$), and DPV022 constructs were also sub-cloned into the pSC66 vector with an N-terminal Flag tag. The transmembrane (TM) domain, the Bcl-2 homology (BH) domains, and the second α -helix ($\alpha 2$) that comprises the putative BH3 domain in FPV039 are indicated.

digestion with EcoRI and BamHI, DPV022 was cloned into the pGEM-T vector, and the construct was sequenced to ensure the absence of errors. DPV022 was sub-cloned into pEGFP-C2 to generate a DPV022 fused to EGFP at the N-terminus. The DPV022 construct is displayed diagrammatically in Figure 2.1.

2.2.9.3. N1L, Puma, Bcl-x_L, Mcl-1, Bid, and tBid. The following constructs were generated using primers listed in Table 2.3. N1L was amplified by PCR from VV strain Copenhagen DNA using the N1L FWD and N1L REV primers. N1L PCR product was cloned into the pGEM-T vector and sub-cloned into pEGFP-C1 to generate an N-terminally tagged EGFP-N1L. To generate pcDNA3-HA-Puma, Puma was excised from pCEP4-HA-Puma (provided by B. Vogelstein, Johns Hopkins University, Baltimore, MD) using the restriction enzymes KpnI and BamHI and ligated into pcDNA3. pEGFP-Bcl-X_L was generated from p(Bluescript)SK-Bcl-X_L (provided by C. Bleackley, University of Alberta, Edmonton, AB) using the BCLXL FWD and BCLXL REV primers. pEGFP-Mcl-1 was generated by excising Mcl-1 from pCR3.1-Mcl-1 (provided by H. Rabinowich, University of Pittsburgh, Pittsburgh, PA) using the restriction enzyme EcoRI, followed by ligation into pEGFP-C3. pcDNA3-Bid-Flag was generated from pCMV5-Bid using the BID FWD and BID REV primers. pcDNA3-tBid-Flag, comprising the caspase-8 cleaved fragment of Bid, was generated from pCMV5-Bid using the BID c8FWD and BID REV primers.

2.3. TRANSFECTIONS

All plasmid DNA used for transfecting cells was prepared using a Maxi Prep Kit as described in section 2.2.7. In general, 50 µl Opti-MEM (Invitrogen) and 2 µl Lipofectamine 2000 (Invitrogen) were combined and incubated at room

temperature for 5 min before being added to 50 μ l Opti-MEM containing 0.25-4 μ g of the indicated plasmid DNA. Following an additional 15 min incubation at room temperature, the DNA-Lipofectamine 2000 mixture (~100 μ l) was added dropwise to a monolayer of 1×10^6 HeLa, HEK 293T, or BMK cells covered in 900 μ l of Opti-MEM. Transfected cells were incubated at 37°C and 5% CO₂ for 2 h before being supplemented with an equal volume of DMEM containing 20% HI-FBS and 200 μ M L-glutamine. When the inhibition of caspase activation was desired, the transfection medium was removed after 2 h and replaced with DMEM containing 10% HI-FBS, 200 μ M L-glutamine, and 50 μ M z.VAD.fmk, a pan-caspase inhibitor (Kamiya Biomedical Company). Transfected cells were incubated at 37°C and 5% CO₂ for approximately 16-18 h before cells were harvested.

2.4. VIRUSES AND THEIR MANIPULATION

2.4.1. Viruses. All viruses used in this study are listed in Table 2.4. WT vaccinia virus (VV) strain Copenhagen, VVCop, and VVCop expressing the enhanced green fluorescent protein (EGFP), VV-EGFP, were kindly provided by G. McFadden (University of Florida, Gainesville, FL). VV strain Copenhagen devoid of E3L, VV Δ E3L, was provided by B. Jacobs (Arizona State University, Tempe, AZ) (31). VVCop lacking the F1L open reading frame (ORF), VV Δ F1L, was generated by disrupting the F1L ORF with the EGFP ORF, as previously described (453). VV strain Western Reserve expressing a Flag-tagged F1L (VWWR-Flag-F1L) was generated as described previously (455). The generation of the recombinant viruses VV-Flag-F1L, VV Δ F1L-Flag-FPV039(1-176), VV Δ F1L-Flag-FPV039(1-94), VV Δ F1L-Flag-FPV039(Δ 41-54), and VV Δ F1L-DPV022 is described in section 2.4.3. All virus stocks except for VV Δ E3L were

Table 2.4. Viruses Used

Virus	Strain	Description/Properties	Source
VVCop	Copenhagen	Wild-type vaccinia virus	G. McFadden
VV-EGFP	Copenhagen	Wild-type vaccinia virus expressing EGFP	G. McFadden
VVΔF1L	Copenhagen	Vaccinia virus lacking F1L	(453)
VVWR-Flag-F1L	Western Reserve	Vaccinia virus strain Western Reserve expressing Flag-tagged F1L	(406)
VV-Flag-F1L	Copenhagen	Vaccinia virus Flag-tagged F1L	This study
VVΔE3L	Copenhagen	Vaccinia virus lacking E3L	(31)
VVΔF1L-Flag-FPV039(1-176)	Copenhagen	Vaccinia virus devoid of F1L but expressing wild-type, Flag-tagged FPV039(1-176)	This study
VVΔF1L-Flag-FPV039(1-94)	Copenhagen	Vaccinia virus devoid of F1L but expressing Flag-tagged FPV039(1-94)	This study
VVΔF1L-Flag-FPV039(Δ41-54)	Copenhagen	Vaccinia virus devoid of F1L but expressing Flag-tagged FPV039(Δ41-54)	This study
VVΔF1L-Flag-DPV022	Copenhagen	Vaccinia virus devoid of F1L but expressing wild-type, Flag-tagged DPV022	This study

propagated in BGMK cells as described previously (408). VV Δ E3L was propagated in BHK cells. All vaccinia viruses used in this study were strain Copenhagen with the exception of VVWR-Flag-F1L, which is strain Western Reserve and labelled accordingly. All viruses were stored at -80°C. Prior to use, viruses were thawed at 37°C and sonicated for 20 s with 0.5 s on/off pulses (Misonix Inc.).

2.4.2. Virus infection protocol. In general, to infect a monolayer of 1×10^6 HeLa, LMH, or BMK cells, 0.5 ml of the appropriate culture medium was added to the monolayer along with the indicated multiplicity of infection (MOI) of virus. Cells were incubated for 1 h at 37°C and 5% CO₂ with gentle rocking every 10 min to allow virus to adhere to the cells. After 1 h, an additional 1 ml of medium was added to the monolayer, cells were incubated at 37°C and 5% CO₂, and the infection was allowed to proceed for the indicated time. Similarly, to infect a monolayer of 7×10^6 HeLa or LMH cells, 3.5 ml of medium was added to the monolayer along with the indicated MOI of virus. Following a 1 h incubation, an additional 7 ml of medium was added, and the infection was allowed to proceed for the indicated time.

To infect Jurkat cells in suspension, 1×10^6 cells were re-suspended in 200 μ l of medium, and the indicated MOI of virus was added. Cells were rotated continuously for 1 h at 37°C and then transferred to a 6-well tissue culture plate containing 0.8 ml of medium per well. Cells were incubated at 37°C and 5% CO₂ for the remainder of the infection.

2.4.3. Generation of recombinant vaccinia viruses. To generate VV-Flag-F1L, a recombinant VVCop expressing Flag-F1L, CV-1 cells were infected at an

MOI of 0.05 with VVCop and transfected with 5 µg of pSC66-Flag-F1L using Lipofectin (Invitrogen). To generate VVΔF1L-Flag-FPV039(1-176), a recombinant VVΔF1L expressing Flag-FPV039(1-176), or VVΔF1L-Flag-FPV039(1-94), a recombinant VVΔF1L expressing Flag-FPV039(1-94), CV-1 cells were infected at an MOI of 0.05 with VVΔF1L and transfected with 5 µg of pSC66-Flag-FPV039(1-176) or pSC66-Flag-FPV039(1-94), respectively, using Lipofectin. To generate VVΔF1L-Flag-FPV039(Δ41-54), a recombinant VVΔF1L expressing Flag-FPV039(Δ41-54), or VVΔF1L-Flag-DPV022, a recombinant VV expressing Flag-DPV022, BGMK cells were infected at an MOI of 0.05 with VVΔF1L and transfected with 5 µg of linearised pSC66-Flag-FPV039(Δ41-54) or pSC66-Flag-DPV022, respectively, using Lipofectin. The pSC66 vector contains two regions of homology to the VV thymidine kinase (TK) gene that flank a *lacZ* gene and its promoter, the gene of interest, and a synthetic poxviral early/late promoter that drives expression of the gene of interest in VV-infected cells only. Following infection and transfection, homologous recombination between the VV TK gene and the TK sequences flanking *lacZ*, the gene of interest, and the poxviral promoter results in the integration of these components into the VV TK gene and the concomitant disruption of the VV TK gene (Fig. 2.2). Recombinant viruses were selected for growth on HuTK^{-/-}-143B cells in the presence of 25 µg/ml 5-deoxy-2'-bromouridine (Sigma-Aldrich), in which VV not possessing a disrupted TK gene was unable to grow. Recombinant viruses were also plaque purified as described in section 2.4.4. and previously (123). The presence of Flag-F1L, Flag-FPV039(1-176), Flag-FPV039(1-94), Flag-FPV039(Δ41-54), and Flag-DPV022 in each recombinant virus was confirmed by PCR, and protein expression was confirmed by Western blotting using the anti-FlagM2 antibody (Sigma-Aldrich).

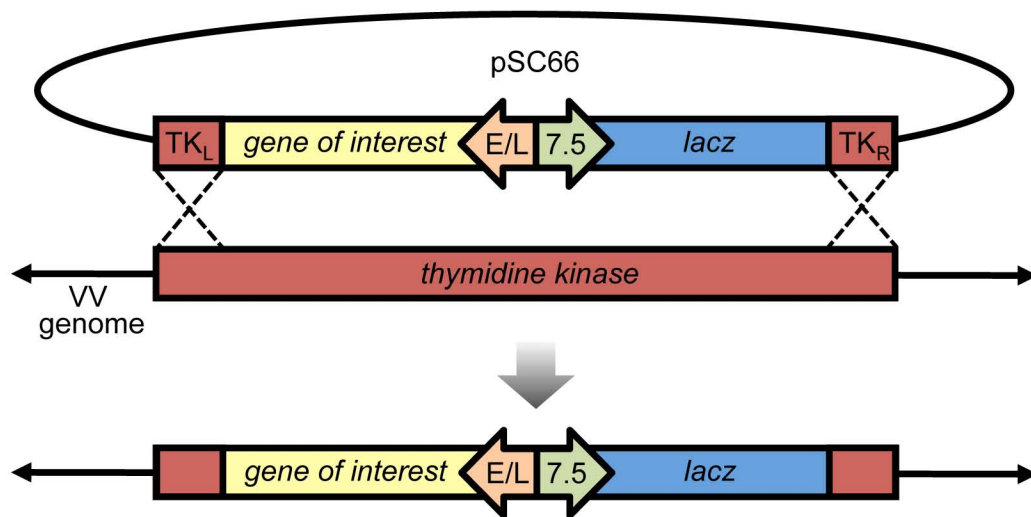


Figure 2.2. Generation of recombinant vaccinia viruses. The pSC66 vector expresses the gene of interest from a synthetic poxviral early/late (E/L) promoter and the *lacZ* gene from the 7.5 promoter. The genes are flanked by a region of homology to the 3' end of the VV *thymidine kinase* gene (TK_L) and the 5' end of the VV *thymidine kinase* gene (TK_R). Following transfection with the pSC66 plasmid and infection with VV, homologous recombination occurs between the TK homologous regions on the pSC66 vector and the *thymidine kinase* gene in the genome of VV. The resulting recombinant viruses have a disrupted *thymidine kinase* gene and express both the gene of interest and β -galactosidase.

2.4.4. Plaque purification. To positively select for VV recombinants, a monolayer of 1×10^6 cells was overlaid with approximately 1 ml of a low melting point agarose mixture (LMP) containing 2.5 ml of 2.5% (w/v) LMP agarose, 2.5 ml 2xDMEM (2.7% w/v DMEM, 88mM NaHCO_3), 1 ml HI-FBS, and 100 μl 5-bromo-4-chloro-3-indolyl- β -D-galactopyranoside (X-gal; Rose Scientific Ltd.) at 100 mg/ml in dimethylformamide (Sigma-Aldrich). The agarose was permitted to solidify at room temperature before the cells were incubated at 37°C and 5% CO_2 for up to 24 h. Because the recombinant viruses produced in this study express the *lacZ* gene product β -galactosidase (see section 2.4.3.), which cleaves X-gal to produce galactose and 5,5'-dibromo-4,4'-dichloroindigo, an insoluble blue precipitate, successful recombination events could be visualised by the appearance of blue VV plaques. Blue plaques were picked using a Pasteur pipette and re-suspended in 100 μl of swelling buffer (10 mM Tris, pH 8.0, 2 mM MgCl_2). Following three freeze/thaw cycles at -80°C and 37°C , respectively, 100 μl of 2xDMEM was added, and the plaques were sonicated (20 s, 0.5 s on/off pulses) before being used to re-infect another monolayer. This process was repeated until only blue plaques were visible.

2.4.5. Preparation of virus chromosomal DNA. Total viral and cellular DNA was isolated and prepared from virus-infected cells using SDS lysis and phenol:chloroform extraction. The medium from an infected monolayer of 1×10^6 cells was removed and replaced with cell lysis buffer containing 1.2% SDS, 50 mM Tris-HCl (pH 8.0), 4 mM EDTA, 4 mM CaCl_2 , and 0.2 mg/ml proteinase K (Roche). After a minimum 4 h incubation at 37°C and 5% CO_2 , the lysed cells were removed to a microfuge tube, and DNA was extracted by vigorous vortexing with half a volume of phenol:chloroform (1:1). Following centrifugation, the

aqueous layer was incubated at 4°C for 10 min with 50 µl of 3M NaCH₃COO and 2.5 volumes of 95% ethanol to precipitate the DNA. DNA was pelleted by centrifugation (9000 x g, 10 min), and the pellet was re-suspended in 50 µl dH₂O.

2.4.6. Preparation of virus stocks. In general, infected BGMK cells (3×10^8 per roller bottle) were harvested using SSC (150 mM NaCl, 15 mM tri-sodium citrate) and pelleted by centrifugation (300 x g, 5 min). The pellet was re-suspended in 20 ml swelling buffer and subjected to three freeze/thaw cycles at -80°C and 37°C. Cell membranes were lysed on ice by dounce homogenisation with a “B” pestle (Bellco Biotechnology) approximately 100 times. Following centrifugation (300 x g, 5 min) of the homogenates, the supernatant was set aside and the pellet was re-suspended in 10 ml swelling buffer. The pellet was dounce homogenised on ice an additional 60 times and centrifuged (300 x g, 5 min). The supernatants were combined and centrifuged (10 000 x g, 1 h) to pellet virus. The virus pellet was re-suspended in 1 ml DMEM.

2.4.7. Quantification of virus. The number of plaque forming units (PFU) per ml of virus stock was quantified by serial dilution and titration of virus on BGMK cells. Briefly, 10 µl of a virus stock was diluted by a factor of 1000 in 990 µl medium, and 100 µl of this dilution was then serially diluted 6 times in 900 µl medium by a factor of 100. The 6 serial dilutions (10^{-2} to 10^{-8}) were used to infect, in duplicate, 6 wells of a tissue culture plate containing a sub-confluent layer of BGMK cells. Following 24-48 h of infection, cells were fixed with neutral-buffered formalin (37% (w/v) formaldehyde (Sigma), pH 7.4; 100 ml 10x PBS) and stained with a solution containing 0.1% (w/v) crystal violet (Sigma-Aldrich) and 20% (v/v) ethanol. Virus plaques were visible as clearings in the monolayer

and counted. The PFU/ml of the virus stock was calculated by multiplying the number of plaques counted in one well by the reciprocal of the dilution factor of that well and then dividing by the volume of medium used to infect that well $[(\# \text{plaques}) \times (1/\text{dilution}) / \text{volume} = \text{PFU/ml}]$. The values from both plates were averaged.

The volume of virus stock used to infect a monolayer of cells at a given MOI (or PFU/cell) was calculated as follows: The number of cells in the monolayer was multiplied by the desired MOI to obtain the total number of PFU required. This value was divided by the concentration of the virus stock (PFU/ml) to obtain the volume of the virus stock necessary to achieve the desired MOI.

2.5. PROTEIN METHODOLOGY

2.5.1. Antibodies. All antibodies and the purpose for which they were used in this study are listed in Table 2.5. The concentration or amount of antibody used and the source of each antibody is also given.

2.5.2. Immunoprecipitations. In general, cells were lysed at 4°C for 2 h in 1 ml of 2% CHAPS lysis buffer containing 2% (w/v) CHAPS (3-[3-cholamidopropyl]-dimethylammonio]-1-propanesulfonate; Sigma-Aldrich), 150 mM NaCl, 50 mM Tris (pH 8.0), and complete, EDTA-free protease inhibitor cocktail tablet (Roche). Following lysis, membranes and other insoluble components were pelleted by centrifugation (9000 x g, 10 min) and removed. Ten percent of the supernatant was reserved as input lysate and subjected to acetone precipitation (section 2.5.3.). Antibody was added to the remainder of the supernatant at the appropriate concentration (Table 2.5.), and the supernatant was incubated at 4°C for 2 h. Following the incubation, 25-40 µl of a 1:1 slurry of lysis buffer and

Table 2.5. Antibodies Used

Antibody	Dilution/Amount	Source
<i>Immunoprecipitation</i>		
Goat anti-EGFP	1 µl	L. Berthiaume
Mouse anti-Bax2D2	1 µg	Trevigen
Mouse anti-Bax6A7	1 µg	BD Biosciences
Mouse anti-FlagM2	1 µg	Sigma-Aldrich
Rabbit anti-BakNT	1-2 µg	Upstate
Rabbit anti-FlagM2	0.8 µg	Sigma-Aldrich
<i>Western Blot</i>		
Mouse anti-β-tubulin	1:2000	ECM Biosciences
Mouse anti-Bak	1:500	PharMingen
Mouse anti-Bax2D2	1:20 000	Trevigen
Mouse anti-EGFP	1:5000	Covance
Mouse anti-FlagHRP	1:2000	Sigma-Aldrich
Mouse anti-HA (12CA5)	1:4000	Roche Diagnostics
Mouse anti-I3L	1:20	D. Evans
Mouse anti-Myc (9E10)	1:2500	M. Barry
Mouse anti-Noxa	1:300	Enzo Life Sciences
Mouse anti-PARP	1:2000	BD Biosciences
Mouse anti-T7	1:5000	Novagen
Rabbit anti-BakNT	1:2000	Upstate
Rabbit anti-BaxN20	1:500	Santa Cruz
Rabbit anti-cleaved caspase-3	1:1000	New England Biolabs
Peroxidase-conjugated AffiniPure donkey anti-mouse	1:30 000	Jackson ImmunoResearch Laboratories Ltd.
Peroxidase-conjugated AffiniPure donkey anti-rabbit	1:30 000	Jackson ImmunoResearch Laboratories Ltd.
<i>Confocal</i>		
Mouse anti-Bax6A7	1:500	BD Biosciences
Mouse anti-dsRNA (J2)	1:200	English and Scientific Consulting Bt.
Mouse anti-I3L	1:100	D. Evans
Mouse anti-Myc (9E10)	1:200	M. Barry
Goat anti-mouse AlexaFluor546	1:400	Molecular Probes
<i>Flow Cytometry</i>		
Mouse anti-BakAb-1	2 µg/ml	Oncogene Research Products
Mouse anti-Bax6A7	2 µg/ml	BD Biosciences
Mouse anti-dsRNA (J2)	2 µg/ml	English and Scientific Consulting Bt.
Mouse anti-NK1.1 (PK136)	2 µg/ml	K. Kane & (244)
Phycoerythrin-conjugated goat anti-mouse	1:100	Jackson ImmunoResearch Laboratories Ltd.

protein A- or protein G-conjugated sepharose beads (GE Healthcare) were added to the supernatant, which was then incubated for an additional 1 h at 4°C. Finally, the supernatant was removed, beads were washed 3 times with 500 µl 2% CHAPS lysis buffer, and the beads were re-suspended in SDS-PAGE loading buffer (see section 2.5.4.).

2.5.3. Acetone precipitation. Protein dissolved in 2% CHAPS lysis buffer was precipitated with the addition of 5 volumes of ice-cold acetone and a 30 min incubation at -20°C. Precipitates were pelleted by centrifugation (9000 x g, 15 min) and re-suspended in SDS-PAGE loading buffer (see section 2.5.4.)

2.5.4. SDS poly-acrylamide gel electrophoresis. SDS poly-acrylamide gel electrophoresis (SDS-PAGE) was performed as described (255). Briefly, the Mini-PROTEAN3 Cell system (Bio-Rad) was used to resolve proteins on 10-15% acrylamide gels. Protein samples were mixed with SDS-PAGE loading buffer containing 10% (w/v) glycerol, 62.5 mM Tris (pH 6.8), 2% (w/v) SDS, 50 mM β-mercaptoethanol, and 0.125% bromophenol blue and boiled at 100°C for 15 min before loading onto the gel. Pre-stained protein molecular weight markers (Fermentas) were used as size ladders for all gels. Gels were run at 150-200 V in buffer containing 25 mM Tris, 190 mM glycine, and 3.5 mM SDS until resolved.

2.5.5. Semi-dry transfer. Proteins resolved by SDS-PAGE were transferred for 2 h at 450 mA from the acrylamide gels to polyvinylidene fluouride (PVDF) membranes (GE Healthcare) using a semi-dry transfer apparatus (Tyler Research) and buffer containing 192 mM glycine, 25 mM Tris, and 20% methanol. Before transfer, PVDF membranes were activated with methanol for

30 s, according to manufacturer's directions. Following transfer, PVDF membranes were blocked for 3-16 h in 5% (w/v) skim milk powder and Tris-buffered saline plus Tween-20 (TBST) containing 200 mM Tris (pH 7.5), 15 mM NaCl, and 0.1% (v/v) Tween-20 (Fisher Scientific).

2.5.6. Western blotting. PVDF membranes were Western blotted with the antibodies and concentrations listed in Table 2.5. Membranes were incubated at room temperature for 3 h or 4°C overnight with between 7-10 ml of primary antibody diluted in either TBST or TBST plus 5% (w/v) skim milk powder. Following incubation with primary antibody, membranes were washed with TBST for 10 min while rocking at room temperature and then incubated for 1 h with the appropriate horse-radish peroxidase (HRP)-conjugated secondary antibody diluted in TBST. If the primary antibody was mouse anti-FlagHRP (Sigma-Aldrich), a FlagM2 antibody conjugated to HRP, then no secondary antibody was added. Finally, membranes were washed 3 times with TBST for 20 min each while rocking at room temperature. Western blots were visualised using enhanced chemiluminescence (ECL) according to the manufacturer's directions (GE Healthcare) and Amersham Hyperfilm ECL (GE Healthcare).

2.5.7. Sequence analyses. Protein sequences obtained from NCBI databases were aligned using AlignX software (Invitrogen) or ClustalW, an online service provided by the European Bioinformatics Institute and the European Molecular Biology Laboratory (www.ebi.ac.uk) (259). The secondary structure of FPV039 was predicted using the online service JPred, provided by the University of Dundee, Scotland (www.compbio.dundee.ac.uk) (85). The transmembrane

domain of FPV039 was predicted using the online service Tmpred, provided by the Swiss node of the European Molecular Biology Net (www.ch.embnet.org).

2.6. ASSAYS

2.6.1. Immunoprecipitations to detect interaction

2.6.1.1. FPV039 and Bak. HEK 293T cells (1×10^6) were transfected using Lipofectamine 2000 with 2 μ g pEGFP-C3, pEGFP-F1L, pEGFP-FPV039(1-176), pEGFP-FPV039(1-94), or pEGFP-FPV039(Δ 41-54) and co-transfected with 2 μ g of pcDNA3-HA-Bak. Cells were lysed in 2% CHAPS lysis buffer, followed by precipitation using goat anti-EGFP antibody (L. Berthiaume, University of Alberta, Edmonton, AB). Immunoprecipitates were Western blotted with mouse anti-EGFP (Covance) or mouse anti-HA (12CA5) (Roche) antibodies, and lysates were Western blotted with mouse anti-EGFP, mouse anti-HA (12CA5), or anti-BakNT (Upstate) antibodies.

Similar experiments were performed in the context of viral infection. HeLa or LMH cells (7×10^6) were infected with VV-EGFP, VV Δ F1L, VVWR-Flag-F1L VV Δ F1L-Flag-FPV039(1-176), or VV Δ F1L-Flag-FPV039(1-94) at an MOI of 5 for six hours or, in the case of VV Δ F1L-Flag-FPV039(1-94), 16 hours. Cells were lysed in 2% CHAPS lysis buffer, followed by precipitation using rabbit anti-BakNT or mouse anti-FlagM2 (Sigma-Aldrich) antibodies. Immunoprecipitates were Western blotted with mouse anti-FlagHRP, rabbit anti-BakNT, or mouse anti-Bak (Pharmingen) antibodies, and lysates were Western blotted with mouse anti-FlagHRP or rabbit anti-BakNT antibodies.

2.6.1.2 FPV039 and Bax. HEK 293T or Bak^{-/-} BMK cells (1×10^6) were transfected using Lipofectamine 2000 with 0.25 μ g pEGFP-C3, 2 μ g pEGFP-

FPV039(1-176), 2 µg pEGFP-FPV039(Δ41-54), 2 µg pEGFP-FPV039(1-94), 4 µg pEGFP-F1L, 2 µg pEGFP-M11L, 2 µg pEGFP-N1L, or 0.5 µg pEGFP-Bcl-2 and 2 µg pcDNA3-HA-Bax. zVAD.fmk (50 µM) was added following transfection to prevent the downstream activation of caspases. Cells were lysed in 2% CHAPS lysis buffer, followed by precipitation using goat anti-EGFP antibody. Immunoprecipitates and lysates were Western blotted with mouse anti-EGFP, mouse anti-HA (12CA5), or rabbit anti-BaxN20 (Santa Cruz) antibodies.

Similar experiments were performed in the context of viral infection. HeLa cells (7×10^6) were infected with VVΔF1L, VV-Flag-F1L, or VVΔF1L-Flag-FPV039(1-176) at an MOI of 5 for 16 hours. Cells were lysed in 2% CHAPS lysis buffer, followed by immunoprecipitation using rabbit anti-FlagM2 (Sigma-Aldrich) or mouse anti-Bax6A7 (BD Biosciences) antibodies. Immunoprecipitates were Western blotted with mouse anti-FlagHRP or mouse anti-Bax2D2 (Trevigen) antibodies, and lysates were Western blotted with mouse anti-FlagHRP, rabbit anti-BaxN20, or mouse anti-Bax2D2 antibodies.

2.6.1.3. FPV039 and BH3-only proteins. HEK 293T cells (1×10^6) were transfected using Lipofectamine 2000 with 0.25 µg pEGFP-C3, 2 µg pEGFP-FPV039(1-176), 0.5 µg pEGFP-Bcl-2, 0.5 µg pEGFP-Bcl-x_L, or 2 µg pEGFP-Mcl-1 and 1 µg of pcDNA3-Flag-Bim_L, pcDNA3-Myc-Bik, pcDNA3-Bmf-T7, pXJ40-HA-Bad, pcDNA3-HA-Puma, pcDNA3-Bid-Flag, pcDNA3-tBid-Flag, or pcDNA3.1-Noxa. zVAD.fmk (50 µM) was added following transfection to prevent the downstream activation of caspases. Cells were lysed in 2% CHAPS lysis buffer, followed by precipitation using goat anti-EGFP antibody. Immunoprecipitates and lysates were Western blotted with mouse anti-FlagHRP, mouse anti-EGFP, anti-Myc (9E10) (M. Barry, University of Alberta, Edmonton,

AB), mouse anti-T7 (Novagen), mouse anti-HA (12CA5), or mouse anti-Noxa (Enzo Life Sciences) antibodies.

2.6.1.4. DPV022 and Bak and Bax. HEK 293T cells (1×10^6) were transfected using Lipofectamine 2000 with 1 μ g pEGFP-C3, 2 μ g pEGFP-FPV039(1-176), 2 μ g pEGFP-M11L, 2 μ g pEGFP-F1L, 2 μ g pEGFP-DPV022, 2 μ g pEGFP-Bcl-x_L, or 2 μ g pEGFP-Bcl-2 and 2 μ g of either pcDNA3-HA-Bak or pcDNA3-HA-Bax. zVAD.fmk (50 μ M) was added following transfection to prevent the downstream activation of caspases. Cells were lysed in 2% CHAPS lysis buffer, followed by precipitation using goat anti-EGFP antibody. Immunoprecipitates and lysates were Western blotted with mouse anti-EGFP or mouse anti-HA (12CA5) antibodies.

Similar experiments were performed in the context of viral infection. HeLa cells (7×10^6) were infected with VV Δ F1L or VV Δ F1L-Flag-DPV022 at an MOI of 2 for 10 h. Cells were lysed in 2% CHAPS lysis buffer and pre-cleared for 30 min with protein A beads. Lysates were split equally into two volumes and immunoprecipitated with either mouse anti-Bax2D2 or rabbit anti-BakNT antibodies. Immunoprecipitates and lysates were Western blotted with mouse anti-FlagHRP, mouse anti-Bak, or mouse anti-Bax2D2 antibodies.

2.6.2. Confocal microscopy to assess sub-cellular localisation

2.6.2.1. Live-cell confocal microscopy to assess localisation of FPV039 and DPV022. To assess the localisation of FPV039, 1×10^6 HeLa cells or LMH cells were grown on 18 mm glass coverslips in modified 3.5 cm cell culture dishes (Corning) and transfected using Lipofectamine 2000 with 2 μ g of pEGFP-C3, pEGFP-F1L, pEGFP-FPV039(1-176), pEGFP-FPV039(Δ 41-54), pEGFP-

FPV039(1-94), pEGFP-FPV039(1-141), or pEGFP-FPV039(142-176). To assess the localisation of DPV022, 1×10^6 HeLa cells were grown on glass bottom no. 1.0 cell culture dishes (MatTek Corporation) and transfected using Lipofectamine 2000 with 0.5 μ g pEGFP-C3 or 2 μ g of pEGFP-DPV022. Mitochondria were labelled with 15 ng/ml of MitoTracker Red CMXRos (Invitrogen). Live cells were examined using a Zeiss LSM510 laser scanning confocal microscope at 543 nm to detect MitoTracker fluorescence and 489 nm to detect EGFP fluorescence.

2.6.2.2. Fixed-cell confocal microscopy to assess localisation of dsRNA, I3L, and Noxa. HeLa cells (5×10^5) seeded on glass coverslips were infected with VVCop, VV Δ F1L, or VV Δ E3L at an MOI of 5 for 4, 12, or 20 h. Cells were subsequently fixed for 5 min in 4% paraformaldehyde (Sigma-Aldrich), permeabilised for 5 min with 0.04% saponin (Sigma-Aldrich), and blocked for 30 min with 30% goat serum (Invitrogen). Cells were incubated with mouse anti-dsRNA (J2) (English and Scientific Consulting Bt.), mouse anti-I3L (D. Evans, University of Alberta, Edmonton, AB), or mouse anti-Noxa antibodies for 1 h and, following that, with goat anti-mouse AlexaFluor546 secondary antibody (Molecular Probes) for 1 h. In between each step, cells were washed with phosphate-buffered saline (PBS; 1.4 M NaCl, 8 mM Na₂HPO₄, 26.8 mM KCl, 17.2 mM KH₂PO₄) plus 1% (v/v) HI-FBS. Coverslips were mounted using mowiol mounting medium (0.096 g/ml mowiol (Calbiochem), 0.24 g/ml glycerol, 0.48% (v/v) PBS (pH 7.4), 0.1% (v/v) N-propyl-gallate (Sigma)) plus 4'6-diamino-2-phenylindole (DAPI) to visualise cell nuclei and virus factories. Cells were examined using a Zeiss LSM710 laser scanning confocal microscope at 405 nm to detect DAPI, and 543 nm to detect the goat anti-mouse AlexaFluor546 secondary antibody.

To detect Myc-Noxa, 5×10^5 HeLa cells were seeded on glass coverslips and transfected with 2 μg of pcDNA3.1-Myc-Noxa. Sixteen hours later, cells were infected with VVCop or VV Δ E3L at an MOI of 5 for 12 h. Cells were prepared as described above, and incubated with mouse anti-Myc (9E10) antibody for 1 h followed by goat anti-mouse AlexaFluor546 secondary antibody for 1 h. Coverslips were mounted using mowiol mounting medium plus DAPI to visualise cell nuclei and virus factories. Cells were examined using a Zeiss LSM710 laser scanning confocal microscope at 405 nm to detect DAPI and 543 nm to detect the goat anti-mouse AlexaFluor546 secondary antibody.

2.6.3. Measurement of mitochondrial membrane potential. Changes in the mitochondrial membrane potential were quantified by staining with tetramethylrhodamine ethyl ester (TMRE) (Invitrogen Life Technologies) (125, 309). HeLa cells (1×10^6) were transfected using Lipofectamine 2000 with 0.5 μg pEGFP-C3, 2 μg pEGFP-FPV039(1-176), 2 μg pEGFP-FPV039(142-176), 4 μg pEGFP-DPV022, 4 μg pEGFP-F1L, 4 μg pEGFP-M11L, 2 μg pEGFP-Bcl-2, 2 μg pEGFP-Bcl-X_L, or 2 μg pEGFP-Mcl-1 and apoptosis was induced by treating cells with 10 ng/ml of tumour necrosis factor α (TNF α ; Roche) and 5 $\mu\text{g}/\text{ml}$ of cycloheximide (ICN Biomedicals Inc.) for 6h or by transfecting cells with 2 μg of pcDNA3-HA-Bak, 0.75 μg of pcDNA3-HA-Bax, or 1 μg of pcDNA3-Flag-Bim_L, pcDNA3-Myc-Bik, pcDNA3-T7-Bmf, pXJ40-HA-Bad, pcDNA3-HA-Puma, pcDNA3-Bid-Flag, pcDNA3-tBid-Flag, or pcDNA3.1-Noxa for 18 h. Following treatment or transfection, cells were washed with PBS and stained for 30 min at 37°C and 5% CO₂ with medium containing 0.2 μM TMRE. Cells were then harvested and re-suspended in PBS plus 1% (v/v) HI-FBS before being analysed by two-colour flow cytometry (FACScan; Becton Dickinson) with TMRE

fluorescence measured through the FL-2 channel equipped with a 585 nm filter (42 nm band pass) and EGFP fluorescence measured through the FL-1 channel equipped with a 489 nm filter (42 nm band pass). Data were acquired on 20 000 cells per sample with fluorescence signals at logarithmic gain, and analysis was performed using CellQuest software. The overall percentage of cells that exhibited a loss in mitochondrial membrane potential was calculated taking into account the cytotoxicity induced by transfection. The number of EGFP-positive, TMRE-negative cells was divided by the total number of EGFP-positive cells to determine the percentage of apoptotic cells in transfected samples treated with an apoptotic stimulus or left untreated. The value obtained for transfected but untreated cells was subtracted from the value obtained for transfected cells also treated with an apoptotic stimulus to give the overall percentage of apoptotic cells.

To assess the expression levels of transfected proteins, parallel transfections were performed for each experiment and whole cell lysates were harvested into SDS-PAGE loading buffer. Following SDS-PAGE, lysates were Western blotted with the following antibodies: mouse anti-EGFP, mouse anti-BakNT, mouse anti-HA (12CA5), mouse anti-FlagHRP, mouse anti-Myc, mouse anti-T7, or mouse anti-Noxa.

Similar experiments were performed in the context of viral infection. WT Jurkat cells or Jurkat cells over-expressing Bcl-2 (1×10^6) were infected at an MOI of 10 for 8 h with VV-EGFP, VV Δ F1L, VV Δ F1L-Flag-FPV039(1-176), or VV Δ F1L-Flag-FPV039(1-94). Cells were stained with TMRE and analysed by two-colour flow cytometry as described above.

2.6.4. Measurement of Bak and Bax activation

2.6.4.1. Measurement of Bak and Bax N-terminus exposure by flow cytometry.

To measure the N-terminal exposure of Bak, 1×10^6 WT Jurkat cells, Jurkat cells over-expressing Bcl-2, or *Bak*^{-/-}/*Bax*^{-/-} Jurkat cells were infected at an MOI of 10 for 4 h with VV-EGFP, VVΔF1L, VVΔF1L-Flag-FPV039(1-176), VVΔF1L-Flag-FPV039(1-94), or VVΔF1L-Flag-DPV022 and then treated with 0.25 μM staurosporine (STS; Sigma-Aldrich) for 2 h. To measure the N-terminal exposure of Bax, 1×10^6 WT Jurkat cells, Jurkat cells over-expressing Bcl-2, or *Bak*^{-/-}/*Bax*^{-/-} Jurkat cells were infected at an MOI of 10 for 6 h with VV-EGFP, VVΔF1L, VVΔF1L-Flag-FPV039(1-176), VVΔF1L-Flag-FPV039(Δ41-54), or VVΔF1L-Flag-DPV022 and then treated with 2 μM STS for 2 h. All cells were fixed for 5 min in PBS plus 0.25% paraformaldehyde and then permeabilised and stained in PBS containing 500 μg/ml digitonin (Sigma-Aldrich) and 2 μg/ml mouse anti-BakAb-1 antibody (Oncogene Research Products) (162, 163), 2 μg/ml mouse anti-Bax6A7 antibody (201), or 2 μg/ml of an isotype control antibody specific for NK1.1 (PK136) (provided by K. Kane, University of Alberta, Edmonton, AB) (244). Following permeabilisation, cells were counterstained with phycoerythrin-conjugated anti-mouse antibody (Jackson ImmunoResearch Laboratories Inc.). In between each step, cells were washed with PBS, and prior to analysis by flow cytometry, cells were re-suspended in PBS plus 1% (v/v) HI-FBS. Antibody staining was analysed by flow cytometry (FACScan; Becton Dickinson) with fluorescence measured through the FL-2 channel equipped with a 585 nm filter (42 nm band pass). Data were acquired on 20 000 cells per sample with fluorescence signals at logarithmic gain, and analysis was performed using CellQuest software.

2.6.4.2. Measurement of Bax N-terminus exposure by fixed-cell confocal microscopy. HeLa cells (5×10^5) were infected with VV-EGFP, VV Δ F1L, VV Δ F1L-Flag-FPV039(1-176), or VV Δ F1L-Flag-FPV039(Δ 41-54) at an MOI of 10 for 24 h. Cells were subsequently fixed in 4% paraformaldehyde, permeabilised with 0.04% saponin, and blocked with PBS plus 1% HI-FBS. Cells were incubated with mouse anti-Bax6A7 antibody for 1 h, followed by goat anti-mouse AlexaFluor546 secondary antibody for 1 h. In between each step, cells were washed with PBS plus 1% (v/v) HI-FBS. Coverslips were mounted in 50% glycerol containing 4 mg/ml N-propyl-gallate (Sigma-Aldrich) and 250 μ g/ml DAPI. Cells were analysed by an LSM510 laser scanning confocal microscope at 543 nm to detect goat anti-mouse AlexaFluor546 and 489 nm to detect EGFP fluorescence. Confocal results were quantified as the percentage of cells displaying anti-Bax6A7-positivity over the total number of cells and given as the mean \pm standard deviation. At least 700 cells were counted per sample, and the standard deviations were calculated from at least 18 different fields of view.

2.6.4.3. Measurement of Bax N-terminus exposure by immunoprecipitation. To assess Bax activation by immunoprecipitation, 7×10^6 HeLa cells were infected at an MOI of 10 for 24 h with VV-EGFP, VV Δ F1L, VV Δ F1L-Flag-FPV039(1-176), or VV Δ F1L-Flag-FPV039(Δ 41-54). Cells were lysed in 2% CHAPS lysis buffer or 1% TRITON X-100 lysis buffer containing 1% (v/v) TRITON X-100, 150 mM NaCl, 50 mM Tris (pH 8.0), and complete, EDTA-free protease inhibitor cocktail tablet, followed by an overnight immunoprecipitation using mouse anti-Bax6A7 antibody. Immunoprecipitates and lysates were Western blotted with rabbit anti-BaxN20 antibody.

2.6.4.4. Assessment of Bax oligomerisation by cross-linking. HEK 293T cells (1×10^6) were transfected with 0.25 μ g pEGFP-C3, 1 μ g pEGFP-FPV039(1-176), 2 μ g pEGFP-FPV039(Δ 41-54), 2 μ g pEGFP-FPV039(1-94), 1 μ g pEGFP-DPV022, or 0.5 μ g pEGFP-Bcl-2 and 0.25 μ g pcDNA-HA-Bax. zVAD.fmk (50 μ M) was added following transfection to prevent the downstream activation of caspases. Cells were lysed in 2% CHAPS lysis buffer. Following lysis, nuclei and membranes were pelleted (9000 x g, 10 min), and the supernatant was incubated with 1 μ M 1,6-bismaleimido-hexane (BMH) (Thermo Scientific) dissolved in DMSO for 30 min. Twenty percent of the lysate was reserved as input lysate and treated with DMSO only. Supernatants were acetone precipitated, and cross-linking was quenched by the addition of SDS-PAGE loading buffer containing 100 mM β -mercaptoethanol. Protein samples were separated by SDS-PAGE and analysed by Western blotting with mouse anti-HA (12CA5) or mouse anti-EGFP antibodies.

2.6.5. Assessment of apoptosis by PARP and caspase-3 cleavage. WT Jurkat, HeLa, WT BMK, or Noxa^{-/-} BMK cells (1×10^6) were infected at an MOI of 5 with VVCop, VV Δ F1L, or VV Δ E3L. Whole-cell lysates were harvested in SDS-PAGE loading buffer at various time points up to 24 hours post-infection (hpi). Following SDS-PAGE, membranes were Western blotted with mouse anti-PARP (BD Biosciences), rabbit anti-cleaved caspase-3 (New England Biolabs), mouse anti-I β L, or mouse anti- β -tubulin (ECM Biosciences) antibodies.

2.6.6. Quantification of dsRNA by flow cytometry. WT Jurkat cells (1×10^6) were infected at an MOI of 5 for 4 or 16 h with VVCop, VV Δ F1L, or VV Δ E3L. Cells infected for 16 h were treated with or without 80 μ g/ml cytosine arabinoside

(AraC; Sigma-Aldrich) for the duration of the infection to inhibit poxviral DNA replication. Cells were fixed for 5 min in PBS plus 0.25% paraformaldehyde and then permeabilised and stained in PBS containing 500 µg/ml digitonin and 2 µg/ml mouse anti-dsRNA (J2) antibody. Following permeabilisation, cells were prepared and analysed as described for Bak and Bax N-terminus exposure in section 2.6.4.1.

2.6.7. Analysis of Noxa expression levels

2.6.7.1. Assessment of Noxa protein levels. HeLa cells (1×10^6) were infected at an MOI of 5 with VVCop or VVΔE3L. Whole-cell lysates were harvested in SDS-PAGE loading buffer at 4, 8, 12, 16, and 24 hpi. Following SDS-PAGE, membranes were Western blotted with mouse anti-Noxa, mouse anti-I3L, mouse anti-β-tubulin, or mouse anti-Bak antibodies.

2.6.7.2. Assessment of Noxa mRNA levels. Noxa mRNA levels were assessed by quantitative real-time PCR, and all primers used for this experiment are listed in Table 2.6. HeLa cells (1×10^6) were infected at an MOI of 5 with VVCop or VVΔE3L. At 2, 4, 8, 12, 16, or 24 hpi, the cell medium was removed from the monolayer and replaced with 1 ml TRIzol (Invitrogen) to lyse the cells and isolate total RNA. After 5 min, the lysate was removed to a microfuge tube and total RNA was extracted with chloroform. Following centrifugation (12 000 x g, 15 min), the aqueous phase was removed to a fresh microfuge tube and RNA was precipitated for 10 min at room temperature with isopropanol. The RNA precipitate was pelleted (12 000 x g, 10 min), and the pellet was washed with 75% ethanol before being re-suspended in RNase-free, diethylpyrocarbonate (DEPC)-treated water (Invitrogen). The concentration of RNA in each sample

Table 2.6. Oligonucleotides Used for Quantitative Real-time PCR

Oligonucleotide	Sequence	Sense ^a	Source
NOXA RT FWD	TCTCAGGAGGTGCACGTTTCATCA	+	IDT
NOXA RT REV	CCCAGCCGCCCAGTCTAATCA	-	IDT
GAPDH RT FWD	CGGAGTCAACGGATTTGGTCG	+	IDT
GAPDH RT REV	AGCCTTCTCCATGGTGGTGAAGAC	-	IDT
ACTB RT FWD	AAATAGCACAGCCTGGATAGCAAC	+	Qiagen
ACTB RT REV	GCACCACACACCTTCTACAATGAG	-	Qiagen

^aSense, +; antisense, -

was determined using a NanoDrop ND-100 Spectrophotometer (NanoDrop). Reverse-transcription reactions to obtain cDNA were performed in a total volume of 20 μ l using a Techgene thermocycler (Techne). Briefly, 2 μ g of total RNA was combined with 25 ng/ μ l Oligo(dT) primers (Invitrogen) and 500 μ M dNTPs (Invitrogen). Following a 5 min incubation at 65°C, the mixture was chilled to 4°C and combined with 5x First-strand Buffer (250 mM Tris-HCl, pH 8.3; 375 mM KCl; 15 mM MgCl₂), 20 mM DTT, and 2 U/ μ l RNaseIN (Promega). The mixture was then incubated at 42°C for 2 min before the addition of 200 U of Superscript II reverse transcriptase (Invitrogen). Real-time PCR reactions were performed in a total volume of 25 μ l in optical PCR plates (Bio-Rad) sealed with a Microsealer B Adhesive Strip (Bio-Rad) using a MyIQ Single Color RT-PCR Detection System thermocycler (Bio-Rad). Briefly, total cDNA was diluted 1/7.5 and 5 μ l was combined with 12.5 μ l iQ SYBR Green Supermix (Bio-Rad) and 200 nM each of NOXA RT FWD and NOXA RT REV, GAPDH RT FWD and GAPDH RT REV, or ACTB RT FWD and ACTB RT REV primers. Real-time PCR reactions were carried out for 55 cycles comprised of a 95°C denaturing step for 30 s, a 54°C annealing step for 30 s, and a 72°C elongation step for 30 s. Data were analysed using the iQ5 Optical System software (V2.1; Bio-Rad), and the level of *Noxa* mRNA relative to either *GAPDH* (which encodes GAPDH) or *ACTB* (which encodes β -actin) mRNA was calculated using the comparative ct method (286, 385).

2.6.8. Colony formation assay. A long-term survival assay was performed as described (64). Briefly, WT MEFs were stably transfected with either pMIH empty vector or pMIH-Flag-DPV022, and expression of Flag-DPV022 was verified by flow cytometry. The mock or DPV022-expressing MEFs were infected with

retrovirus expressing empty pMIG vector or pMIG-Bim_s2A. Since cloning into the pMIG vector places the BH3-only sequence upstream of an internal ribosome entry site (IRES) and the EGFP ORF, pMIG clones express the relevant BH3-only protein and EGFP simultaneously and to similar levels. EGFP positive cells (and, therefore, BH3-only positive cells) were sorted by FACS and seeded on to 6 well plates (150 cells/well). The MEFs infected with the retrovirus expressing Bim_s2A were cultured with or without 1 μ M of ABT-737. Cells were incubated for 5 days and the number of EGFP positive clones was scored using a fluorescent microscope. *This experiment was performed by T. Okamoto in the laboratory of D. Huang (Walter and Eliza Hall Institute, Parkville, Australia).*

2.6.9. Yeast colony assay. *Saccharomyces cerevisiae* W303 α cells were co-transformed with pGALL(TRP1) vector only, pGALL(TRP1)-Bcl-x_L, or pGALL(TRP1)-DPV022 and pGALL(TRP1)-Bak or pGALL(TRP1)-Bax. pGALL(TRP1) places genes under the control of a galactose inducible promoter (178). Cells were spotted as 5-fold serial dilutions onto medium containing 2% w/v galactose (inducing, “ON”), which induces protein expression, or 2% w/v glucose (repressing, “OFF”), which prevents protein expression, as previously described (215). Plates were incubated for 48 h at 30°C and then photographed. *This experiment was performed by T. Okamoto in the laboratory of D. Huang (Walter and Eliza Hall Institute, Parkville, Australia).*

CHAPTER THREE

FOWLPOX VIRUS ENCODES A BCL-2 HOMOLOGUE THAT PROTECTS CELLS FROM APOPTOTIC DEATH THROUGH INTERACTION WITH THE PRO-APOPTOTIC PROTEIN BAK

A version of this chapter has been published:

Banadyga L., Gerig J., Stewart T., and M. Barry. 2007. *Journal of Virology*.

81(20):11032-45. Copyright 2007. American Society for Microbiology.

All of the experiments included within this chapter were performed by L. Banadyga with the exception of Figure 3.5B, which was performed by J. Gerig under the supervision of L. Banadyga. pEGFP-FPV039 (Δ 41-54) was cloned by J. Gerig under the supervision of L. Banadyga. The original manuscript was written by L. Banadyga with a major editorial contribution by M. Barry.

3.1. BRIEF INTRODUCTION

Given the unique homology between fowlpox virus FPV039 and cellular Bcl-2 proteins (4), we sought to determine what role FPV039 played in the modulation of apoptosis. We demonstrate here that FPV039 localised to the mitochondria where it maintained the integrity of the MOM by constitutive interaction with the pro-apoptotic protein Bak. Concordantly, FPV039 also inhibited apoptosis induced by Bak over-expression. FPV039 expressed in the context of viral infection retained its ability to interact with Bak and rendered cells resistant to apoptosis. Furthermore, infection with a recombinant VV expressing FPV039 prevented Bak conformational change, a prerequisite for cytochrome *c* release and apoptosis. Together, our data indicate that FPV039 is a functional Bcl-2 homologue that inhibits apoptosis by neutralising the pro-apoptotic Bcl-2 family member Bak.

3.2. RESULTS

3.2.1. Fowlpox virus encodes a Bcl-2 homologue. Genomic sequencing of fowlpox virus revealed a putative Bcl-2 homologue encoded by the open reading frame FPV039 (4). Similar to most anti-apoptotic Bcl-2 proteins, FPV039 is predicted to contain a series of α -helices that closely align with those determined from the structure of Bcl-2 (Fig. 3.1A). In addition, FPV039 possesses conserved BH1 and BH2 domains; however, FPV039 lacks obvious BH3 and BH4 domains and is unusually short, owing to the absence of an unstructured loop region present in Bcl-2 (Fig. 3.1A and B). Alignment of the BH1 domain of FPV039 with several cellular Bcl-2 proteins indicates that FPV039 possesses a highly conserved BH1 domain characterised by the presence of the “NWGR” sequence (amino acids 82 to 85) (Fig. 3.1B). Likewise, the BH2 domain of FPV039 bears

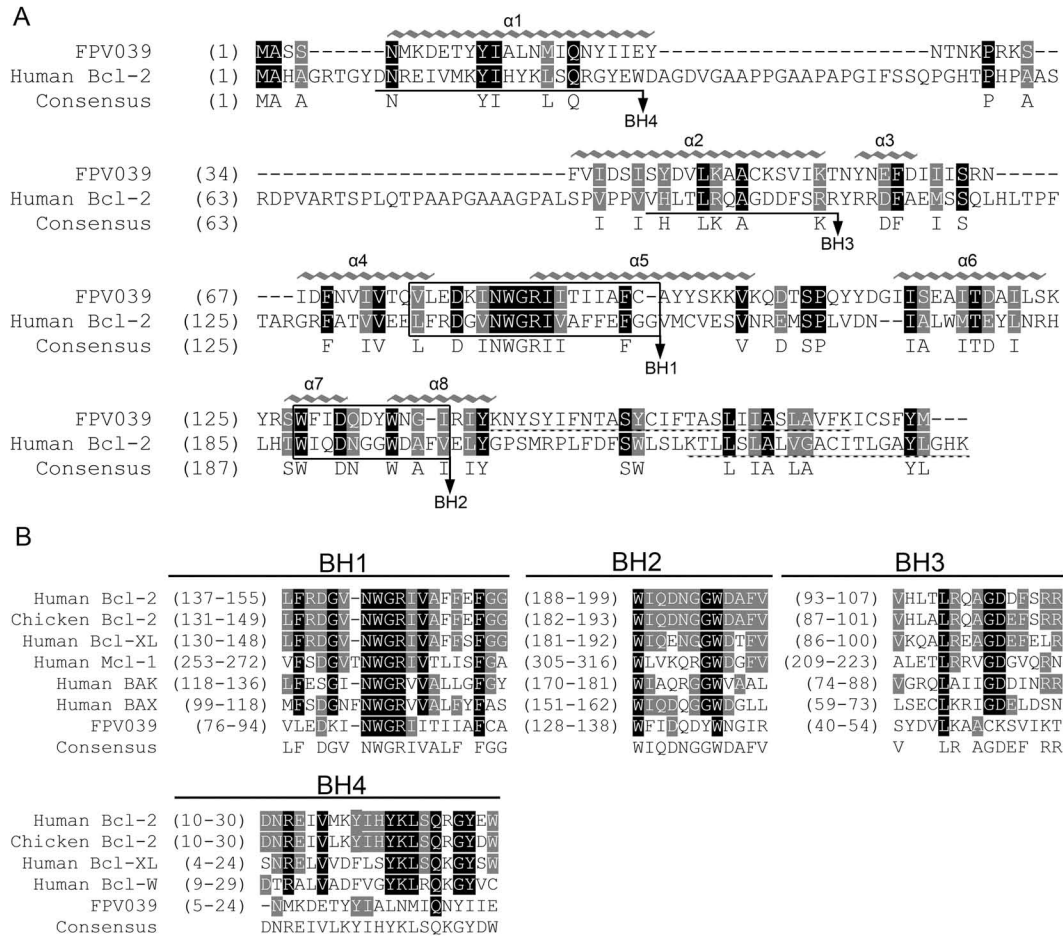


Figure 3.1. Alignment of FPV039 with human Bcl-2. (A) FPV039 is predicted to contain eight α -helices (JPred) and demonstrates significant homology to human Bcl-2 within the BH1 and BH2 domains. Predicted α -helices are indicated (α 1- α 8), and the transmembrane domains of Bcl-2 and FPV039 are underlined (dashed line). (B) Alignment of BH1, BH2, BH3, and BH4 domains from various Bcl-2 family members with FPV039. Identical amino acids are highlighted in black, and similar amino acids are highlighted in grey (ClustalW) (A & B).

sequence homology to the same domain in cellular Bcl-2 proteins (Fig. 3.1B). Importantly, G84 and R85 of the BH1 domain and W128 of the BH2 domain in FPV039 correspond to the same residues in cellular Bcl-2 proteins that are critical for anti-apoptotic function (167, 482). Although FPV039 lacks key residues usually conserved within the BH3 domain, the predicted α -helix 2 of FPV039 corresponds with the α -helix in Bcl-2 that defines the BH3 domain (Fig. 3.1A). Similarly, α -helix 1 in Bcl-2, which contains the BH4 domain, also aligns with a predicted α -helical region in FPV039, suggesting that, despite lacking obvious sequence homology, FPV039 may be structurally and functionally homologous to Bcl-2. These discrepancies in sequence conservation between FPV039 and Bcl-2 may highlight substantial, and possibly critical, functional differences.

3.2.2. FPV039 is a tail-anchored protein that localises to the mitochondria.

Bcl-2 proteins possess C-terminal “tail anchors” that typically target them to the ER membrane or the MOM (47, 281, 382). Sequence analysis of FPV039 demonstrated the presence of a 26 amino acid hydrophobic domain flanked by positively charged lysines at positions 141 and 169 of FPV039, suggesting that FPV039 may localise to intracellular membranes (Fig. 3.1A). Therefore, to determine the subcellular localisation pattern of FPV039, HeLa cells were transiently transfected with pEGFP, pEGFP-F1L, or pEGFP-FPV039(1-176) and analysed by confocal microscopy (Fig. 3.2). Cells transfected with pEGFP alone showed a diffuse fluorescence pattern indicative of uniform distribution throughout the cell that did not display co-localisation with MitoTracker, a mitochondrial specific dye that labels the mitochondria (Fig. 3.2, a-c). As a control, cells transfected with pEGFP-F1L, which expresses an EGFP-tagged

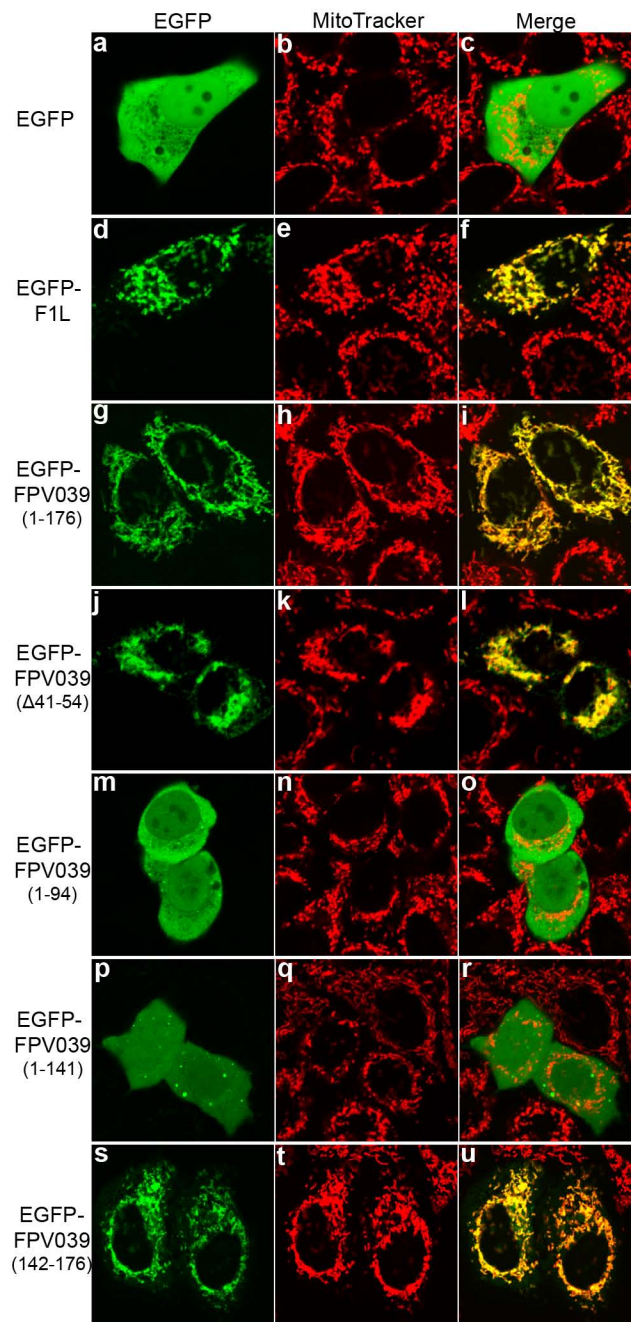


Figure 3.2. FPV039 localises to the mitochondria in mammalian cells. HeLa cells were transfected with the indicated EGFP-tagged constructs, and mitochondria were stained with MitoTracker dye. Co-localisation was visualised by confocal microscopy.

version of the VV-encoded F1L protein (406), showed a punctate fluorescence pattern that overlapped with MitoTracker (Fig. 3.2, d-f). Similarly, cells expressing wild-type EGFP-FPV039(1-176) displayed a punctate fluorescence pattern that co-localised with MitoTracker, indicating that FPV039 also localised to the mitochondria (Fig. 3.2, g-i). Deletion of the region in FPV039 predicted to encode an α -helical BH3 domain in other anti-apoptotic Bcl-2 proteins did not affect localisation of EGFP-FPV039(Δ 41-54) to the mitochondria (Fig. 3.2, j-l) since this construct retains the C-terminal TM domain.

To determine whether or not the C-terminal domain of FPV039 was necessary for mitochondrial localisation of FPV039, three mutated constructs were generated. Cells transfected with pEGFP-FPV039(1-94), which expresses a protein truncated immediately after the BH1 domain and therefore lacks the downstream BH2 and putative TM domain, showed a diffuse cytoplasmic distribution that did not co-localise with MitoTracker (Fig. 3.2, m-o). These results suggested that the C-terminal 82 amino acids were important for the mitochondrial localization of FPV039. A second mutant construct, pEGFP-FPV039(1-141), which expresses a protein that lacks only the 35 C-terminal amino acids, was used to refine the domain required for mitochondrial localisation. Cells transfected with pEGFP-FPV039(1-141) displayed diffuse localisation throughout the cell and failed to co-localise with MitoTracker (Fig. 3.2, p-r). In contrast, cells transfected with pEGFP-FPV039(142-176), expressing a protein comprised of only the C-terminal 35 amino acids appended to the C-terminus of EGFP, displayed a punctate green fluorescence pattern similar to pEGFP-F1L and pEGFP-FPV039 (1-176) (Fig. 3.2, s-u). Co-localisation with MitoTracker indicated that the C-terminal 35 amino acids of

FPV039 are necessary and sufficient for promoting localisation to the mitochondria.

Because fowlpox virus is a natural pathogen of various poultry species (97, 434, 435), including chickens, we wanted to confirm the localisation of FPV039 in a physiologically relevant context. Chicken leghorn male hepatocellular carcinoma (LMH) cells were transfected with pEGFP-FPV039(1-176), pEGFP-FPV039(1-94), pEGFP-FPV039(1-141), or pEGFP-FPV039(142-176) and analysed by confocal microscopy (Fig. 3.3). The co-localisation observed in LMH cells precisely reflected the co-localisation of the same constructs observed in HeLa cells (Fig. 3.2). EGFP-FPV039(1-176) and EGFP-FPV039(142-176) localised predominantly to the mitochondria (Fig. 3.3, a-c & j-l). Conversely, EGFP-FPV039(1-94) and EGFP-FPV039(1-141) exhibited a cytoplasmic distribution that did not co-localise with the mitochondria (Fig. 3.3, d-i). Together, these data indicate that FPV039 is capable of localising to the mitochondria in human and chicken cells.

3.2.3. FPV039 inhibits TNF α -induced loss of mitochondrial membrane potential. The apparent sequence homology between FPV039 and cellular Bcl-2 proteins coupled with the observed localisation of FPV039 to the mitochondria suggested that FPV039 may play a role in modulating apoptosis. To determine whether FPV039 was sufficient to inhibit apoptosis, HeLa cells were transfected with pEGFP, pEGFP-Bcl-2, pEGFP-F1L, pEGFP-FPV039(1-176), or pEGFP-FPV039(142-176). Transiently transfected cells were subsequently treated with TNF α to induce apoptosis, and uptake of TMRE, a dye that fluorescently labels healthy, respiring mitochondria, was used as an indicator of apoptosis (Fig. 3.4A) (125, 309). To ensure the phenomena we were observing were specific to cells

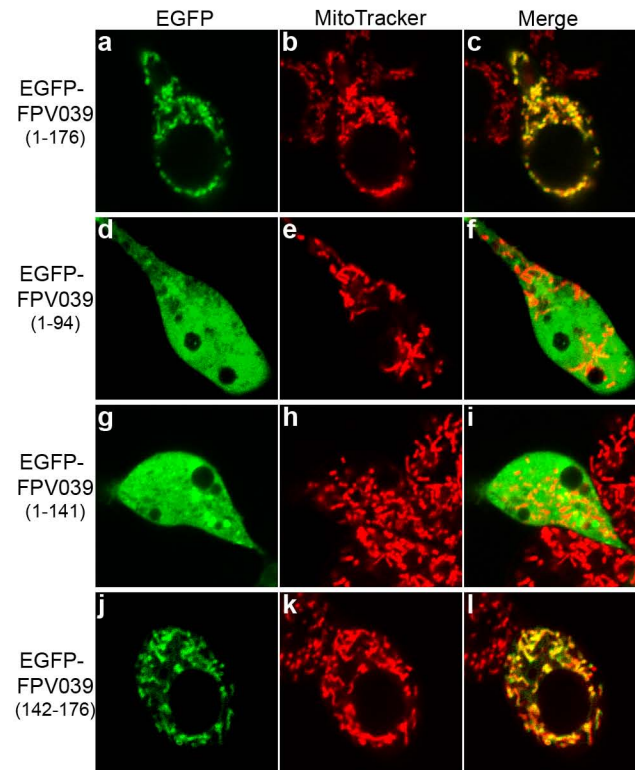


Figure 3.3. FPV039 localises to the mitochondria in chicken cells. Chicken LMH cells were transfected with the indicated EGFP-tagged constructs, and mitochondria were stained with MitoTracker dye. Co-localisation was visualised by confocal microscopy.

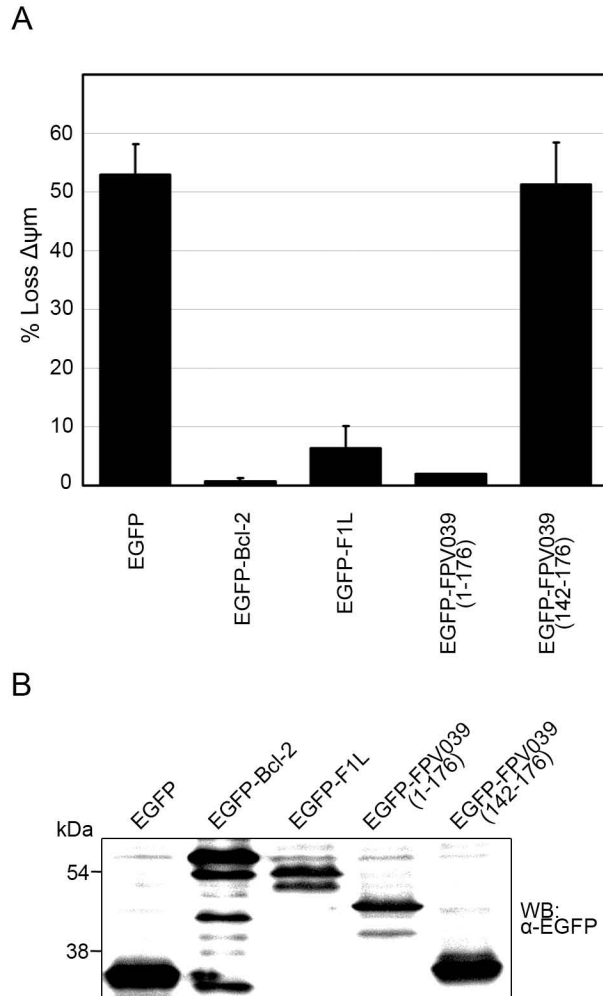


Figure 3.4. FPV039 inhibits TNF α -induced apoptosis. (A) HeLa cells were transfected with pEGFP, pEGFP-Bcl-2, pEGFP-F1L, pEGFP-FPV039(1-176), or pEGFP-FPV039(141-176) and treated with 10 ng/ml TNF α and 5 μ g/ml cycloheximide for 6h. Apoptosis was assessed in EGFP-positive cells by quantifying TMRE fluorescence via flow cytometry, and the percentage of cells that demonstrated a loss of mitochondrial membrane potential ($\Delta\psi_m$) is given as the y-axis. Standard deviations were calculated from three independent experiments. (B) HeLa cells were transfected in a parallel experiment, and the expression level of each EGFP-tagged construct was assessed by Western blotting (WB) whole cell lysates.

expressing the transfected proteins, only EGFP-expressing cells were analysed for TMRE fluorescence. After TNF α treatment, 53% of cells expressing EGFP alone exhibited loss of mitochondrial membrane potential, whereas less than 1% of cells transfected with EGFP-Bcl-2 and only 6% of cells expressing EGFP-F1L showed a drop in TMRE fluorescence. These data agree with previous studies and indicate that both Bcl-2 and the VV-encoded protein F1L protect cells from TNF α -induced apoptosis (406). Similarly, expression of EGFP-FPV039(1-176) also inhibited apoptosis, with only 2% of transfected cells exhibiting a loss of mitochondrial membrane potential after TNF α treatment. Conversely, cells expressing EGFP-FPV039(142-176) provided no protection, with 51% of transfected cells exhibiting a loss in TMRE fluorescence.

To ensure that differences in protein expression levels were not influencing the ability of the EGFP-tagged constructs to inhibit apoptosis, expression levels were analysed by Western blotting (Fig. 3.4B). HeLa cells transfected with either pEGFP or pEGFP-FPV039(142-176) showed the highest levels of protein expression; however, neither construct was capable of inhibiting apoptosis. EGFP-Bcl-2, EGFP-F1L, and EGFP-FPV039(1-176) were expressed at lower levels, but all of these constructs protected against TNF α -induced apoptosis. Together, these data clearly demonstrate that FPV039 is an anti-apoptotic protein capable of inhibiting TNF α -induced apoptosis.

3.2.4. FPV039 interacts with the pro-apoptotic protein Bak and inhibits Bak-induced apoptosis. Loss of the mitochondrial membrane potential and subsequent induction of apoptosis is governed by the Bcl-2 family of proteins and requires the activity of at least one of two pro-apoptotic proteins, Bak or Bax (282, 459, 502). Two other poxviral anti-apoptotic proteins, M11L and F1L,

which, unlike FPV039, display little sequence homology to members of the Bcl-2 family, constitutively interact with and inhibit Bak activity (450, 453). Accordingly, we wanted to ascertain if FPV039 also interacted with Bak. HEK 293T cells were co-transfected with pEGFP, pEGFP-F1L, pEGFP-FPV039(1-176), pEGFP-FPV039(1-94), or pEGFP-FPV039(Δ 41-54) and pcDNA3-HA-Bak and lysed in 2% CHAPS, a detergent that preserves the conformational integrity of Bcl-2 family members (200, 201). Immunocomplexes were precipitated with an anti-EGFP antibody and subsequent Western blotting was performed with an anti-HA or anti-Bak antibody (Fig. 3.5A). In agreement with previous studies, an interaction between EGFP-F1L and HA-Bak was detected (453). Using this approach, an interaction between EGFP-FPV039(1-176) and HA-Bak was also observed. Significantly, no co-immunoprecipitation was observed in cells transfected with EGFP or HA-Bak alone, confirming the specificity of the interaction between EGFP-FPV039(1-176) and HA-Bak. To ensure that we were precipitating equal amounts of the EGFP-tagged proteins, we subjected the lysates and immunoprecipitations to Western blotting with an anti-EGFP antibody, and the results indicated that each EGFP-tagged protein was expressed and precipitated at approximately equal levels. Although EGFP alone was highly expressed and readily precipitated, this protein exhibited no interaction with HA-Bak.

Two mutant FPV039 constructs were employed to refine the domains within FPV039 required for its interaction with Bak (Fig. 3.5B). EGFP-FPV039(1-94) failed to interact with HA-Bak, suggesting that the BH2 domain and the TM domain play critical functional roles. Additionally, although FPV039 lacks a domain with obvious sequence homology to the BH3 domain of human Bcl-2 (Fig. 3.1), secondary structural analysis predicted an α -helix (α 2) in FPV039

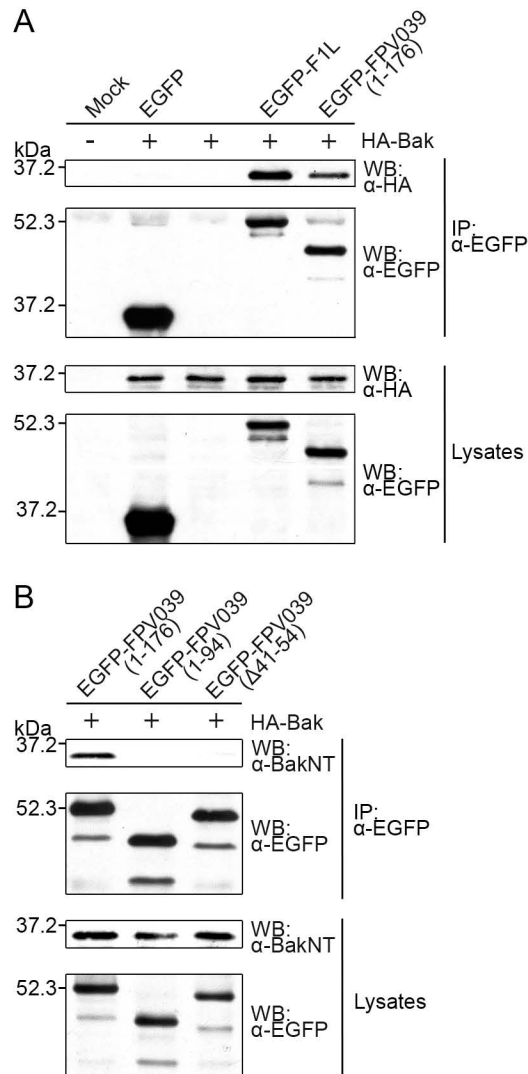


Figure 3.5. FPV039 interacts with the pro-apoptotic protein Bak. (A) HEK 293T cells were co-transfected with either pEGFP, pEGFP-F1L, or pEGFP-FPV039(1-176) and pcDNA3-HA-Bak. Following lysis in 2% CHAPS buffer, lysates were immunoprecipitated (IP) with an anti-EGFP antibody and Western blotted (WB) with anti-EGFP or anti-HA antibodies to detect interactions. Cell lysates were Western blotted with anti-HA or anti-EGFP antibodies to determine expression of HA-Bak and EGFP-tagged proteins, respectively. (B) Deletion of the BH3 and BH2 domains of FPV039 abrogates interaction with Bak. HEK 293T cells were co-transfected with pEGFP-FPV039(1-176), pEGFP-FPV039(1-94), or pEGFP-FPV039(Δ41-54) and pcDNA3-HA-Bak. Following lysis in 2% CHAPS buffer, lysates were immunoprecipitated (IP) with an anti-EGFP antibody and Western blotted (WB) with anti-EGFP or anti-HA antibodies to detect interactions. Lysates were Western blotted with anti-BakNT or anti-EGFP antibodies to determine expression of HA-Bak and EGFP-tagged proteins, respectively. *The experiment depicted in (B) was performed by J. Gerig under the supervision of L. Banadyga.*

(amino acids 41-54) that aligns with the BH3 α -helix of human Bcl-2 (Fig. 3.1A), suggesting that this region may be important for interaction with Bak. To determine if amino acids 41-54 of FPV039 were critical for interaction with Bak, we generated an EGFP-tagged version of FPV039 lacking amino acids 41-54, EGFP-FPV039(Δ 41-54). No interaction by co-immunoprecipitation was detected between Bak and EGFP-FPV039(Δ 41-54), indicating that, despite lacking homology to the BH3 domain of anti-apoptotic Bcl-2 proteins, this region was required for Bak interaction (Fig. 3.5B). Together, these data demonstrate that, like cellular Bcl-2 proteins and viral proteins, such as M11L and F1L, FPV039 also interacts with Bak (1, 90, 450, 453).

Since FPV039 clearly interacted with Bak, we next wanted to determine whether FPV039 could inhibit apoptosis induced by over-expression of Bak. Ectopic over-expression of Bak saturates the mitochondria with Bak, artificially inducing its activation and leading to apoptosis (76). HeLa cells were co-transfected with pEGFP, pEGFP-Bcl-2, pEGFP-F1L, pEGFP-FPV039(1-176), or pEGFP-FPV039(142-176) and pcDNA3-HA-Bak. Apoptosis was quantified by staining cells with TMRE to determine the percent loss of the mitochondrial membrane potential, and EGFP-expressing cells were analysed by flow cytometry (Fig. 3.6A). EGFP expression alone was unable to prevent the loss of the mitochondrial membrane potential induced by HA-Bak, with almost 30% of cells exhibiting decreased TMRE fluorescence. A loss of mitochondrial membrane potential in cells expressing EGFP-Bcl-2 was undetectable, and less than 5% of cells expressing EGFP-F1L exhibited a drop in TMRE fluorescence, indicating that both Bcl-2 and F1L protect against Bak-induced apoptosis. EGFP-FPV039(1-176) also inhibited Bak-induced apoptosis, with approximately only 1% of transfected cells showing a decrease in TMRE fluorescence. The

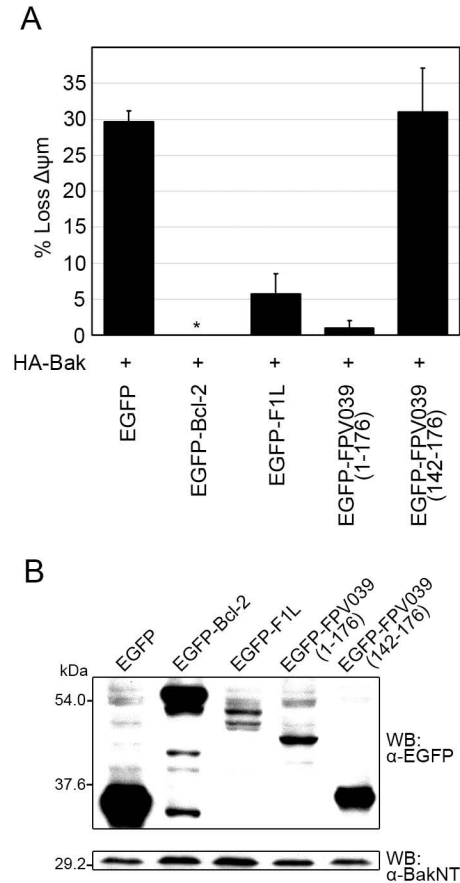


Figure 3.6. FPV039 inhibits Bak-induced apoptosis. (A) HeLa cells were co-transfected with pEGFP, pEGFP-Bcl-2, pEGFP-F1L, pEGFP-FPV039(1-176), or pEGFP-FPV039(141-176) and pcDNA3-HA-Bak. Eighteen hours post transfection, apoptosis was assessed in EGFP-positive cells by quantifying TMRE fluorescence via flow cytometry, and the percentage of cells that demonstrated a loss of mitochondrial membrane potential ($\Delta\psi_m$) is given as the y-axis. The asterisk (*) denotes complete protection when cells were transfected with pEGFP-Bcl-2. Standard deviations were calculated from three independent experiments. (B) HeLa cells were transfected in a parallel experiment, and the expression level of each EGFP-tagged construct and HA-Bak was assessed by Western blotting (WB) whole cell lysates.

activity of wild-type FPV039 contrasted sharply with that of EGFP-FPV039(142-176), where greater than 30% of cells transfected with this construct lost their mitochondrial membrane potential as a result of HA-Bak over-expression.

Protein expression levels were analysed via Western blotting to ensure that differences in the protective abilities of the EGFP-tagged proteins were not a result of differences in expression of either the EGFP-tagged proteins or HA-Bak (Fig. 3.6B). EGFP and EGFP-FPV039(142-176) were robustly expressed, but neither prevented apoptosis induced by HA-Bak. EGFP-Bcl-2, EGFP-F1L, and EGFP-FPV039(1-176) were expressed at slightly varied levels, which correlated with the ability to inhibit apoptosis. HA-Bak was equally expressed in all samples. Collectively, these data imply that FPV039 is capable of interacting with the pro-apoptotic protein Bak and preventing the induction of apoptosis.

3.2.5. FPV039 interacts with endogenous Bak during vaccinia virus infection. To further elucidate the anti-apoptotic mechanism of FPV039 during virus infection, we constructed two recombinant viruses using the previously generated VV strain Copenhagen lacking its natural apoptotic inhibitor, F1L, VV Δ F1L (453). Using homologous recombination, we generated VV Δ F1L-Flag-FPV039(1-176), which expresses wild-type FPV039, and VV Δ F1L-Flag-FPV039(1-94), which expresses a truncated FPV039 lacking the 82 amino acids immediately C-terminal of the BH1 domain.

To determine if FPV039 was able to interact with Bak in the context of infection, we infected HeLa cells with VV Δ F1L, VVWR-Flag-F1L, VV Δ F1L-Flag-FPV039(1-176), or VV Δ F1L-Flag-FPV039(1-94) and immunoprecipitated cell lysates with an anti-Flag antibody (Fig. 3.7A). Subsequent Western blotting of the precipitates using an anti-Bak antibody revealed that Flag-tagged FPV039(1-

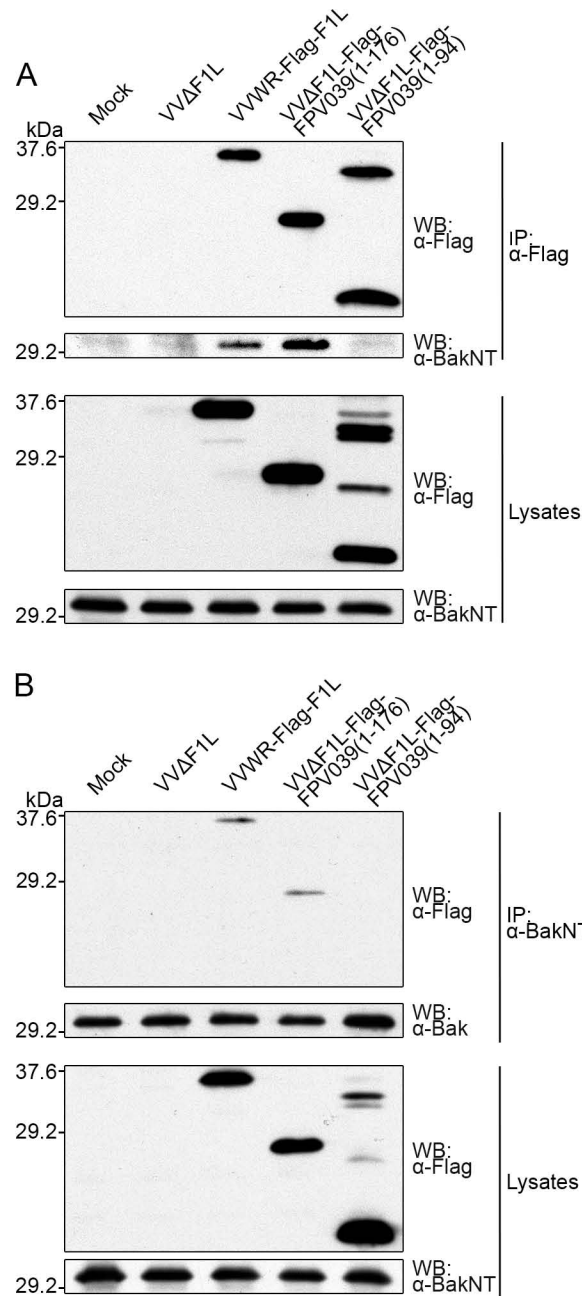


Figure 3.7. FPV039 interacts with endogenous Bak during vaccinia virus infection. (A) HeLa cells were mock infected or infected with VVΔF1L, VVWR-Flag-F1L, VVΔF1L-Flag-FPV039(1-176), VVΔF1L-Flag-FPV039(1-94) at an MOI of 5. Twelve hours post-infection, cells were lysed in 2% CHAPS buffer and immunoprecipitated (IP) with anti-Flag antibody and Western blotted (WB) with anti-BakNT or anti-Flag antibodies to detect interactions. Cell lysates were Western blotted with anti-Flag-HRP or anti-BakNT antibodies to determine expression levels of Flag-tagged proteins and endogenous Bak, respectively. (B) Reciprocal immunoprecipitations were performed with anti-BakNT antibody followed by Western blotting with anti-FlagHRP antibody to detect interactions. Cell lysates were Western blotted with anti-Flag-HRP or anti-BakNT antibodies to determine expression levels.

176) interacted with endogenous Bak during infection. Conversely, Flag-tagged FPV039(1-94), which lacks the BH2 region and the C-terminal TM domain, was unable to interact with Bak during virus infection, despite being precipitated and expressed at equal or greater levels. Flag-F1L also interacted with Bak, as previously shown (453), but no interaction was observed in the lysates from cells infected with VV Δ F1L, confirming the specificity of the interaction between the Flag-tagged proteins and endogenous Bak. Western blotting these samples with anti-Flag antibodies revealed that each Flag-tagged protein was precipitated equally and equal levels were expressed in the lysates. Notably, Western blotting of lysates infected with VV Δ F1L-Flag-FPV039(1-94) showed a pattern indicative of ubiquitination (Fig. 3.7A & B), which we routinely observed for this mutant as well as FPV039(1-176). To confirm the interaction, we performed the reciprocal immunoprecipitation, using an anti-Bak antibody, and again showed that both F1L and FPV039 interacted with Bak during infection (Fig. 3.7B). Western blotting of infected cell lysates indicated that endogenous Bak and each Flag-tagged protein were expressed at equal levels. Importantly, the interactions observed between virally-expressed FPV039 and endogenous Bak reflect those observed between ectopically expressed EGFP-tagged proteins and HA-Bak (Fig. 3.5).

We next sought to confirm the ability of FPV039 to interact with chicken Bak, a presumably important and natural interaction partner. LMH cells were infected with VV Δ F1L, VVWR-Flag-F1L, or VV Δ F1L-Flag-FPV039(1-176), and the lysates were immunoprecipitated with either an anti-Flag (Fig. 3.8B) or anti-Bak (Fig. 3.8C) antibody. Because of the paucity of reagents available to study Bcl-2 proteins in chickens, we relied on rabbit anti-human BakNT, an antibody generated against human Bak (131). Overall, chicken Bak and human Bak share

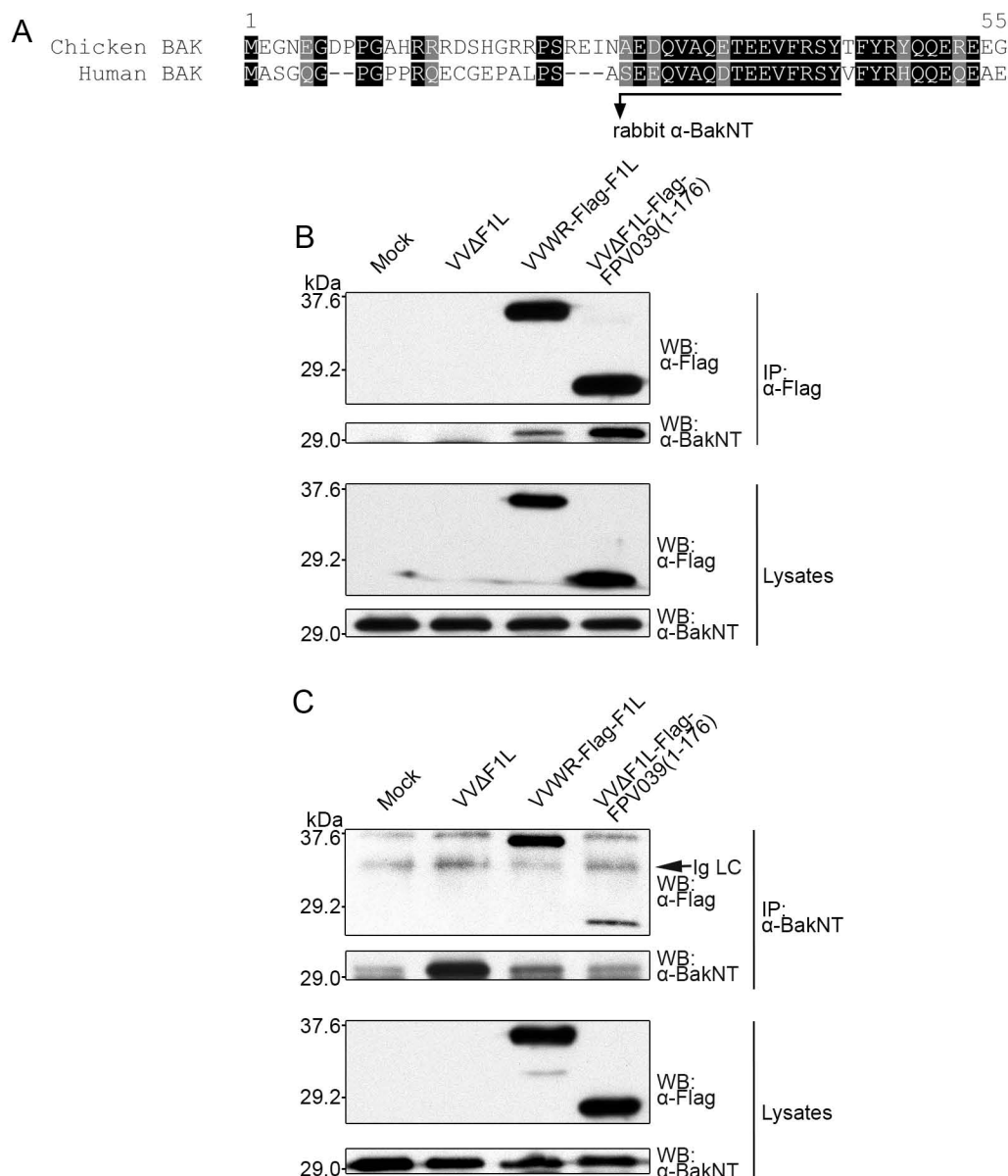


Figure 3.8. FPV039 interacts with endogenous Bak in chicken cells. (A) Amino acid alignment of the N-terminal portion of chicken Bak and human Bak, with the immunogen used to generate the human Bak-specific antibody, rabbit anti-BakNT, indicated by underlining. Identical amino acids are highlighted in black, and similar amino acids are highlighted in grey (ClustalW). (B) LMH cells were mock-infected or infected with VV Δ F1L, VVWR-Flag-F1L, or VV Δ F1L-Flag-FPV039(1-176). Twelve hours post-infection, cells were lysed in 2% CHAPS buffer and immunoprecipitated (IP) with anti-Flag antibody and Western blotted (WB) with anti-BakNT or anti-Flag antibodies to detect interactions. Cell lysates were Western blotted with anti-Flag or anti-Bak antibodies to determine expression levels of Flag-tagged proteins or endogenous Bak. (C) Reciprocal immunoprecipitations were performed with anti-BakNT antibody followed by Western blotting with anti-BakNT to detect interactions. Cell lysates were Western blotted with anti-BakNT or anti-Flag antibodies to determine expression levels. The immunoglobulin light chain (Ig LC) is indicated by an arrow.

approximately 60% amino acid identity; however, the immunogen used to generate rabbit anti-human BakNT was a 16 amino acid peptide of human Bak that shares approximately 80% identity with chicken Bak (Fig. 3.8A). Indeed, anti-BakNT detected a single band from LMH whole cell lysates running at the predicted size of chicken Bak (Fig. 3.8A & B, lowest panel). Immunoprecipitation of cell lysates with an anti-Flag antibody followed by Western blotting with anti-BakNT revealed an interaction between chicken Bak and both Flag-F1L and Flag-FPV039(1-176) (Fig. 3.8B). No interaction was observed in the lysates from cells infected with VV Δ F1L. Western blotting the immunoprecipitates with anti-Flag revealed that Flag-F1L and Flag-FPV039(1-176) were precipitated in equal amounts, and Western blotting of infected cell lysates showed that the Flag-tagged proteins and endogenous chicken Bak were equally expressed. To confirm the interaction, a reciprocal immunoprecipitation was performed. Infected cell lysates were immunoprecipitated with anti-BakNT and subsequently Western blotted with an anti-Flag antibody (Fig. 3.8C). As expected, both Flag-F1L and Flag-FPV039(1-176) interacted with chicken Bak, and no interaction was observed in lysates from cells infected with VV Δ F1L. Anti-BakNT precipitated approximately equal amounts of Bak in mock-, VVWR-Flag-F1L-, and VV Δ F1L-Flag-FPV039(1-176)-infected cells. More Bak was immunoprecipitated in VV Δ F1L infected cells, but, as expected, no protein co-precipitated. All Flag-tagged proteins and endogenous Bak were expressed at equal levels. The results in chicken cells precisely mirror those obtained in human cells and lend further support to the idea that FPV039 is a functional Bcl-2 homologue.

3.2.6. FPV039 inhibits apoptosis induced by virus infection. We have previously shown that the VV protein F1L is a potent inhibitor of apoptosis and that, in the absence of F1L, VV infection induces apoptosis (453). To ascertain whether FPV039 could functionally replace F1L as an inhibitor of VV-induced apoptosis, Jurkat cells were infected with either VV-EGFP, VV Δ F1L, VV Δ F1L-Flag-FPV039(1-176), or VV Δ F1L-Flag-FPV039(1-94), and the ability of these viruses to inhibit apoptosis was quantified using two-colour flow cytometric analysis (Fig. 3.9). Apoptosis was measured by quantifying the loss of the mitochondrial membrane potential using TMRE staining in EGFP positive cells since each virus expressed EGFP. Using this experimental approach, the majority of cells infected with VV-EGFP, which encodes F1L, maintained their mitochondrial membrane potential following infection for eight hours (Fig. 3.9, a). Conversely, 23% of cells infected with VV Δ F1L, which induces apoptosis, exhibited a loss of mitochondrial membrane potential (Fig. 3.9, b) (453). Similar to VV-EGFP-infected cells, cells infected with VV Δ F1L-Flag-FPV039(1-176) did not demonstrate a loss in mitochondrial membrane potential, suggesting that expression of FPV039 is sufficient to inhibit apoptosis induced by VV lacking the anti-apoptotic protein F1L (Fig. 3.9, c). Infection with VV Δ F1L-Flag-FPV039(1-94), however, failed to completely protect cells from virus-induced apoptosis, perhaps offering partial protection (Fig. 3.9, d). Jurkat cells over-expressing Bcl-2 were completely resistant to the loss of mitochondrial membrane potential regardless of the virus used to infect them (Fig. 3.9, e-h). Together, these data demonstrate that FPV039, despite lacking sequence homology to F1L, is capable of inhibiting apoptosis induced by VV infection.

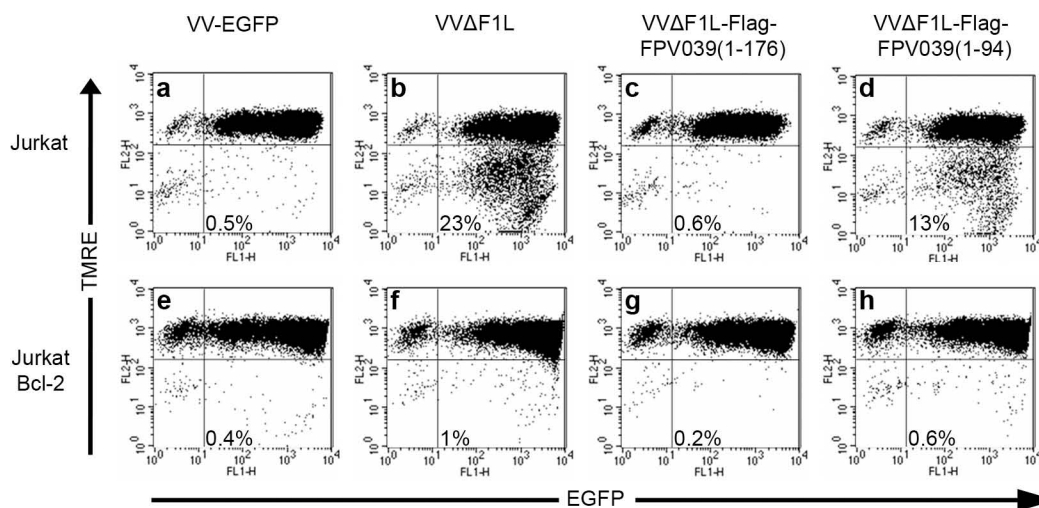


Figure 3.9. FPV039 inhibits virus-induced apoptosis. Wild-type Jurkat (a to d) or Jurkat cells over-expressing Bcl-2 (e to h) were infected with VV-EGFP, VVΔF1L, VVΔF1L-Flag-FPV039(1-176) or VVΔF1L-Flag-FPV039(1-94) at an MOI of 10. After 8 h, apoptosis was quantified via flow cytometry by measuring loss of the mitochondrial membrane potential as detected by TMRE fluorescence in EGFP-positive cells. The percentage of cells infected and exhibiting a loss in mitochondrial membrane potential is indicated in the lower right quadrant. Data were acquired on 20 000 cells per sample, and the data shown is representative of three or more independent experiments.

3.2.7. FPV039 inhibits the activation-associated conformational change of

Bak. Given that FPV039 interacted with Bak (Figs. 3.5, 3.7, & 3.8) and inhibited apoptosis in response to a variety of different stimuli (Figs. 3.4, 3.6, & 3.9), we wanted to determine whether FPV039 functioned by inhibiting the activity of Bak. Bak oligomerisation and disruption of mitochondrial integrity is preceded by a conformational change in Bak resulting in the exposure of its N-terminus, which serves as an indicator of Bak activation and impending apoptotic death (162, 163, 458). Therefore, to determine if FPV039 inhibited Bak activity, we assessed the activation-associated exposure of the N-terminus of Bak. Jurkat cells were infected with either VV-EGFP, VV Δ F1L, VV Δ F1L-Flag-FPV039(1-176), or VV Δ F1L-Flag-FPV039(1-94), and the activation of Bak was induced by treatment with staurosporine (STS). The exposure of the Bak N-terminus was detected by staining with the conformational specific antibody anti-BakAb-1 and quantified by flow cytometry (Fig. 3.10) (162, 163). Untreated Jurkat cells displayed a low level of fluorescence, attributable to non-specific antibody binding; however, upon STS treatment, fluorescence intensity increased, indicating a change in Bak conformation and exposure of the N-terminal epitope recognised by the antibody (Fig. 3.10, a). Infection with VV-EGFP inhibited the exposure of the Bak N-terminus upon treatment with STS, as previously shown (Fig. 3.10, b) (453). Infection with VV Δ F1L, however, did not inhibit STS-induced Bak activation, but was instead a potent inducer of apoptosis, capable of inducing Bak activation in the absence of staurosporine (Fig. 3.10, c). In contrast, Jurkat cells infected with VV Δ F1L-Flag-FPV039(1-176) exhibited no increase in fluorescence intensity associated with Bak conformational change, whether treated with staurosporine or not (Fig. 3.10, d), indicating that FPV039, like F1L, is capable of inhibiting the activation of Bak. This effect was not seen in Jurkat cells infected with VV Δ F1L-

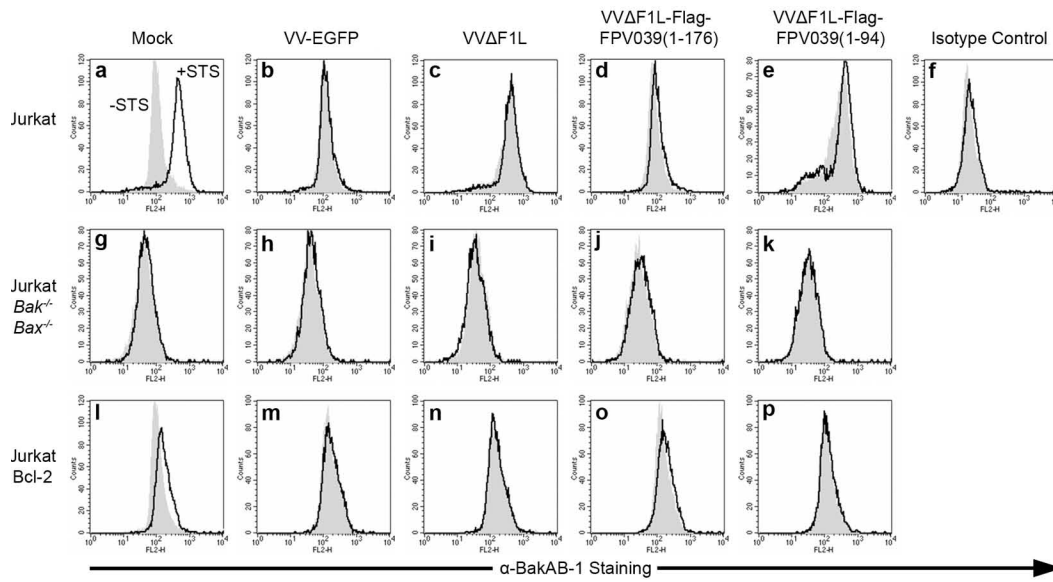


Figure 3.10. FPV039 inhibits the conformational activation of Bak. Wild-type Jurkat cells (a to f), Jurkat cells devoid of Bak and Bax (*Bak*^{-/-}/*Bax*^{-/-}) (g to k), or Jurkat cells over-expressing Bcl-2 (l to p) were mock infected or infected with VV-EGFP, VVΔF1L, VVΔF1L-Flag-FPV039(1-176), or VVΔF1L-Flag-FPV039(1-94) at an MOI of 10 for 4h and then treated with 250 nM staurosporine (STS) for 2h to induce apoptosis. Exposure of the N-terminus of Bak was monitored by flow cytometry using the confirmation specific anti-BakAb-1 antibody or an isotype control antibody (NK1.1). Untreated cells, shaded histogram; staurosporine treated cells, open histogram. Data are representative of at least three independent experiments.

Flag-FPV039(1-94), which, whether treated with STS or not, exhibited an almost complete shift in fluorescence intensity (Fig. 3.10, e). An increase in fluorescence intensity was not observed in Jurkat cells treated with STS and stained with an isotype control antibody, confirming the specificity of our antibody (Fig. 3.10, f). To ensure that our assay was specifically measuring Bak, we repeated the experiments in Jurkat cells lacking both Bak and Bax (451). In each case, no detectable increase in fluorescence activity was observed, further confirming the specificity of the anti-BakAb-1 antibody (Fig. 3.10, g-k). Moreover, over-expression of Bcl-2 inhibited the exposure of the Bak N-terminus in response to both infection and STS treatment, as previously shown (Fig. 3.10, l-p) (163, 453). Together, these data indicate that FPV039 is capable of inhibiting Bak conformational change and activation, providing a mechanistic explanation of the ability of FPV039 to inhibit apoptosis.

CHAPTER FOUR

THE FOWLPOX VIRUS BCL-2 HOMOLOGUE, FPV039, INTERACTS WITH ACTIVATED BAX AND A DISCRETE SUBSET OF BH3-ONLY PROTEINS TO INHIBIT APOPTOSIS

A version of this chapter has been published:

Banadyga L., Veugelers K., Campbell S., and M. Barry. 2009. *Journal of Virology*. 83(14):7085-98. Copyright 2009. American Society for Microbiology.

All of the experiments included within this chapter were performed by L. Banadyga. pEGFP-N1L, pcDNA3-HA-Puma, pEGFP-Bcl-x_L, pEGFP-Mcl-1, pcDNA3-Bid-Flag, pcDNA3-tBid-Flag were cloned by K. Veugelers, and VVΔF1L strain Copenhagen was generated by S. Campbell. The original manuscript was written by L. Banadyga with editorial contribution by M. Barry.

4.1. BRIEF INTRODUCTION

Although FPV039 interacted with Bak and prevented Bak conformational activation, Bax, the other critical pro-apoptotic Bcl-2 family member, must also be inactivated to effectively inhibit apoptosis. Accordingly, we wanted to determine whether FPV039, in addition to inactivating Bak, could inactivate Bax. We report here that FPV039 inhibited Bax activity and prevented critical steps in Bax activation. FPV039 did not appear to interact with endogenous inactive Bax; however, FPV039 was able to interact with active Bax. Moreover, FPV039 inhibited apoptosis induced by the BH3-only proteins and interacted with both Bim_L and Bik. Together, these data strongly suggest that FPV039 inhibits apoptosis by inactivating multiple pro-apoptotic Bcl-2 proteins, including the critical Bak and Bax, as well as a discrete subset of BH3-only proteins.

4.2. RESULTS

4.2.1. FPV039 inhibits apoptosis induced by Bax. Permeabilisation of the MOM and the concomitant progression of apoptosis can be induced independently by either Bak or Bax (76, 282, 338, 459). Because we have shown previously that FPV039 inhibited apoptosis induced by over-expression of Bak (Chapter 3), we wanted to determine if FPV039 could likewise inhibit apoptosis induced by Bax over-expression. HeLa cells were transfected with pEGFP; pEGFP-FPV039(1-176), which expresses full-length FPV039; pEGFP-FPV039(142-176), which expresses only the C-terminal TM tail of FPV039; or pEGFP-Bcl-2, the prototypical cellular anti-apoptotic protein, and apoptosis was triggered by expression of HA-Bax. Apoptosis was then quantified in transfected (EGFP positive) cells by measuring the fluorescence intensity of TMRE, a fluorescent dye taken up exclusively by healthy mitochondria with an intact

membrane potential (Fig. 4.1A) (125, 309). Over-expression of Bax resulted in the artificial activation of Bax (243, 475) and subsequent loss of the mitochondrial membrane potential in 45% of cells expressing EGFP, indicating that EGFP is not able to protect cells from apoptosis. However, when EGFP-Bcl-2 was over-expressed along with Bax, apoptosis was significantly inhibited. Similarly, full-length EGFP-FPV039(1-176) also inhibited Bax-induced apoptosis, with only 10% of transfected cells exhibiting a loss in mitochondrial membrane potential. Conversely, EGFP-FPV039(142-176), the TM tail of FPV039, did not protect against Bax-induced apoptosis, with more than 50% of transfected cells displaying a loss in mitochondrial membrane potential.

To ensure that differences in the expression levels of either the EGFP-tagged proteins or HA-Bax were not influencing the results of this assay, we analysed protein expression by Western blot (Fig. 4.1B). EGFP-Bcl-2 was expressed at a slightly higher level than EGFP-FPV039(1-176), and this correlated with their respective abilities to inhibit apoptosis. EGFP and EGFP-FPV039(142-176) were robustly expressed; however, neither was able to inhibit apoptosis. In each case, HA-Bax was expressed to equally high levels. Together these data indicate that, in addition to inhibiting apoptosis induced by the pro-apoptotic protein Bak, FPV039 also inhibits apoptosis induced by the over-expression of Bax.

4.2.2. FPV039 inhibits the conformational activation of Bax. Prior to the loss of mitochondrial membrane potential and the induction of apoptosis, Bax undergoes a series of conformational changes that result in its activation. In addition to the exposure of the C-terminal TM domain of Bax, Bax reveals an N-terminal epitope that can be specifically detected by the antibody anti-Bax6A7

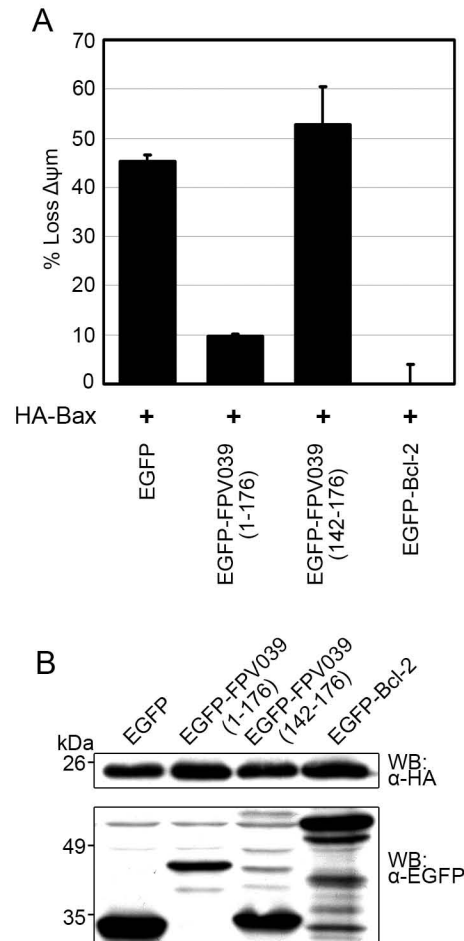


Figure 4.1. FPV039 inhibits Bax-induced apoptosis. (A) HeLa cells were co-transfected with either pEGFP, pEGFP-FPV039(1-176), pEGFP-FPV039(142-176), or pEGFP-Bcl-2 and pcDNA3-HA-Bax. Eighteen hours post-transfection, apoptosis was assessed in EGFP-positive cells by quantifying TMRE fluorescence via flow cytometry, and the percentage of cells that demonstrated a loss of mitochondrial membrane potential ($\Delta\psi_m$) is given as the y-axis. Standard deviations were calculated from three independent experiments. (B) HeLa cells were transfected in a parallel experiment, and the expression level of each EGFP-tagged construct and HA-Bax was assessed by Western blotting (WB) whole cell lysates.

(201). Detection of this N-terminal epitope therefore serves as a marker for Bax activation and impending apoptosis (201). Given that FPV039 inhibited apoptosis induced by Bax over-expression, we sought to determine if FPV039 also prevented the activation of Bax. HeLa cells were infected with one of various recombinant VVs at an MOI of 10, and Bax activation was visualised by confocal microscopy using the conformation-specific antibody, anti-Bax6A7 (Fig. 4.2A). Because each recombinant virus also expressed EGFP, green fluorescence served as a marker of infection. HeLa cells infected with VV Δ F1L, a VV devoid of the anti-apoptotic protein F1L, induced Bax activation (Fig. 4.2A, d-f), whereas both VV-EGFP, a wild-type VV, and VV Δ F1L-Flag-FPV039(1-176), a VV devoid of F1L but expressing WT FPV039, significantly inhibited Bax activation (Fig. 4.2A, a-c & g-i). VV Δ F1L-Flag-FPV039(Δ 41-54), which expresses a mutated form of FPV039 lacking the putative BH3 domain, was unable to prevent Bax activation (Fig. 4.2A, j-l). These results were quantified by counting cells positive for anti-Bax6A7 staining (Fig. 4.2B).

To confirm the ability of FPV039 to inhibit Bax activation, we infected HeLa cells with the same panel of recombinant viruses and immunoprecipitated activated Bax from cell lysates using anti-Bax6A7 (Fig. 4.3). When lysed in 2% CHAPS, a detergent that does not artificially alter Bax conformation (200, 201), activated Bax was precipitated detectably from cells infected with VV Δ F1L or VV Δ F1L-Flag-FPV039(Δ 41-54) and not from cells infected with VV-EGFP or VV Δ F1L-Flag-FPV039(1-176), confirming the ability of both F1L and FPV039 to inhibit Bax activation. Conversely, when cells were lysed in 1% TRITON X-100, a detergent that artificially activates Bax (200, 201), Bax was precipitated from all infected cells, validating the ability of anti-Bax6A7 to detect activated Bax.

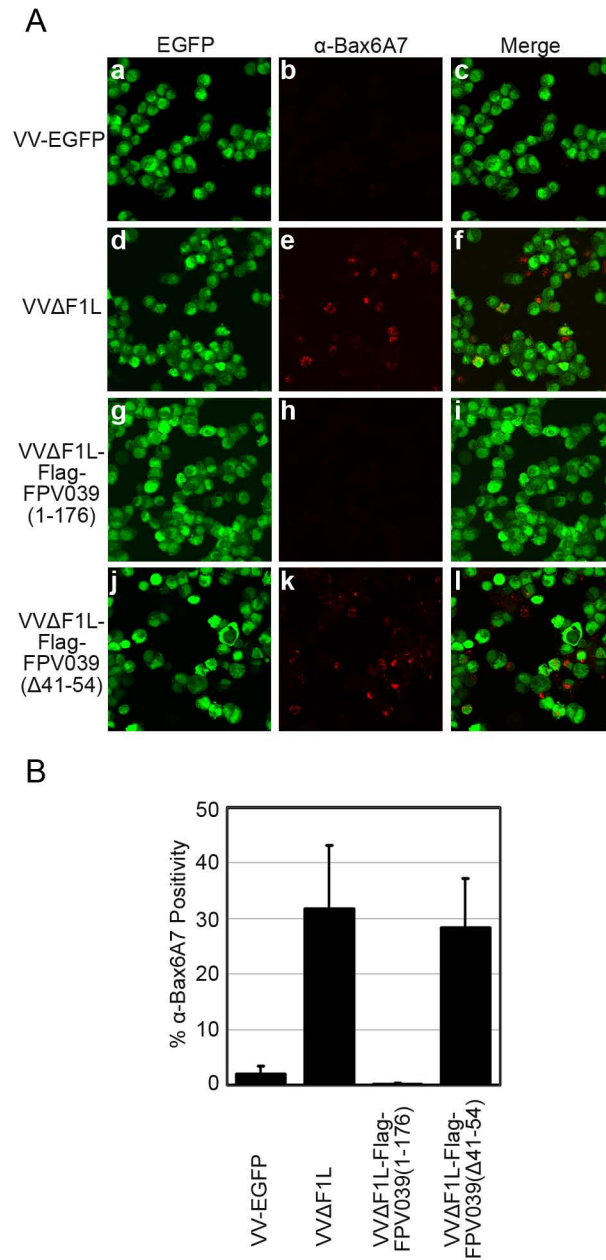


Figure 4.2. FPV039 inhibits Bax activity. (A) HeLa cells were infected with VV-EGFP, VV Δ F1L, VV Δ F1L-Flag-FPV039(1-176), or VV Δ F1L-Flag-FPV039(Δ 41-54) at an MOI of 10 for 24 hours. Following fixation and permeabilisation, Bax activation was visualised with anti-Bax6A7 antibody. (B) Microscopy analysis was quantified as the percentage of cells displaying Bax activation (mean \pm S.D.).

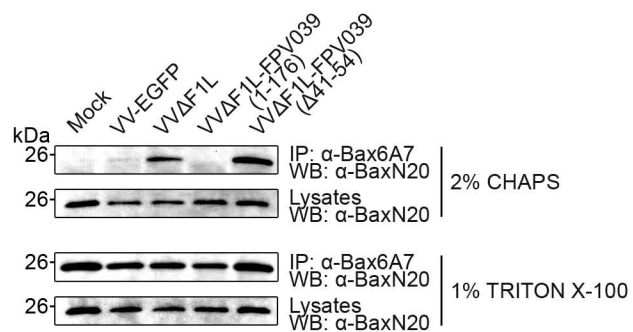


Figure 4.3. FPV039 inhibits Bax activity. HeLa cells were infected with VV-EGFP, VVΔF1L, VVΔF1L-Flag-FPV039(1-176), or VVΔF1L-Flag-FPV039(Δ41-54) at an MOI of 10 for 24 hours. Cells were lysed using either 2% CHAPS or 1% TRITON X-100, and activated Bax was immunoprecipitated (IP) with anti-Bax6A7 antibody and Western blotted (WB) with anti-BaxN20 antibody.

We also used a flow cytometry-based assay to precisely detect and quantify Bax conformational change. Jurkat cells were infected with VV-EGFP, VV Δ F1L, VV Δ F1L-Flag-FPV039(1-176), or VV Δ F1L-Flag-FPV039(Δ 41-54), and the activation of Bax was induced by treatment with staurosporine (STS), a potent apoptotic stimulus (419). Activation-associated exposure of the Bax N-terminus was detected by staining with anti-Bax6A7 and quantified by flow cytometry (Fig. 4.4). Jurkat cells mock infected and left untreated displayed a basal level of fluorescence attributable to nonspecific antibody binding (Fig. 4.4, a). Upon STS treatment of mock-infected cells, however, fluorescence intensity increased, indicating that Bax became activated and underwent a conformational change exposing its N-terminus to binding by the anti-Bax6A7 antibody (Fig. 4.4, a). Conversely, cells infected with VV-EGFP completely inhibited the activation of Bax upon STS treatment due to the endogenous expression of F1L (Fig. 4.4, b). This phenomenon was dependent on the presence of F1L because cells infected with VV Δ F1L were not protected from STS-induced Bax activation (Fig. 4.4, c). Importantly, and in agreement with the previous experiments (Fig. 4.2 & 4.3), cells infected with VV Δ F1L-Flag-FPV039(1-176) were resistant to Bax activation induced by STS (Fig. 4.4, d), whereas cells infected with VV Δ F1L-Flag-FPV039(Δ 41-54) were not (Fig. 4.4, e). No increase in fluorescence intensity was observed in Jurkats stained with an isotype control antibody, confirming the specificity of anti-Bax6A7 for conformationally active Bax (Fig. 4.4, f). Moreover, Jurkat cells deficient in both Bak and Bax did not exhibit an increase in fluorescence after infection or STS treatment, again confirming the specificity of our assay for Bax (Fig. 4.4, g-k). Jurkat cells over-expressing anti-apoptotic Bcl-2 were completely resistant to Bax activation (Fig. 4.4, l-p). Together, these data indicate that FPV039, like both F1L and Bcl-2, is capable of

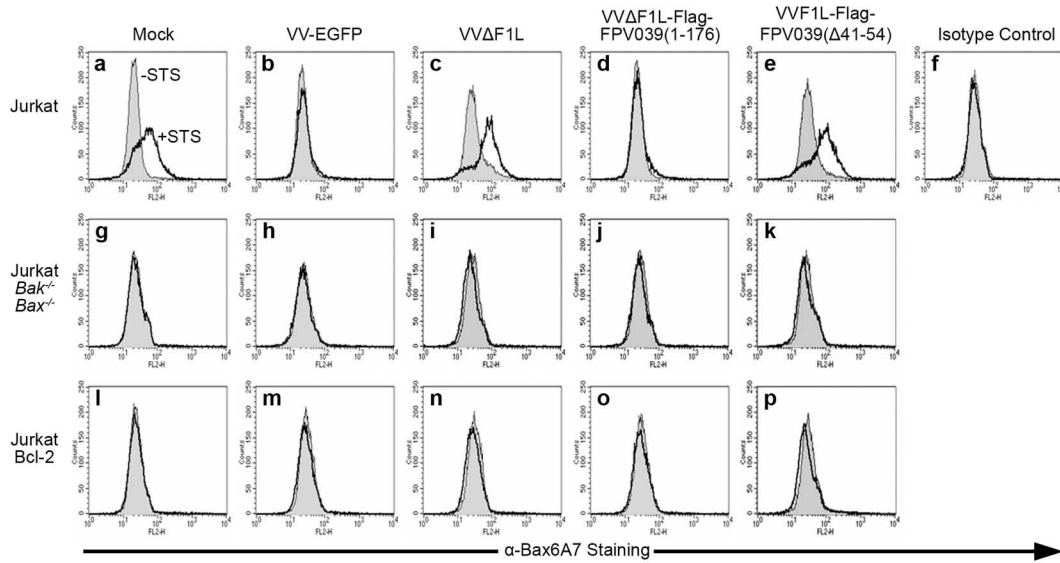


Figure 4.4. FPV039 inhibits the conformational activation of Bax. Wild-type Jurkat cells (a to f), Jurkat cells devoid of Bak and Bax (*Bak*^{-/-}/*Bax*^{-/-}) (g to k), or Jurkat cells over-expressing Bcl-2 (l to p) were infected with VV-EGFP, VVΔF1L, VVΔF1L-Flag-FPV039(1-176), or VVΔF1L-Flag-FPV039(Δ41-54) at an MOI of 5 for 6 hours and then treated with 2 μM staurosporine (STS) for 2 h to induce apoptosis. Exposure of the N-terminus of Bax was monitored by flow cytometry using the confirmation-specific anti-Bax6A7 antibody or an isotype control antibody (NK1.1). Untreated cells, shaded histogram; staurosporine treated cells, open histogram. Data are representative of at least three independent experiments.

inhibiting the activation-associated exposure of the Bax N-terminus during virus infection and in response to potent apoptotic stimuli (200, 426).

4.2.3. FPV039 inhibits Bax oligomerisation. Subsequent to the conformational changes that result in Bax activation, Bax forms high molecular weight oligomers on the surface of the MOM that facilitate the loss of the mitochondrial membrane potential and the release of pro-apoptotic cytochrome c (8, 10, 11). The formation of Bax oligomers therefore represents the penultimate step in the induction of apoptosis by Bax. Because FPV039 inhibited the conformational activation of Bax, we wanted to determine whether FPV039 could also inhibit the consequent formation of Bax oligomers. To this end, HEK 293T cells were transfected with a panel of EGFP-tagged FPV039 constructs and HA-Bax, followed by lysis with 2% CHAPS and treatment with bis-maleimido-hexane (BMH), a chemical cross-linker that irreversibly conjugates proteins at sulfhydryl groups (403). In this way, Bax oligomers could be preserved and visualised by SDS-PAGE and Western blot (Fig. 4.5). Over-expression of HA-Bax alone, which is sufficient to induce apoptosis (Fig. 4.1), resulted in the formation of an approximately 44 kDa Bax dimer and a 66 kDa Bax trimer, both represented on Western blot by distinct bands two and three times the size of monomeric Bax, present as a 22 kDa band. Additionally, higher-order oligomers of Bax were represented by the high-molecular weight bands visible above 85 kDa (Fig. 4.5, lane 2). EGFP alone, as expected, did not prevent the formation of Bax oligomers (Fig. 4.5, lane 3). Importantly, EGFP-FPV039(1-176), like EGFP-Bcl-2, prevented the oligomerisation of Bax (Fig. 4.5, lanes 4 and 7), whereas EGFP-FPV039(Δ 41-54), which lacks the putative BH3 domain, and EGFP-FPV039(1-94), which lacks the BH2 and TM domains, were unable to prevent Bax

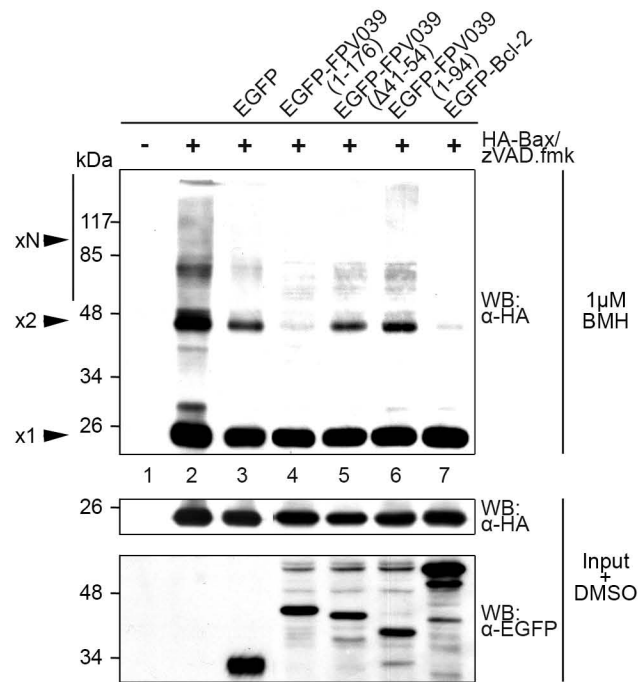


Figure 4.5. FPV039 inhibits Bax oligomerisation. HeLa cells were co-transfected with pEGFP, pEGFP-FPV039(1-176), pEGFP-FPV039(Δ41-54), pEGFP-FPV039(1-94), or pEGFP-Bcl-2 and pcDNA3-HA-Bax. zVAD.fmk was added following transfection to prevent the activation of caspases. Cells were lysed in 2% CHAPS, and cell lysates were treated with 1 μM 1,6-bismaleimido-hexane (BMH) and Western blotted (WB) with anti-HA antibody to detect Bax oligomers (upper panel). A portion of the lysates (input) was treated with DMSO alone and subjected to Western blotting with either anti-HA or anti-EGFP antibodies to determine expression levels of the transfected proteins (lower two panels). x1, Bax monomer; x2, Bax dimer; xN, higher-order Bax oligomers.

oligomerisation (Fig. 4.5, lanes 5 and 6). Moreover, Western blotting of the lysates before the addition of BMH revealed that HA-Bax was expressed at similar levels in each case, as were all FPV039 constructs (Fig. 4.5, bottom two panels). Thus, in addition to inhibiting the conformational activation of Bax, FPV039 also inhibited Bax oligomerisation, the penultimate step in the induction of apoptosis by Bax.

4.2.4. FPV039 interacts with Bax. The ability of FPV039 to inhibit Bax activation and prevent Bax-induced apoptosis implied that FPV039 might interact with Bax. To determine whether FPV039 interacted with Bax, HEK 293T cells were transfected with pEGFP, pEGFP-FPV039(1-176), pEGFP-FPV039(Δ 41-54), pEGFP-FPV039(1-94), or pEGFP-Bcl-2 and pcDNA3-HA-Bax, followed by lysis in 2% CHAPS. Complexes were immunoprecipitated with an anti-EGFP antibody and Western blotted with an anti-Bax antibody (Fig. 4.6A). Using this approach, an interaction between EGFP-FPV039(1-176) and HA-Bax was detected. Importantly, FPV039 lacking the cryptic BH3 domain, EGFP-FPV039(Δ 41-54), or the BH2 and TM domains, EGFP-FPV039(1-94), was unable to interact with Bax, suggesting that the interaction depended on specific functional domains of FPV039. As expected, EGFP-Bcl-2 interacted with Bax, serving as a positive control in this experiment (482, 488). No Bax was precipitated in cells expressing HA-Bax alone or co-expressing HA-Bax along with EGFP, further confirming the specificity of the interaction between FPV039 and Bax. Although each EGFP-tagged protein was precipitated equally (Fig. 4.6A, second panel), lysates were also Western blotted to ensure that all proteins were expressed at comparable levels. Notably, HA-Bax was similarly expressed in each case, as were all FPV039 constructs (Fig. 4.6A, bottom two panels). These data provide

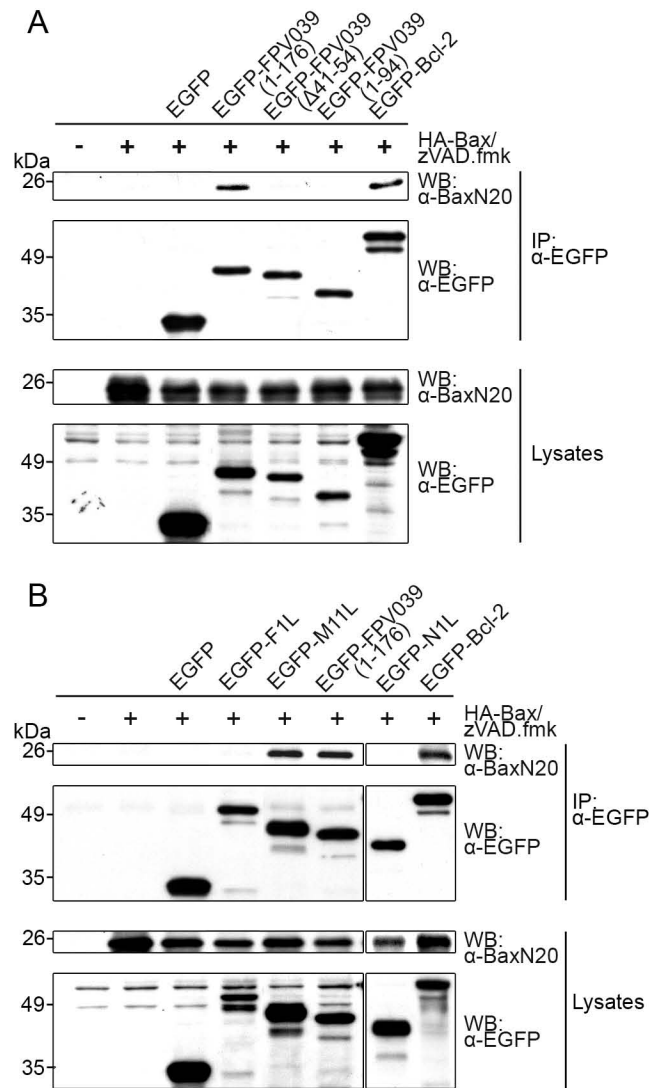


Figure 4.6. FPV039 interacts with Bax. (A) HEK 293T cells were co-transfected with pEGFP, pEGFP-FPV039(1-176), pEGFP-FPV039(Δ41-54), pEGFP-FPV039(1-94), or pEGFP-Bcl-2 and pcDNA3-HA-Bax, followed by lysis with 2% CHAPS. Cell lysates were immunoprecipitated (IP) with anti-EGFP antibody and Western blotted (WB) with either anti-BaxN20 or anti-EGFP antibodies to detect interaction. Cell lysates were Western blotted with anti-BaxN20 or anti-EGFP antibodies to determine the expression levels of HA-Bax or the EGFP-tagged proteins, respectively. (B) HEK 293T cells were co-transfected with pEGFP, pEGFP-F1L, pEGFP-M11L, pEGFP-FPV039(1-176), pEGFP-N1L, or pEGFP-Bcl-2 and pcDNA3-HA-Bax. Immunoprecipitations and Western blotting were performed as in (A). zVAD.fmk was added following transfection to prevent the activation of caspases.

convincing evidence that FPV039 interacts with Bax and that this interaction is dependent on Bcl-2 functional domains, including the cryptic BH3 domain.

In an effort to compare FPV039 with other poxviral inhibitors of apoptosis, we performed a second co-immunoprecipitation experiment and included EGFP-F1L or EGFP-N1L, both anti-apoptotic proteins encoded by VV, and EGFP-M11L, the anti-apoptotic protein encoded by myxoma virus (Fig. 4.6B). As previously shown, M11L, like FPV039, exhibited an interaction with Bax, whereas F1L failed to interact with Bax (251, 409, 426). Contrary to previously published results (89), N1L did not exhibit an interaction with Bax in this assay.

We excluded the possibility that FPV039 was interacting with Bax through an interaction with Bak by repeating the immunoprecipitations in Bak-deficient baby mouse kidney cells. Cells were transfected with pEGFP, pEGFP-Bcl-2, or pEGFP-FPV039(1-176) and co-transfected with pcDNA3-HA-Bax. Following lysis and immunoprecipitation, Western blot analysis revealed that FPV039, like Bcl-2, was able to interact with Bax even in the absence of Bak (Fig. 4.7). These data collectively suggest that FPV039 interacts with Bax, a property not necessarily shared among other poxviral inhibitors of apoptosis, like F1L and N1L.

4.2.5. FPV039 interacts with endogenous activated Bax. During transient transfection, Bax is over-expressed and, consequently, activated. Although we demonstrated that FPV039 interacted with Bax in the context of over-expression, we wanted to determine if FPV039 could also interact with endogenous Bax in the context of virus infection, when the majority of Bax is apparently not activated (Fig. 4.2, 4.3, & 4.4). To address this question, HeLa cells were infected with VV Δ F1L, VV-Flag-F1L, which expresses a Flag-tagged version of the anti-

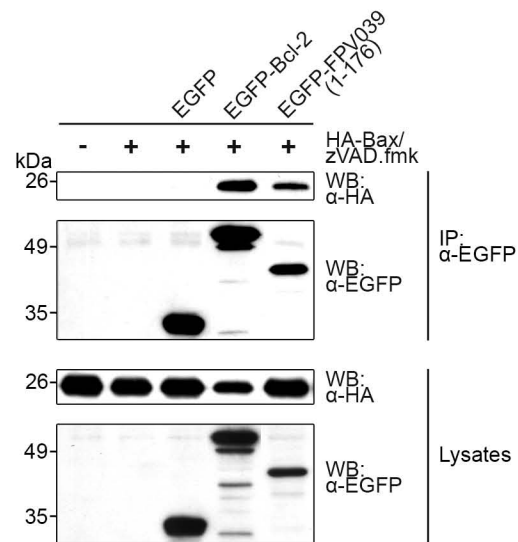


Figure 4.7. FPV039 interacts with Bax in the absence of Bak. *Bak*^{-/-} baby mouse kidney (BMK) cells were co-transfected with pEGFP, pEGFP-Bcl-2, or pEGFP-FPV039(1-176) and pcDNA3-HA-Bax, followed by lysis with 2% CHAPS. Cell lysates were immunoprecipitated (IP) with anti-EGFP antibody and Western blotted (WB) with either anti-HA or anti-EGFP antibodies to detect interactions. Cell lysates were Western blotted with anti-HA or anti-EGFP antibodies to determine the expression levels of HA-Bax or the EGFP-tagged proteins, respectively. zVAD.fmk was added following transfection to prevent the activation caspases.

apoptotic protein F1L, or VV Δ F1L-Flag-FPV039(1-176), which expresses full-length Flag-FPV039. Cell lysates were first immunoprecipitated with an anti-Flag antibody and Western blotted with an anti-Bax antibody to detect an interaction (Fig. 4.8A). Despite robust precipitation and expression of FPV039, an interaction between FPV039 and endogenous Bax was not observed in this experiment. Similarly, F1L also failed to interact with endogenous Bax during virus infection, as previously shown (426). Our inability to detect Bax by precipitating FPV039 suggested that the expression of FPV039 potentially prevented Bax activation (Fig. 4.1 to 4.5) and therefore pre-empted an interaction between FPV039 and active Bax at the mitochondria. However, we wondered whether FPV039 could interact with the minute levels of endogenous, active Bax that might be present during infection. To specifically precipitate any activated Bax that might be present, we performed a reciprocal immunoprecipitation this time using anti-Bax6A7 (Fig. 4.8B). As expected, the amount of immunoprecipitated active Bax varied among the infected samples in this experiment, with the most Bax precipitated from cells infected with the apoptotic virus VV Δ F1L and dramatically less Bax precipitated from cells infected with either of the anti-apoptotic viruses, VV-Flag-F1L and VV Δ F1L-Flag-FPV039. Precipitation of active Bax resulted in the co-precipitation of FPV039, indicating, along with Figures 4.6 and 4.7, that FPV039 interacted with endogenous active Bax. Precipitation of active Bax also co-precipitated F1L, albeit to a lesser extent, which agrees with the observed ability of F1L to interact with artificially activated Bax in the presence of the detergent TRITON X-100 (426). Although we were able to detect Flag-FPV039 by precipitating active Bax (Fig. 4.8B), we were unable to detect Bax by precipitating Flag-FPV039 (Fig. 4.8A). Since FPV039 is a potent inhibitor of Bax activation (Fig. 4.1 to 4.5), the vast majority of

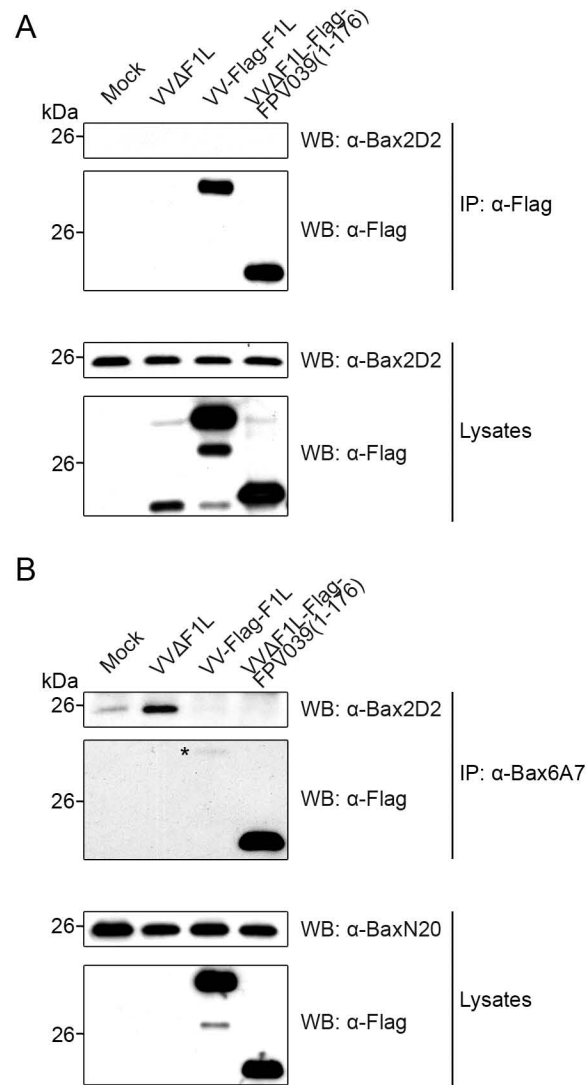


Figure 4.8. FPV039 interacts with endogenous active Bax during vaccinia virus infection. HeLa cells were mock infected or infected at an MOI of 5 with VVΔF1L, VV-Flag-F1L, or VVΔF1L-Flag-FPV039(1-176). Sixteen hours post-infection, cells were lysed in 2% CHAPS, and cell lysates were immunoprecipitated (IP) with either anti-Flag (**A**) or anti-Bax6A7 (**B**) antibodies and Western blotted (WB) with either anti-Flag or anti-Bax2D2 (**A & B**) antibodies. Cell lysates were Western blotted with anti-Bax2D2 and anti-Flag (**A**) or anti-BaxN20 and anti-Flag (**B**) antibodies to determine expression levels. The asterisk (*) indicates Flag-F1L (**B**).

Bax within a cell expressing FPV039 is inactive and presumably unable to interact with FPV039. Thus, the small minority of activated Bax that interacts with FPV039 (such as might be observed in Fig. 4.8A) is likely below the level of detection that can be achieved by Western blotting using our antibodies. Together, these data suggest that FPV039, like Bcl-2 and Bcl-x_L (39, 115, 496), is capable of interacting with activated Bax.

4.2.6. FPV039 inhibits apoptosis induced by BH3-only proteins. The BH3-only proteins are pro-apoptotic members of the Bcl-2 family that induce apoptosis by facilitating the activation of both Bak and Bax (73). Given that FPV039 is a potent inhibitor of apoptosis, we wondered whether FPV039 was also capable of inhibiting cell death induced by the over-expression of BH3-only proteins. To this end, HeLa cells were transfected with pEGFP, pEGFP-FPV039(1-176), pEGFP-Bcl-2, pEGFP-Bcl-x_L, or pEGFP-Mcl-1 and co-transfected with a plasmid encoding one of eight BH3-only proteins. Apoptosis was then quantified in transfected (EGFP positive) cells by measuring the fluorescence intensity of TMRE (Fig. 4.9). EGFP alone was unable to prevent apoptosis induced by the over-expression of Bim_L, Bik, Bmf, or Bad, each of which induced apoptosis in over 40% of the cells. Conversely, co-expression of either EGFP-Bcl-2 or EGFP-FPV039(1-176) reduced apoptosis to less than 1% (Fig. 4.9A-D). Similarly, full-length Bid and active tBid induced apoptosis in approximately 50% of cells co-expressing EGFP, and this was reduced to less than 10% upon expression of EGFP-Bcl-x_L or EGFP-FPV039(1-176) (Fig. 4.9F & G). Over-expression of Puma and Noxa induced apoptosis in only 26% and 14% of cells, respectively, but this was reduced to less than 5% upon co-expression of EGFP-Bcl-2, EGFP-Mcl-1, or EGFP-FPV039(1-176) (Fig. 4.9E & H). Lysates of transfected cells

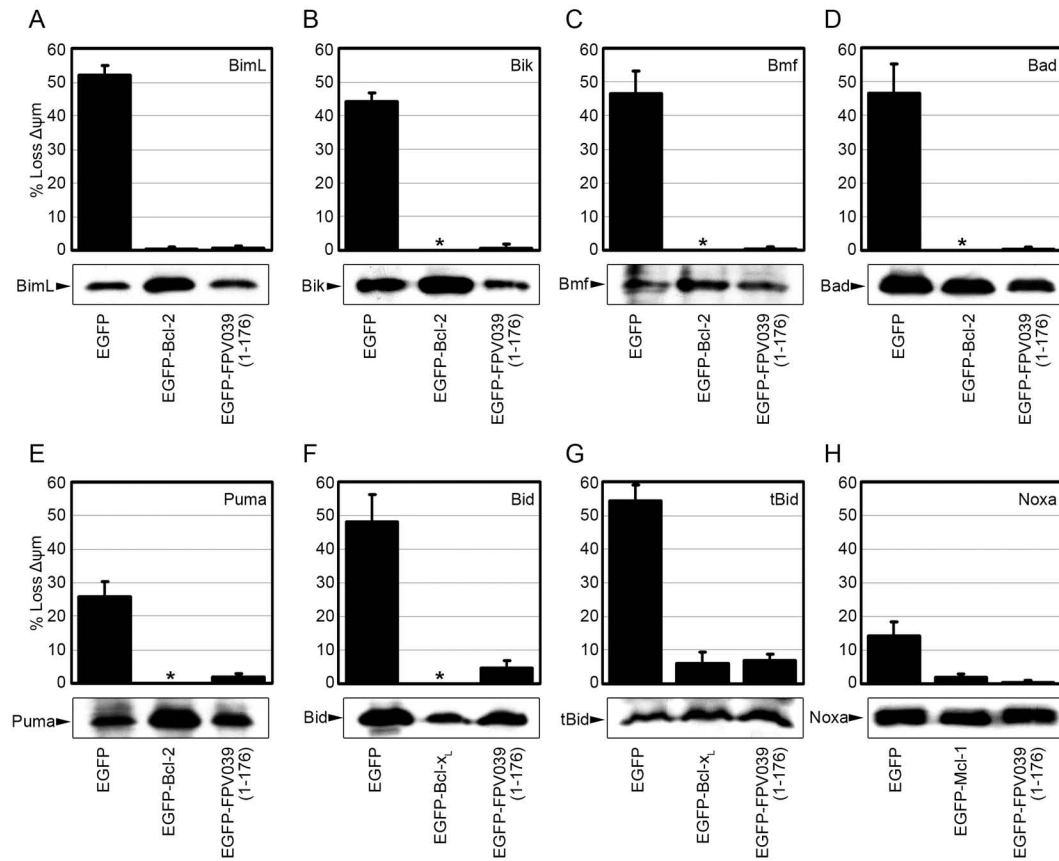


Figure 4.9. FPV039 inhibits apoptosis induced by BH3-only proteins. HeLa cells were co-transfected with pEGFP and pEGFP-FPV039(1-176) along with one of the following BH3-only proteins and the relevant cellular Bcl-2 protein: (A) pcDNA3-Flag-Bim_L and pEGFP-Bcl-2, (B) pcDNA3-Myc-Bik and pEGFP-Bcl-2, (C) pcDNA3-T7-Bmf and pEGFP-Bcl-2, (D) pXJ40-HA-Bad and pEGFP-Bcl-2, (E) pcDNA3-HA-Puma and pEGFP-Bcl-2, (F) pcDNA3-Bid-Flag and pEGFP-Bcl-x_L, (G) pcDNA3-tBid-Flag and pEGFP-Bcl-x_L, (H) pcDNA3.1-Myc-Noxa and pEGFP-Mcl-1. Eighteen hours post-transfection, apoptosis was assessed in EGFP-positive cells by quantifying TMRE fluorescence via flow cytometry, and the percentage of cells that demonstrated a loss of mitochondrial membrane potential ($\Delta\psi_m$) is given as the y-axis. Standard deviations were calculated from three independent experiments. Whole cell lysates from parallel experiments were Western blotted with the following antibodies to determine expression levels of the BH3-only proteins: anti-Flag (A, F, & G), anti-Myc (B), anti-T7 (C), anti-HA (D & E), anti-Noxa (H). The asterisk (*) indicates complete protection by EGFP-Bcl-2 or EGFP-Bcl-x_L.

showed that, in each case, BH3-only proteins were being expressed. Together these data indicate that FPV039 is able to inhibit apoptosis induced by the over-expression of Bim_L, Bik, Bmf, Bad, Puma, Bid, tBid, and Noxa.

4.2.7. FPV039 interacts with a subset of BH3-only proteins. Given the ability of FPV039 to inhibit apoptosis induced by all eight BH3-only proteins tested, we next sought to determine whether FPV039 could also interact with BH3-only proteins. One BH3-only protein in particular, Bim, is thought to directly activate Bax and has been previously shown by our lab to be required for VV-induced apoptosis (426). To determine if FPV039 was capable of interacting with Bim, HEK 293T cells were transfected with pEGFP, pEGFP-F1L, pEGFP-M11L, pEGFP-FPV039(1-176), or pEGFP-Bcl-2 and co-transfected with pcDNA3-Bim_L. Following lysis in 2% CHAPS, EGFP was precipitated using an anti-EGFP antibody, and Western blotting was subsequently performed using both anti-Flag and anti-EGFP antibodies (Fig. 4.10). As expected, EGFP-Bcl-2 exhibited an interaction with Bim_L, whereas EGFP alone did not (333). Interestingly, EGFP-FPV039(1-176) also precipitated Bim_L, suggesting that, like Bcl-2, FPV039 was capable of interacting with Bim_L. Additionally, EGFP-M11L, which has been previously shown to interact with Bim_{EL} (251), also interacted with Bim_L, as did EGFP-F1L, as previously shown (426). Each EGFP-tagged protein was precipitated at equal levels (Fig. 4.10, second panel), and Western blotting of the lysates confirmed that the EGFP-tagged proteins, as well as Bim_L, were expressed at comparable levels in each case (Fig. 4.10, third and fourth panel).

We next examined the ability of FPV039 to interact with seven other BH3-only proteins. Using a similar transfection and immunoprecipitation procedure as described for Bim_L, we confirmed the interaction between each BH3-only protein

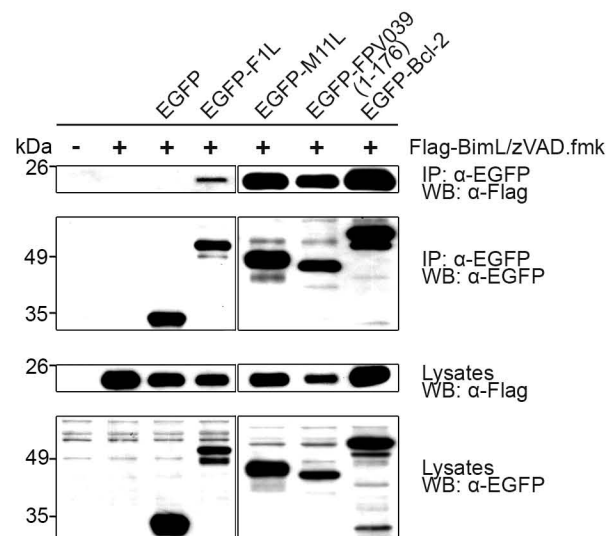


Figure 4.10. FPV039 interacts with Bim_L. HeLa cells were co-transfected with pEGFP, pEGFP-F1L, pEGFP-M11L, pEGFP-FPV039(1-176), or pEGFP-Bcl-2 and pcDNA3-Flag-Bim_L, followed by lysis with 2% CHAPS. Cell lysates were immunoprecipitated (IP) with anti-EGFP antibody and Western blotted (WB) with either anti-Flag or anti-EGFP antibodies to detect interaction. Cell lysates were Western blotted with anti-Flag or anti-EGFP antibodies to determine expression levels. zVAD.fmk was added following transfection to prevent the activation of caspases.

and the appropriate EGFP-tagged, anti-apoptotic Bcl-2 family protein (Fig. 4.11). As expected, Bik, Bmf, Bad, and Puma all co-precipitated with EGFP-Bcl-2 (Fig. 4.11A-D), whereas Bid and tBid co-precipitated with EGFP-Bcl-x_L (Fig. 4.11E & F) and Noxa co-precipitated with Mcl-1 (Fig. 4.11G). Interestingly, only Bik co-precipitated with EGFP-FPV039(1-176) to significant levels, suggesting that Bik and FPV039 interacted (Fig. 4.11A). In each case, EGFP was precipitated at equal levels, and the lysates show that expression of the EGFP-tagged proteins, as well as the BH3-only proteins, was comparable (Fig. 4.11A-G, bottom three panels). Thus, it is clear from these data that FPV039 is capable of interacting with only two BH3-only proteins: Bim_L and Bik.

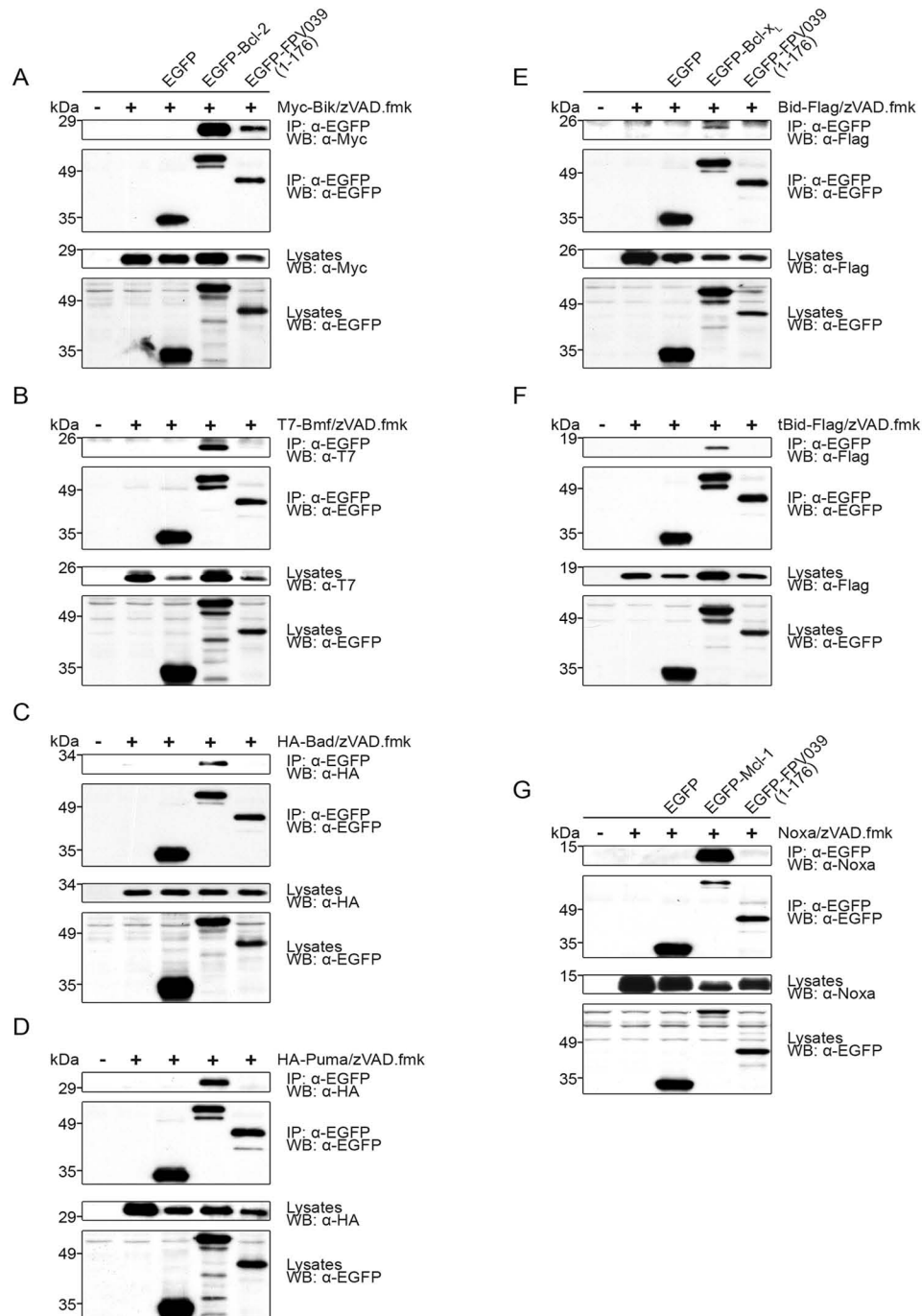


Figure 4.11. FPV039 interacts with a subset of BH3-only proteins. HEK 293T cells were co-transfected with pEGFP and pEGFP-FPV039(1-176) along with one of the following BH3-only proteins and the relevant cellular Bcl-2 protein: **(A)** pcDNA3-Myc-Bik and pEGFP-Bcl-2, **(B)** pcDNA3-T7-Bmf and pEGFP-Bcl-2, **(C)** pXJ40-HA-Bad and pEGFP-Bcl-2, **(D)** pcDNA3-HA-Puma and pEGFP-Bcl-2, **(E)** pcDNA3-Bid-Flag and pEGFP-Bcl-x_L, **(F)** pcDNA3-tBid-Flag and pEGFP-Bcl-x_L, **(G)** pcDNA3.1-Myc-Noxa and pEGFP-Mcl-1. zVAD.fmk was added following transfection to prevent the activation of caspases. Cells were lysed with 2% CHAPS and immunoprecipitated (IP) with anti-EGFP antibody. Immunoprecipitates and cell lysates were Western blotted (WB) with anti-EGFP and anti-Myc **(A)**, anti-T7 **(B)**, anti-HA **(C & D)**, anti-Flag **(E & F)**, or anti-Noxa **(G)** antibodies.

CHAPTER FIVE

DEERPOX VIRUS ENCODES AN INHIBITOR OF APOPTOSIS THAT REGULATES BAK AND BAX

A version of this chapter has been submitted to *Journal of Virology*:

Banadyga L., Lam S-C., Okamoto T., Kvensakul M., Huang D.C., and M. Barry.
2011. *Journal of Virology*. 85(5). Copyright 2011. American Society for
Microbiology.

All of the experiments included within this chapter were performed by L. Banadyga with the exception of Figures 5.2, 5.3, 5.5A, 5.6A, 5.8A, and 5.9A, which were performed by S-C. Lam under the supervision of L. Banadyga, and Figures 5.4, 5.7, and 5.11, which were performed by T. Okamoto. pEGFP-DPV022 was sub-cloned by S-C. Lam under the supervision of L. Banadyga. psc66-Flag-DPV022 was cloned by T. Okamoto. The original manuscript was written by L. Banadyga with editorial contributions by M. Kvensakul, D. Huang, and M. Barry.

5.1. BRIEF INTRODUCTION

Surprisingly, although DPV022, encoded by deerpox virus, lacks obvious sequence homology with cellular Bcl-2 proteins, DPV022 possesses limited regions of homology with both M11L and F1L (2). Based on this homology, we hypothesised that DPV022 would inhibit apoptosis, and we sought to characterise the mechanism of action. Here we show that like cellular Bcl-2 proteins and both M11L and F1L, DPV022 localised to the mitochondria where it inhibited apoptosis induced by TNF α . DPV022 directly interacted with both exogenous Bak and Bax and inhibited apoptosis induced by Bak and Bax over-expression. Moreover, DPV022 was able to inhibit apoptosis even when all endogenous anti-apoptotic Bcl-2 proteins were neutralised. In the context of virus infection, DPV022 interacted with endogenous Bak and Bax and inhibited their conformational activation. Together, our data indicate that DPV022 is an inhibitor of apoptosis that might be exploited to better understand the regulation of cell death.

5.2. RESULTS

5.1.1. DPV022 shares sequence homology with F1L and M11L but not Bcl-2 family proteins. F1L, encoded by VV, and M11L, encoded by myxoma virus, share no obvious sequence similarity with each other or other known modulators of apoptosis. It was therefore surprising that, upon sequencing of the deerpox virus genome, the open reading frame DPV022 was discovered to share 27% amino acid sequence identity with F1L (2). Alignment of the F1L and DPV022 amino acid sequences revealed identical amino acids distributed throughout the two proteins but not necessarily localised to any particular region, including the regions corresponding to the highly divergent F1L BH-like domains (Fig. 5.1A)

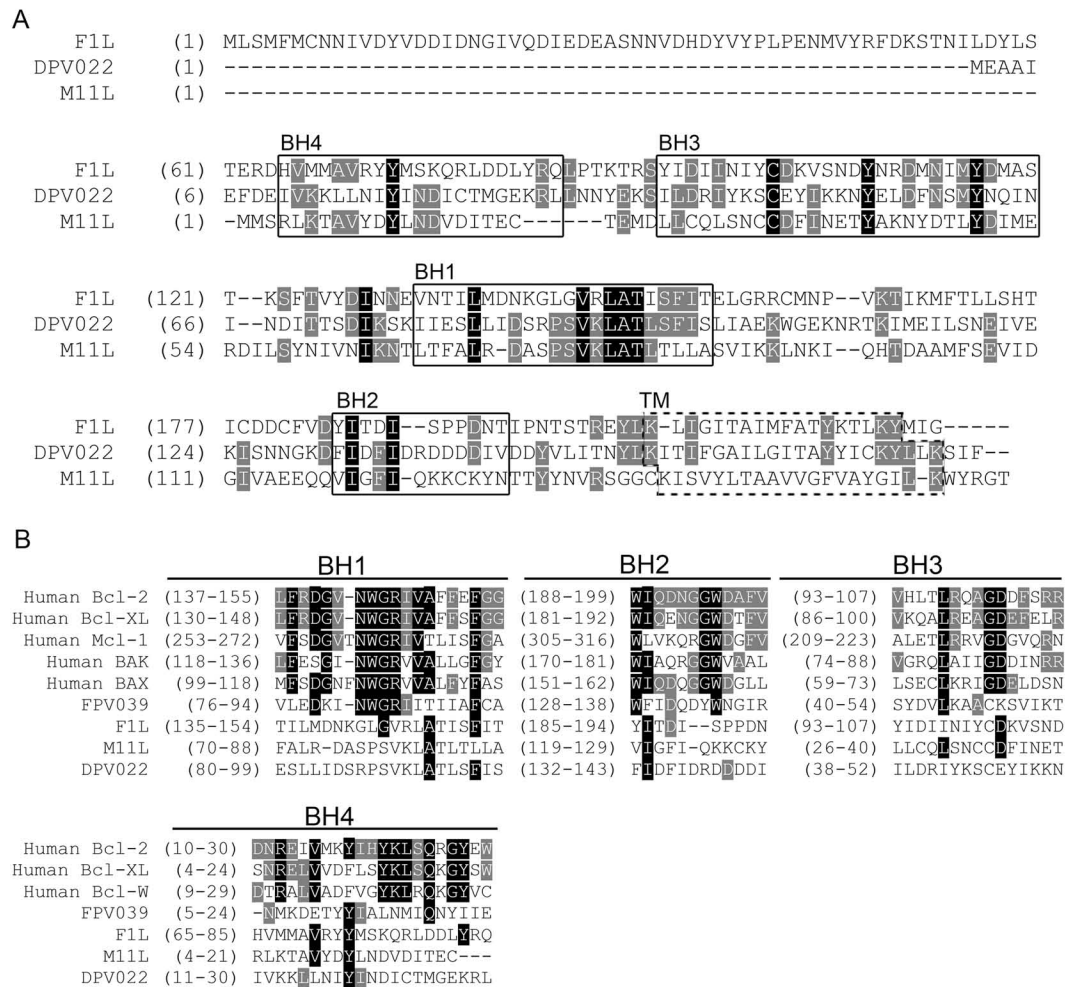


Figure 5.1. DPV022 shares regions of sequence homology with F1L and M11L but not cellular Bcl-2 proteins. (A) DPV022 shares regions of sequence homology with both F1L and M11L, particularly in the regions corresponding to F1L BH-like domains (boxed). The transmembrane (TM) domains for F1L and M11L and the putative TM domain for DPV022 are indicated (dashed box). (B) Alignment of BH1-4 domains from various cellular and viral Bcl-2 proteins with corresponding regions of DPV022. Amino acids conserved among all three proteins are highlighted in black, and amino acids conserved among two of the three proteins are highlighted in grey (AlignX) (A & B).

(53). Interestingly, DPV022 also possesses 23% amino acid identity with M11L (Fig. 5.1A). Alignment of M11L and DPV022 amino acid sequences likewise showed identical amino acids distributed throughout the two proteins (Fig. 5.1A). Many of the amino acids shared by DPV022 and F1L differed from the amino acids shared by DPV022 and M11L, suggesting that DPV022 may represent an evolutionary intermediate between F1L and M11L. Moreover, although relatively few amino acids were identical among all three proteins, a number of identical amino acids were clustered within the regions corresponding to the highly divergent BH-like domains of F1L and M11L, particularly BH3 and BH1 (Fig. 5.1A) (53, 251, 252). These putative BH-like domains in DPV022, however, bear little sequence identity to the BH domains present in cellular Bcl-2 family proteins or the poxviral Bcl-2 homologue, FPV039 (Fig. 5.1B) (53). Like Bcl-2 family proteins and both F1L and M11L, DPV022 is predicted to possess a C-terminal hydrophobic domain responsible for targeting the protein to intracellular membranes, such as the mitochondria (Fig. 5.1A). Therefore, based on sequence identity and the predicted presence of a C-terminal TM tail, we hypothesised that DPV022 would act at the mitochondria to inhibit apoptosis.

5.2.2. DPV022 localises to the mitochondria and inhibits apoptosis. Most cellular Bcl-2 proteins and viral inhibitors of apoptosis possess hydrophobic C-terminal TM domains that post-translationally anchor the proteins to an intracellular membrane (47). Sub-cellular localisation to the mitochondria is typical for cellular Bcl-2 proteins and, in many cases, a pre-requisite for their anti-apoptotic function (281, 382). Sequence analysis of DPV022 revealed a C-terminal hydrophobic region that may act as a tail anchor (Fig. 5.1A). To determine whether DPV022 localised to the mitochondria, HeLa cells were

transfected with pEGFP or pEGFP-DPV022 and analysed by live-cell confocal microscopy (Fig. 5.2). Cells transfected with pEGFP displayed a diffuse, cytoplasmic fluorescence pattern that did not co-localise with MitoTracker, a dye that specifically labels mitochondria. Conversely, cells transfected with pEGFP-DPV022 displayed a punctate fluorescence pattern that co-localised with MitoTracker, indicating that, like F1L and M11L, DPV022 is a mitochondria-localised protein.

Given that DPV022 bears limited sequence homology to F1L and M11L, two well-characterised poxviral inhibitors of apoptosis, we next sought to determine whether DPV022 could inhibit apoptosis. HeLa cells were transfected with pEGFP, pEGFP-DPV022, pEGFP-FPV039, pEGFP-M11L, pEGFP-F1L, or pEGFP-Bcl-2 and treated with TNF α to induce apoptosis. Cells were stained with TMRE, a fluorescent dye incorporated by healthy, respiring mitochondria, and apoptosis was quantified via flow cytometric analysis of EGFP-expressing cells (Fig. 5.3A) (125, 309). Nearly 40% of cells expressing EGFP exhibited a decrease in TMRE staining upon TNF α treatment, indicating loss of mitochondrial membrane potential and the induction of apoptosis. Cells expressing EGFP-FPV039, the anti-apoptotic Bcl-2 homologue encoded by fowlpox virus, EGFP-M11L, or EGFP-F1L were protected from the loss of mitochondrial membrane potential, with apoptosis prevented in at least 92% of transfected cells. EGFP-Bcl-2, the proto-typical anti-apoptotic member of the cellular Bcl-2 family, prevented TNF α -induced apoptosis in 96% of transfected cells. Importantly, cells expressing EGFP-DPV022 were also protected from the induction of apoptosis, with only 3% of transfected cells exhibiting a loss in mitochondrial membrane potential. To ensure that differences in expression levels did not affect the inhibition of apoptosis, cell lysates were analysed (Fig. 5.3B). Although EGFP-

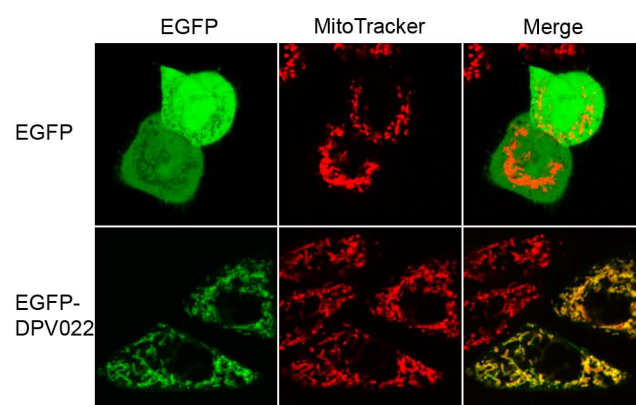


Figure 5.2. DPV022 localises to the mitochondria. HeLa cells were transfected with pEGFP or pEGFP-DPV022, and mitochondria were stained with MitoTracker dye. Co-localisation was visualised by confocal microscopy. *This experiment was performed by S-C. Lam under the supervision of L. Banadyga.*

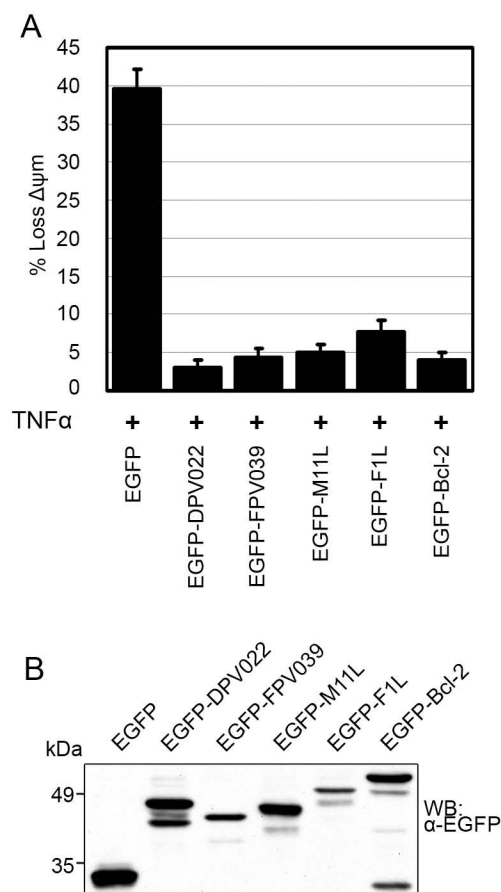


Figure 5.3. DPV022 inhibits TNF α -induced apoptosis. (A) HeLa cells were transfected with pEGFP, pEGFP-DPV022, pEGFP-FPV039, pEGFP-M11L, pEGFP-F1L, or pEGFP-Bcl-2 and treated with 10 ng/ml TNF α and 5 μ g/ml cycloheximide for 6 h. Apoptosis was assessed in EGFP-positive cells by quantifying TMRE fluorescence via flow cytometry, and the percentage of cells that demonstrated a loss of mitochondrial membrane potential ($\Delta\psi_m$) is given as the y-axis. Standard deviations were calculated from three independent experiments. (B) HeLa cells were transfected in a parallel experiment, and the expression level of each EGFP-tagged construct was assessed by Western blotting (WB) whole cell lysates. *The experiment depicted in (A) was performed by S-C. Lam under the supervision of L. Banadyga.*

FPV039 and EGFP-F1L were expressed to lower levels than the other EGFP-tagged proteins, both were potent inhibitors of apoptosis. EGFP alone was expressed at the highest level, but it was not protective (Fig. 5.3B). Together, these data demonstrate that DPV022 is a mitochondria-localised protein capable of inhibiting apoptosis induced by activation of the death receptor pathway in HeLa cells, presumably by interfering with events at the mitochondria.

5.2.3. DPV022 interacts with Bak and inhibits Bak-induced apoptosis. The intrinsic apoptotic pathway is ultimately regulated at the mitochondria by the pro-apoptotic proteins Bak and Bax (282, 459, 502). Activation of Bak results in the release of cytochrome *c* from the mitochondria and the subsequent induction of apoptosis (458). Bak activity is inhibited by constitutive interaction with the cellular anti-apoptotic proteins Bcl-x_L and Mcl-1 (94, 470) as well as several viral inhibitors of apoptosis, including FPV039, F1L, and M11L (Chapter 3 and (450, 453)). To determine if DPV022 was capable of directly interacting with Bak, we used a heterologous model system based on the yeast *Saccharomyces cerevisiae*, which lacks endogenous Bcl-2 family proteins (Fig. 5.4). Because *S. cerevisiae* do not have the equivalent components of the mammalian death machinery, they do not undergo apoptosis in a manner similar to mammalian cells. Nonetheless, over-expression of pro-apoptotic Bax or Bak results in growth arrest and loss of yeast colony formation, potentially due to disruption of mitochondrial function (174, 210, 379). Yeast cells can be rescued from this growth arrest by over-expression of mammalian anti-apoptotic proteins, such as Bcl-x_L, which leads to robust colony growth in the spotting assay (174, 379). Thus, in this well-established functional assay (139, 161, 215, 489), expression of Bak blocks yeast growth, which can be rescued by over-expression of anti-

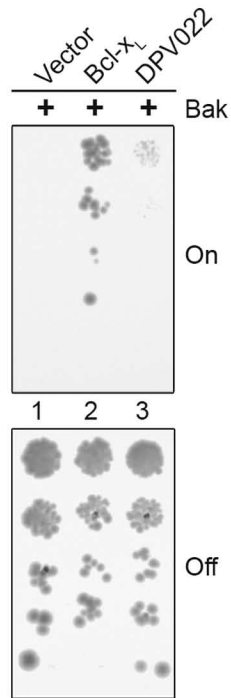


Figure 5.4. DPV022 interacts with Bak in the absence of all other Bcl-2 family proteins. *S. cerevisiae* were co-transformed with the indicated plasmids and standardised concentrations were spotted in serial dilutions vertically down the plate. Galactose-containing media (On) induced the expression of Bak, whereas glucose-containing media (Off) repressed the expression of Bak. Colony growth reflects resistance to Bak-induced growth suppression. *This experiment was performed by T. Okamoto.*

apoptotic Bcl-2 proteins (Fig. 5.4, "On"). Yeast were serially diluted and duplicate-plated vertically on medium containing either galactose, to induce the expression of Bak (Fig. 5.4, "On"), or glucose, to repress the expression of Bak (Fig. 5.4, "Off"). As expected, yeast expressing only Bak did not produce any colonies. (Fig. 5.4, lane 1, "On") (423); however, co-expression of Bcl-x_L, which interacts with Bak, efficiently rescued yeast growth and resulted in colony formation. Likewise, co-expression of DPV022 neutralised Bak and allowed the growth of the yeast (Fig. 5.4, lane 3, "On"). Compared to Bcl-x_L, fewer colonies grew when DPV022 was co-expressed with Bak, which may be due to different expression levels between Bcl-x_L and DPV022. Regardless, this data suggests that DPV022 can directly engage Bak and neutralise its activity in the absence of any other mammalian Bcl-2 proteins. Yeast plated on glucose-containing medium produced a similar number of colonies in each case, indicating that expression of Bak was being repressed and that equivalent concentrations of yeast were plated (Fig. 5.4, "Off"). To further confirm the ability of DPV022 to interact with Bak, HEK 293T cells were transfected with pEGFP, pEGFP-FPV039, pEGFP-M11L, pEGFP-F1L, pEGFP-Bcl-x_L, or pEGFP-DPV022 and pcDNA3-HA-Bak, and cells were lysed in buffer containing 2% CHAPS, a detergent that does not artificially affect the conformation of Bcl-2 family proteins (200, 201). Cell lysates were immunoprecipitated with an anti-EGFP antibody followed by Western blotting with either an anti-HA or an anti-EGFP antibody (Fig. 5.4A & B). Consistent with previous data, an interaction between HA-Bak and EGFP-FPV039, EGFP-M11L, and EGFP-F1L was observed (Fig. 5.5A) (Chapter 3 and (450, 453)). EGFP-Bcl-x_L, a cellular Bcl-2 family protein, also interacted with HA-Bak, as expected (Fig. 5.5B) (470). Similarly, EGFP-DPV022 precipitated HA-Bak, suggesting that the two proteins interact (Fig. 5.5A & B).

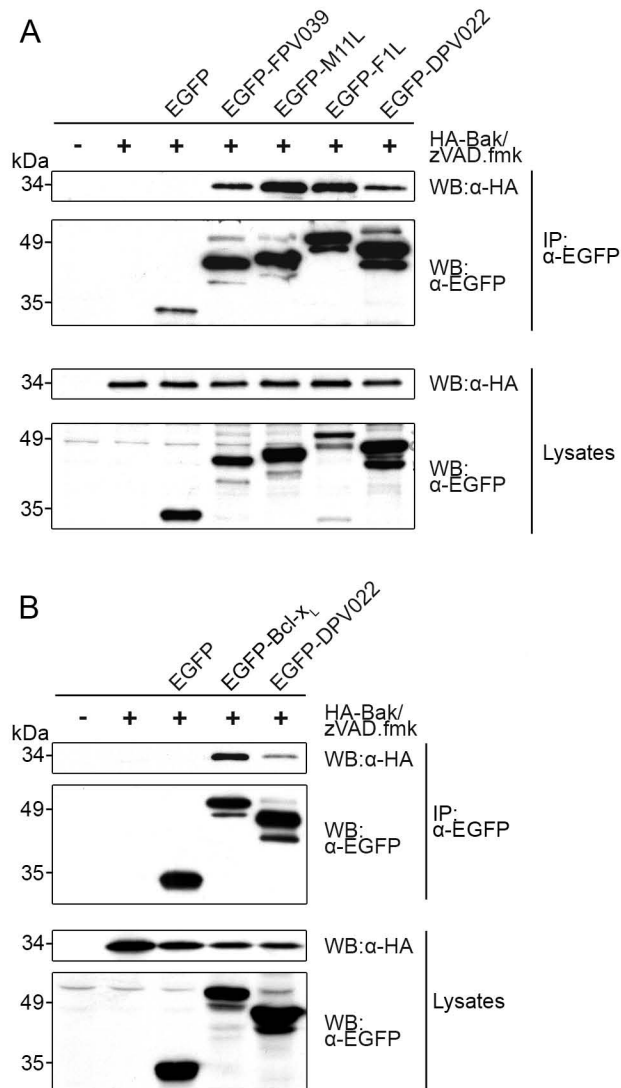


Figure 5.5. DPV022 interacts with ectopically expressed Bak. (A & B) HEK 293T cells were co-transfected with pEGFP, pEGFP-FPV039, pEGFP-M11L, pEGFP-F1L, or pEGFP-DPV022 and pcDNA3-HA-Bak (A) or pEGFP, pEGFP-Bcl-x_L, or pEGFP-DPV022 and pcDNA3-HA-Bak (B). zVAD.fmk was added after transfection to prevent caspase activation. Following lysis in 2% CHAPS buffer, lysates were immunoprecipitated (IP) with an anti-EGFP antibody and subjected to Western blotting (WB) with anti-EGFP or anti-HA antibodies to detect an interaction. Cell lysates were Western blotted with anti-EGFP or anti-HA antibodies to determine expression levels of EGFP-tagged proteins and HA-Bak, respectively. *The experiment depicted in (A) was performed by S-C. Lam under the supervision of L. Banadyga.*

EGFP-tagged proteins were precipitated from cell lysates at equal levels, and all constructs were expressed (Fig. 5.5A & B).

Transient over-expression of Bak results in its activation and the subsequent induction of apoptosis (76). Given that DPV022 interacted with Bak, we investigated whether DPV022 could inhibit Bak-induced apoptosis. HeLa cells were transfected with pEGFP, pEGFP-DPV022, pEGFP-FPV039, pEGFP-M11L, or pEGFP-Bcl-2 and co-transfected with HA-Bak. Apoptosis was then quantified via TMRE staining and flow cytometric analysis (Fig. 5.6A). EGFP was unable to protect against the apoptosis triggered by Bak over-expression, with 39% of cells exhibiting loss of mitochondrial membrane potential. Conversely, the two viral proteins, EGFP-FPV039 and EGFP-M11L, as well as the anti-apoptotic cellular protein EGFP-Bcl-2, prevented Bak-induced apoptosis. Likewise, EGFP-DPV022 was a potent inhibitor of Bak-induced apoptosis, with less than 2% of cells exhibiting loss of mitochondrial membrane potential. HA-Bak and all EGFP-tagged proteins were expressed in each case (Fig. 5.6B). Thus, DPV022 is capable of interacting with Bak and inhibiting apoptosis induced by Bak over-expression.

5.2.4. DPV022 interacts with Bax and inhibits Bax-induced apoptosis. Both Bak and Bax are independently able to facilitate the release of cytochrome c and induce apoptosis (282, 459, 502). Therefore, to effectively inhibit apoptosis Bax must also be inactivated. To determine whether DPV022 is able to directly engage and neutralise Bax, we used an approach identical to that described for Bak (Fig. 5.4). Expression of Bcl-x_L rescued yeast from growth arrest induced by Bax expression, as did expression of DPV022 (Fig. 5.7, “On”), suggesting that DPV022 directly interacts with and inhibits Bax. Duplicate-plating of the yeast

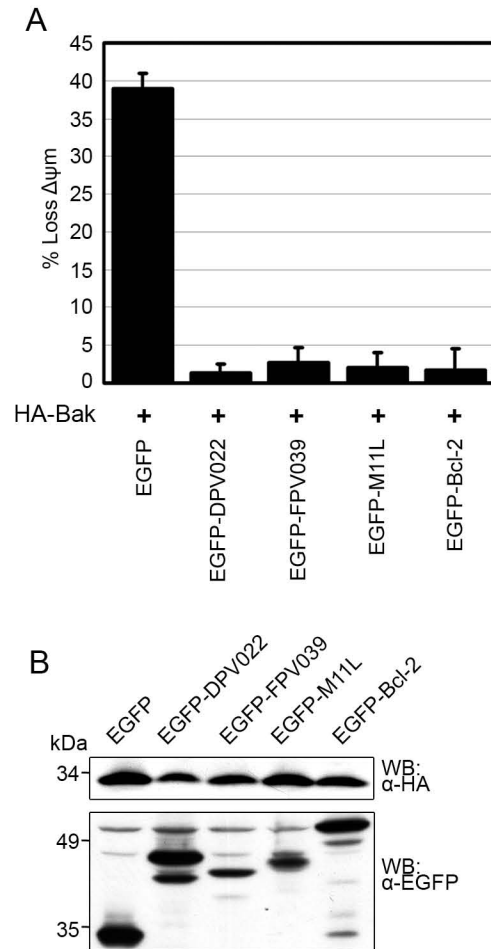


Figure 5.6. DPV022 inhibits Bak-induced apoptosis. (A) HeLa cells were co-transfected with pEGFP, pEGFP-DPV022, pEGFP-FPV039, pEGFP-M11L, or pEGFP-Bcl-2 and pcDNA3-HA-Bak. Apoptosis was assessed in EGFP-positive cells by quantifying TMRE fluorescence via flow cytometry, and the percentage of cells that demonstrated a loss of mitochondrial membrane potential ($\Delta\psi_m$) is given as the y-axis. Standard deviations were calculated from three independent experiments. (B) HeLa cells were transfected in a parallel experiment, and the expression level of each EGFP-tagged construct and HA-Bak was assessed by Western blotting (WB) whole cell lysates. *The experiment depicted in (A) was performed by S-C. Lam under the supervision of L. Banadyga.*

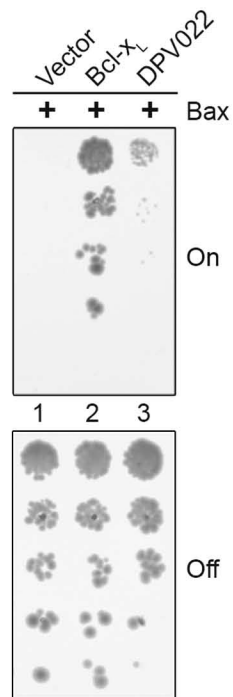


Figure 5.7 DPV022 interacts with Bax in the absence of all other Bcl-2 family proteins. *S. cerevisiae* were co-transformed with the indicated plasmids and standardised concentrations were spotted in serial dilutions vertically down the plate. Galactose-containing media (On) induced the expression of Bax, whereas glucose-containing media (Off) repressed the expression of Bax. Colony growth reflects resistance to Bax-induced growth suppression. *This experiment was performed by T. Okamoto.*

onto glucose-containing medium indicated that Bax expression was repressed and equivalent concentrations of yeast were being plated (Fig. 5.7, "Off"). The interaction between DPV022 and Bax was then confirmed by co-immunoprecipitation (Fig. 5.8A & B). As expected, EGFP-FPV039 and EGFP-M11L both precipitated HA-Bax, whereas EGFP-F1L did not (Fig. 5.8A) (Chapter 4 and (409, 426)). The cellular anti-apoptotic protein EGFP-Bcl-2, which is known to interact with Bax, also precipitated Bax in this assay (Fig. 5.8B) (482, 488). Importantly, EGFP-DPV022 robustly precipitated Bax, indicating an interaction between the two proteins (Fig. 5.8A & B). In each case, EGFP-tagged proteins were precipitated and all proteins were expressed (Fig. 5.8A & B).

Similar to Bak over-expression, over-expression of Bax also induces apoptosis (243, 475). In order to assess whether DPV022 could inhibit Bax-induced apoptosis, HeLa cells were transfected with pEGFP, pEGFP-DPV022, pEGFP-FPV039, pEGFP-M11L, or pEGFP-Bcl-2 and HA-Bax. Apoptosis was then quantified via TMRE staining and flow-cytometric analysis (Fig. 5.9A). Bax induced almost 50% apoptosis in cells expressing EGFP alone; however, cells expressing EGFP-FPV039, EGFP-M11L, or EGFP-Bcl-2 were all protected from apoptosis, each with less than 5% of transfected cells exhibiting loss of mitochondrial membrane potential. Less than 1% of cells expressing EGFP-DPV022 exhibited a loss in mitochondrial membrane potential, indicating that DPV022 was a potent inhibitor of Bax-induced apoptosis. HA-Bax and all EGFP-tagged proteins were expressed in each case (Fig. 5.9B).

Following the activation of Bax and prior to the induction of apoptosis, Bax forms homo-oligomers in the MOM that are thought to assemble a pore sufficiently large to release cytochrome *c* (8, 10, 11). To confirm the ability of

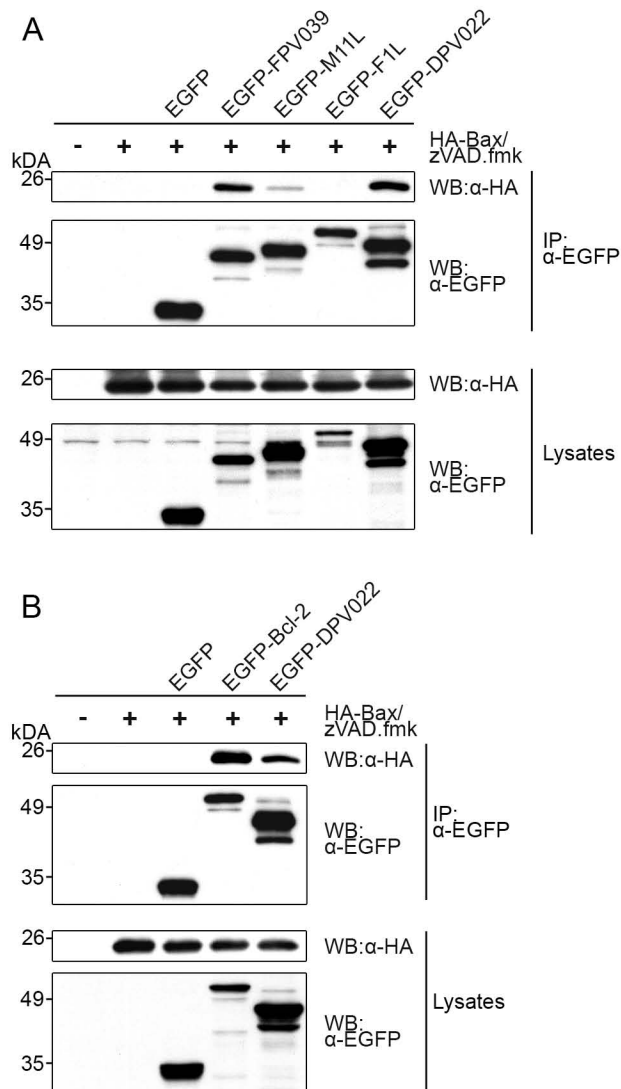


Figure 5.8. DPV022 interacts with ectopically expressed Bax. (A & B) HEK 293T cells were co-transfected with pEGFP, pEGFP-FPV039, pEGFP-M11L, pEGFP-F1L, or pEGFP-DPV022 and pcDNA3-HA-Bax (A) or pEGFP, pEGFP-Bcl-2, or pEGFP-DPV022 and pcDNA3-HA-Bax (B). zVAD.fmk was added after transfection to prevent caspase activation. Following lysis in 2% CHAPS buffer, lysates were immunoprecipitated (IP) with an anti-EGFP antibody and subjected to Western blotting (WB) with anti-EGFP or anti-HA antibodies to detect an interaction. Cell lysates were Western blotted with anti-EGFP or anti-HA antibodies to determine expression levels of EGFP-tagged proteins and HA-Bax, respectively. *The experiment depicted in (A) was performed by S-C. Lam under the supervision of L. Banadyga.*

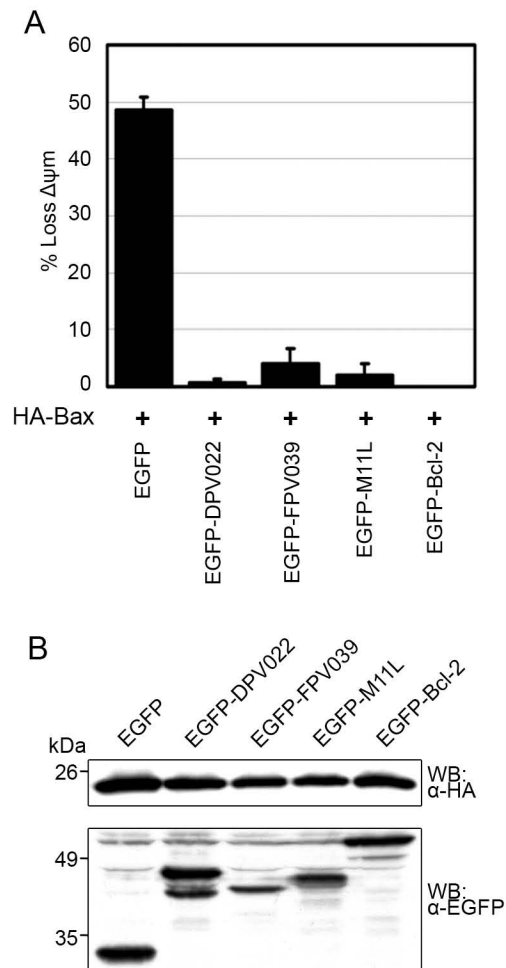


Figure 5.9. DPV022 inhibits Bax-induced apoptosis. (A) HeLa cells were co-transfected with pEGFP, pEGFP-DPV022, pEGFP-FPV039, pEGFP-M11L, or pEGFP-Bcl-2 and pcDNA3-HA-Bax. Apoptosis was assessed in EGFP-positive cells by quantifying TMRE fluorescence via flow cytometry, and the percentage of cells that demonstrated a loss of mitochondrial membrane potential ($\Delta\psi_m$) is given as the y-axis. Standard deviations were calculated from three independent experiments. (B) HeLa cells were transfected in a parallel experiment, and the expression level of each EGFP-tagged construct and HA-Bax was assessed by Western blotting (WB) whole cell lysates. *The experiment depicted in (A) was performed by S-C. Lam under the supervision of L. Banadyga.*

DPV022 to inhibit Bax-induced apoptosis, we assessed the formation of Bax homo-oligomers in the presence of DPV022. HEK 293T cells were transfected with pEGFP, pEGFP-Bcl-2, or pEGFP-DPV022 and HA-Bax. Following lysis in buffer containing 2% CHAPS, cell lysates were treated with the covalent cross-linker BMH. Bax oligomers could thus be preserved and visualised by Western blot after SDS-PAGE (Fig. 5.10). Because over-expression of Bax induces apoptosis, HA-Bax expression alone was sufficient to induce the formation of Bax homo-oligomers, and 44 kDa Bax dimers, 66 kDa Bax trimers, and multiple higher-order Bax oligomers were clearly visible. Co-expression of EGFP alone was unable to prevent Bax oligomerisation, whereas expression of either EGFP-Bcl-2 or EGFP-DPV022 completely prevented Bax oligomerisation. Cell lysates confirmed that HA-Bax and each EGFP-tagged construct were expressed. Together, these data demonstrate that DPV022 is able to interact with Bax, inhibit Bax oligomerisation, and prevent Bax-induced apoptosis.

5.2.5. DPV022 replaces the cellular anti-apoptotic Bcl-2 proteins. Given that DPV022 appeared to rescue Bax and Bak-induced growth arrest in yeast by directly engaging both pro-apoptotic Bcl-2 proteins, we sought to determine if this was also the case in a mammalian system. MEFs stably expressing DPV022 were retrovirally transduced to express the BH3-only protein Bim_S2A, a Bim mutant that only engages Mcl-1 (Fig. 5.11A) (264). Additionally, cells were treated with the Bad BH3 mimetic ABT-737, which neutralises the anti-apoptotic proteins Bcl-2, Bcl-x_L, and Bcl-w (Fig. 5.11A) (337, 444). Thus, the combination of ABT-737 and Bim_S2A potentially neutralises all endogenous anti-apoptotic Bcl-2 proteins (264). Apoptosis was measured as a function of cell colony formation, with the colonies produced by MEFs transduced with a pMIG empty vector

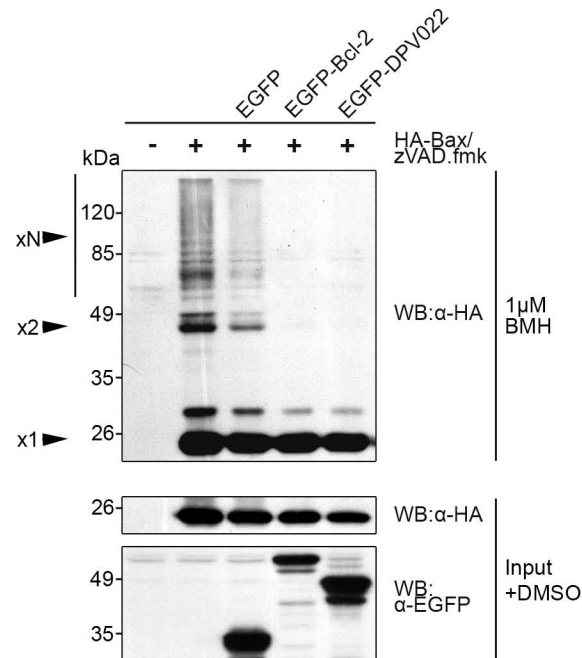


Figure 5.10 DPV022 inhibits Bax oligomerisation. HEK 293T cells were co-transfected with pEGFP, pEGFP-Bcl-2, or pEGFP-DPV022 and pcDNA3-HA-Bax. zVAD.fmk was added after transfection to prevent the activation of caspases. Following lysis in 2% CHAPS buffer, cells were treated with 1 μM 1,6-bismaleimido-hexane (BMH) and Western blotted (WB) with anti-HA to detect Bax oligomers (upper panel). A portion of the lysates (input) was treated with dimethylsulfoxide (DMSO) alone and subjected to Western blotting with either anti-HA or anti-EGFP antibodies to determine expression levels of the transfected proteins (lower two panels). x1, Bax monomer; x2, Bax dimer; xN, higher-order Bax oligomers.

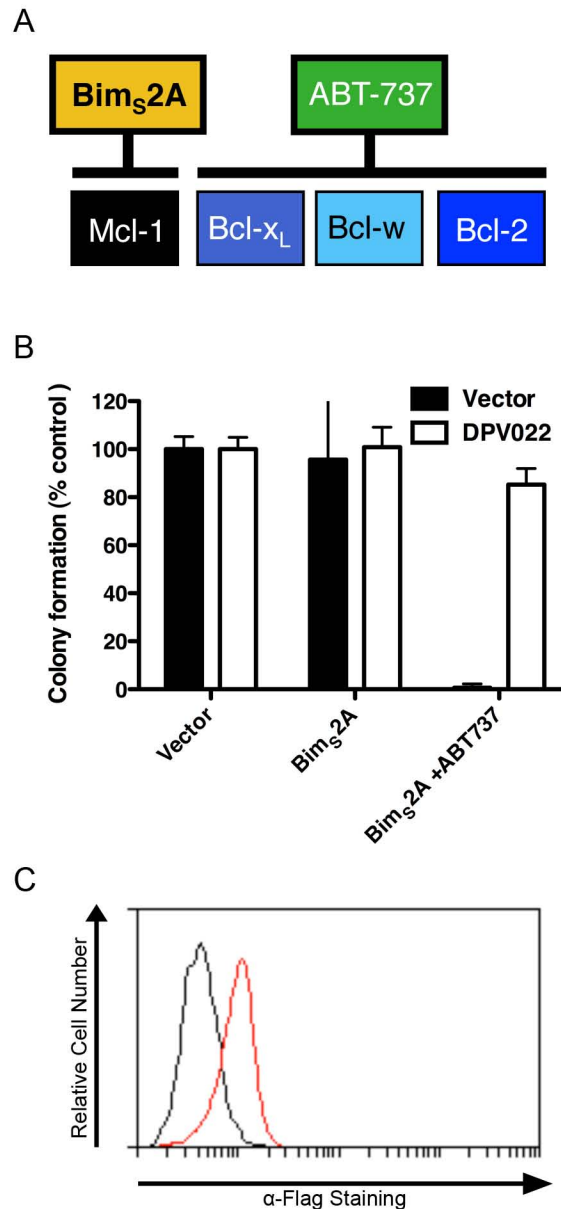


Figure 5.11. DPV022 can replace the endogenous anti-apoptotic Bcl-2 proteins. (A) Binding and neutralisation of the endogenous mammalian anti-apoptotic proteins by Bim_S2A and ABT-737. (B) Wild-type MEFs expressing pMIH empty vector or Flag-DPV022 were infected with a retrovirus expressing the empty pMIG vector or Bim_S2A. EGFP-positive MEFs were sorted and incubated for 5 days. MEFs infected with the retrovirus expressing Bim_S2A were cultured with or without 1 μ M ABT-737. The number of colonies formed by MEFs infected with the empty virus represents 100% colony formation. Standard deviations were calculated from two independent experiments. (C) The flow cytometric histogram indicating the expression of Flag-DPV022 (red line) compared to cells mock transfected with pMIH (black line). *This experiment was performed by T. Okamoto.*

retrovirus arbitrarily set to 100% (Fig. 5.11B). MEFs expressing pMIH empty vector or DPV022 and Bim_S2A, which neutralises only Mcl-1, showed no significant defect in colony formation, as expected. Treatment of MEFs expressing DPV022 and Bim_S2A with ABT-737, to neutralise all anti-apoptotic Bcl-2 proteins, resulted in only a small decrease in colony formation. Conversely, treatment of the MEFs expressing empty vector and Bim_S2A with ABT-737 resulted in the complete loss of colony formation. These data suggest that even when all cellular anti-apoptotic Bcl-2 proteins are neutralised, DPV022 is still able to promote colony growth and, therefore, inhibit apoptosis. The expression of Flag-DPV022 was confirmed by flow cytometry (Fig. 5.11C).

5.2.6. DPV022 interacts with endogenous Bak and Bax during virus infection. Although DPV022 interacted with Bak and Bax, we wanted to confirm these interactions by assessing the ability of DPV022 to interact with endogenous Bak and Bax in the context of virus infection. We therefore made use of the recombinant vaccinia viruses VVΔF1L, which lacks the anti-apoptotic F1L (453) and VVΔF1L-Flag-DPV022, which lacks F1L but expresses a Flag-tagged DPV022. Following infection, HeLa cells were lysed in buffer containing 2% CHAPS, and lysates were immunoprecipitated with either an anti-Bak or an anti-Bax antibody. Lysates were subsequently Western blotted with an anti-Flag antibody to detect interactions (Fig. 5.12). Immunoprecipitation of Bak pulled down Flag-DPV022, indicating that DPV022 interacts with endogenous Bak in the context of infection (Fig. 5.12, first panel). Similarly, DPV022 co-precipitated with Bax, suggesting that DPV022 and endogenous Bax also interact (Fig. 5.12, second panel). Endogenous Bak and Bax were expressed at equal levels in all cases, as was Flag-DPV022 (Fig. 5.12, bottom three panels). Together, these

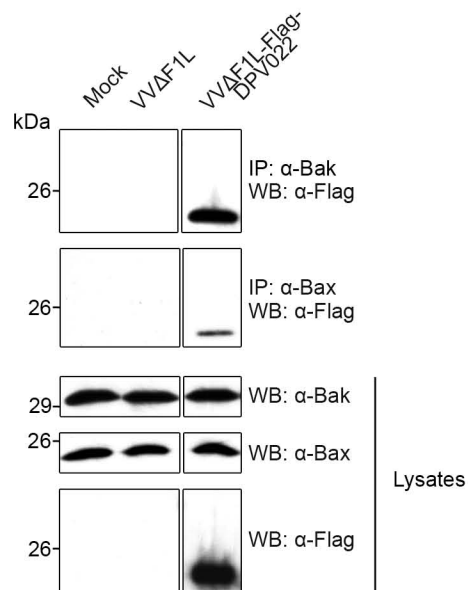


Figure 5.12. DPV022 interacts with endogenous Bak and Bax during virus infection. HeLa cells were mock infected or infected at an MOI of 2 with VVΔF1L or VVΔF1L-Flag-DPV022. Ten hours post-infection, cells were lysed in 2% CHAPS buffer and immunoprecipitated (IP) with either anti-Bak or anti-Bax antibodies and Western blotted (WB) with anti-Flag, anti-Bak, or anti-Bax antibodies to detect interactions. Cell lysates were Western blotted with anti-Bak, anti-Bax, or anti-Flag antibodies to determine expression levels.

data suggest that DPV022 retains its ability to interact with endogenous Bak and Bax in the context of virus infection.

5.2.7. DPV022 inhibits the conformational activation of Bak and Bax during

virus infection. When transiently over-expressed, DPV022 was a potent inhibitor of apoptosis induced by TNF α treatment or Bak and Bax over-expression. To determine if DPV022 expressed by VV could inhibit the activation of Bak, we used a flow cytometry-based assay to detect the activation-associated conformational change of Bak. Jurkat cells were mock infected or infected with VV-EGFP, VV Δ F1L, or VV Δ F1L-Flag-DPV022 and treated with staurosporine (STS), a potent apoptotic stimulus (419). Prior to Bak homo-oligomerisation and the release of cytochrome c, Bak undergoes a series of conformational changes that result in the exposure of an N-terminal epitope that can be detected by staining with anti-BakAb-1 and quantified by flow cytometry (Fig 5.13) (162, 163). Mock-infected Jurkat cells not treated with STS displayed a basal level of fluorescence, likely a result of non-specific antibody binding (Fig. 5.13, a). After STS treatment, however, the fluorescence intensity of mock-infected Jurkat cells increased substantially, indicating that Bak was activated and had undergone a conformational change exposing its N-terminus to binding by anti-BakAb-1 (Fig. 5.13, a). Cells infected with VV-EGFP, which expresses F1L, completely prevented the activation of Bak during virus infection alone and after STS treatment (Fig. 5.13, b), as previously observed (Chapter 3 and (453)). Conversely, VV Δ F1L, which lacks F1L, in combination with STS treatment showed robust Bak activation, whereas infection with VV Δ F1L alone resulted in a less robust activation of Bak, presumably due to the slower induction of apoptosis during VV infection (Fig. 5.13, c) (454). Infection with VV Δ F1L-

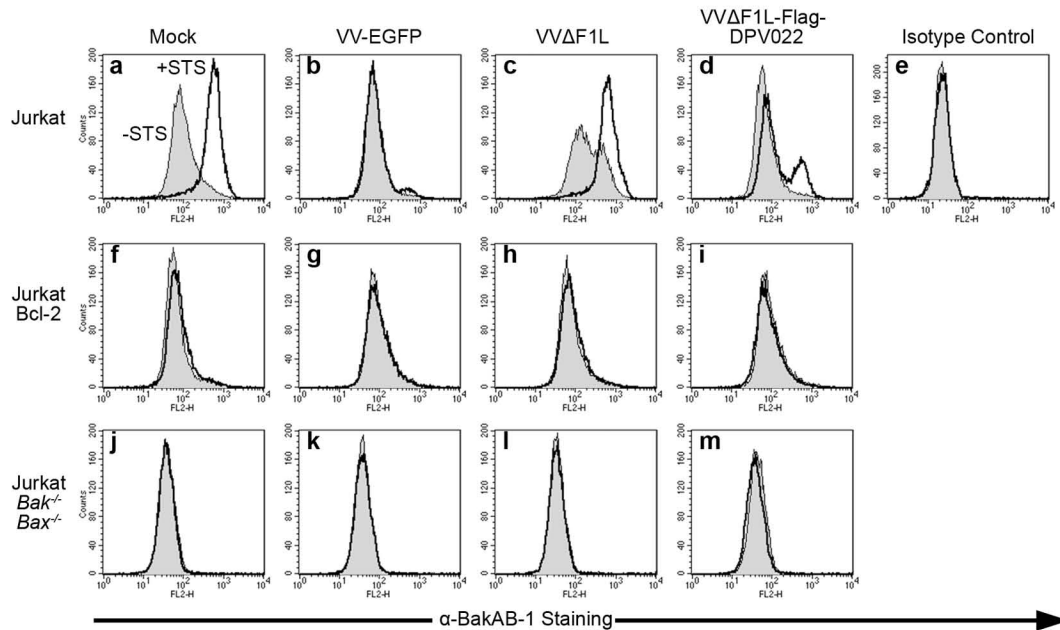


Figure 5.13. DPV022 inhibits the conformational activation of Bak. Wild-type Jurkat cells (a to e), Jurkat cells over-expressing Bcl-2 (f to i), and Jurkat cells devoid of Bak and Bax (j to m) were infected with VV-EGFP, VVΔF1L, or VVΔF1L-Flag-DPV022 at an MOI of 10 for 4 h and then treated with 250 nM staurosporine (STS) for 2 h to induce apoptosis. Exposure of the N-terminus of Bak was monitored by flow cytometry using the anti-BakAb-1 antibody or an isotype control antibody (NK1.1). Shaded histograms, untreated cells; open histograms, STS-treated cells. Data are representative of at least three independent experiments.

DPV022 inhibited the activation of Bak; however, DPV022 was unable to completely prevent the activation of Bak upon treatment with STS (Fig. 5.13, d). No increase in fluorescence intensity was observed in Jurkat cells stained with an isotype control antibody, confirming the specificity of anti-BakAb-1 (Fig. 5.13, e). Additionally, Jurkat cells over-expressing the cellular anti-apoptotic protein Bcl-2 were resistant to Bak activation in all cases (Fig. 5.13, f-i), and activated Bak was undetectable in Jurkat cells devoid of both Bak and Bax (Fig. 5.13, j-m), again confirming the specificity of our assay. These data demonstrate that, like F1L, DPV022 can inhibit the activation of Bak induced by virus infection alone. Unlike F1L, however, DPV022 was incapable of inhibiting all Bak activation following the additional apoptotic stimulus provided by STS.

Similar to Bak, Bax also undergoes a series of activation-associated conformational changes that result in the re-localisation of Bax from the cytoplasm to the mitochondria and the exposure of an N-terminal epitope. To determine if DPV022 could inhibit Bax activation, we performed a similar assay as above using an antibody specific for the activation-associated N-terminus of Bax, anti-Bax6A7 (Fig. 5.14) (201). Mock-infected Jurkat cells displayed a basal level of fluorescence that increased after treatment with STS, indicating that Bax had been activated and the N-terminal epitope had been exposed to binding by anti-Bax6A7 (Fig. 5.14, a). VV-EGFP completely prevented the activation of Bax during infection alone and following treatment with STS (Fig. 5.14, b). Although VV Δ F1L infection alone did not induce the activation of Bax, perhaps because of its slower activation kinetics (237), VV Δ F1L was unable to prevent Bax activation induced by STS treatment (Fig. 5.14, c). Importantly, infection with VV Δ F1L-Flag-DPV022 completely prevented the activation of Bax following treatment with STS, indicating that DPV022, like F1L, can inhibit Bax activity (Fig. 5.14, d).

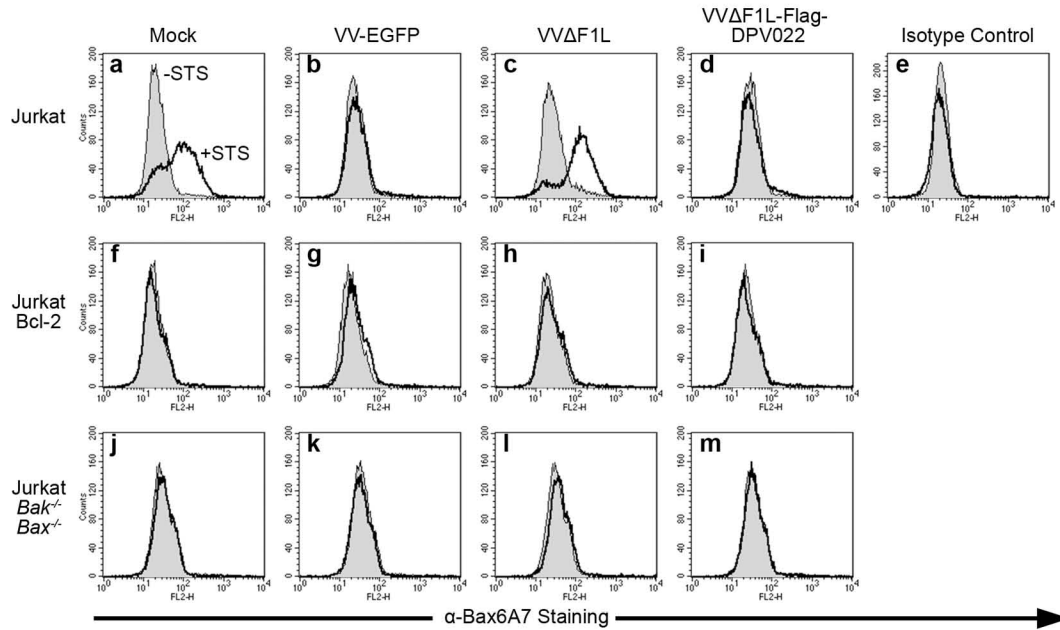


Figure 5.14. DPV022 inhibits the conformational activation of Bax. Wild-type Jurkat cells (a to e), Jurkat cells over-expressing Bcl-2 (f to i), and Jurkat cells devoid of Bak and Bax (j to m) were infected with VV-EGFP, VVΔF1L, or VVΔF1L-Flag-DPV022 at an MOI of 10 for 6 h and then treated with 2 μ M staurosporine (STS) for 2 h to induce apoptosis. Exposure of the N-terminus of Bax was monitored by flow cytometry using the anti-Bax6A7 antibody or an isotype control antibody (NK1.1). Shaded histograms, untreated cells; open histograms, STS-treated cells. Data are representative of at least three independent experiments.

Staining with an isotype control antibody confirmed the specificity of anti-Bax6A7 (Fig. 5.14, e), and no Bax activation was observed in Jurkat cells over-expressing Bcl-2 or devoid of both Bak and Bax, further validating our assay (Fig. 5.14, f-m). Thus, even in the context of virus infection, DPV022 is able to inhibit the activation of Bax.

CHAPTER SIX

THE ROLE OF NOXA, DOUBLE-STRANDED RNA, AND E3L IN THE APOPTOTIC RESPONSE TO VACCINIA VIRUS INFECTION

The results contained within this chapter consist of unpublished material.

All of the experiments included within this chapter were performed by L. Banadyga. The original manuscript was written by L. Banadyga with editorial contribution by M. Barry.

6.1. BRIEF INTRODUCTION

Many viruses, including poxviruses, encode proteins that inhibit apoptosis at the mitochondria, so it is logical to assume that virus infection, itself, produces signals that ultimately promote the activation of Bak and Bax. Following this logic, it is also safe to assume that BH3-only proteins, the upstream activators of Bak and Bax, are responsible for sensing virus-related cellular stresses and subsequently activating Bak and Bax. Unfortunately, little is known about the nature of these viral signals and how they result in BH3-only activation. Indeed, we know that both Bim_L and Bad contribute to the apoptotic response to VV infection (358, 426); however, it is unclear how or why these particular BH3-only proteins are activated in the first place.

Interestingly, several recent reports have described a role for the BH3-only protein Noxa in virus-induced apoptosis (157, 257, 413). Noxa expression is upregulated following infection with a variety of viruses and appears to contribute significantly to the induction of apoptosis by vesicular stomatitis virus and encephalomyocarditis virus (157, 257, 413). Similarly, synthetic dsRNA also induces the upregulation of Noxa and Noxa-dependent apoptosis (257, 413). Because dsRNA is an inevitable by-product of viral infection, it has accordingly been proposed that dsRNA is the signal responsible for Noxa upregulation and, possibly, post-translational activation during virus infection (413).

Using the highly attenuated strain of VV known as modified vaccinia virus Ankara (MVA), Fischer and colleagues recently demonstrated that Noxa is critical to MVA-induced apoptosis (137). These authors showed that MVA induced Noxa-dependent apoptosis but only when E3L, the VV dsRNA-binding protein, was absent (137). Intriguingly, MVA devoid of E3L induced apoptosis even in the presence of F1L, a potent anti-apoptotic protein (137, 455). Together, these data

implicate Noxa and possibly dsRNA as important players in poxvirus-induced apoptosis; however, the mechanisms of Noxa upregulation and activation have yet to be addressed in the context of a poxvirus infection. Furthermore, how Noxa instigates apoptosis at the mitochondria and why MVA F1L was seemingly unable to prevent this from occurring are still unanswered questions. As such, we sought to understand whether Noxa and dsRNA also contribute to the apoptotic response to WT VV, with the ultimate goal of defining the mechanism behind Noxa activation and its pro-apoptotic activity. Here we demonstrate that WT VV devoid of E3L (VV Δ E3L) induced apoptosis, even when F1L was present, and that dsRNA levels appeared to be increased during infection with VV Δ E3L. Importantly, Noxa was upregulated upon VV infection and, interestingly, localised, along with dsRNA, around the virus factories in VV Δ E3L-infected cells. Finally, preliminary data suggest that Noxa was also critical to the induction of VV-induced apoptosis. Together, this study provides insight into the poxvirus-associated signals that initiate apoptosis, and it lays the groundwork for future detailed analyses of Noxa-dependent cell death.

6.2. RESULTS

6.2.1. Vaccinia virus devoid of E3L induces apoptosis even in the presence of F1L. Infection with WT VV strain Copenhagen (VVCop) has been shown previously to protect cells against the induction of apoptosis by virus infection, itself, or by additional apoptotic stimuli (454). In contrast, VV devoid of F1L, a protein that interferes with cellular Bcl-2 family members to inhibit apoptosis, induces cell death upon infection and is unable to prevent cell death induced by extraneous apoptotic stimuli (453, 455). To confirm these results, Jurkat (Fig. 6.1A) or HeLa (Fig. 6.1B) cells were infected at an MOI of 5 with VVCop or a

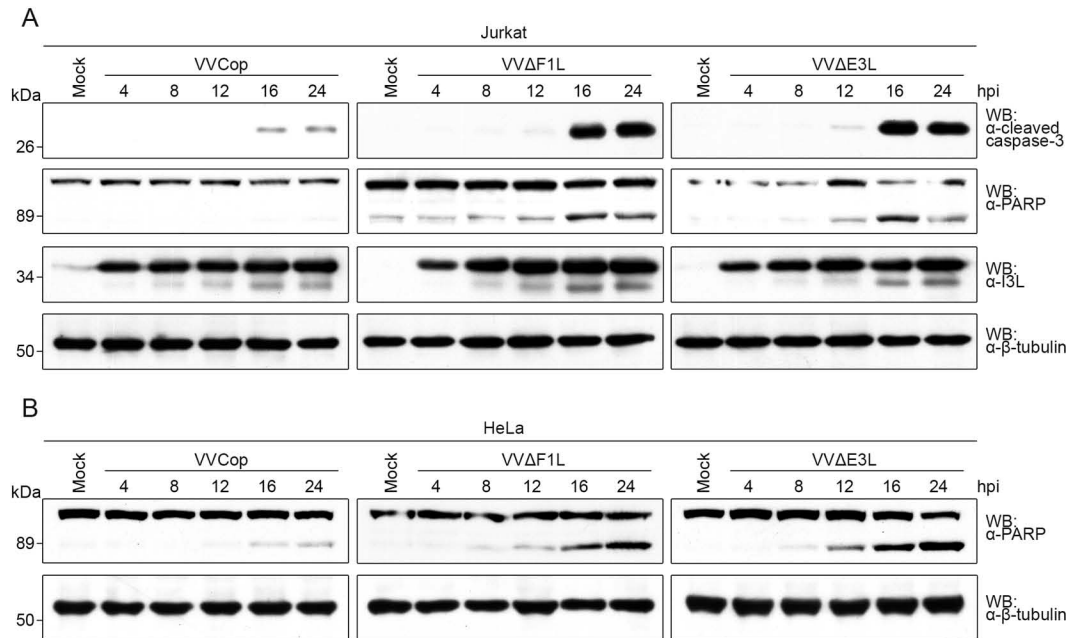


Figure 6.1. Vaccinia virus devoid of F1L or E3L, but not wild-type vaccinia virus, induce apoptosis. Wild-type Jurkat (A) or HeLa cells (B) were infected with VVCop, VVΔF1L, or VVΔE3L at an MOI of 5. Whole cell lysates were harvested at 4, 8, 12, 16, and 24 h post-infection (hpi), and apoptosis was assessed by Western blotting (WB) with an anti-PARP antibody and an anti-cleaved caspase-3 antibody. Infection was confirmed by Western blotting with anti-I3L antibody, and Western blotting with anti-β-tubulin antibody served as a loading control.

mutant VVCop lacking F1L (VV Δ F1L), and cell lysates were harvested over a 24 h time course. The induction of apoptosis was assessed by Western blotting for cleaved, and therefore activated, caspase-3 as well as poly (ADP-ribose) polymerase (PARP), which is cleaved by active caspase-3 late during apoptosis (429). Infection with VVCop resulted in only a minimal amount of cleaved caspase-3, which was not apparent until late during infection (Fig. 6.1A). Likewise, VVCop did not induce the cleavage of PARP in Jurkat cells, even after 24 h of infection, and HeLa cells demonstrated only small amounts of PARP cleavage at 16 and 24 h after infection (Fig. 6.1A & B). In contrast, Jurkat cells infected with VV Δ F1L exhibited caspase-3 cleavage as early as 8 h post-infection, and significant levels were visible by 16 and 24 h post-infection (Fig. 6.1A). Pronounced PARP cleavage was visible in both Jurkat and HeLa cells by 8 h post-infection and levels increased up to 24 h, as indicated on Western blot by the appearance of the 89 kDa cleavage product below full-length PARP (Fig. 6.1A & B). Western blotting for I3L, a VV protein produced at early and intermediate times post-infection (370), confirmed that Jurkat cells were infected (Fig. 6.1A), and Western blotting for β -tubulin served as a loading control (Fig. 6.1A & B). These data confirm that the VV devoid of F1L induces apoptosis.

F1L, however, is not the only protein encoded by VV that inhibits apoptosis. VV lacking E3L, a protein responsible for sequestering virally-produced dsRNA and inhibiting protein kinase R (PKR), also induces apoptosis upon infection (59, 137, 235, 266). Jurkat cells infected at an MOI of 5 with a mutant VV devoid of E3L (VV Δ E3L) demonstrated caspase-3 cleavage as early as 8 h post-infection, with significant levels visible by 16 and 24 h post-infection (Fig. 6.1A). Similarly, PARP cleavage was observed in Jurkat and HeLa cells as early as 8 h post-infection, and levels of cleaved PARP increased up to 24 h after

infection (Fig. 6.1A & B). Infection in Jurkat cells was confirmed by I3L expression (Fig. 6.1A), and consistent loading was confirmed by Western blotting for β -tubulin (Fig. 6.1A & B). Thus, like F1L, E3L also plays a role in preventing apoptosis induced by VV infection. Importantly, however, VV devoid of E3L appears to induce apoptosis even when F1L is present. Such a phenomenon has been observed by others using the related, but highly attenuated, virus MVA (137).

6.2.2. Increased levels of dsRNA are detected upon infection with VV Δ E3L.

dsRNA is a by-product of the replication of many different viruses, including VV, which produces dsRNA probably as a result of symmetrical transcription from viral late genes (83, 84, 121). Because dsRNA is produced almost exclusively during virus infection, it serves as a potent trigger of multiple immune responses, including apoptosis (216). Upon binding to dsRNA, the cellular protein PKR becomes activated and goes on to phosphorylate and inactivate the cellular translation initiation factor eIF-2 α , effectively shutting down host and viral mRNA translation and inhibiting viral replication (130, 265, 267, 273). However, activated PKR has also been shown to induce apoptosis, a phenomenon that, at least during VV infection, also appears to be triggered by dsRNA (235, 266). To counter these effects, VV E3L binds and sequesters viral dsRNA, thereby preventing the activation of PKR and its anti-viral activity (59). We therefore became interested in the production of VV dsRNA, the stimulus that might ultimately be responsible for triggering cell death in VV Δ E3L-infected cells despite the presence of F1L. To examine the amount of dsRNA produced during virus infection, HeLa cells were mock infected or infected with VVCop, VV Δ F1L, or VV Δ E3L at an MOI of 5 for 4, 12, and 20 h, and dsRNA was visualised by

confocal microscopy using an antibody that recognises dsRNA in a sequence-independent manner (Fig. 6.2A) (386). dsRNA was not observed in mock-infected cells at any time point, consistent with dsRNA being a product of VV infection (Fig. 6.2A, a-c). At 4 h post-infection, no dsRNA was observed in VVCop- or VV Δ F1L-infected cells, whereas a few cells infected with VV Δ E3L were positive for dsRNA (Fig. 6.2A, d, g, j). By 12 h post-infection, dsRNA could be detected in cells infected with VVCop or VV Δ F1L, but significantly more dsRNA was observed in cells infected with VV Δ E3L (Fig. 6.2A, e, h, k). After 20 h of infection, the amount of dsRNA detected in cells infected with either VVCop or VV Δ F1L had increased compared to the 12 h time point and appeared closer, although still less than, the amount of dsRNA observed 20 h post-infection with VV Δ E3L (Fig. 6.2A, f, i, l).

To quantify the accumulation of dsRNA during VV infection, we devised a flow cytometric assay using the same anti-dsRNA antibody employed in Fig. 6.2A. Jurkat cells were infected with VVCop, VV Δ F1L, or VV Δ E3L at an MOI of 5 for 4 or 16 h, and dsRNA was quantified via flow cytometry (Fig. 6.2B). After 4 h of infection, the percentage of cells infected with VVCop or VV Δ F1L and positive for dsRNA was close to zero, whereas over 10% of the cells infected with VV Δ E3L were positive for dsRNA, reflecting our observations by confocal microscopy. By 16 h post-infection, almost 30% of VV Δ E3L-infected cells were dsRNA positive, while only 10% to 14% of cells infected with VVCop or VV Δ F1L exhibited dsRNA positivity. To ensure that we were detecting dsRNA in this assay, we treated cells with cytosine arabinoside (AraC), a drug that inhibits poxviral DNA replication and therefore prevents viral late gene transcription and the synthesis of dsRNA. Cells infected with VVCop or VV Δ F1L and treated with AraC for 16 h demonstrated no dsRNA positivity, and VV Δ E3L-infected cells

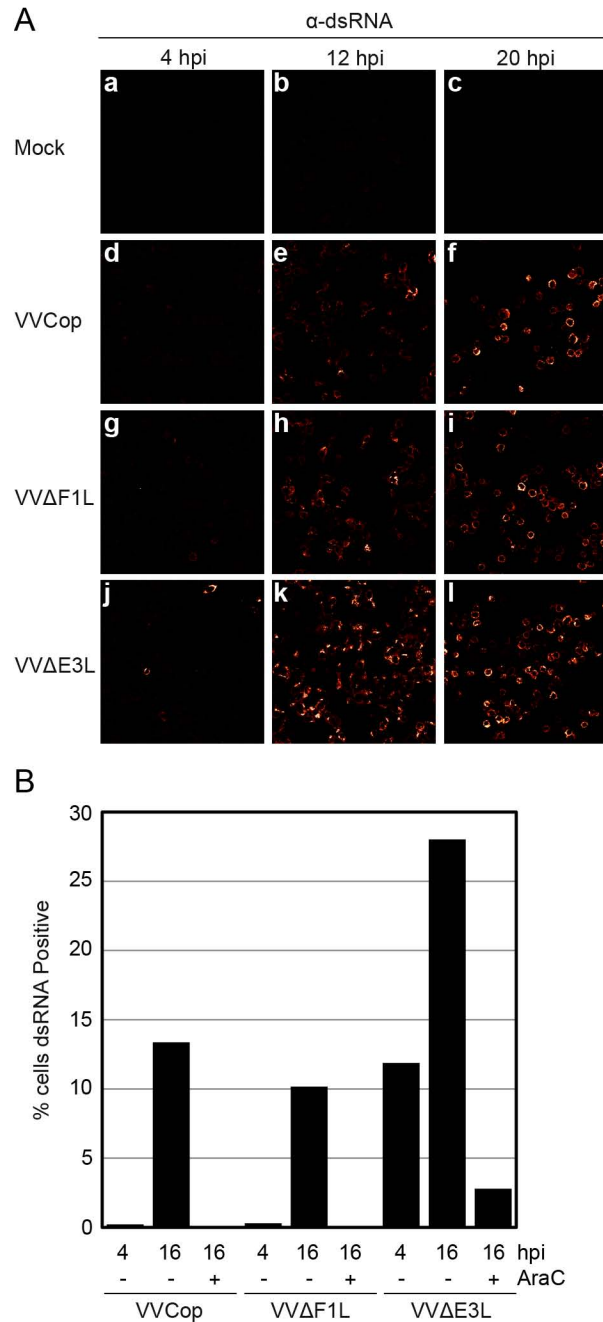


Figure 6.2. Increased levels of dsRNA are detected upon VV Δ E3L infection. (A) HeLa cells were mock infected (a to c) or infected with VVCop (d to f), VV Δ F1L (g to i), or VV Δ E3L (j to l) at an MOI of 5. Four, 12, and 20 h post-infection (hpi) cells were fixed and permeabilised, and dsRNA was visualised by confocal microscopy using an antibody specific for dsRNA, anti-dsRNA (J2). (B) Wild-type Jurkat cells were infected with VVCop, VV Δ F1L, or VV Δ E3L at an MOI of 5. Four or 16 h post-infection (hpi) cells were fixed and permeabilised, and the percentage of cells positive for dsRNA was quantified by flow cytometry using anti-dsRNA (J2) antibody. Cells harvested at 16 hpi were treated with or without cytosine arabinoside (AraC) to inhibit poxviral late gene expression and dsRNA synthesis.

treated with AraC exhibited a drop in dsRNA positivity to less than 5%. Together, these data suggest that VV Δ E3L infection results in increased levels of dsRNA compared to infection with either VVCop or VV Δ F1L. However, these data do not rule out the possibility that, in the absence of E3L, dsRNA is more readily bound by antibody.

6.2.3. dsRNA produced during VV Δ E3L infection localises around virus factories. The confocal analysis of dsRNA production during VV infection (Fig. 6.2A) revealed a peculiar localisation of dsRNA in VV Δ E3L-infected cells. To examine this localisation in more detail, HeLa cells were mock infected or infected with VVCop, VV Δ F1L, or VV Δ E3L at an MOI of 5 for 12 h, and dsRNA was visualised at a higher resolution by confocal microscopy using the anti-dsRNA antibody (Fig. 6.3A). As expected, no dsRNA was observed in mock-infected cells (Fig. 6.3A, a-c). Although dsRNA could be detected in a small proportion of cells infected with either VVCop or VV Δ F1L, the majority of cells exhibited no dsRNA (Fig. 6.3A, d-i). Notably, virus factories, the DNA-rich sites of VV transcription and replication, were visible by DAPI staining as faint, globular structures adjacent to the larger and denser nuclei, indicating that both cells were infected with VVCop or VV Δ F1L (Fig. 6.3A, d, g). Conversely, cells infected with VV Δ E3L possessed multiple smaller and denser virus factories, each of which was surrounded by dsRNA (Fig. 6.3A, j-o). To confirm that these structures were virus factories, we stained VV Δ E3L infected cells with an antibody specific for I3L, a VV DNA binding protein that localises exclusively to virus factories (Fig. 6.3B) (370). To our knowledge, this is the first study to examine the localisation of dsRNA during VV infection, and the results indicate that dsRNA produced by VV Δ E3L localises around virus factories.

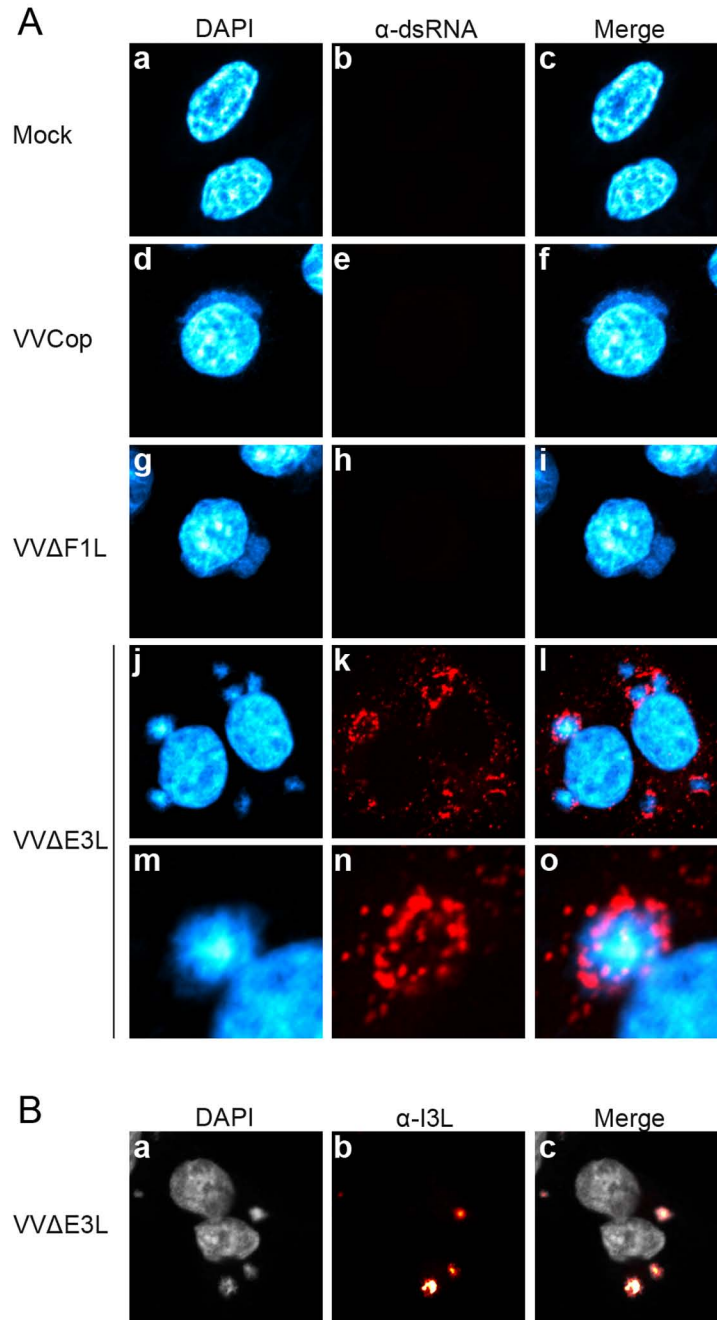


Figure 6.3. dsRNA localises around VV Δ E3L virus factories. (A) HeLa cells were mock infected (a to c) or infected with VVCop (d to f), VV Δ F1L (g to i), or VV Δ E3L (j to l) at an MOI of 5 for 12 h. Following fixation and permeabilisation, cells were stained with DAPI to visualise the nuclei and virus factories (bright blue) and anti-dsRNA(J2) antibody to visualise dsRNA (red). Cells were analysed by confocal microscopy. Enlarged images of the VV Δ E3L virus factories displayed in panels j to l are provided in panels m to o. (B) HeLa cells were infected with VV Δ E3L at an MOI of 5 for 12 h. Following fixation and permeabilisation, cells were stained with DAPI to visualise the nuclei and virus factories (grey) and anti-I3L antibody to visualise I3L (bright red). Cells were analysed by confocal microscopy.

6.2.4. The BH3-only protein Noxa is upregulated during vaccinia virus infection. Noxa, a 54 amino acid protein belonging to the pro-apoptotic BH3-only subgroup of Bcl-2 family proteins, is upregulated in response to dsRNA treatment as well as infection by numerous viruses, including vesicular stomatitis virus, sendai virus, encephalomyocarditis virus, measles virus, and herpes simplex virus 1 (157, 257, 334, 413). Additionally, Noxa has been shown to contribute to the apoptotic response induced by these viruses, as well as VV (137, 157, 257, 413). To determine whether VV infection results in a similar upregulation of Noxa, HeLa cells were infected with wild-type VVCop at an MOI of 5, and Noxa protein levels were assessed by Western blotting cell lysates harvested over a 24 h time course (Fig. 6.4A). Uninfected cells showed negligible levels of Noxa protein, but as early as 4 h post-infection with VVCop, Noxa protein levels increased significantly. Noxa expression remained stable at 8 and 12 h post-infection; however, a substantial increase in Noxa levels was observed at 16 h post-infection and again at 24 h post-infection. Virus infection was confirmed by Western blotting for the viral early protein I3L, and Western blotting for β -tubulin and Bak served as a loading control. Although Noxa protein levels appeared to increase over the course of VV infection, we wanted to determine if *Noxa* mRNA levels showed a corresponding increase. HeLa cells were infected with VVCop at an MOI of 5, cDNA was generated from total cellular RNA harvested over a 24 h time course, and the levels of *Noxa* mRNA were determined by quantitative real-time PCR (Fig. 6.4B). *Noxa* mRNA increased by over 30 and 90 fold relative to *GAPDH* and *ACTB* transcript levels, respectively, during the course of a 24 h infection. Similar to the protein levels observed in Fig. 6.4A, *Noxa* mRNA also increased substantially 24 h post-infection. Thus,

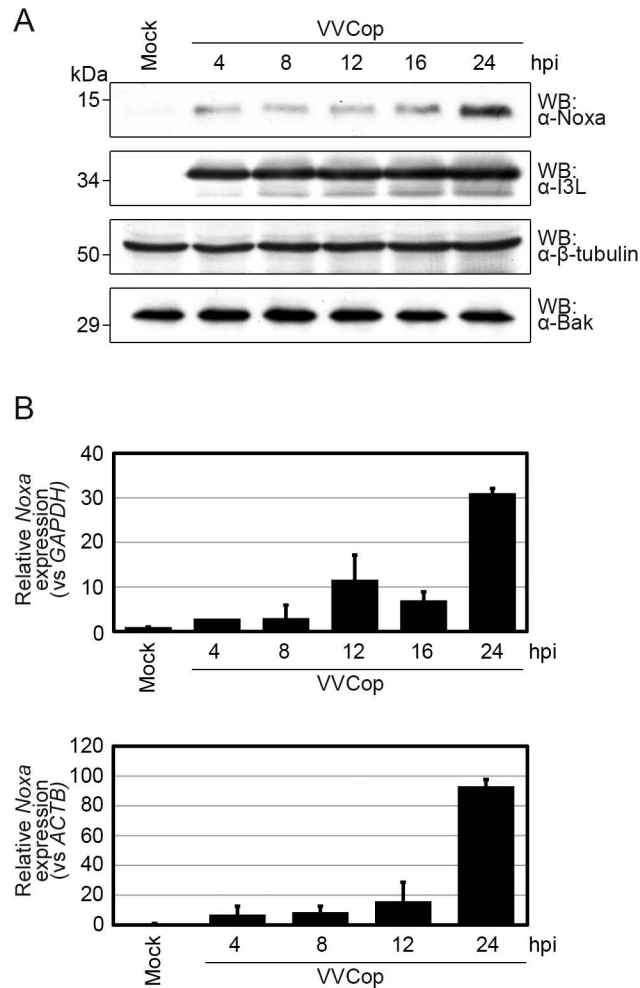


Figure. 6.4. The BH3-only protein Noxa is upregulated during VVCop infection. (A) HeLa cells were infected with VVCop at an MOI of 5. Whole cell lysates were harvested at 4, 8, 12, 16, and 24 h post-infection (hpi), and Noxa protein expression was assessed by Western blotting (WB) with anti-Noxa antibody. Infection was confirmed by Western blotting with anti-I3L antibody, and Western blotting with anti- β -tubulin and anti-Bak antibodies served as a loading control. (B) HeLa cells were infected with VVCop at an MOI of 5. At the indicated time points, total cellular RNA was harvested and subjected to reverse-transcriptase PCR to obtain cDNA. Quantitative real-time PCR was performed using primers specific to *Noxa*, *GAPDH*, and *ACTB* mRNA. Expression of *Noxa* mRNA is given relative to *GAPDH* expression (upper panel) or *ACTB* expression (lower panel). Standard deviations were calculated from three (*GAPDH*) or two (*ACTB*) independent experiments, except for the *GAPDH* 4 h timepoint, which was performed only once.

infection with wild-type VVCop resulted in the upregulation of both Noxa protein and mRNA.

Given that Noxa expression may be upregulated, in part, by dsRNA treatment (413) and that VV Δ E3L infection resulted in increased dsRNA levels, we next sought to determine the Noxa protein and mRNA expression patterns in VV Δ E3L-infected cells. Similar to VVCop-infected cells, cells infected with VV Δ E3L showed an increase in Noxa protein levels by 16 h post-infection and an additional increase at 24 h (Fig. 6.5A). As in Fig. 6.4, Western blotting for β -tubulin and Bak served as a loading control. Moreover, Noxa mRNA levels increased by over 20 fold relative to *ACTB* mRNA over the course of infection, again with a substantial increase in transcript levels at 24 h post-infection (Fig. 6.5B). Together, these data demonstrate that VV, like many other viruses, induces the upregulation, or at least stabilisation, of Noxa protein and mRNA. Additionally, upregulation of Noxa occurred independently of E3L, perhaps suggesting that the increased amount of dsRNA present in VV Δ E3L-infected cells plays little role in inducing Noxa expression during VV infection.

6.2.5. The BH3-only protein Noxa also localises to VV Δ E3L virus factories.

Noxa may be post-translationally activated to induce apoptosis in response to dsRNA—possibly through a direct interaction between Noxa and dsRNA—and this might comprise the mechanism by which Noxa contributes to the induction of apoptosis by a variety of viruses (413). Given the apparent upregulation of Noxa during VV infection and the peculiar localisation of dsRNA in VV Δ E3L-infected cells, we sought to examine the localisation of Noxa in the context of VV infection. HeLa cells were mock infected or infected at an MOI of 5 with VVCop or VV Δ E3L, and Noxa localisation was analysed by confocal microscopy using a

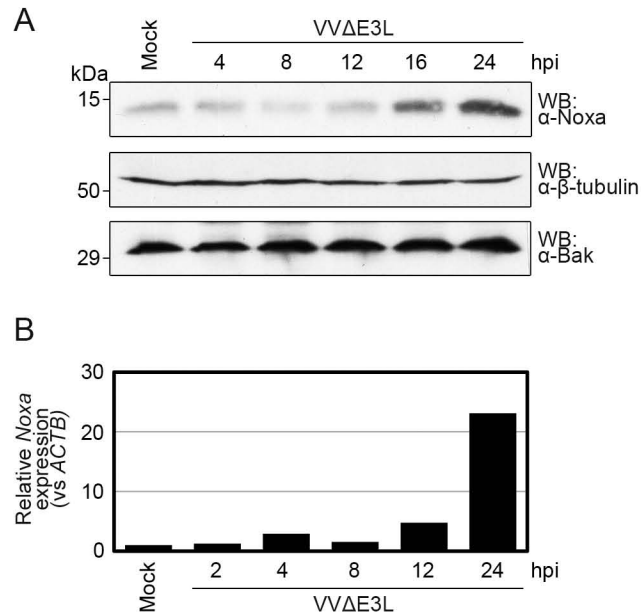


Figure 6.5. Noxa is upregulated during VVΔE3L infection. (A) HeLa cells were infected with VVΔE3L at an MOI of 5. Whole cell lysates were harvested at 4, 8, 12, 16, and 24 h post-infection (hpi), and Noxa protein expression was assessed by Western blotting (WB) with anti-Noxa antibody. Western blotting with anti-β-tubulin and anti-Bak antibodies served as a loading control. (B) HeLa cells were infected with VVΔE3L at an MOI of 5. At the indicated time points, total cellular RNA was harvested and subjected to reverse-transcriptase PCR to obtain cDNA. Quantitative real-time PCR was performed using primers specific to *Noxa* and *ACTB* mRNA. Expression of *Noxa* mRNA is given relative to *ACTB* expression.

monoclonal antibody specific for Noxa (Fig. 6.6). Both mock-infected and VVCop-infected cells showed Noxa distributed diffusely throughout the cell (Fig. 6.6, a-i). In contrast, cells infected with VVΔE3L showed Noxa almost entirely localised in a punctate pattern to the virus factory (Fig. 6.6, j-o). To confirm the localisation of Noxa using a different antibody, HeLa cells were transfected with pcDNA-Myc-Noxa and, 16 h later, mock infected or infected at an MOI of 5 with VVCop or VVΔE3L for an additional 12 h. The localisation of Myc-tagged Noxa was analysed in transfected and infected cells by confocal microscopy using an anti-Myc antibody (Fig. 6.7). Similar to the results in Fig. 6.6, mock-infected and VVCop-infected cells showed a diffuse distribution of Myc-Noxa throughout the cell (Fig. 6.7, a-f). However, in VVΔE3L-infected cells, Myc-Noxa, like endogenous Noxa observed in Fig. 6.6, appeared to localise to the virus factories (Fig. 6.7, g-l). Intriguingly, these results suggest that in VVΔE3L-infected cells, Noxa is localised to a site identical, or at least proximal, to dsRNA. Whether Noxa co-localises with dsRNA or interacts directly with dsRNA remains to be determined.

6.2.6. Noxa contributes to vaccinia virus-induced apoptosis. Because Noxa was upregulated upon VV infection and localised to VVΔE3L virus factories, similar to dsRNA, a proposed activating ligand for Noxa, we investigated the contribution that Noxa makes to VV-induced apoptosis. WT or *Noxa*^{-/-} baby mouse kidney (BMK) cells were infected at an MOI of 5 with either VVCop or VVΔE3L, and the induction of apoptosis was assessed in cell lysates harvested over the course of 12 h by Western blotting for PARP cleavage (Fig. 6.8). During the first 6 h of infection, no discernible PARP cleavage is detected in WT or *Noxa*^{-/-} cells infected with VVΔE3L, indicating that apoptosis is not occurring or

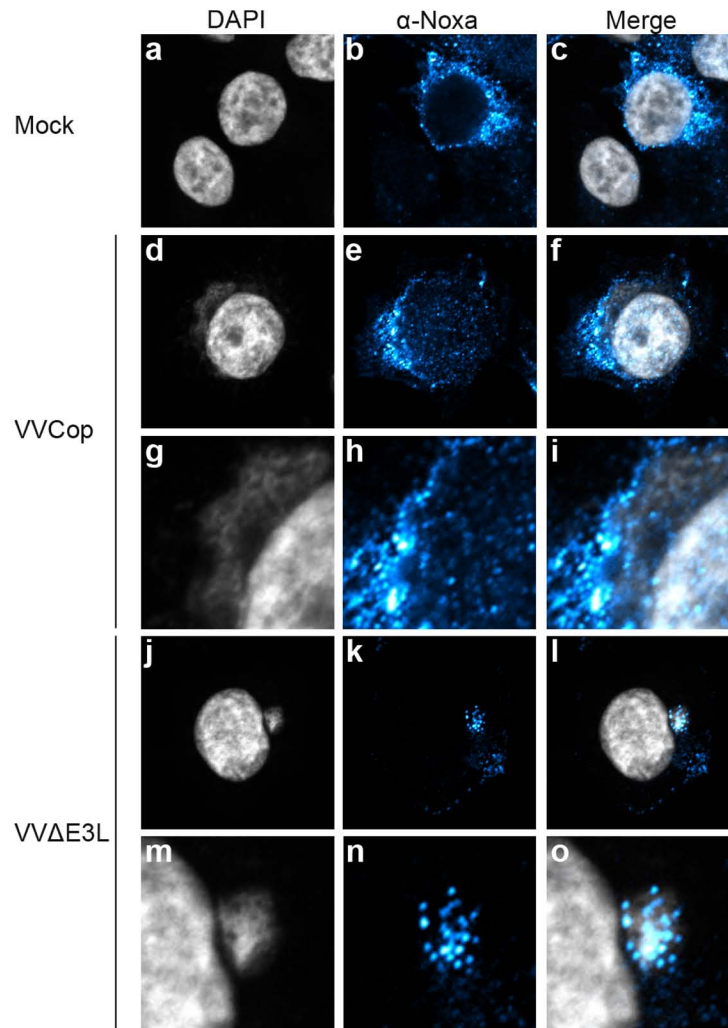


Figure 6.6. Endogenous Noxa localises to VVΔE3L virus factories. HeLa cells were mock infected (a to c) or infected with VVCop (d to i) or VVΔE3L (j to o) at an MOI of 5 for 12 h. Following fixation and permeabilisation, cells were stained with DAPI to visualise the nuclei and virus factories (grey) and anti-Noxa antibody to visualise endogenous Noxa (bright blue). Cells were analysed by confocal microscopy. Enlarged images of the VVCop virus factory displayed in panels d to f are provided in panels g to i, and enlarged images of the VVΔE3L virus factory displayed in panels j to l are provided in panels m to o.

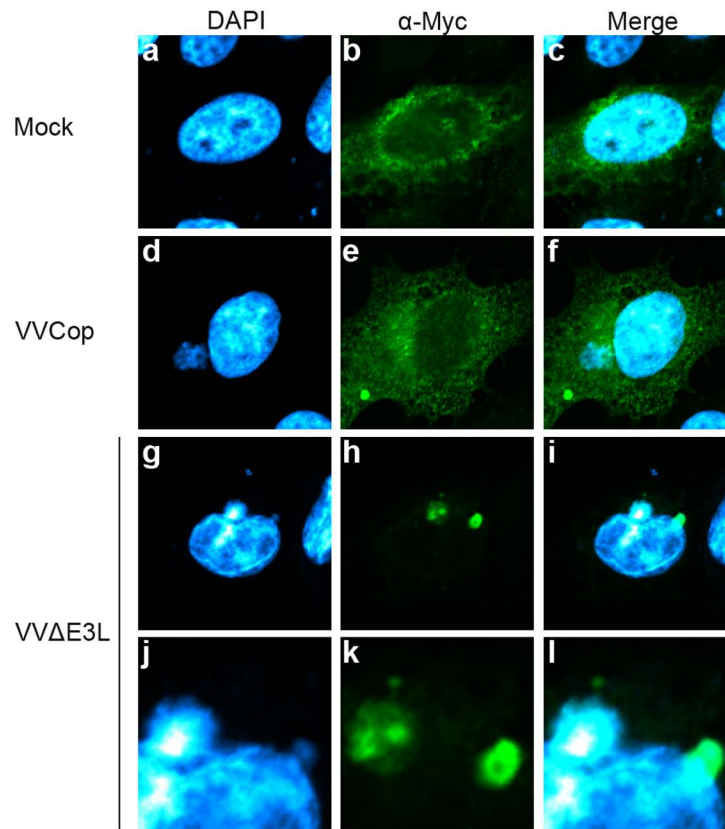


Figure 6.7. Ectopically expressed Myc-Noxa localises to VVΔE3L virus factories. HeLa cells were transfected with pcDNA3.1-Myc-Noxa (a to i) and, 16 h later, were mock infected (a to c) or infected with VVCop (d to f) or VVΔE3L (g to i) at an MOI of 5 for an additional 12 h. Following fixation and permeabilisation, cells were stained with DAPI to visualise the nuclei and virus factories (bright blue) and anti-Myc antibody to visualise transfected Myc-Noxa (green). Cells were analysed by confocal microscopy. Enlarged images of the VVΔE3L virus factories displayed in panels g to i are provided in panels j to l.

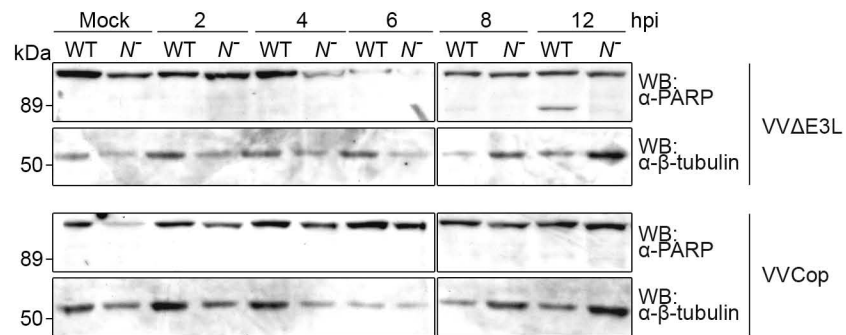


Figure 6.8. Noxa-deficient cells undergo reduced apoptosis during VVΔE3L infection. Wild-type (WT) and Noxa-deficient (*N*⁻) baby mouse kidney (BMK) cells were infected with VVΔE3L or VVCop at an MOI of 5. Whole cell lysates were harvested at 2, 4, 6, 8, and 12 h post-infection (hpi), and apoptosis was assessed by Western blotting (WB) with anti-PARP antibody. Western blotting with anti-β-tubulin antibody served as a loading control.

has not yet progressed to the relatively late stage of PARP cleavage. By 8 h post-infection, however, cleaved PARP was detected in WT BMKs infected with VV Δ E3L but not in *Noxa*^{-/-} BMKs infected with the same virus. At 12 h post-infection with VV Δ E3L the difference is even more dramatic, with the amount of cleaved PARP in WT BMKs significantly greater than the amount observed in *Noxa*^{-/-} BMKs. Conversely, WT or *Noxa*^{-/-} BMKs infected with VVCop did not display appreciable PARP cleavage at any time point up to 12 h, indicating that apoptosis was not occurring in these cells. For each set of infections, Western blotting for β -tubulin served as a loading control. Together these data suggest that cells deficient in Noxa exhibit reduced or delayed apoptosis when infected with VV Δ E3L compared to WT cells, implicating Noxa as an important player in the apoptotic response to VV infection.

CHAPTER SEVEN

DISCUSSION

7.1. POXVIRUSES INHIBIT APOPTOSIS

Apoptosis comprises an important and powerful part of the immune system (98, 183). As obligate intracellular parasites, viruses depend on healthy host cells to complete their replication cycle and facilitate a productive infection; accordingly, many viruses, including poxviruses, encode proteins that interfere with apoptosis (35, 373). Because Bcl-2 family proteins and, in particular, Bak and Bax, play a critical role in determining cellular fate, they make attractive targets for viral manipulation and subversion. By understanding how viral proteins inactivate Bak and Bax to inhibit apoptosis we have gained, and will continue to gain, insight into both viral biology and the regulation of the cellular death machinery. To this end, the present study sought to characterise the putative function and mechanism of action of two poxviral inhibitors of apoptosis, FPV039 and DPV022.

7.1.1. FPV039 and the vBcl-2-like proteins. Every chordopoxvirus described to date, with the exception of molluscum contagiosum virus, encodes, or is predicted to encode, a protein that inhibits apoptosis by interfering with the Bcl-2 family of proteins (155). Despite the prevalence of this particular immune evasion strategy among poxviruses, only members of the *Avipoxvirus* genus, of which fowlpox virus is the prototypical member, encode proteins with obvious sequence similarity to cellular Bcl-2 (cBcl-2) family members (4, 438). The fowlpox virus protein FPV039 was initially identified as a Bcl-2 homologue based on sequence analysis that revealed the presence of an obvious BH1 and BH2 domain and a C-terminal TM domain (Fig. 3.1) (4). However, FPV039 lacks obvious BH3 and BH4 domains, which are thought to be required for anti-apoptotic function (4). As such, FPV039 differs markedly from anti-apoptotic

cBcl-2 proteins, such as Bcl-2 and Bcl-x_L, which possess all four BH domains (75, 483). On the contrary, FPV039 does not differ in this respect from other viral inhibitors of apoptosis, which, in general, exhibit considerably less conservation within the BH domains, if they are present at all (95, 176, 355). Besides FPV039, only KSBcl-2 and A179L possess well conserved BH1 and BH2 domains (3, 67, 326). In fact, the BH1 domains of these three proteins are nearly identical to their cellular counterparts and, unlike other viral BH1 domains, retain the entire “NWGR” sequence motif that is unfailingly conserved and functionally critical for cBcl-2 proteins (Fig. 3.1B) (95, 174, 176). BHRF1, BALF1, and E1B 19K have less well conserved BH1 and BH2 domains (95, 176), and, more recently, putative BH-like domain sequences have been identified in several other viral inhibitors of apoptosis (53, 117, 251, 252, 345).

Aside from the conservation of a few BH domains, as degenerate as they may be, viral anti-apoptotic proteins possess little in common with each other at the amino acid sequence level (95, 176, 425). Such differences belied initial attempts to understand precisely how these viral proteins were preventing apoptosis in the context of the Bcl-2 family of proteins with which they interfered. However, the abundance of structural data now available for both cBcl-2 proteins and viral inhibitors of apoptosis has made it clear that viruses are regulating apoptosis in a manner analogous to cBcl-2 proteins. KSBcl-2 and BHRF1 were both shown to adopt α -helical structures similar to those of cBcl-2 proteins, despite sharing only a BH1, BH2, and TM domain in common with their cellular counterparts (205, 206). This was the first evidence suggesting that the primary amino acid sequence of viral Bcl-2 homologues does not have to be identical to that of cBcl-2 family members in order to assume a similar structure and inhibit apoptosis.

Based on cBcl-2 structural information, we predicted the presence of a series of α -helices in FPV039 that closely aligned with those determined from the structure of Bcl-2 (Fig. 3.1A) (351). All of the predicted α -helices possessed by FPV039 corresponded closely with the same helices in Bcl-2, structurally confirming the presence of the BH1 and BH2 domains. Moreover, two of the predicted helices aligned with the BH3- and BH4-containing helices of Bcl-2, suggesting functional relevance. Indeed, deletion of amino acids 41 to 54 in FPV039, which correspond to the BH3 domain and α -helix 2 of human Bcl-2, ablated the ability of FPV039 to interact with Bak and Bax and inhibit apoptosis, providing evidence of a “cryptic” BH3 domain in FPV039. Despite the lack of sequence homology, the fact that the FPV039 BH3 domain was critical to the function of FPV039 strongly suggests that it, along with the more conserved BH1 and BH2 domains, contributes to the formation of a hydrophobic binding groove similar to that observed in cellular anti-apoptotic Bcl-2 proteins and necessary for mediating the interactions with Bak and Bax. We suspect that FPV039 also possesses a cryptic BH4 domain, comprised of the predicted α -helix 1, although the importance of this helix remains untested. Thus, we predict that, like KSBcl-2 and BHRF1, FPV039 is structurally and functionally homologous to cBcl-2 proteins even in the absence of absolute fidelity to Bcl-2 primary sequence. This and other evidence implies that the structural equivalent of a BH domain may be just as relevant, if not more so, than the presence of a canonical BH domain sequence.

The idea that structure plays a critical role in the function of viral inhibitors of apoptosis was bolstered by the publication of structures for the poxviral inhibitors of apoptosis M11L and F1L (117, 251, 252). Although M11L may possess a BH3-like domain (450), F1L shares no obvious sequence identity with

cBcl-2 proteins, and neither M11L nor F1L share significant sequence homology with each other (455). Nonetheless, both M11L and F1L adopt structures that are strikingly similar to cBcl-2 proteins, and this structure plays a critical role in the ability of these proteins to interact with cBcl-2 family members and inhibit apoptosis (117, 251, 252). Surprisingly, additional structural and sequence analysis of F1L revealed the presence of highly divergent BH-like domains (53). Moreover, structure-based alignment of Orf virus ORFV125 uncovered a similar Bcl-2-like structure, and sequence analysis again revealed the presence of BH-like domains (461). Even HCMV vMIA, which inhibits apoptosis in a manner completely unlike any known cellular or viral protein, has been predicted to be structurally similar to Bcl-x_L and possess BH-like domains (345).

With the identification of each new “cryptic” or “degenerate” or “highly-divergent” BH domain, usually in viral proteins, the canonically described sequences of the BH domains becomes less and less relevant. It is a reflection of the advancement in the field of apoptosis that BH domains are now less beholden to a specific amino acid sequence and more accurately described in terms of their structural composition. Indeed, the identification of the putative F1L BH4-like domain, comprised of F1L α -helix 1, prompted the re-definition of the BH4 domain as a structural motif rather than an amino acid sequence (252). Previously, viral Bcl-2 homologues, such as KSBcl-2 and BHRF1, were designated as such based solely on primary sequence identity with cellular Bcl-2 proteins (176). However, it is now clear that the presence or absence of the canonical BH domain sequence in these viral proteins may be of little consequence to their function. Far more important is overall structural homology and, specifically, the biochemical properties of the amino acids that make up these viral proteins. Accordingly, and regardless of their amino acid sequence, it

is logical to refer to the viral proteins discussed here, including M11L, F1L, and FPV039, as viral Bcl-2-like (vBcl-2) proteins, given that both the structure and function of these proteins parallels that of cBcl-2 proteins.

The family of vBcl-2 proteins may even extend beyond proteins that modulate apoptosis at the mitochondria. Poxviruses have recently been shown to encode a variety of proteins that all adopt a Bcl-2-like fold (155, 158). Interestingly, the VV protein N1L possesses a Bcl-2-like structure and has been shown to inhibit both NF- κ B signalling and apoptosis (89). However, Cooray and colleagues provided evidence that contradicted N1L's role as an NF- κ B inhibitor and demonstrated, instead, that N1L interacts with Bax, Bad, and Bid to inhibit apoptosis. In contrast, we were unable to detect an interaction between Bax and N1L (Fig. 4.6B), and N1L showed no anti-apoptotic activity in our hands (K. Veugelers and M. Barry, personal communication). Whether N1L can truly be classified as an inhibitor of apoptosis remains to be determined, but it is certainly not the case that a protein with a Bcl-2-like structure must function to inhibit apoptosis. A52R and B14R, both VV-encoded proteins that share little sequence homology with each other, fold like Bcl-2 proteins, and inhibit NF- κ B signalling through TLRs but have no effect on apoptosis (158). Indeed, A52R and B14R lack the hydrophobic binding groove required by Bcl-2 family members to interact with pro-apoptotic Bcl-2 proteins and inhibit apoptosis (158). Additionally, Gonzalez and Esteban have recently proposed that like N1L, A52R, and B14R, VV proteins A46R, K7R, N2L, and C1L all possess a Bcl-2-like fold and should be grouped within the same protein family (155). Of these proteins, only N1L has been shown to modulate apoptosis, and all of them are demonstrated or suspected inhibitors of TLR signalling. Overall, it seems as though poxviruses

have co-opted the Bcl-2 protein structure and employed it for inhibiting apoptosis as well as other signalling pathways.

7.1.2. FPV039 inhibits apoptosis. Given the unique homology between FPV039 and cBcl-2 proteins, we sought to determine what role FPV039 played in the modulation of apoptosis. We hypothesised that, like cBcl-2 proteins, FPV039 would function through interactions with members of the Bcl-2 family, which tightly regulates the mitochondrial events leading to apoptosis. Specifically, Bak and Bax, the two pro-apoptotic proteins absolutely required for the induction of apoptosis, represent a crucial junction in the regulation of cell death, and other vBcl-2 proteins have been shown to inhibit apoptosis by interfering with their pro-apoptotic activity (95, 176).

Accordingly, we initially showed that FPV039 localised to the mitochondria where it interacted with both human and chicken Bak in the context of virus infection and during transient over-expression (Fig. 3.2, 3.3, 3.5, 3.7, & 3.8). FPV039 inhibited apoptosis induced by Bak over-expression and TNF α treatment in mammalian cells (Fig. 3.4 & 3.6), and it functionally replaced F1L to inhibit VV-induced cell death (Fig. 3.9). In response to both VV infection and STS treatment, FPV039 also prevented the conformational activation of Bak, a key step towards Bak oligomerisation and MOMP (Fig. 3.10) (162, 163, 458), confirming the functional relevance of the interaction between the two proteins. Thus, we established that FPV039 was a potent anti-apoptotic protein. However, because Bak and Bax often function redundantly, Bax must also be inactivated to inhibit apoptosis (282, 459, 502). We therefore went on to demonstrate that FPV039 inhibited apoptosis induced by Bax over-expression (Fig. 4.1) and prevented the formation of Bax oligomers (Fig. 4.5), which, like Bak oligomers,

ultimately facilitate the release of cytochrome *c* and the commitment to apoptosis (8, 10, 11). Moreover, in the context of virus infection, FPV039 functionally replaced F1L and prevented the conformational activation of Bax (Fig. 4.2 – 4.4), a step that is thought to occur immediately after Bax re-localisation to the MOM and just prior to Bax oligomerisation (54, 156, 199, 256, 324, 474). We also demonstrated that FPV039 interacted with Bax during transient transfection, in both the presence and absence of Bak (Fig. 4.6 & 4.7), when Bax was over-expressed and activated. Additionally, FPV039 interacted with endogenous Bax during virus infection but only when active Bax was specifically precipitated (Fig. 4.8), suggesting that FPV039 interacts with active but not inactive Bax. Further, FPV039 inhibited apoptosis induced by the upstream activators of Bax and Bak, the BH3-only proteins, and interacted with at least two of them: Bim_L and Bik (Fig. 4.9 – 4.11). All together, FPV039 appears to be a robust and potent viral inhibitor of apoptosis (Fig. 7.1).

Because Bak and Bax can independently commit the cell to death, a virus must inactivate both to efficiently inhibit apoptosis. Since Bak, unlike Bax, resides constitutively at the mitochondria, its inhibition is relatively straightforward (Fig. 7.2). In healthy cells, Bak is held in an inactive complex by Bcl-x_L and Mcl-1, and, upon the induction of apoptosis, conformational changes in Bak can promote additional inhibitory interactions with Bcl-2 (94, 115, 470). Several viral proteins inhibit Bak activity in ostensibly the same manner. M11L, F1L, and ORFV125 constitutively interact with Bak, and both F1L and ORFV125 have been shown to prevent the conformational activation of Bak and the associated exposure of an N-terminal epitope (450, 453, 460). Presumably, M11L also inhibits Bak conformational activation, but this has not been specifically addressed. We have demonstrated here that FPV039 interacted with Bak and,

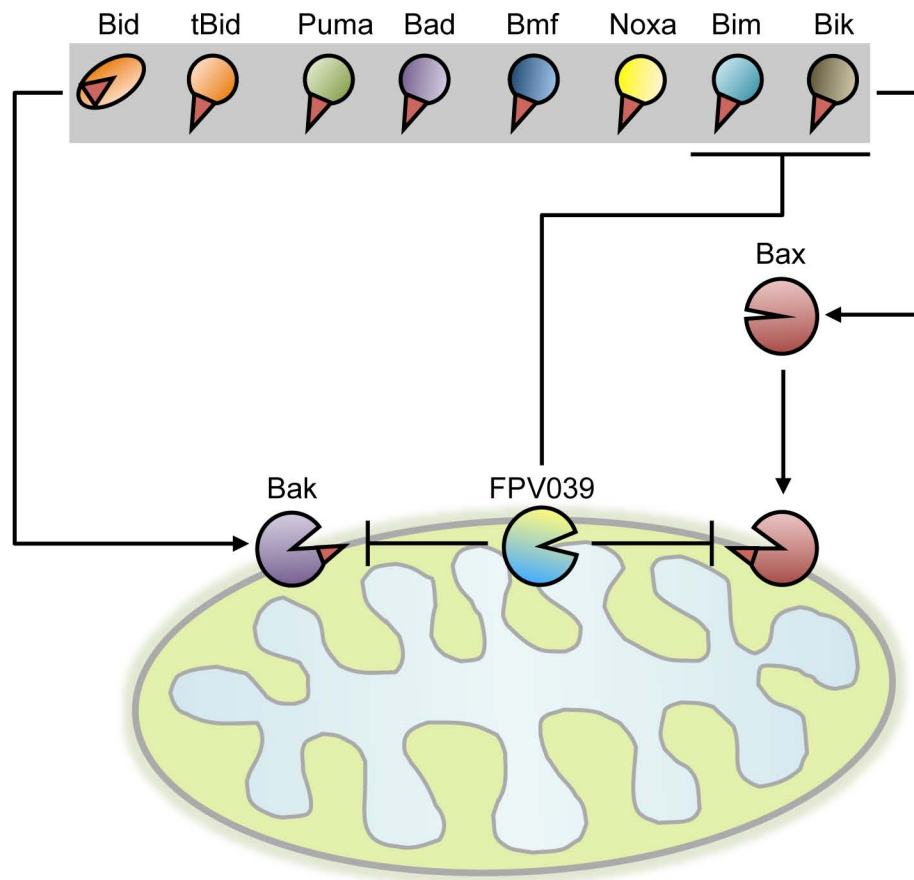


Figure 7.1. FPV039 inhibits apoptosis. FPV039 localises to the mitochondria where it interacts with Bak to inhibit Bak activation. FPV039 also interacts with two BH3-only proteins, Bim_L and Bik, presumably to prevent the activation of Bax. However, in situations where Bax becomes activated regardless, FPV039 is still able to interact with active Bax and inhibit its activity. Although we only detected an interaction between FPV039 and Bim_L and Bik, FPV039 prevented apoptosis induced by Bim_L and Bik as well as Bid, tBid, Bad, Noxa, Bmf, and Puma.

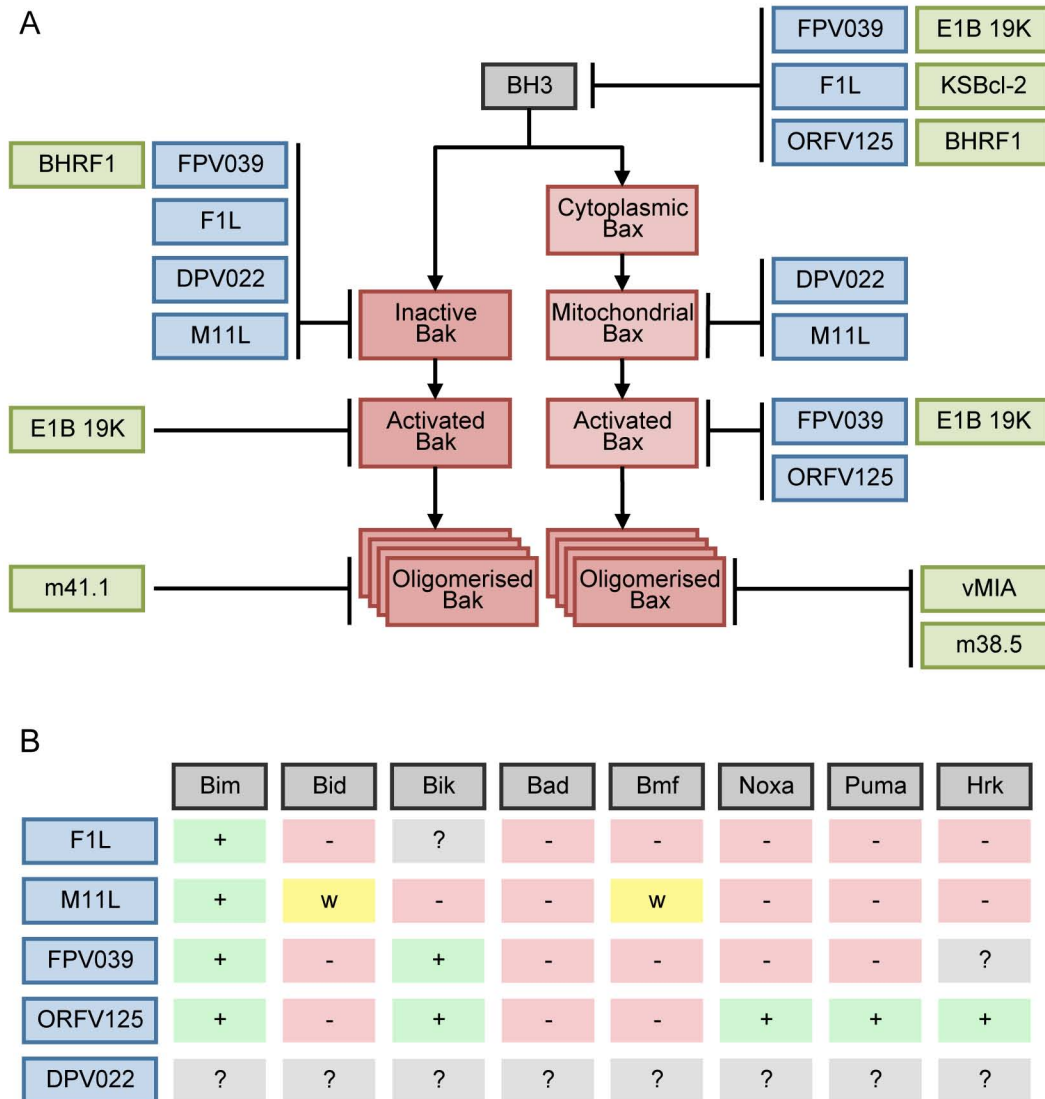


Figure 7.2. The inhibition of Bak and Bax activity by vBcl-2 proteins. (A) BH3-only proteins activate Bak and Bax to induce their homo-oligomerisation and subsequent apoptosis. vBcl-2 proteins inhibit the steps leading to Bak and Bax activation at multiple points, as indicated in this schematic. Poxviral vBcl-2 proteins are coloured blue and other vBcl-2 proteins from other viruses are coloured in green. “Activated Bak/Bax” denotes the active conformation of Bak/Bax with the N-terminal epitope exposed. “Cytoplasmic Bax” denotes cytoplasmic, inactive Bax, whereas “mitochondrial Bax” denotes Bax that has integrated into the mitochondrial outer membrane but not yet undergone conformational activation. The stacked Bak/Bax boxes depict Bak/Bax homo-oligomers. (B) The interactions observed between poxviral vBcl-2 proteins and BH3-only proteins (251, 252, 426, 461). +, binding; -, no binding; w, weak binding; ?, no data.

like F1L, inhibited Bak conformational activation, suggesting that FPV039 constitutively sequesters Bak in an inactive complex. Curiously, although ORFV125 also prevents Bak activation, it appears not to interact with Bak, a phenomenon that may be linked to ORFV125's ability to interact with the upstream BH3-only proteins (461). Nevertheless, with the exception of ORFV125, all poxviral vBcl-2 proteins neutralise Bak by the same, or at least a similar, manner. Interestingly, the case is somewhat different for E1B 19K, which preferentially interacts with the conformationally activated form of Bak, similar to Bcl-2 (92, 93). E1B 19K has also been demonstrated to bind Bak upon its release from Mcl-1 during the course of adenovirus infection (94), and, in this case, Bak is presumably in an active conformation. A similar phenomenon has recently been described for F1L, which sequesters Bak upon its release from Mcl-1 during the course of VV infection (53), and, by extension, this may hold true for the other poxviral vBcl-2 proteins, including FPV039. Whether F1L was interacting with activated Bak, in this case, was unclear (53). Indeed, the ability of FPV039 and other poxviral inhibitors of apoptosis to interact with activated Bak has not been strictly investigated and cannot, therefore, be ruled out.

The regulation and activation of Bax is more complicated than that of Bak, making its inactivation by vBcl-2 proteins equally complicated. Bax exists as an inactive monomer in the cytoplasm of healthy cells and must, upon receipt of an apoptotic stimulus, be activated to translocate to the MOM where additional conformational changes occur in Bax before it is capable of promoting MOMP (10, 11, 156, 199, 200, 474). The multiple steps required for Bax activation are reflected in the variety of mechanisms that viral proteins employ to inhibit this activation (Fig. 7.2). tBid-induced activation of Bax results in its translocation to the MOM and the activation-associated exposure of the Bax N-terminus before

E1B 19K interacts with Bax and inhibits the remainder of the downstream events that lead to Bax-mediated MOMP (92, 350). M11L, on the other hand, inhibits Bax one step earlier. During myxoma virus infection, unknown apoptotic signals induce the activation of Bax and its translocation to the MOM where M11L interacts with Bax and prevents its conformational activation (409). Conversely, F1L does not interact with Bax and appears to inhibit the earliest steps in Bax activation, preventing the translocation of Bax to the mitochondria in the first place and thereby preventing all downstream Bax activation steps (426). A similar mechanism may be behind the inhibition of Bax by FPV039. Similar to F1L, FPV039 did not readily interact with Bax during virus infection, even though Bax conformational activation and apoptosis is inhibited, suggesting that FPV039, like F1L, inhibits Bax activation at a step upstream of its translocation to the MOM. Unlike F1L, however, FPV039 was able to interact with Bax in the context of its transient over-expression, a situation in which Bax exists in the active conformation (243, 475). Moreover, selective immunoprecipitation of active Bax during virus infection revealed that active Bax could be bound by FPV039. Notably, a small amount of F1L was also precipitated along with active Bax; however, the amount of F1L precipitated was miniscule compared to FPV039 and its relevance is uncertain, especially given the fact that F1L does not interact with over-expressed Bax (Fig. 4.6 & 4.8). Thus, it appears as if FPV039 functions upstream of Bax to prevent the majority of Bax activation but, in cases where Bax becomes activated regardless, FPV039 is still able to bind activated Bax and presumably inhibit its pro-apoptotic function. Subsequent to our study, it was demonstrated that ORFV125 interacts with active, but not inactive, Bax to prevent MOMP, suggesting that ORFV125 may function in a similar manner to FPV039 (461).

The ability of FPV039 to inhibit Bax activation in the absence of an interaction with inactive Bax is undoubtedly linked to the upstream activators of Bax and Bak, the BH3-only proteins. Indeed, in some cases viral proteins appear able to inhibit apoptosis not because of a direct interaction with Bak or Bax but, instead, because of an interaction with a distinct set of BH3-only proteins (Fig. 7.2). We demonstrated that FPV039 inhibited apoptosis induced by the over-expression of eight BH3-only proteins and interacted detectably with Bim_L and Bik. Bim has been implicated in the direct activation of Bax (55, 144, 175, 249), and the importance of Bim_L as an activator of Bax during virus infection is underscored by the ability of F1L to inhibit Bax activation by inactivating Bim_L (426). Likewise, Bik has also been shown to trigger the activation of Bax (151, 152). It is therefore tempting to speculate that the interactions observed between FPV039 and Bim_L and Bik are critical to FPV039's ability to inhibit Bax activation. How FPV039 inhibited apoptosis induced by the other six BH3-only proteins with which it did not interact is uncertain. It seems likely, however, that, because BH3-only proteins require Bak and Bax to induce apoptosis (502), the ability of FPV039 to neutralise Bak and Bax rendered the remaining BH3-only proteins impotent. ORFV125 also interacts with Bim and Bik, as well as Puma, Noxa, and Hrk, suggesting that ORFV125 may similarly rely on the inhibition of BH3-only proteins to prevent Bax activation. Besides FPV039, F1L, and ORFV125, several other viral proteins have been shown to interact with one or more of the BH3-only proteins. In particular, KSBcl-2 interacts with Bim, Bik, Bid, Noxa, Puma, Bmf, and Hrk but not Bak or Bax, suggesting that inhibition of BH3-only proteins alone is sufficient to prevent Bak- and Bax-mediated apoptosis (67, 138). Likewise, BHRF1 interacts with Bim, Bid, and Puma but not Bax (92, 105, 138, 430). Although an interaction between

BHRF1 and Bak has been observed, recent data suggests that it is the ability of BHRF1 to interact with Bim, not Bak, that correlates with its anti-apoptotic activity (105). Similarly, while E1B 19K also interacts with both Bak and Bax, interaction with Bim and Bik alone may be sufficient to prevent apoptosis (411). The functional consequences of ASFV A179L's ability to interact with a subset of BH3-only proteins is as yet unclear, given that it also interacts with Bak and Bax (141). In fact, just because a viral protein exhibits an interaction with a BH3-only protein does not necessarily mean that that interaction is functionally relevant, and in some cases it may even be deleterious. For example, despite our evidence that M11L interacted with Bim_L (Fig. 4.10) and other evidence that M11L interacts strongly with Bim_{EL} (251), the anti-apoptotic activity of M11L correlates with binding to Bak and Bax and not Bim (251). Moreover, Bik has been shown to induce apoptosis despite an observed interaction with E1B 19K (173), and Bim_S induces apoptosis even in the presence of M11L (251). Thus, it is possible that some BH3-only proteins may be able to overcome viral inhibition of apoptosis and/or regulate the vBcl-2 proteins. Regardless of the functional outcome, it is worth noting that, like the cellular anti-apoptotic Bcl-2 proteins, vBcl-2 proteins, including FPV039, appear to bind only a specific subset of BH3-only proteins. Although the determinants of, and the functional basis for, these disparate binding profiles remain to be determined, the ability of viral proteins to inhibit cell death is probably not confined to their ability to interact with Bak and Bax. Inactivating the upstream BH3-only proteins may, in many cases, be an equally effective strategy.

But why exactly should BH3-only proteins be involved at all in the strategies that viruses employ to inhibit apoptosis? After all, Bak and Bax are the ultimate gatekeepers of apoptosis and their direct inhibition therefore represents

the most parsimonious method of preventing apoptosis. BH3-only proteins, on the other hand, are activated by a variety of different stimuli and their expression is often dependent on cell type—as a result, BH3-only proteins represent a much bigger and varied target (287). It is possible that some of the interactions observed between viral proteins and BH3-only proteins are pleiotropic “side-effects” of the more important interactions with Bak and Bax, all of which involve the viral protein binding to the BH3 domain of the cellular protein. Alternatively, perhaps there is some selective advantage to preventing Bax activation in the first place or inhibiting apoptosis at every possible step in order to afford the most complete protection possible. Bim, a so-called activator BH3-only protein, is potentially pro-apoptotic and appears to play a significant role in the direct activation of Bax and the induction of apoptosis by several different viruses. Indeed, the fact that many viral proteins, including FPV039, F1L, M11L, ORFV125, A179L, BHRF1, and KSBcl-2, interact with Bim suggests that the interaction might be relevant, particularly in the context of preventing Bax activation (92, 141, 251, 426, 461). The “life-cycle” of the virus and its evolutionary relationship with its host also probably influence the mechanism the virus employs to inhibit apoptosis. Perhaps, the most extreme example is that of the cytomegalovirus inhibitors of apoptosis. Both HCMV vMIA and MCMV m38.5 recruit Bax to the mitochondria and facilitate its conformational activation and oligomerisation prior to interacting with Bax and inhibiting apoptosis (14, 15, 223, 331, 356). The ability of vMIA to interact with Bak, however, is disputed and vMIA is unable to inhibit Bak-induced cell death (14, 331). m38.5 is also unable to interact with Bak and inhibit Bak induced death, but, in compensation, MCMV encodes an additional protein, m41.1, that appears to specifically inhibit Bak (52). An analogous protein has yet to be identified in HCMV, leading to the speculation

that HCMV replication is confined to cells in which Bax is dominant over Bak (14). A similar phenomenon, developed over evolutionary time, might contribute to the cBcl-2 binding profiles of other viral proteins, especially regarding their ability to bind BH3-only proteins. Unfortunately, unlike the case for cellular anti-apoptotic Bcl-2 proteins, there are few standardised, systematic comparisons of the cBcl-2 interaction partners of viral proteins. In the absence of definitive data, it is difficult to draw any certain conclusions about which interactions are the most functionally relevant and why this might be the case.

Taken together, our data suggest a model for FPV039-mediated inhibition of apoptosis that involves both indirect and direct inactivation of Bak and Bax, the two critical pro-apoptotic Bcl-2 proteins (Fig. 7.1). The ability of FPV039 to interact with Bim and Bik, two BH3-only proteins known to activate Bax, suggests that FPV039 may counter apoptosis by inhibiting Bim and Bik and preventing the initial activation of Bax. In particular, Bim appears to be a crucial activator of apoptosis in response to VV infection (426) and several viral proteins, including F1L, demonstrate an interaction with Bim, suggesting that the ability of FPV039 to interact robustly with Bim_L is physiologically relevant. Thus, it may be that by sequestering and inactivating certain BH3-only proteins, FPV039 is able to indirectly inhibit Bax activation during virus infection. Conceivably, because inactive Bax resides in the cytoplasm (199, 474) and FPV039 localises to the MOM, suppression of Bax activation by BH3-only proteins would keep Bax and FPV039 physically separated, explaining our inability to co-precipitate Bax when precipitating Flag-tagged FPV039 during virus infection (Fig. 4.8). Nevertheless, the ability of FPV039 to interact with active Bax may be physiologically significant in conditions where (1) Bax becomes activated by BH3-only proteins not repressed by FPV039 or where (2) Bax becomes activated by cellular factors that

are independent of regulation by Bcl-2 family members. Indeed, such a phenomenon has been described for the cellular anti-apoptotic proteins Bcl-2 and Bcl-x_L. Both Bcl-2 and Bcl-x_L interact with Bax only upon receipt of an apoptotic stimulus (39, 115, 496), when Bax becomes activated and translocates to the MOM. Furthermore, Bcl-x_L can sequester the BH3-only protein tBid to prevent Bax activation in the first place, but, in cases where Bax becomes activated regardless, Bcl-x_L can also sequester active Bax to prevent its subsequent oligomerisation (39, 289). In this case, sequestration of both tBid and active Bax each contribute significantly to the inhibition of apoptosis (39). It therefore seems likely that FPV039 may inhibit the activation of Bax in a manner analogous to Bcl-x_L. It is not known whether FPV039's ability to interact with BH3-only proteins also helps prevent the activation of Bak, as might be the case for ORFV125 (460, 461). However, because Bak is constitutively localised to the MOM where it interacts with FPV039, the simplest explanation for inhibition would be that FPV039 directly inactivates Bak independent of BH3-only activity. Regardless, given the ability of FPV039 to interact with Bak, as well as active Bax and certain BH3-only proteins, it is evident that FPV039 targets multiple pro-apoptotic Bcl-2 family members to inhibit apoptosis.

7.1.3. DPV022 inhibits apoptosis. The sequencing of the deerpox virus genome revealed the presence of DPV022, yet another putative inhibitor of apoptosis unique among the already characterised family of poxvirus vBcl-2 proteins. DPV022 lacks obvious sequence identity with cellular Bcl-2 proteins, but, surprisingly, it possesses discrete and limited regions of sequence identity with both M11L and F1L (Fig. 5.1). M11L and F1L, themselves, share no sequence identity and, aside from their similar structures, are typically

considered to be unrelated. Much of the sequence identity among these three proteins is concentrated within the regions of DPV022 that correspond to the BH-like domains recently identified in F1L and M11L (117, 251, 252). Strikingly, the “LAT” motif (corresponding to amino acids 147-149 in F1L) within the BH1 region is conserved among all three proteins, highlighting the importance of the BH1-like domain to the function of these proteins. In fact, A148 in F1L and the corresponding A82 in M11L occupy structurally important positions in the F1L and M11L binding grooves, and mutation of A82 in M11L abrogates its interaction with Bak and Bax (251, 252). The corresponding A93 in DPV022 is therefore likely to play a critical role in the ability of DPV022 to inhibit apoptosis. Interestingly, however, the majority of identical amino acids shared between M11L and DPV022 are not the same amino acids shared between F1L and DPV022. Besides A82 of M11L, DPV022 shares M11L amino acids I37, Y41, and F122, all of which have been implicated to play key roles in the ability of M11L to inhibit apoptosis (251). Except for M11L Y41, none of these critical amino acids are shared with F1L. Conversely, F1L F152 has been suggested to be critical to the ability of F1L to inhibit apoptosis, and, along with both flanking residues, F152 is shared between F1L and DPV022 but not M11L (252). Two additional F1L amino acids, V104 and G144, are critical to F1L’s ability to interact with Bak but are not conserved in DPV022 (53). Notably, however, the valine in F1L (V104) aligns with the similarly hydrophobic isoleucine in M11L (I37) and DPV022 (I49), and because F1L V104 and M11L I37 are demonstrated or predicted critical amino acids, it is likely that I49 is also critical to DPV022 function (53, 251). Thus, at the primary sequence level, DPV022 represents a kind of intermediate between M11L and F1L, making its mechanism of action an

interesting target for further research, especially in comparison with M11L and F1L.

We demonstrated here that DPV022 localised to mitochondria (Fig. 5.2) where it inhibited apoptosis induced by a variety of stimuli, probably a result of DPV022's ability to interact with and inactivate both Bak and Bax. Like most poxviral vBcl-2 proteins, DPV022 interacted constitutively with Bak, inhibited Bak-induced apoptosis, and prevented Bak conformational activation during VV infection (Fig. 5.4 – 5.6, 5.12, & 5.13). Curiously, however, when these VV-infected cells were stimulated with STS, DPV022 was unable to completely inhibit the activation of Bak (Fig. 5.13). This result differs from those obtained with other poxviral inhibitors of apoptosis, namely F1L and FPV039, which completely inhibited Bak activation induced by virus infection and STS treatment (453). It is possible that the apoptotic stimuli provided by virus infection concomitant with STS treatment overwhelmed the ability of DPV022 to inhibit apoptosis or perhaps induced apoptosis via an additional pathway not inhibited by DPV022. Moreover, DPV022, which presumably evolved to interfere with apoptosis in its natural host, mule deer, may be less efficient at interacting with the human Bak or human BH3-only proteins that were used in our experiments (see section 7.1.4.).

Interestingly, DPV022 also interacted with Bax, both during transfection with over-expressed Bax and during VV infection with endogenous Bax (Fig. 5.7, 5.8, & 5.12). This differs from the mechanism employed by F1L, which does not interact with Bax, presumably because F1L inhibits the upstream BH3-only proteins to prevent Bax activation and translocation to the MOM in the first place (426). Likewise, although FPV039 has the ability to interact with activated Bax, it, like F1L, appears to prevent the activation of Bax in the first place.

Conversely, for an interaction between DPV022 and endogenous Bax to be possible, Bax must be activated and induced to translocate to the MOM where DPV022 is located. Once at the MOM, we speculate that DPV022 interacts with Bax to prevent its conformational activation and subsequent oligomerisation (Fig. 5.10 & 5.14). This mechanism of action is almost identical to that of M11L, which relies on the activation of Bax—probably by signals induced by virus infection itself—and its translocation to the MOM before interacting with Bax and inhibiting its activity (409).

The observation that DPV022 circumvents cell death by directly targeting Bak and Bax was reinforced by the demonstration that DPV022, alone, was sufficient to prevent the activation of Bak and Bax when all cellular anti-apoptotic Bcl-2 proteins were inactivated (Fig. 5.11). These data support the idea that DPV022 interacts with Bak and Bax to hold them in an inactive conformation, but they do not rule out the possibility that DPV022 interacts with a subset of BH3-only proteins to further pre-empt the activation of Bak and Bax. Indeed the ability of DPV022 to interact with and inhibit the activity of BH3-only proteins is the subject of ongoing research. In the meantime, it is interesting to speculate that, given the apparent inability of DPV022 to prevent the initial activation of Bax, which is presumably mediated by BH3-only proteins, DPV022 anti-apoptotic activity might correlate with its direct inhibition of Bak and Bax rather than any ability to interact with BH3-only proteins. Such a mechanism has recently been proposed for M11L (251).

Given the amino acid identity shared between DPV022, M11L, and F1L, it is likely that DPV022 also folds like a Bcl-2 family protein. The residues conserved among these three poxviral proteins, and the ability of DPV022 to interact with Bak and Bax, also suggests that DPV022 retains the hydrophobic

binding groove necessary for the homo- and heterotypic interactions that characterise Bcl-2 proteins (352). In the future, it will be interesting to determine whether the intriguing differences in amino acid sequence between DPV022 and other poxviral inhibitors of apoptosis account for the mechanistic and functional differences observed in this study. Additionally, DPV022 encoded by a different strain of deerpox virus differs from the one used in this study by three amino acids (2), and preliminary evidence suggests that its ability to inhibit apoptosis is less robust (D. Huang, personal communication). Whether or not the difference in amino acids affects the ability of DPV022 to bind Bak, Bax, or even BH3-only proteins will be addressed in the future.

7.1.4. The evolution of poxviral vBcl-2 proteins. Given that almost every poxvirus encodes a protein to inhibit the activity of Bak and Bax, it is obvious that inhibition of the intrinsic apoptotic cascade is of paramount importance to the poxvirus replication cycle. Yet the diversity of vBcl-2 proteins encoded by poxviruses is extensive, and each vBcl-2 appears to achieve the goal of apoptosis inhibition in a slightly different way, by interacting with different members of the cellular Bcl-2 family. Poxviruses are renowned for “capturing” genes from the host cells they infect and re-purposing them to their own advantage (207). Therefore, it is possible that multiple, independent acquisitions of cBcl-2 proteins led to the diversity of vBcl-2 proteins we see today. However, sequence analysis strongly suggests that DPV022 is related to both M11L and F1L, and all three proteins are grouped closely together on an unrooted phylogenetic tree, arguing for a single common ancestor (Fig. 7.3A) (132). Moreover, the *DPV022*, *F1L*, and *M11L* genes, along with all the orthologues of both F1L and M11L, are found at a similar location within the virus genome and

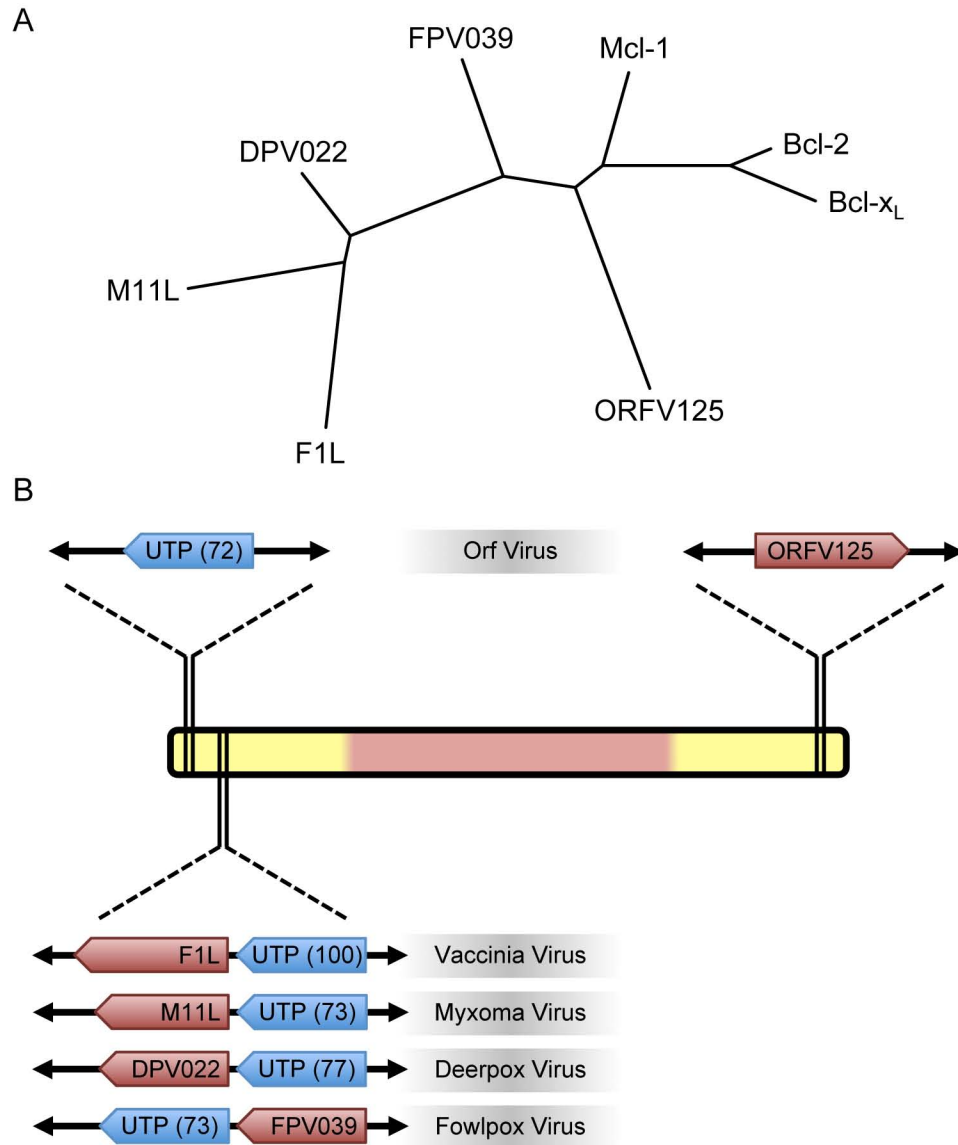


Figure 7.3. The evolutionary relationship of poxviral vBcl-2 proteins. (A) The unrooted phylogenetic tree was generated from the amino acid sequence alignments of the indicated proteins using the programmes PROTDIST, FITCH, and DRAWTREE, part of the PHYLIP package, using the default settings (132). (B) A schematic of the chordopoxvirus genome with the general location of the vBcl-2 genes and the dUTPase genes ("UTP") given for the indicated viruses. The number in parentheses given for each dUTPase gene indicates the percentage of amino acid similarity shared between that gene and the dUTPase gene encoded by vaccinia virus strain Copenhagen.

are each immediately preceded by a gene encoding the highly conserved poxviral dUTPase (Fig. 7.3B). These data therefore imply that F1L, M11L, and DPV022, despite sharing little sequence identity, are the products of divergent evolution from a common progenitor. A similar phenomenon has been observed between the human and murine CMV proteins, vMIA and m38.5, which lack sequence identity but are encoded in homologous positions in the viral genome (298). Conversely, ORFV125 appears to have evolved separately from F1L, M11L, and DPV022. It is predicted to be a phylogenetically distant relative of the other poxviral vBcl-2 proteins, and the *ORFV125* gene is encoded in a different genomic position, far away from the dUTPase gene (Fig. 7.3).

Whether FPV039 also evolved from the same ancestral protein as F1L, M11L, and DPV022 is a matter of debate. Although FPV039's amino acid sequence is considerably different from all other poxviral vBcl-2 proteins, a fact reflected in phylogenetic analysis, the *FPV039* gene is found in the same genome position as *F1L*, *M11L*, and *DPV022* and is flanked by the dUTPase gene (Fig. 7.3). Notably, however, instead of preceding the FPV039 gene, the dUTPase gene immediately follows it. The fowlpox virus genome, although similar in overall structure to the genomes of other chordopoxviruses, is nonetheless highly divergent and has been subject to numerous gene rearrangements (305). The argument could be made that such rearrangements might have flipped the dUTPase gene to the other side of the *FPV039* gene relative to *F1L*, *M11L*, and *DPV022*. Conversely, the same argument could be invoked as an explanation for the proximity of the two genes in the first place, the dUTPase gene having been rearranged to a position immediately downstream of *FPV039* by coincidence.

Regardless of their evolutionary relatedness, if one accepts that the ancestor (or ancestors) of the poxviral vBcl-2 proteins were cBcl-2 proteins, the question then becomes why has structural homology but not sequence similarity been preserved? And more specifically, why has sequence identity been preserved in the BH1 and BH2 domains of FPV039 but not the BH3 and BH4 domains? The answers surely lie in the selection pressures that these proteins have faced over evolutionary time. For example, the various levels of negative regulation imposed on cellular Bcl-2 family members have likely resulted in the preservation of only the minimal functional elements and the loss of regulatory elements in vBcl-2s. The lack of BH4 or N-terminal sequence conservation in FPV039 may reflect the loss of a phosphorylation site typically present in the BH4 domain of Bcl-2 that negatively regulates Bcl-2 (168). Furthermore, similar to other vBcl-2 proteins, FPV039 is predicted to lack the unstructured “loop” domain normally present between the BH3 and BH4 domains of Bcl-2 and Bcl-x_L, making FPV039 a comparably smaller protein (Fig. 3.1A). This loop acts as a negative regulatory domain sensitive to inhibitory phosphorylation (336, 478) and caspase-3-mediated cleavage that converts Bcl-2 and Bcl-x_L from anti-apoptotic to pro-apoptotic proteins (30, 66, 81, 159). Several of the herpesvirus vBcl-2 proteins bypass this level of control and are resistant to caspase cleavage (33, 95, 176, 355), and the structures of both M11L and F1L suggest that the unstructured loop is absent in these proteins (117, 251, 252). Additionally, some Bcl-2 family members, such as Mcl-1, are regulated by ubiquitination. Ongoing investigations in our laboratory are attempting to address whether ubiquitination also plays a role in regulating vBcl-2 proteins, including FPV039 and F1L, both of which are heavily ubiquitinated upon expression (Chapter 3, S. Campbell and M. Barry, unpublished data, and (443)). Overall, however, the lack of sequence

identity may be the result of an absence of selection pressure rather than its presence. The structure of both cellular and vBcl-2 proteins plays a demonstrated and important role in their ability to modulate apoptosis, and strict adherence to the canonical BH domain sequences is clearly unnecessary for vBcl-2 function. Thus, without the requirement to preserve the specific BH domain sequences, vBcl-2 proteins may be free to diverge at the amino acid level, with the only requirement being structural preservation. Intriguingly, if FPV039 truly shares a common ancestor with F1L, M11L, and DPV022, why FPV039 should have preserved its BH1 and BH2 domains, while the others did not, is a fascinating and unanswered question.

7.1.5. Of chickens and deer. FPV039 presumably evolved to counteract the avian members of the Bcl-2 family, and we have demonstrated that FPV039 does, in fact, interact with endogenous chicken Bak (Fig. 3.8). It would be interesting to confirm all of the interactions demonstrated in this study using the avian homologues of the relevant human Bcl-2 proteins, for it is not necessarily certain that the binding profiles would be identical. Unfortunately, of the chicken Bcl-2 family members that have been identified to date, only the Bmf and Bid homologues have been functionally characterised in chicken cells (111, 154). This, coupled with the incompletely annotated chicken genome and the paucity of reagents available, has so far prevented a detailed examination of avian apoptosis. The situation is similar among cervids, for which even less genomic data exists and no Bcl-2 homologues have been identified. Nevertheless, the fact that DPV022 and FPV039 are both capable of interacting with human Bcl-2 proteins and inhibiting apoptosis in human cells underscores the evolutionary relatedness of the apoptotic programme and provides indirect evidence that the

avian and cervid death machinery operates in a similar manner to that of humans.

The role that these anti-apoptotic proteins play during the course of a natural infection with either fowlpox or deerpox virus is also unclear. Although, given the importance of apoptosis to the host immune system, it is likely that FPV039 and DPV022 act as major virulence factors. Indeed, myxoma virus devoid of M11L is highly attenuated in rabbits (339), and this is almost certainly the case in mice infected with ectromelia virus devoid of its F1L orthologue, although the relevant experiments have yet to be performed. Moreover, natural fowlpox virus infection results in epithelial hyperplasia (61, 62), making it tempting to speculate that FPV039 is involved in promoting or at least maintaining the pro-survival signals that might be necessary to sustain this cellular proliferation. Similar, albeit highly contentious, roles have been proposed for the herpesvirus vBcl-2 proteins in the etiology of EBV- and KSHV-mediated cancers (176). Unfortunately, defining the *in vivo* function of FPV039 and DPV022 awaits animal study, something that, although intellectually rewarding, is neither urgent nor technically practical. Instead, FPV039 and DPV022, as well as other vBcl-2 proteins, will continue to prove useful for the biochemical dissection of an important human process we still do not fully understand: apoptosis.

From a timely and practical standpoint, however, it is also imperative that we understand how FPV039, in particular, influences apoptosis in mammalian cells. Live fowlpox virus is currently being pursued as a recombinant vaccine vector for a variety of diseases, including HIV/AIDS (37, 399). Although fowlpox virus is incapable of replicating in mammalian cells and causing a productive infection, mammalian cells do support the transcription and translation of native

or recombinantly inserted early genes (404). As such, understanding how FPV039 interacts with Bcl-2 proteins and inhibits apoptosis in a mammalian context may have significant implications in the development of vaccines and gene therapy vectors using fowlpox virus.

7.1.6. More than meets the eye? Although interference with cellular Bcl-2 proteins may be the primary and most important aspect of vBcl-2 function, it is possible that vBcl-2 proteins, including FPV039 and DPV022, inhibit additional aspects of the cellular apoptotic machinery. Mitochondria are dynamic organelles that are constantly undergoing fission and fusion within the cell (296). Cellular Bcl-2 proteins, including Bak, Bax, and Bcl-x_L, are thought to regulate mitochondrial morphology, at least in part, by interacting with several unrelated proteins that directly promote mitochondrial fission or fusion (371). Moreover, dramatic mitochondrial fission has been observed during MOMP, and it is currently a matter of debate as to whether this fission contributes to apoptosis or is simply a result of apoptosis (75, 222). Paradoxically, vMIA has been shown to promote mitochondrial fission without inducing apoptosis and independent of its ability to interact with Bax (300, 345, 374). Whether or not mitochondrial fission even contributes to virus infection and whether other vBcl-2 proteins also influence mitochondrial morphology has yet to be examined in depth. Additionally, it has been proposed that F1L directly interacts with and inhibits caspase-9 to further prevent intrinsic apoptosis at a step downstream of cytochrome c release (492). Whether other poxviral vBcl-2 proteins possess this function is unknown, but it would be especially interesting to know if DPV022, given the limited homology that it shares with F1L, or if F1L orthologues, given their unique and variable N-terminal repeat sequences, also inhibit caspase-9.

Investigation of FPV039, DPV022, and other vBcl-2 proteins beyond their role in inhibiting Bcl-2 family members should be pursued in an effort to identify additional, perhaps unexpected, new mechanisms for inhibiting cell death or modulating other host cell pathways.

7.1.7. To infinity and beyond. FPV039 and DPV022, along with other vBcl-2 proteins such as M11L and F1L, are powerful tools for dissecting the complex biochemical mechanisms that control cellular fate in all metazoans. These viral inhibitors of apoptosis have evolved to inhibit apoptosis in discrete yet functionally equivalent manners, and understanding precisely how they achieve this inhibition will help elucidate the role that apoptosis plays in infection and disease, including cancer. It is clear that Bak and Bax are critically important to the apoptosis induced by virus infection, but given that some vBcl-2 proteins, such as FPV039 and F1L, inhibit Bax activation in the first place, BH3-only proteins must also be relevant to the anti-viral apoptotic response. With respect to poxviruses, why have several different viruses with ostensibly similar replication cycles employed different mechanisms for achieving the same goal? Are these subtle differences relevant during natural virus infection or are they idiosyncrasies left over from separate evolutionary paths? However, instead of asking “why” perhaps we should be asking the more interesting questions “how” and “what.” How, for example, are the different binding profiles of these vBcl-2 proteins accounted for by their sequence? Obviously, the common structure shared by cellular and viral Bcl-2 proteins is critical, but we have yet to thoroughly characterise the structural determinants of function for vBcl-2 proteins and compare them to the same determinants identified in cBcl-2 proteins. Furthermore, what role, if any, do conformational changes play in vBcl-2 protein

activity? It is now well established that the structural conformations of both anti- and pro-apoptotic cellular Bcl-2 proteins are not static and undergo complex rearrangements at multiple points in the apoptotic cascade (75, 483). Based on structural similarities, it might be presumed that the same conformational changes occur in vBcl-2 proteins, but the rigorous structural and functional analyses applied to cBcl-2 proteins have yet to be applied to vBcl-2 proteins. Defining the molecular details that govern vBcl-2 function will undoubtedly support the kind of comparative studies between cellular and viral Bcl-2 proteins needed to truly understand the regulation of apoptosis. Nonetheless, a complete understanding of the regulation of apoptosis must be accompanied by an understanding of the signals that kick-start the cellular death machinery in the first place.

7.2. VACCINIA VIRUS INDUCES APOPTOSIS

Because poxviruses encode proteins that inhibit apoptosis by interacting with Bcl-2 family members at the mitochondria, common sense implies that poxvirus infection must produce signals that activate the intrinsic apoptotic pathway. BH3-only proteins are the apical sensors of cell stress in this pathway, and they are activated, either translationally or post-transcriptionally, in response to a variety of stimuli, including virus infection (287). Once activated, BH3-only proteins propagate apoptosis by inactivating anti-apoptotic Bcl-2 proteins and activating Bak and Bax (146). Thus, it is likely that poxvirus infection results in the activation of one or more BH3-only protein that contributes to pro-apoptotic signals normally neutralised by vBcl-2 proteins. Indeed, Bim and Bad have both been shown to contribute to the apoptotic response to VV infection (358, 426). However, whether other BH3-only proteins are activated in response to poxvirus

infection and what infection-related signals are responsible for this activation remain largely unknown. Based on intriguing results obtained with other viruses, including the highly attenuated MVA (137, 157, 257, 413), the present study sought to characterise the apoptotic response to VV infection mediated by the BH3-only protein Noxa.

Initially we noted that VV devoid of E3L (VV Δ E3L) induced apoptosis even though F1L was ostensibly still being expressed (Fig. 6.1). Given that E3L functions to bind dsRNA, an inevitable by-product of virus infection and a potent inducer of apoptosis (216), we wondered whether the apoptosis we observed was ultimately being induced by dsRNA, in the absence of any E3L to bind and sequester it. In agreement with this idea, dsRNA levels appeared to be elevated in cells infected with VV Δ E3L compared to cells infected with WT VV strain Copenhagen (VVCop) or VV devoid of F1L (VV Δ F1L) (Fig. 6.2). Interestingly, the dsRNA produced during VV Δ E3L infection localised around the virus factories, which, to our knowledge, has not been previously observed (Fig. 6.3). Although dsRNA can induce apoptosis by activating multiple pathways, it is now becoming clear that dsRNA is critical to the activation of the BH3-only protein Noxa (157, 257, 413). dsRNA, as well as infection with a variety of viruses, results in Noxa upregulation and possibly post-translational activation (157, 257, 413). Likewise, we demonstrated here that Noxa is upregulated following VV infection (Fig. 6.4 & 6.5). We were somewhat surprised to find that Noxa also localised around the virus factories during VV Δ E3L infection, perhaps supporting the idea of a physical and functional link between Noxa and dsRNA (Fig. 6.6 & 6.7) (413). Concordantly, we observed that, in the absence of Noxa, the apoptosis induced by VV Δ E3L infection was mitigated, indicating that Noxa contributes to the apoptotic response to VV (Fig. 6.8). We hypothesise that

during VVCop infection, regardless of whether or not Noxa is present, apoptosis does not occur because E3L binds and sequesters the virally-produced dsRNA. Conversely, we predict that during infection with VV Δ E3L, Noxa becomes activated in response to dsRNA, which is no longer bound by E3L, and contributes to apoptosis. In the absence of Noxa, this additional pro-apoptotic signal would not be instigated (Fig. 7.4).

Noxa has previously been shown to be critical for apoptosis induced by infection with vesicular stomatitis virus (VSV) and encephalomyocarditis virus (EMCV) (157, 257, 413). Similarly, Noxa also appears to induce apoptosis triggered by synthetic dsRNA (413). It is therefore tempting to speculate that the dsRNA produced during VSV or EMCV infection is the initial signal that activates Noxa-mediated apoptosis, and it is likely that this phenomenon applies to a wide variety of viruses. Indeed, such a model agrees with our data suggesting that Noxa contributes to VV-induced apoptosis and other data indicating that apoptosis induced by MVA also relies on Noxa (137). Yet in most cases, the mechanism behind Noxa-mediated apoptosis is unclear. It is well established that Noxa interacts with, and inhibits the activity of, Mcl-1 and Bcl-2A1 (56, 64, 271), but the inactivation of only two of the five anti-apoptotic Bcl-2 proteins is unlikely to be sufficient for apoptosis to proceed. Intriguingly, Sun and Leaman showed that Noxa interacts with Bax following dsRNA treatment or EMCV infection, and this may represent a means by which Noxa induces apoptosis (413). This mechanism of action seems at odds with the established dogma that Noxa acts solely as a sensitiser BH3-only protein (56, 64, 249, 271); however, a recent report has provided evidence that Noxa, as well as several other alleged sensitiser BH3-only proteins, may possess varying degrees of “activator” activity (119). In support of Sun and Leaman’s data, Du and colleagues demonstrate

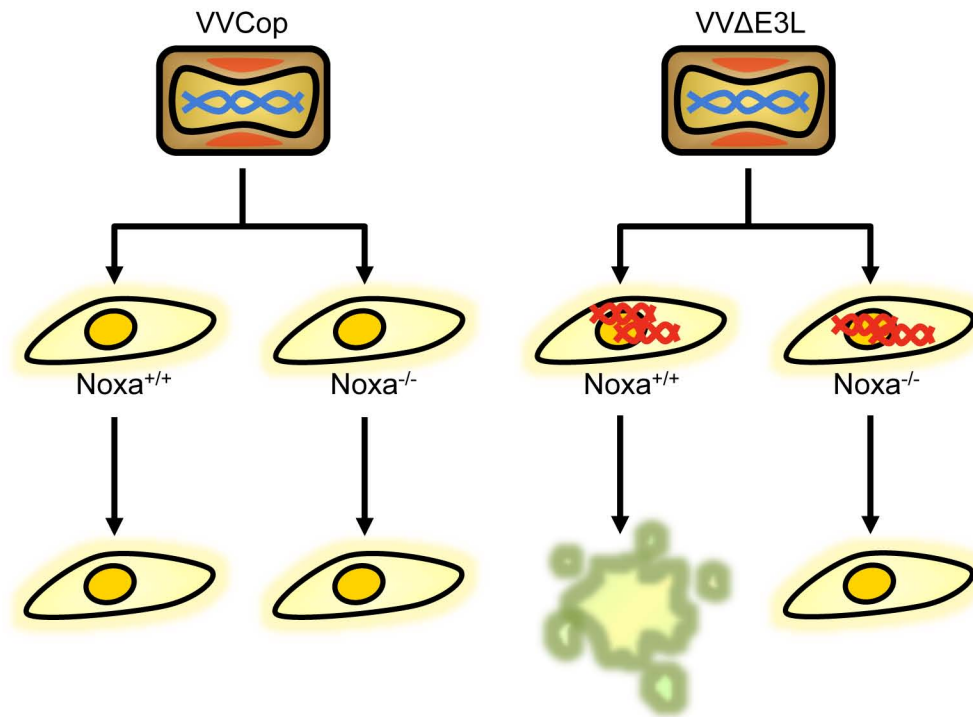


Figure 7.4. Working hypothesis for the role of Noxa during VVΔE3L infection. During VVCop infection, regardless of whether or not Noxa is present, apoptosis does not occur because E3L binds and sequesters the virally-produced dsRNA. However, upon infection with VVΔE3L, Noxa becomes activated in response to dsRNA, which is no longer bound by E3L, and contributes to apoptosis. In the absence of Noxa to detect dsRNA, this additional pro-apoptotic signal is absent.

that the Noxa BH3-only domain, alone, is capable of activating Bax (119). Accordingly, future experiments will determine whether during VVCop or VV Δ E3L infection Noxa exhibits an interaction with Bax or, possibly, Bak. Similarly, it would be interesting to know if VV infection releases Noxa from its interaction with Mcl-1 or Bcl-2A1 and whether this release correlates with the induction of apoptosis. Because the events at the mitochondria are what ultimately facilitate MOMP and the commitment to apoptosis, it is surprising that more studies have not yet focused on the mechanism Noxa employs to induce apoptosis following virus infection.

Before Noxa can influence events at the mitochondria, however, it may need to be post-translationally activated. A cytoplasmic Noxa mutant lacking its mitochondrial targeting domain is capable of interacting with Bax in the cytoplasm but only after treatment with dsRNA (413). Thus, either Noxa is somehow being activated to bind an inactive Bax and/or Bax is being activated to bind Noxa. In support of the former, a putative dsRNA-binding domain has been identified in the N-terminus of Noxa, suggesting that a direct interaction between dsRNA and Noxa may be responsible for Noxa activation (D. Leaman, personal communication). Interestingly, we observed that Noxa localised around the virus factories during VV Δ E3L infection (Fig. 6.6 & 6.7), placing Noxa in proximity to the excess dsRNA that is produced upon infection with VV Δ E3L. Although only conjecture at this point, it is possible that Noxa interacts with the dsRNA in these cells and that this interaction contributes to the activation of Noxa. Examining the co-localisation of Noxa and dsRNA is a critical and obvious first step in understanding the relationship between the two. Verification of dsRNA-mediated, post-translational activation of Noxa is therefore the goal of future studies.

Regardless of whether or not Noxa is post-translationally activated, it is clear that a large part of its regulation is transcriptional. VSV, sendai virus (SV), EMCV, measles virus (MV), and herpes simplex virus 1 (HSV-1) all increase Noxa expression (157, 257, 413), and we have shown here that VV infection similarly resulted in an upregulation of Noxa protein and transcript (Fig. 6.4 & 6.5). Although we do not know which transcription factors were responsible for VV-induced Noxa upregulation, it has been shown that VSV, SV, MV, and probably EMCV all rely on IRF1/3/7 and CREB to promote Noxa transcription (157, 257, 413). It is possible that VV infection activates Noxa expression in a similar manner; however, it is not necessarily the only way. The *Noxa* gene promoter has response elements for many transcription factors, including p53, and may contain other, as yet unidentified elements (354). Indeed, infection with HSV-1 results in the robust activation of the Noxa promoter independent of the IRF, p53, and CREB response elements (257). Interestingly, dsRNA also results in the upregulation of Noxa dependent on IRF and CREB signalling, perhaps suggesting that the dsRNA produced by VSV, SV, MV, and EMCV—but not HSV-1—triggers the activation of IRF1, 3, or 7 and CREB and the resulting upregulation of Noxa. If this were the case, it would not be surprising if RIG-I or Mda5 proved to be the pattern recognition receptor responsible for recognising dsRNA and inciting the response that eventually results in Noxa upregulation. Notably, however, cells infected with VVCop or VV Δ E3L showed similar levels of Noxa upregulation, even though VV Δ E3L infection appears to produce considerably more dsRNA. These data seem to suggest that VV-induced upregulation of Noxa is mediated by some aspect of infection intrinsic to both VVCop and VV Δ E3L. Further studies are required in order to understand how

VV infection upregulates Noxa, and identification of the relevant transcription factors would be a good place to start.

Our interest in investigating the link between VV Δ E3L infection and apoptosis led us to examine the production of dsRNA during infection (Fig. 6.2). The dramatically increased levels of dsRNA observed during VV Δ E3L infection may help explain why VV Δ E3L was so potently apoptotic, but it is unclear why so much dsRNA was being produced in the first place. One possible, albeit unsatisfying, explanation is that the amount of dsRNA produced during infection is similar for VVCop, VV Δ F1L, and VV Δ E3L but that in the former two cases the presence of E3L bound to the dsRNA obstructed antibody binding. Further investigation using multiple methods will be necessary to rule out this explanation and identify others. In retrospect, it was not surprising to find the dsRNA localised around the virus factories (Fig. 6.3), given that virus factories serve as the sites of viral transcription implicated in the ultimate production of dsRNA (316). In general, this observation agrees with a previous report by Katsafanas and Moss, who showed the localisation of viral mRNA in and around virus factories (225). To our knowledge, however, this is the first time that the distribution of VV dsRNA has been examined and found to be proximal to virus factories. That this phenomenon appears to be more pronounced during VV Δ E3L infection, as opposed to VVCop or VV Δ F1L infection, is probably related to the increased production (or, as discussed, detection) of dsRNA in VV Δ E3L-infected cells and/or the obviously different architecture of the VV Δ E3L virus factories. The virus factories produced by VV Δ E3L appeared denser, more numerous, and scattered throughout the cytoplasm compared to those produced by either VVCop or VV Δ F1L. Perhaps a greater number of dense virus factories correspondingly increases the quantity and density of the dsRNA produced,

making it easier to visualise. Notably, in cases where dsRNA was detectable in cells infected with VVCop or VV Δ F1L it appeared proximal to the larger and more diffuse factories produced by these viruses, suggesting that the localisation of dsRNA may be similar regardless of the presence of E3L. Why many small virus factories were visible in VV Δ E3L-infected cells in the first place is not apparent. It is worth noting that the number of virus factories per cell roughly corresponded to the MOI of the infection, perhaps implying that the merger of individually derived virus factories into one larger virus factory—a phenomenon that has been reported for VV (225)—is prevented or delayed in the absence of E3L.

There are several additional experiments that will need to be performed in order to fully understand the preliminary observations made in this study. Importantly, a more in-depth analysis of the involvement of E3L is required. The localisation of E3L was not addressed in this study, although E3L has been observed by others to be localised within the nucleus (485), diffusely throughout the cytoplasm (457), and within and around the virus factories (225). Future experiments will determine whether E3L co-localises with dsRNA, as we would predict, or Noxa, which, like E3L, may also be a dsRNA-binding protein. Furthermore, can transiently over-expressed E3L inhibit apoptosis in response to dsRNA treatment in the presence and/or absence of Noxa? Knowing the answer to this question might help address the mechanism of Noxa activation. Additional experiments must also be performed to address the role of PKR, which is undoubtedly active during VV Δ E3L infection (143). PKR-deficient cells infected with VV Δ E3L undergo considerably less apoptosis (494), and it would be interesting to determine whether the contribution that Noxa makes to VV-induced apoptosis is still observable or perhaps even more pronounced in the absence of PKR. It would also be interesting to examine the production and localisation of

dsRNA and the morphology of VV Δ E3L virus factories in a PKR-deficient context. The role of dsRNA could be further assessed using a temperature-sensitive VV mutant that loses the activity of A18R, a helicase that limits VV transcript elongation, and produces excess dsRNA at the restrictive temperature (254, 477). Such a virus would be useful because E3L would still be present.

Despite the preliminary nature of this study, our data, and data obtained during MVA infection (137), suggest a model in which Noxa contributes to the induction of apoptosis by VV (Fig. 7.5). Upon VV Δ E3L infection, Noxa expression is upregulated and dsRNA accumulates around the virus factories. Noxa is then recruited to the virus factories by an interaction with dsRNA, whereupon it becomes post-translationally activated. Activated Noxa is then able to promote the induction of apoptosis at the mitochondria, possibly through a direct interaction with Bax. Similar events likely occur during the course of infection with WT virus, but this is currently a matter of speculation. Surprisingly, F1L appears incapable of inhibiting the apoptosis induced by VV Δ E3L infection. The reason for this is unclear, although it may be that E3L and F1L inhibit separate but parallel signalling pathways that both lead to apoptosis. F1L is unable to interact with Noxa (L. Banadyga, unpublished data) and does not interact with Bax, so perhaps the Noxa-mediated activation of Bax is beyond the inhibitory capabilities of F1L. Such an idea, while captivating, is highly speculative. Although Noxa appears to be playing an important and interesting role in the apoptotic response to VV, further investigation is required.

7.3. SUMMARY

The neat and orderly removal of surplus, damaged, infected, or otherwise unwanted cells appears, at first glance, to be a relatively simple physiological

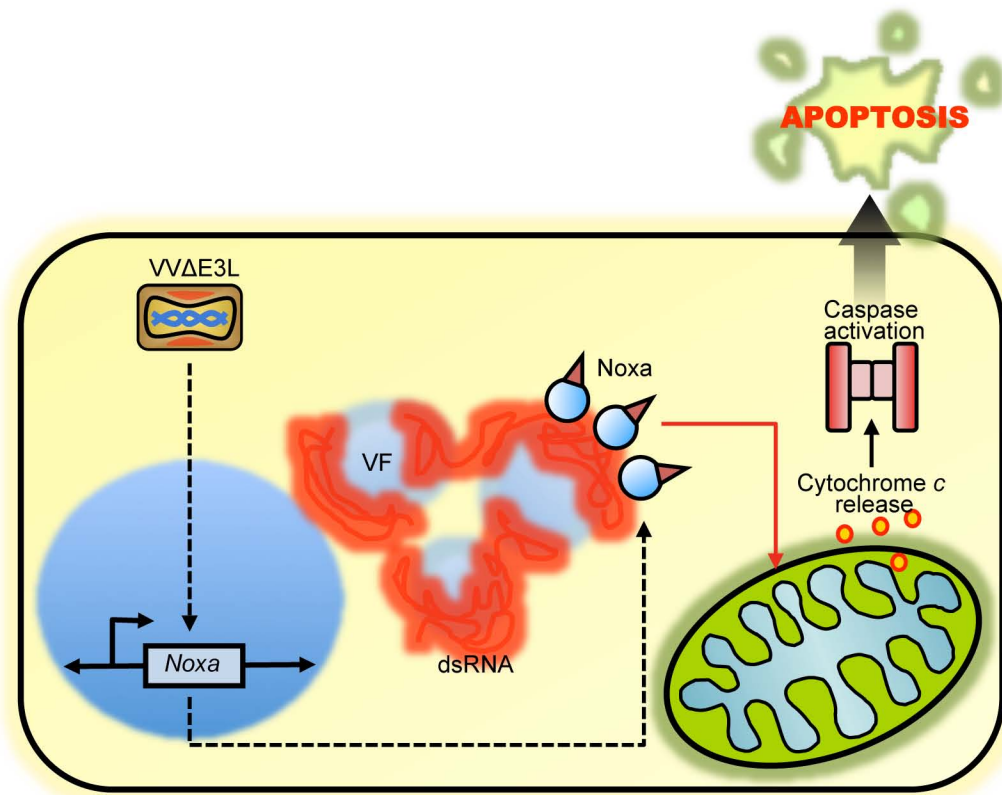


Figure 7.5. Noxa contributes to vaccinia virus-induced apoptosis. Our data support a preliminary model in which Noxa contributes to the induction of apoptosis by VV. Upon VVΔE3L infection, Noxa expression is upregulated and dsRNA accumulates around the virus factories. Noxa may be recruited to a location proximal to the virus factories by an interaction with dsRNA, whereupon binding to dsRNA post-translationally activates Noxa. Activated Noxa would then be able to promote the induction of apoptosis at the mitochondria, possibly through a direct interaction with Bax.

process. Over the past several decades, however, we have been routinely humbled by the vast, complex, and peculiar signalling pathways that regulate apoptosis. The Bcl-2 family of proteins, in particular, and their ability to control the fate of the cell have proven both fascinating and frustrating to study. Although we understand how the Bcl-2 family regulates apoptosis in general terms, we are only now beginning to comprehend how these proteins function at the molecular level. And it is only with such a detailed understanding of apoptosis that we can hope, in turn, to understand the diseases, such as cancer, that are caused by apoptotic dysfunction.

Perhaps no one “understands” the intricacies of apoptosis better than the viruses that must thwart it in order to survive. Poxviruses encode numerous different proteins that all inhibit apoptosis at the mitochondria but do so by interfering with the Bcl-2 family of proteins in slightly different ways. Here we have characterised two poxviral vBcl-2 proteins, FPV039, encoded by fowlpox virus, and DPV022, encoded by deerpox virus. It is our hope and belief that these and other vBcl-2 proteins can be used as tools to further dissect the cellular signalling pathways that govern cell death, particularly those culminating in the activation of Bak and Bax. Accordingly, we have also taken the first steps towards characterising the initial events that trigger apoptosis upon vaccinia virus infection, and with further study we hope to gain a better understanding of the apical signals that instigate apoptosis in the first place. The continued use of poxviruses as model systems to study apoptosis can be expected to contribute invaluablely to our greater scientific appreciation in such matters of life and death.

REFERENCES

1. **Adams, J. M., and S. Cory.** 2001. Life-or-death decisions by the Bcl-2 protein family. *Trends Biochem Sci* **26**:61-6.
2. **Afonso, C. L., G. Delhon, E. R. Tulman, Z. Lu, A. Zsak, V. M. Becerra, L. Zsak, G. F. Kutish, and D. L. Rock.** 2005. Genome of deerpox virus. *J Virol* **79**:966-77.
3. **Afonso, C. L., J. G. Neilan, G. F. Kutish, and D. L. Rock.** 1996. An African swine fever virus Bcl-2 homolog, 5-HL, suppresses apoptotic cell death. *J Virol* **70**:4858-63.
4. **Afonso, C. L., E. R. Tulman, Z. Lu, L. Zsak, G. F. Kutish, and D. L. Rock.** 2000. The genome of fowlpox virus. *J Virol* **74**:3815-31.
5. **Akao, Y., Y. Otsuki, S. Kataoka, Y. Ito, and Y. Tsujimoto.** 1994. Multiple subcellular localization of bcl-2: detection in nuclear outer membrane, endoplasmic reticulum membrane, and mitochondrial membranes. *Cancer Res* **54**:2468-71.
6. **Alcami, A., A. Khanna, N. L. Paul, and G. L. Smith.** 1999. Vaccinia virus strains Lister, USSR and Evans express soluble and cell-surface tumour necrosis factor receptors. *J Gen Virol* **80** (Pt 4):949-59.
7. **Altmann, M., and W. Hammerschmidt.** 2005. Epstein-Barr virus provides a new paradigm: a requirement for the immediate inhibition of apoptosis. *PLoS Biol* **3**:e404.
8. **Annis, M. G., E. L. Soucie, P. J. Dlugosz, J. A. Cruz-Aguado, L. Z. Penn, B. Leber, and D. W. Andrews.** 2005. Bax forms multispinning monomers that oligomerize to permeabilize membranes during apoptosis. *Embo J* **24**:2096-103.
9. **Antonsson, B., F. Conti, A. Ciavatta, S. Montessuit, S. Lewis, I. Martinou, L. Bernasconi, A. Bernard, J. J. Mermoud, G. Mazzei, K. Maundrell, F. Gambale, R. Sadoul, and J. C. Martinou.** 1997. Inhibition of Bax channel-forming activity by Bcl-2. *Science* **277**:370-2.
10. **Antonsson, B., S. Montessuit, S. Lauper, R. Eskes, and J. C. Martinou.** 2000. Bax oligomerization is required for channel-forming activity in liposomes and to trigger cytochrome c release from mitochondria. *Biochem J* **345 Pt 2**:271-8.
11. **Antonsson, B., S. Montessuit, B. Sanchez, and J. C. Martinou.** 2001. Bax is present as a high molecular weight oligomer/complex in the mitochondrial membrane of apoptotic cells. *J Biol Chem* **276**:11615-23.
12. **Aouacheria, A., F. Brunet, and M. Gouy.** 2005. Phylogenomics of life-or-death switches in multicellular animals: Bcl-2, BH3-Only, and BNip families of apoptotic regulators. *Mol Biol Evol* **22**:2395-416.
13. **Aoyagi, M., D. Zhai, C. Jin, A. E. Aleshin, B. Stec, J. C. Reed, and R. C. Liddington.** 2007. Vaccinia virus N1L protein resembles a B cell lymphoma-2 (Bcl-2) family protein. *Protein Sci* **16**:118-24.
14. **Arnoult, D., L. M. Bartle, A. Skaletskaya, D. Poncet, N. Zamzami, P. U. Park, J. Sharpe, R. J. Youle, and V. S. Goldmacher.** 2004. Cytomegalovirus cell death suppressor vMIA blocks Bax- but not Bak-mediated apoptosis by binding and sequestering Bax at mitochondria. *Proc Natl Acad Sci U S A* **101**:7988-93.
15. **Arnoult, D., A. Skaletskaya, J. Estaquier, C. Dufour, and V. S. Goldmacher.** 2008. The murine cytomegalovirus cell death suppressor m38.5 binds Bax and blocks Bax-mediated mitochondrial outer membrane permeabilization. *Apoptosis* **13**:1100-10.

16. **Bae, J., C. P. Leo, S. Y. Hsu, and A. J. Hsueh.** 2000. MCL-1S, a splicing variant of the antiapoptotic BCL-2 family member MCL-1, encodes a proapoptotic protein possessing only the BH3 domain. *J Biol Chem* **275**:25255-61.
17. **Baglioni, C., M. A. Minks, and P. A. Maroney.** 1978. Interferon action may be mediated by activation of a nuclease by pppA2'p5'A2'p5'A. *Nature* **273**:684-7.
18. **Baines, C. P., R. A. Kaiser, N. H. Purcell, N. S. Blair, H. Osinska, M. A. Hambleton, E. W. Brunskill, M. R. Sayen, R. A. Gottlieb, G. W. Dorn, J. Robbins, and J. D. Molkentin.** 2005. Loss of cyclophilin D reveals a critical role for mitochondrial permeability transition in cell death. *Nature* **434**:658-62.
19. **Baines, C. P., R. A. Kaiser, T. Sheiko, W. J. Craigen, and J. D. Molkentin.** 2007. Voltage-dependent anion channels are dispensable for mitochondrial-dependent cell death. *Nat Cell Biol* **9**:550-5.
20. **Bakhshi, A., J. P. Jensen, P. Goldman, J. J. Wright, O. W. McBride, A. L. Epstein, and S. J. Korsmeyer.** 1985. Cloning the chromosomal breakpoint of t(14;18) human lymphomas: clustering around JH on chromosome 14 and near a transcriptional unit on 18. *Cell* **41**:899-906.
21. **Baksh, S., S. Tommasi, S. Fenton, V. C. Yu, L. M. Martins, G. P. Pfeifer, F. Latif, J. Downward, and B. G. Neel.** 2005. The tumor suppressor RASSF1A and MAP-1 link death receptor signaling to Bax conformational change and cell death. *Mol Cell* **18**:637-50.
22. **Balachandran, S., C. N. Kim, W. C. Yeh, T. W. Mak, K. Bhalla, and G. N. Barber.** 1998. Activation of the dsRNA-dependent protein kinase, PKR, induces apoptosis through FADD-mediated death signaling. *EMBO J* **17**:6888-902.
23. **Balachandran, S., P. C. Roberts, L. E. Brown, H. Truong, A. K. Pattnaik, D. R. Archer, and G. N. Barber.** 2000. Essential role for the dsRNA-dependent protein kinase PKR in innate immunity to viral infection. *Immunity* **13**:129-41.
24. **Barry, M., and R. C. Bleackley.** 2002. Cytotoxic T lymphocytes: all roads lead to death. *Nat Rev Immunol* **2**:401-9.
25. **Barry, M., J. A. Heibin, M. J. Pinkoski, S. F. Lee, R. W. Moyer, D. R. Green, and R. C. Bleackley.** 2000. Granzyme B short-circuits the need for caspase 8 activity during granule-mediated cytotoxic T-lymphocyte killing by directly cleaving Bid. *Mol Cell Biol* **20**:3781-94.
26. **Barry, M., S. T. Wasilenko, T. L. Stewart, and J. M. Taylor.** 2004. Apoptosis regulator genes encoded by poxviruses. *Prog Mol Subcell Biol* **36**:19-37.
27. **Bartlett, N., J. A. Symons, D. C. Tschärke, and G. L. Smith.** 2002. The vaccinia virus N1L protein is an intracellular homodimer that promotes virulence. *J Gen Virol* **83**:1965-76.
28. **Basanez, G., A. Nechushtan, O. Drozhinin, A. Chanturiya, E. Choe, S. Tutt, K. A. Wood, Y. Hsu, J. Zimmerberg, and R. J. Youle.** 1999. Bax, but not Bcl-xL, decreases the lifetime of planar phospholipid bilayer membranes at subnanomolar concentrations. *Proc Natl Acad Sci U S A* **96**:5492-7.
29. **Basanez, G., J. C. Sharpe, J. Galanis, T. B. Brandt, J. M. Hardwick, and J. Zimmerberg.** 2002. Bax-type apoptotic proteins porate pure lipid

- bilayers through a mechanism sensitive to intrinsic monolayer curvature. *J Biol Chem* **277**:49360-5.
30. **Basanez, G., J. Zhang, B. N. Chau, G. I. Maksaev, V. A. Frolov, T. A. Brandt, J. Burch, J. M. Hardwick, and J. Zimmerberg.** 2001. Pro-apoptotic cleavage products of Bcl-xL form cytochrome c-conducting pores in pure lipid membranes. *J Biol Chem* **276**:31083-91.
 31. **Beattie, E., K. L. Denzler, J. Tartaglia, M. E. Perkus, E. Paoletti, and B. L. Jacobs.** 1995. Reversal of the interferon-sensitive phenotype of a vaccinia virus lacking E3L by expression of the reovirus S4 gene. *J Virol* **69**:499-505.
 32. **Beattie, E., E. B. Kauffman, H. Martinez, M. E. Perkus, B. L. Jacobs, E. Paoletti, and J. Tartaglia.** 1996. Host-range restriction of vaccinia virus E3L-specific deletion mutants. *Virus Genes* **12**:89-94.
 33. **Bellows, D. S., B. N. Chau, P. Lee, Y. Lazebnik, W. H. Burns, and J. M. Hardwick.** 2000. Antiapoptotic herpesvirus Bcl-2 homologs escape caspase-mediated conversion to proapoptotic proteins. *J Virol* **74**:5024-31.
 34. **Bellows, D. S., M. Howell, C. Pearson, S. A. Hazlewood, and J. M. Hardwick.** 2002. Epstein-Barr virus BALF1 is a BCL-2-like antagonist of the herpesvirus antiapoptotic BCL-2 proteins. *J Virol* **76**:2469-79.
 35. **Benedict, C. A., P. S. Norris, and C. F. Ware.** 2002. To kill or be killed: viral evasion of apoptosis. *Nat Immunol* **3**:1013-8.
 36. **Bertin, J., R. C. Armstrong, S. Otilie, D. A. Martin, Y. Wang, S. Banks, G. H. Wang, T. G. Senkevich, E. S. Alnemri, B. Moss, M. J. Lenardo, K. J. Tomaselli, and J. I. Cohen.** 1997. Death effector domain-containing herpesvirus and poxvirus proteins inhibit both Fas- and TNFR1-induced apoptosis. *Proc Natl Acad Sci U S A* **94**:1172-6.
 37. **Beukema, E. L., M. P. Brown, and J. D. Hayball.** 2006. The potential role of fowlpox virus in rational vaccine design. *Expert Rev Vaccines* **5**:565-77.
 38. **Bildfell, R. J., K. A. Thompson, M. Moerdyk-Schauwecker, L. Jin, P. L. Wolff, and C. M. Gillin.** 2010. Experimental deerpox infection in black-tailed deer (*Odocoileus hemionus columbianus*). *J Wildl Dis* **46**:33-45.
 39. **Billen, L. P., C. L. Kokoski, J. F. Lovell, B. Leber, and D. W. Andrews.** 2008. Bcl-XL inhibits membrane permeabilization by competing with Bax. *PLoS Biol* **6**:e147.
 40. **Birnbaum, M. J., R. J. Clem, and L. K. Miller.** 1994. An apoptosis-inhibiting gene from a nuclear polyhedrosis virus encoding a polypeptide with Cys/His sequence motifs. *J Virol* **68**:2521-8.
 41. **Blasco, R., N. B. Cole, and B. Moss.** 1991. Sequence analysis, expression, and deletion of a vaccinia virus gene encoding a homolog of profilin, a eukaryotic actin-binding protein. *J Virol* **65**:4598-608.
 42. **Bleicken, S., M. Classen, P. V. Padmavathi, T. Ishikawa, K. Zeth, H. J. Steinhoff, and E. Bordignon.** 2010. Molecular details of Bax activation, oligomerization, and membrane insertion. *J Biol Chem* **285**:6636-47.
 43. **Bogner, C., B. Leber, and D. W. Andrews.** 2010. Apoptosis: embedded in membranes. *Curr Opin Cell Biol* **22**:1-7.
 44. **Boise, L. H., M. Gonzalez-Garcia, C. E. Postema, L. Ding, T. Lindsten, L. A. Turka, X. Mao, G. Nunez, and C. B. Thompson.** 1993. bcl-x, a bcl-2-related gene that functions as a dominant regulator of apoptotic cell death. *Cell* **74**:597-608.

45. **Boldin, M. P., T. M. Goncharov, Y. V. Goltsev, and D. Wallach.** 1996. Involvement of MACH, a novel MORT1/FADD-interacting protease, in Fas/APO-1- and TNF receptor-induced cell death. *Cell* **85**:803-15.
46. **Boone, R. F., R. P. Parr, and B. Moss.** 1979. Intermolecular duplexes formed from polyadenylylated vaccinia virus RNA. *J Virol* **30**:365-74.
47. **Borgese, N., S. Colombo, and E. Pedrazzini.** 2003. The tale of tail-anchored proteins: coming from the cytosol and looking for a membrane. *J Cell Biol* **161**:1013-9.
48. **Boulakia, C. A., G. Chen, F. W. Ng, J. G. Teodoro, P. E. Branton, D. W. Nicholson, G. G. Poirier, and G. C. Shore.** 1996. Bcl-2 and adenovirus E1B 19 kDa protein prevent E1A-induced processing of CPP32 and cleavage of poly(ADP-ribose) polymerase. *Oncogene* **12**:529-35.
49. **Boyd, J. M., G. J. Gallo, B. Elangovan, A. B. Houghton, S. Malstrom, B. J. Avery, R. G. Ebb, T. Subramanian, T. Chittenden, R. J. Lutz, and et al.** 1995. Bik, a novel death-inducing protein shares a distinct sequence motif with Bcl-2 family proteins and interacts with viral and cellular survival-promoting proteins. *Oncogene* **11**:1921-8.
50. **Brandt, T. A., and B. L. Jacobs.** 2001. Both carboxy- and amino-terminal domains of the vaccinia virus interferon resistance gene, E3L, are required for pathogenesis in a mouse model. *J Virol* **75**:850-6.
51. **Brun, A., C. Rivas, M. Esteban, J. M. Escribano, and C. Alonso.** 1996. African swine fever virus gene A179L, a viral homologue of bcl-2, protects cells from programmed cell death. *Virology* **225**:227-30.
52. **Cam, M., W. Handke, M. Picard-Maureau, and W. Brune.** 2010. Cytomegaloviruses inhibit Bak- and Bax-mediated apoptosis with two separate viral proteins. *Cell Death Differ* **17**:655-65.
53. **Campbell, S., B. Hazes, M. Kvansakul, P. Colman, and M. Barry.** 2010. Vaccinia virus F1L interacts with Bak using highly divergent Bcl-2 homology domains and replaces the function of Mcl-1. *J Biol Chem* **285**:4695-708.
54. **Cartron, P. F., H. Arokium, L. Oliver, K. Meflah, S. Manon, and F. M. Vallette.** 2005. Distinct domains control the addressing and the insertion of Bax into mitochondria. *J Biol Chem* **280**:10587-98.
55. **Cartron, P. F., T. Gallenne, G. Bougras, F. Gautier, F. Manero, P. Vusio, K. Meflah, F. M. Vallette, and P. Juin.** 2004. The first alpha helix of Bax plays a necessary role in its ligand-induced activation by the BH3-only proteins Bid and PUMA. *Mol Cell* **16**:807-18.
56. **Certo, M., V. Del Gaizo Moore, M. Nishino, G. Wei, S. Korsmeyer, S. A. Armstrong, and A. Letai.** 2006. Mitochondria primed by death signals determine cellular addiction to antiapoptotic BCL-2 family members. *Cancer Cell* **9**:351-65.
57. **Chakrabarti, S., J. R. Sisler, and B. Moss.** 1997. Compact, synthetic, vaccinia virus early/late promoter for protein expression. *Biotechniques* **23**:1094-7.
58. **Chang, H. W., and B. L. Jacobs.** 1993. Identification of a conserved motif that is necessary for binding of the vaccinia virus E3L gene products to double-stranded RNA. *Virology* **194**:537-47.
59. **Chang, H. W., J. C. Watson, and B. L. Jacobs.** 1992. The E3L gene of vaccinia virus encodes an inhibitor of the interferon-induced, double-

- stranded RNA-dependent protein kinase. *Proc Natl Acad Sci U S A* **89**:4825-9.
60. **Chattopadhyay, S., J. T. Marques, M. Yamashita, K. L. Peters, K. Smith, A. Desai, B. R. Williams, and G. C. Sen.** 2010. Viral apoptosis is induced by IRF-3-mediated activation of Bax. *EMBO J* **29**:1762-73.
61. **Cheevers, W. P., D. J. O'Callaghan, and C. C. Randall.** 1968. Biosynthesis of host and viral deoxyribonucleic acid during hyperplastic fowlpox infection in vivo. *J Virol* **2**:421-9.
62. **Cheevers, W. P., and C. C. Randall.** 1968. Viral and cellular growth and sequential increase of protein and DNA during fowlpox infection in vivo (32700). *Proc Soc Exp Biol Med* **127**:401-5.
63. **Chen, G., P. E. Branton, E. Yang, S. J. Korsmeyer, and G. C. Shore.** 1996. Adenovirus E1B 19-kDa death suppressor protein interacts with Bax but not with Bad. *J Biol Chem* **271**:24221-5.
64. **Chen, L., S. N. Willis, A. Wei, B. J. Smith, J. I. Fletcher, M. G. Hinds, P. M. Colman, C. L. Day, J. M. Adams, and D. C. Huang.** 2005. Differential targeting of prosurvival Bcl-2 proteins by their BH3-only ligands allows complementary apoptotic function. *Mol Cell* **17**:393-403.
65. **Chen-Levy, Z., and M. L. Cleary.** 1990. Membrane topology of the Bcl-2 proto-oncogenic protein demonstrated in vitro. *J Biol Chem* **265**:4929-33.
66. **Cheng, E. H., D. G. Kirsch, R. J. Clem, R. Ravi, M. B. Kastan, A. Bedi, K. Ueno, and J. M. Hardwick.** 1997. Conversion of Bcl-2 to a Bax-like death effector by caspases. *Science* **278**:1966-8.
67. **Cheng, E. H., J. Nicholas, D. S. Bellows, G. S. Hayward, H. G. Guo, M. S. Reitz, and J. M. Hardwick.** 1997. A Bcl-2 homolog encoded by Kaposi sarcoma-associated virus, human herpesvirus 8, inhibits apoptosis but does not heterodimerize with Bax or Bak. *Proc Natl Acad Sci U S A* **94**:690-4.
68. **Cheng, E. H., T. V. Sheiko, J. K. Fisher, W. J. Craigen, and S. J. Korsmeyer.** 2003. VDAC2 inhibits BAK activation and mitochondrial apoptosis. *Science* **301**:513-7.
69. **Cheng, E. H., M. C. Wei, S. Weiler, R. A. Flavell, T. W. Mak, T. Lindsten, and S. J. Korsmeyer.** 2001. BCL-2, BCL-X(L) sequester BH3 domain-only molecules preventing BAX- and BAK-mediated mitochondrial apoptosis. *Mol Cell* **8**:705-11.
70. **Chinnaiyan, A. M., K. O'Rourke, M. Tewari, and V. M. Dixit.** 1995. FADD, a novel death domain-containing protein, interacts with the death domain of Fas and initiates apoptosis. *Cell* **81**:505-12.
71. **Chinnaiyan, A. M., C. G. Tepper, M. F. Seldin, K. O'Rourke, F. C. Kischkel, S. Hellbardt, P. H. Krammer, M. E. Peter, and V. M. Dixit.** 1996. FADD/MORT1 is a common mediator of CD95 (Fas/APO-1) and tumor necrosis factor receptor-induced apoptosis. *J Biol Chem* **271**:4961-5.
72. **Chiou, S. K., C. C. Tseng, L. Rao, and E. White.** 1994. Functional complementation of the adenovirus E1B 19-kilodalton protein with Bcl-2 in the inhibition of apoptosis in infected cells. *J Virol* **68**:6553-66.
73. **Chipuk, J. E., and D. R. Green.** 2008. How do BCL-2 proteins induce mitochondrial outer membrane permeabilization? *Trends Cell Biol* **18**:157-64.
74. **Chipuk, J. E., T. Kuwana, L. Bouchier-Hayes, N. M. Droin, D. D. Newmeyer, M. Schuler, and D. R. Green.** 2004. Direct activation of Bax

- by p53 mediates mitochondrial membrane permeabilization and apoptosis. *Science* **303**:1010-4.
75. **Chipuk, J. E., T. Moldoveanu, F. Llambi, M. J. Parsons, and D. R. Green.** 2010. The BCL-2 family reunion. *Mol Cell* **37**:299-310.
 76. **Chittenden, T., E. A. Harrington, R. O'Connor, C. Flemington, R. J. Lutz, G. I. Evan, and B. C. Guild.** 1995. Induction of apoptosis by the Bcl-2 homologue Bak. *Nature* **374**:733-6.
 77. **Choi, S. S., I. C. Park, J. W. Yun, Y. C. Sung, S. I. Hong, and H. S. Shin.** 1995. A novel Bcl-2 related gene, Bfl-1, is overexpressed in stomach cancer and preferentially expressed in bone marrow. *Oncogene* **11**:1693-8.
 78. **Chou, J. J., H. Li, G. S. Salvesen, J. Yuan, and G. Wagner.** 1999. Solution structure of BID, an intracellular amplifier of apoptotic signaling. *Cell* **96**:615-24.
 79. **Cleary, M. L., and J. Sklar.** 1985. Nucleotide sequence of a t(14;18) chromosomal breakpoint in follicular lymphoma and demonstration of a breakpoint-cluster region near a transcriptionally active locus on chromosome 18. *Proc Natl Acad Sci U S A* **82**:7439-43.
 80. **Cleary, M. L., S. D. Smith, and J. Sklar.** 1986. Cloning and structural analysis of cDNAs for bcl-2 and a hybrid bcl-2/immunoglobulin transcript resulting from the t(14;18) translocation. *Cell* **47**:19-28.
 81. **Clem, R. J., E. H. Cheng, C. L. Karp, D. G. Kirsch, K. Ueno, A. Takahashi, M. B. Kastan, D. E. Griffin, W. C. Earnshaw, M. A. Veluona, and J. M. Hardwick.** 1998. Modulation of cell death by Bcl-XL through caspase interaction. *Proc Natl Acad Sci U S A* **95**:554-9.
 82. **Clemens, M. J., and B. R. Williams.** 1978. Inhibition of cell-free protein synthesis by pppA2'p5'A2'p5'A: a novel oligonucleotide synthesized by interferon-treated L cell extracts. *Cell* **13**:565-72.
 83. **Colby, C., and P. H. Duesberg.** 1969. Double-stranded RNA in vaccinia virus infected cells. *Nature* **222**:940-4.
 84. **Colby, C., C. Jurale, and J. R. Kates.** 1971. Mechanism of synthesis of vaccinia virus double-stranded ribonucleic acid in vivo and in vitro. *J Virol* **7**:71-6.
 85. **Cole, C., J. D. Barber, and G. J. Barton.** 2008. The Jpred 3 secondary structure prediction server. *Nucleic Acids Res* **36**:W197-201.
 86. **Condit, R. C., N. Moussatche, and P. Traktman.** 2006. In a nutshell: structure and assembly of the vaccinia virion. *Adv Virus Res* **66**:31-124.
 87. **Conradt, B., and H. R. Horvitz.** 1998. The *C. elegans* protein EGL-1 is required for programmed cell death and interacts with the Bcl-2-like protein CED-9. *Cell* **93**:519-29.
 88. **Consortium, I. C. G. S.** 2004. Sequence and comparative analysis of the chicken genome provide unique perspectives on vertebrate evolution. *Nature* **432**:695-716.
 89. **Cooray, S., M. W. Bahar, N. G. Abrescia, C. E. McVey, N. W. Bartlett, R. A. Chen, D. I. Stuart, J. M. Grimes, and G. L. Smith.** 2007. Functional and structural studies of the vaccinia virus virulence factor N1 reveal a Bcl-2-like anti-apoptotic protein. *J Gen Virol* **88**:1656-66.
 90. **Cory, S., D. C. Huang, and J. M. Adams.** 2003. The Bcl-2 family: roles in cell survival and oncogenesis. *Oncogene* **22**:8590-607.

91. **Coultas, L., D. C. Huang, J. M. Adams, and A. Strasser.** 2002. Pro-apoptotic BH3-only Bcl-2 family members in vertebrate model organisms suitable for genetic experimentation. *Cell Death Differ* **9**:1163-6.
92. **Cross, J. R., A. Postigo, K. Blight, and J. Downward.** 2008. Viral pro-survival proteins block separate stages in Bax activation but changes in mitochondrial ultrastructure still occur. *Cell Death Differ* **15**:997-1008.
93. **Cuconati, A., K. Degenhardt, R. Sundararajan, A. Ansel, and E. White.** 2002. Bak and Bax function to limit adenovirus replication through apoptosis induction. *J Virol* **76**:4547-58.
94. **Cuconati, A., C. Mukherjee, D. Perez, and E. White.** 2003. DNA damage response and MCL-1 destruction initiate apoptosis in adenovirus-infected cells. *Genes Dev* **17**:2922-32.
95. **Cuconati, A., and E. White.** 2002. Viral homologs of BCL-2: role of apoptosis in the regulation of virus infection. *Genes Dev* **16**:2465-78.
96. **Czabotar, P. E., P. M. Colman, and D. C. Huang.** 2009. Bax activation by Bim? *Cell Death Differ* **16**:1187-91.
97. **Damon, I.** 2007. Poxviruses. *In* D. M. Knipe and P. M. Howley (ed.), *Fields Virology*, 5th ed, vol. II. Lippincott Williams & Wilkins, Philadelphia, PA.
98. **Danial, N. N., and S. J. Korsmeyer.** 2004. Cell death: critical control points. *Cell* **116**:205-19.
99. **Day, C. L., L. Chen, S. J. Richardson, P. J. Harrison, D. C. Huang, and M. G. Hinds.** 2005. Solution structure of prosurvival Mcl-1 and characterization of its binding by proapoptotic BH3-only ligands. *J Biol Chem* **280**:4738-44.
100. **Degenhardt, K., R. Sundararajan, T. Lindsten, C. Thompson, and E. White.** 2002. Bax and Bak independently promote cytochrome C release from mitochondria. *J Biol Chem* **277**:14127-34.
101. **Dejean, L. M., S. Martinez-Caballero, L. Guo, C. Hughes, O. Teijido, T. Ducret, F. Ichas, S. J. Korsmeyer, B. Antonsson, E. A. Jonas, and K. W. Kinnally.** 2005. Oligomeric Bax is a component of the putative cytochrome c release channel MAC, mitochondrial apoptosis-induced channel. *Mol Biol Cell* **16**:2424-32.
102. **Deng, L., P. Dai, W. Ding, R. D. Granstein, and S. Shuman.** 2006. Vaccinia virus infection attenuates innate immune responses and antigen presentation by epidermal dendritic cells. *J Virol* **80**:9977-87.
103. **Denisov, A. Y., M. S. Madiraju, G. Chen, A. Khadir, P. Beauparlant, G. Attardo, G. C. Shore, and K. Gehring.** 2003. Solution structure of human BCL-w: modulation of ligand binding by the C-terminal helix. *J Biol Chem* **278**:21124-8.
104. **Desagher, S., A. Osen-Sand, A. Nichols, R. Eskes, S. Montessuit, S. Lauper, K. Maundrell, B. Antonsson, and J. C. Martinou.** 1999. Bid-induced conformational change of Bax is responsible for mitochondrial cytochrome c release during apoptosis. *J Cell Biol* **144**:891-901.
105. **Desbien, A. L., J. W. Kappler, and P. Marrack.** 2009. The Epstein-Barr virus Bcl-2 homolog, BHRF1, blocks apoptosis by binding to a limited amount of Bim. *Proc Natl Acad Sci U S A* **106**:5663-8.
106. **Deveraux, Q. L., R. Takahashi, G. S. Salvesen, and J. C. Reed.** 1997. X-linked IAP is a direct inhibitor of cell-death proteases. *Nature* **388**:300-4.

107. **Dewson, G., and R. M. Kluck.** 2009. Mechanisms by which Bak and Bax permeabilise mitochondria during apoptosis. *J Cell Sci* **122**:2801-8.
108. **Dewson, G., T. Kratina, P. Czabotar, C. L. Day, J. M. Adams, and R. M. Kluck.** 2009. Bak activation for apoptosis involves oligomerization of dimers via their alpha6 helices. *Mol Cell* **36**:696-703.
109. **Dewson, G., T. Kratina, H. W. Sim, H. Puthalakath, J. M. Adams, P. M. Colman, and R. M. Kluck.** 2008. To trigger apoptosis, Bak exposes its BH3 domain and homodimerizes via BH3:groove interactions. *Mol Cell* **30**:369-80.
110. **Dey, M., C. Cao, A. C. Dar, T. Tamura, K. Ozato, F. Sicheri, and T. E. Dever.** 2005. Mechanistic link between PKR dimerization, autophosphorylation, and eIF2alpha substrate recognition. *Cell* **122**:901-13.
111. **Diaz-Gil, G., F. Gomez-Esquer, D. Agudo, J. Delcan, F. Martinez-Arribas, C. Rivas, J. Schneider, M. A. Palomar, and R. Linares.** 2006. Characterization of a human Bid homologue protein from *Gallus gallus*. *Gene* **372**:26-32.
112. **Dijkers, P. F., R. H. Medema, J. W. Lammers, L. Koenderman, and P. J. Coffe.** 2000. Expression of the pro-apoptotic Bcl-2 family member Bim is regulated by the forkhead transcription factor FKHR-L1. *Curr Biol* **10**:1201-4.
113. **Ding, J., Z. Zhang, G. J. Roberts, M. Falcone, Y. Miao, Y. Shao, X. C. Zhang, D. W. Andrews, and J. Lin.** 2010. Bcl-2 and Bax interact via the BH1-3 groove-BH3 motif interface and a novel interface involving the BH4 motif. *J Biol Chem* **285**:28749-63.
114. **DiPerna, G., J. Stack, A. G. Bowie, A. Boyd, G. Kotwal, Z. Zhang, S. Arvikar, E. Latz, K. A. Fitzgerald, and W. L. Marshall.** 2004. Poxvirus protein N1L targets the I-kappaB kinase complex, inhibits signaling to NF-kappaB by the tumor necrosis factor superfamily of receptors, and inhibits NF-kappaB and IRF3 signaling by toll-like receptors. *J Biol Chem* **279**:36570-8.
115. **Dlugosz, P. J., L. P. Billen, M. G. Annis, W. Zhu, Z. Zhang, J. Lin, B. Leber, and D. W. Andrews.** 2006. Bcl-2 changes conformation to inhibit Bax oligomerization. *Embo J* **25**:2287-96.
116. **Dobbelstein, M., and T. Shenk.** 1996. Protection against apoptosis by the vaccinia virus SPI-2 (B13R) gene product. *J Virol* **70**:6479-85.
117. **Douglas, A. E., K. D. Corbett, J. M. Berger, G. McFadden, and T. M. Handel.** 2007. Structure of M11L: A myxoma virus structural homolog of the apoptosis inhibitor, Bcl-2. *Protein Sci* **16**:695-703.
118. **Du, C., M. Fang, Y. Li, L. Li, and X. Wang.** 2000. Smac, a mitochondrial protein that promotes cytochrome c-dependent caspase activation by eliminating IAP inhibition. *Cell* **102**:33-42.
119. **Du, H., J. Wolf, B. Schafer, T. Moldoveanu, J. E. Chipuk, and T. Kuwana.** 2010. BH3-domains other than Bim and Bid can directly activate BAX/BAK. *J Biol Chem*.
120. **Duckett, C. S., V. E. Nava, R. W. Gedrich, R. J. Clem, J. L. Van Dongen, M. C. Gilfillan, H. Shiels, J. M. Hardwick, and C. B. Thompson.** 1996. A conserved family of cellular genes related to the baculovirus iap gene and encoding apoptosis inhibitors. *EMBO J* **15**:2685-94.

121. **Duesberg, P. H., and C. Colby.** 1969. On the biosynthesis and structure of double-stranded RNA in vaccinia virus-infected cells. *Proc Natl Acad Sci U S A* **64**:396-403.
122. **Dussmann, H., M. Rehm, C. G. Concannon, S. Anguissola, M. Wurstle, S. Kacmar, P. Voller, H. J. Huber, and J. H. Prehn.** 2010. Single-cell quantification of Bax activation and mathematical modelling suggest pore formation on minimal mitochondrial Bax accumulation. *Cell Death Differ* **17**:278-90.
123. **Earl, P. L., B. Moss, L. S. Wyatt, M. W. Carroll.** 1998. Generation of Recombinant Vaccinia Viruses, p. 16.17.1 - 16.17.19. *In* R. B. Frederick M. Ausubel, Robert E. Kingston, David D. Moore, J.G. Seidman, John A. Smith, Kevin Struhl (ed.), *Current Protocols in Molecular Biology*. John Wiley and Sons Inc., New York, N. Y.
124. **Eckelman, B. P., G. S. Salvesen, and F. L. Scott.** 2006. Human inhibitor of apoptosis proteins: why XIAP is the black sheep of the family. *EMBO Rep* **7**:988-94.
125. **Ehrenberg, B., V. Montana, M. D. Wei, J. P. Wuskell, and L. M. Loew.** 1988. Membrane potential can be determined in individual cells from the nernstian distribution of cationic dyes. *Biophys J* **53**:785-94.
126. **Eskes, R., S. Desagher, B. Antonsson, and J. C. Martinou.** 2000. Bid induces the oligomerization and insertion of Bax into the outer mitochondrial membrane. *Mol Cell Biol* **20**:929-35.
127. **Esposito, J. J., and F. Fenner.** 2001. Poxviruses. *In* D. M. Knipe and P. M. Howley (ed.), *Fields Virology*, 4th ed, vol. II. Lippincott Williams & Wilkins, Philadelphia, PA.
128. **Everett, H., M. Barry, S. F. Lee, X. Sun, K. Graham, J. Stone, R. C. Bleackley, and G. McFadden.** 2000. M11L: a novel mitochondria-localized protein of myxoma virus that blocks apoptosis of infected leukocytes. *J Exp Med* **191**:1487-98.
129. **Everett, H., M. Barry, X. Sun, S. F. Lee, C. Frantz, L. G. Berthiaume, G. McFadden, and R. C. Bleackley.** 2002. The myxoma poxvirus protein, M11L, prevents apoptosis by direct interaction with the mitochondrial permeability transition pore. *J Exp Med* **196**:1127-39.
130. **Farrell, P. J., K. Balkow, T. Hunt, R. J. Jackson, and H. Trachsel.** 1977. Phosphorylation of initiation factor eIF-2 and the control of reticulocyte protein synthesis. *Cell* **11**:187-200.
131. **Farrow, S. N., J. H. White, I. Martinou, T. Raven, K. T. Pun, C. J. Grinham, J. C. Martinou, and R. Brown.** 1995. Cloning of a bcl-2 homologue by interaction with adenovirus E1B 19K. *Nature* **374**:731-3.
132. **Felsenstein, J.** 2004. PHYLIP (Phylogeny Inference Package) version 3.6. Distributed by the author. Department of Genome Sciences, University of Washington, Seattle.
133. **Fenner, F., and B. M. Comben.** 1958. [Genetic studies with mammalian poxviruses. I. Demonstration of recombination between two strains of vaccina virus.]. *Virology* **5**:530-48.
134. **Fenner, F., D. A. Henderson, I. Arita, Z. Jezek, and I. D. Ladnyi.** 1988. Smallpox and Its Eradication. World Health Organization, Geneva.
135. **Fernandez, Y., M. Verhaegen, T. P. Miller, J. L. Rush, P. Steiner, A. W. Opipari, Jr., S. W. Lowe, and M. S. Soengas.** 2005. Differential regulation of noxa in normal melanocytes and melanoma cells by proteasome inhibition: therapeutic implications. *Cancer Res* **65**:6294-304.

136. **Finlay, B. B., and G. McFadden.** 2006. Anti-immunology: evasion of the host immune system by bacterial and viral pathogens. *Cell* **124**:767-82.
137. **Fischer, S. F., H. Ludwig, J. Holzapfel, M. Kvensakul, L. Chen, D. C. Huang, G. Sutter, M. Knese, and G. Hacker.** 2006. Modified vaccinia virus Ankara protein F1L is a novel BH3-domain-binding protein and acts together with the early viral protein E3L to block virus-associated apoptosis. *Cell Death Differ* **13**:109-18.
138. **Flanagan, A. M., and A. Letai.** 2008. BH3 domains define selective inhibitory interactions with BHRF-1 and KSHV BCL-2. *Cell Death Differ* **15**:580-8.
139. **Fletcher, J. I., S. Meusburger, C. J. Hawkins, D. T. Riglar, E. F. Lee, W. D. Fairlie, D. C. Huang, and J. M. Adams.** 2008. Apoptosis is triggered when prosurvival Bcl-2 proteins cannot restrain Bax. *Proc Natl Acad Sci U S A* **105**:18081-7.
140. **Foghsgaard, L., and M. Jaattela.** 1997. The ability of BHRF1 to inhibit apoptosis is dependent on stimulus and cell type. *J Virol* **71**:7509-17.
141. **Galindo, I., B. Hernaez, G. Diaz-Gil, J. M. Escribano, and C. Alonso.** 2008. A179L, a viral Bcl-2 homologue, targets the core Bcl-2 apoptotic machinery and its upstream BH3 activators with selective binding restrictions for Bid and Noxa. *Virology* **375**:561-72.
142. **Gao, S., W. Fu, M. Durrenberger, C. De Geyter, and H. Zhang.** 2005. Membrane translocation and oligomerization of hBok are triggered in response to apoptotic stimuli and Bnip3. *Cell Mol Life Sci* **62**:1015-24.
143. **Garcia, M. A., E. F. Meurs, and M. Esteban.** 2007. The dsRNA protein kinase PKR: virus and cell control. *Biochimie* **89**:799-811.
144. **Gavathiotis, E., M. Suzuki, M. L. Davis, K. Pitter, G. H. Bird, S. G. Katz, H. C. Tu, H. Kim, E. H. Cheng, N. Tjandra, and L. D. Walensky.** 2008. BAX activation is initiated at a novel interaction site. *Nature* **455**:1076-81.
145. **George, N. M., J. J. Evans, and X. Luo.** 2007. A three-helix homooligomerization domain containing BH3 and BH1 is responsible for the apoptotic activity of Bax. *Genes Dev* **21**:1937-48.
146. **Giam, M., D. C. Huang, and P. Bouillet.** 2008. BH3-only proteins and their roles in programmed cell death. *Oncogene* **27 Suppl 1**:S128-36.
147. **Gibson, L., S. P. Holmgreen, D. C. Huang, O. Bernard, N. G. Copeland, N. A. Jenkins, G. R. Sutherland, E. Baker, J. M. Adams, and S. Cory.** 1996. bcl-w, a novel member of the bcl-2 family, promotes cell survival. *Oncogene* **13**:665-75.
148. **Gil, J., and M. Esteban.** 2000. The interferon-induced protein kinase (PKR), triggers apoptosis through FADD-mediated activation of caspase 8 in a manner independent of Fas and TNF-alpha receptors. *Oncogene* **19**:3665-74.
149. **Gil, J., M. A. Garcia, P. Gomez-Puertas, S. Guerra, J. Rullas, H. Nakano, J. Alcami, and M. Esteban.** 2004. TRAF family proteins link PKR with NF-kappa B activation. *Mol Cell Biol* **24**:4502-12.
150. **Gil, J., J. Rullas, M. A. Garcia, J. Alcami, and M. Esteban.** 2001. The catalytic activity of dsRNA-dependent protein kinase, PKR, is required for NF-kappaB activation. *Oncogene* **20**:385-94.
151. **Gillissen, B., F. Essmann, V. Graupner, L. Starck, S. Radetzki, B. Dorken, K. Schulze-Osthoff, and P. T. Daniel.** 2003. Induction of cell

- death by the BH3-only Bcl-2 homolog Nbk/Bik is mediated by an entirely Bax-dependent mitochondrial pathway. *Embo J* **22**:3580-90.
152. **Gillissen, B., F. Essmann, P. G. Hemmati, A. Richter, A. Richter, I. Oztop, G. Chinnadurai, B. Dorken, and P. T. Daniel.** 2007. Mcl-1 determines the Bax dependency of Nbk/Bik-induced apoptosis. *J Cell Biol* **179**:701-15.
 153. **Goldmacher, V. S., L. M. Bartle, A. Skaletskaya, C. A. Dionne, N. L. Kedersha, C. A. Vater, J. W. Han, R. J. Lutz, S. Watanabe, E. D. Cahir McFarland, E. D. Kieff, E. S. Mocarski, and T. Chittenden.** 1999. A cytomegalovirus-encoded mitochondria-localized inhibitor of apoptosis structurally unrelated to Bcl-2. *Proc Natl Acad Sci U S A* **96**:12536-41.
 154. **Gomez-Esquer, F., M. A. Palomar, I. Rivas, J. Delcan, R. Linares, and G. Diaz-Gil.** 2008. Characterization of the BH3 protein Bmf in *Gallus gallus*: identification of a novel chicken-specific isoform. *Gene* **407**:21-9.
 155. **Gonzalez, J. M., and M. Esteban.** 2010. A poxvirus Bcl-2-like gene family involved in regulation of host immune response: sequence similarity and evolutionary history. *Virol J* **7**:59.
 156. **Goping, I. S., A. Gross, J. N. Lavoie, M. Nguyen, R. Jemmerson, K. Roth, S. J. Korsmeyer, and G. C. Shore.** 1998. Regulated targeting of BAX to mitochondria. *J Cell Biol* **143**:207-15.
 157. **Goubau, D., R. Romieu-Mourez, M. Solis, E. Hernandez, T. Mesplede, R. Lin, D. Leaman, and J. Hiscott.** 2009. Transcriptional reprogramming of primary macrophages reveals distinct apoptotic and anti-tumoral functions of IRF-3 and IRF-7. *Eur J Immunol* **39**:527-40.
 158. **Graham, S. C., M. W. Bahar, S. Cooray, R. A. Chen, D. M. Whalen, N. G. Abrescia, D. Alderton, R. J. Owens, D. I. Stuart, G. L. Smith, and J. M. Grimes.** 2008. Vaccinia virus proteins A52 and B14 Share a Bcl-2-like fold but have evolved to inhibit NF-kappaB rather than apoptosis. *PLoS Pathog* **4**:e1000128.
 159. **Grandgirard, D., E. Studer, L. Monney, T. Belser, I. Fellay, C. Borner, and M. R. Michel.** 1998. Alphaviruses induce apoptosis in Bcl-2-overexpressing cells: evidence for a caspase-mediated, proteolytic inactivation of Bcl-2. *Embo J* **17**:1268-78.
 160. **Green, D. R., and J. E. Chipuk.** 2008. Apoptosis: Stabbed in the BAX. *Nature* **455**:1047-9.
 161. **Greenhalf, W., C. Stephan, and B. Chaudhuri.** 1996. Role of mitochondria and C-terminal membrane anchor of Bcl-2 in Bax induced growth arrest and mortality in *Saccharomyces cerevisiae*. *FEBS Lett* **380**:169-75.
 162. **Griffiths, G. J., B. M. Corfe, P. Savory, S. Leech, M. D. Esposti, J. A. Hickman, and C. Dive.** 2001. Cellular damage signals promote sequential changes at the N-terminus and BH-1 domain of the pro-apoptotic protein Bak. *Oncogene* **20**:7668-76.
 163. **Griffiths, G. J., L. Dubrez, C. P. Morgan, N. A. Jones, J. Whitehouse, B. M. Corfe, C. Dive, and J. A. Hickman.** 1999. Cell damage-induced conformational changes of the pro-apoptotic protein Bak in vivo precede the onset of apoptosis. *J Cell Biol* **144**:903-14.
 164. **Gubser, C., S. Hue, P. Kellam, and G. L. Smith.** 2004. Poxvirus genomes: a phylogenetic analysis. *J Gen Virol* **85**:105-17.

165. **Guerra, S., A. Caceres, K. P. Knobeloch, I. Horak, and M. Esteban.** 2008. Vaccinia virus E3 protein prevents the antiviral action of ISG15. *PLoS Pathog* **4**:e1000096.
166. **Guo, B., D. Zhai, E. Cabezas, K. Welsh, S. Nouraini, A. C. Satterthwait, and J. C. Reed.** 2003. Humanin peptide suppresses apoptosis by interfering with Bax activation. *Nature* **423**:456-61.
167. **Gurudutta, G. U., Y. K. Verma, V. K. Singh, P. Gupta, H. G. Raj, R. K. Sharma, and R. Chandra.** 2005. Structural conservation of residues in BH1 and BH2 domains of Bcl-2 family proteins. *FEBS Lett* **579**:3503-7.
168. **Hallin, U., E. Kondo, Y. Ozaki, H. Hagberg, F. Shibasaki, and K. Blomgren.** 2006. Bcl-2 phosphorylation in the BH4 domain precedes caspase-3 activation and cell death after neonatal cerebral hypoxic-ischemic injury. *Neurobiol Dis* **21**:478-86.
169. **Han, J., C. Flemington, A. B. Houghton, Z. Gu, G. P. Zambetti, R. J. Lutz, L. Zhu, and T. Chittenden.** 2001. Expression of bbc3, a pro-apoptotic BH3-only gene, is regulated by diverse cell death and survival signals. *Proc Natl Acad Sci U S A* **98**:11318-23.
170. **Han, J., L. A. Goldstein, W. Hou, and H. Rabinowich.** 2007. Functional linkage between NOXA and Bim in mitochondrial apoptotic events. *J Biol Chem* **282**:16223-31.
171. **Han, J., D. Modha, and E. White.** 1998. Interaction of E1B 19K with Bax is required to block Bax-induced loss of mitochondrial membrane potential and apoptosis. *Oncogene* **17**:2993-3005.
172. **Han, J., P. Sabbatini, D. Perez, L. Rao, D. Modha, and E. White.** 1996. The E1B 19K protein blocks apoptosis by interacting with and inhibiting the p53-inducible and death-promoting Bax protein. *Genes Dev* **10**:461-77.
173. **Han, J., P. Sabbatini, and E. White.** 1996. Induction of apoptosis by human Nbk/Bik, a BH3-containing protein that interacts with E1B 19K. *Mol Cell Biol* **16**:5857-64.
174. **Hanada, M., C. Aime-Sempe, T. Sato, and J. C. Reed.** 1995. Structure-function analysis of Bcl-2 protein. Identification of conserved domains important for homodimerization with Bcl-2 and heterodimerization with Bax. *J Biol Chem* **270**:11962-9.
175. **Harada, H., B. Quearry, A. Ruiz-Vela, and S. J. Korsmeyer.** 2004. Survival factor-induced extracellular signal-regulated kinase phosphorylates BIM, inhibiting its association with BAX and proapoptotic activity. *Proc Natl Acad Sci U S A* **101**:15313-7.
176. **Hardwick, J. M., and D. S. Bellows.** 2003. Viral versus cellular BCL-2 proteins. *Cell Death Differ* **10 Suppl 1**:S68-76.
177. **Hartmann, R., P. L. Norby, P. M. Martensen, P. Jorgensen, M. C. James, C. Jacobsen, S. K. Moestrup, M. J. Clemens, and J. Justesen.** 1998. Activation of 2'-5' oligoadenylate synthetase by single-stranded and double-stranded RNA aptamers. *J Biol Chem* **273**:3236-46.
178. **Hawkins, C. J., S. L. Wang, and B. A. Hay.** 1999. A cloning method to identify caspases and their regulators in yeast: identification of Drosophila IAP1 as an inhibitor of the Drosophila caspase DCP-1. *Proc Natl Acad Sci U S A* **96**:2885-90.
179. **Hayajneh, W. A., A. M. Colberg-Poley, A. Skaletskaya, L. M. Bartle, M. M. Lesperance, D. G. Contopoulos-Ioannidis, N. L. Kedersha, and V. S. Goldmacher.** 2001. The sequence and antiapoptotic functional

- domains of the human cytomegalovirus UL37 exon 1 immediate early protein are conserved in multiple primary strains. *Virology* **279**:233-40.
180. **Heath-Engel, H. M., N. C. Chang, and G. C. Shore.** 2008. The endoplasmic reticulum in apoptosis and autophagy: role of the BCL-2 protein family. *Oncogene* **27**:6419-33.
 181. **Hegde, R., S. M. Srinivasula, Z. Zhang, R. Wassell, R. Mukattash, L. Cilenti, G. DuBois, Y. Lazebnik, A. S. Zervos, T. Fernandes-Alnemri, and E. S. Alnemri.** 2002. Identification of Omi/HtrA2 as a mitochondrial apoptotic serine protease that disrupts inhibitor of apoptosis protein-caspase interaction. *J Biol Chem* **277**:432-8.
 182. **Henderson, S., D. Huen, M. Rowe, C. Dawson, G. Johnson, and A. Rickinson.** 1993. Epstein-Barr virus-coded BHRF1 protein, a viral homologue of Bcl-2, protects human B cells from programmed cell death. *Proc Natl Acad Sci U S A* **90**:8479-83.
 183. **Hengartner, M. O.** 2000. The biochemistry of apoptosis. *Nature* **407**:770-6.
 184. **Hengartner, M. O., R. E. Ellis, and H. R. Horvitz.** 1992. *Caenorhabditis elegans* gene *ced-9* protects cells from programmed cell death. *Nature* **356**:494-9.
 185. **Hengartner, M. O., and H. R. Horvitz.** 1994. Activation of *C. elegans* cell death protein CED-9 by an amino-acid substitution in a domain conserved in Bcl-2. *Nature* **369**:318-20.
 186. **Hengartner, M. O., and H. R. Horvitz.** 1994. *C. elegans* cell survival gene *ced-9* encodes a functional homolog of the mammalian proto-oncogene *bcl-2*. *Cell* **76**:665-76.
 187. **Hershko, T., and D. Ginsberg.** 2004. Up-regulation of Bcl-2 homology 3 (BH3)-only proteins by E2F1 mediates apoptosis. *J Biol Chem* **279**:8627-34.
 188. **Hickish, T., D. Robertson, P. Clarke, M. Hill, F. di Stefano, C. Clarke, and D. Cunningham.** 1994. Ultrastructural localization of BHRF1: an Epstein-Barr virus gene product which has homology with *bcl-2*. *Cancer Res* **54**:2808-11.
 189. **Hijikata, M., N. Kato, T. Sato, Y. Kagami, and K. Shimotohno.** 1990. Molecular cloning and characterization of a cDNA for a novel phorbol-12-myristate-13-acetate-responsive gene that is highly expressed in an adult T-cell leukemia cell line. *J Virol* **64**:4632-9.
 190. **Hiller, G., K. Weber, L. Schneider, C. Parajsz, and C. Jungwirth.** 1979. Interaction of assembled progeny pox viruses with the cellular cytoskeleton. *Virology* **98**:142-53.
 191. **Hinds, M. G., M. Lackmann, G. L. Skea, P. J. Harrison, D. C. Huang, and C. L. Day.** 2003. The structure of Bcl-w reveals a role for the C-terminal residues in modulating biological activity. *EMBO J* **22**:1497-507.
 192. **Hockenbery, D., G. Nunez, C. Milliman, R. D. Schreiber, and S. J. Korsmeyer.** 1990. Bcl-2 is an inner mitochondrial membrane protein that blocks programmed cell death. *Nature* **348**:334-6.
 193. **Hovanessian, A. G., and J. Justesen.** 2007. The human 2'-5'oligoadenylate synthetase family: unique interferon-inducible enzymes catalyzing 2'-5' instead of 3'-5' phosphodiester bond formation. *Biochimie* **89**:779-88.

194. **Hovanessian, A. G., J. Wood, E. Meurs, and L. Montagnier.** 1979. Increased nuclease activity in cells treated with pppA2'p5'A2'p5' A. *Proc Natl Acad Sci U S A* **76**:3261-5.
195. **Hsu, H., H. B. Shu, M. G. Pan, and D. V. Goeddel.** 1996. TRADD-TRAF2 and TRADD-FADD interactions define two distinct TNF receptor 1 signal transduction pathways. *Cell* **84**:299-308.
196. **Hsu, H., J. Xiong, and D. V. Goeddel.** 1995. The TNF receptor 1-associated protein TRADD signals cell death and NF-kappa B activation. *Cell* **81**:495-504.
197. **Hsu, S. Y., A. Kaipia, E. McGee, M. Lomeli, and A. J. Hsueh.** 1997. Bok is a pro-apoptotic Bcl-2 protein with restricted expression in reproductive tissues and heterodimerizes with selective anti-apoptotic Bcl-2 family members. *Proc Natl Acad Sci U S A* **94**:12401-6.
198. **Hsu, S. Y., P. Lin, and A. J. Hsueh.** 1998. BOD (Bcl-2-related ovarian death gene) is an ovarian BH3 domain-containing proapoptotic Bcl-2 protein capable of dimerization with diverse antiapoptotic Bcl-2 members. *Mol Endocrinol* **12**:1432-40.
199. **Hsu, Y. T., K. G. Wolter, and R. J. Youle.** 1997. Cytosol-to-membrane redistribution of Bax and Bcl-X(L) during apoptosis. *Proc Natl Acad Sci U S A* **94**:3668-72.
200. **Hsu, Y. T., and R. J. Youle.** 1998. Bax in murine thymus is a soluble monomeric protein that displays differential detergent-induced conformations. *J Biol Chem* **273**:10777-83.
201. **Hsu, Y. T., and R. J. Youle.** 1997. Nonionic detergents induce dimerization among members of the Bcl-2 family. *J Biol Chem* **272**:13829-34.
202. **Hu, F. Q., C. A. Smith, and D. J. Pickup.** 1994. Cowpox virus contains two copies of an early gene encoding a soluble secreted form of the type II TNF receptor. *Virology* **204**:343-56.
203. **Hu, S., C. Vincenz, M. Buller, and V. M. Dixit.** 1997. A novel family of viral death effector domain-containing molecules that inhibit both CD-95- and tumor necrosis factor receptor-1-induced apoptosis. *J Biol Chem* **272**:9621-4.
204. **Huang, B., M. Eberstadt, E. T. Olejniczak, R. P. Meadows, and S. W. Fesik.** 1996. NMR structure and mutagenesis of the Fas (APO-1/CD95) death domain. *Nature* **384**:638-41.
205. **Huang, Q., A. M. Petros, H. W. Virgin, S. W. Fesik, and E. T. Olejniczak.** 2002. Solution structure of a Bcl-2 homolog from Kaposi sarcoma virus. *Proc Natl Acad Sci U S A* **99**:3428-33.
206. **Huang, Q., A. M. Petros, H. W. Virgin, S. W. Fesik, and E. T. Olejniczak.** 2003. Solution structure of the BHRF1 protein from Epstein-Barr virus, a homolog of human Bcl-2. *J Mol Biol* **332**:1123-30.
207. **Hughes, A. L., and R. Friedman.** 2005. Poxvirus genome evolution by gene gain and loss. *Mol Phylogenet Evol* **35**:186-95.
208. **Hughes, A. L., S. Irausquin, and R. Friedman.** 2009. The evolutionary biology of poxviruses. *Infect Genet Evol* **10**:50-9.
209. **Imaizumi, K., M. Tsuda, Y. Imai, A. Wanaka, T. Takagi, and M. Tohyama.** 1997. Molecular cloning of a novel polypeptide, DP5, induced during programmed neuronal death. *J Biol Chem* **272**:18842-8.
210. **Ink, B., M. Zornig, B. Baum, N. Hajibagheri, C. James, T. Chittenden, and G. Evan.** 1997. Human Bak induces cell death in

- Schizosaccharomyces pombe with morphological changes similar to those with apoptosis in mammalian cells. *Mol Cell Biol* **17**:2468-74.
211. **Inohara, N., L. Ding, S. Chen, and G. Nunez.** 1997. harakiri, a novel regulator of cell death, encodes a protein that activates apoptosis and interacts selectively with survival-promoting proteins Bcl-2 and Bcl-X(L). *EMBO J* **16**:1686-94.
 212. **Inohara, N., D. Ekhterae, I. Garcia, R. Carrio, J. Merino, A. Merry, S. Chen, and G. Nunez.** 1998. Mtd, a novel Bcl-2 family member activates apoptosis in the absence of heterodimerization with Bcl-2 and Bcl-XL. *J Biol Chem* **273**:8705-10.
 213. **Inohara, N., T. S. Gourley, R. Carrio, M. Muniz, J. Merino, I. Garcia, T. Koseki, Y. Hu, S. Chen, and G. Nunez.** 1998. Diva, a Bcl-2 homologue that binds directly to Apaf-1 and induces BH3-independent cell death. *J Biol Chem* **273**:32479-86.
 214. **Inoue, S., J. Riley, T. W. Gant, M. J. Dyer, and G. M. Cohen.** 2007. Apoptosis induced by histone deacetylase inhibitors in leukemic cells is mediated by Bim and Noxa. *Leukemia* **21**:1773-82.
 215. **Jabbour, A. M., M. A. Puryer, J. Y. Yu, T. Lithgow, C. D. Riffkin, D. M. Ashley, D. L. Vaux, P. G. Ekert, and C. J. Hawkins.** 2006. Human Bcl-2 cannot directly inhibit the *Caenorhabditis elegans* Apaf-1 homologue CED-4, but can interact with EGL-1. *J Cell Sci* **119**:2572-82.
 216. **Jacobs, B. L., and J. O. Langland.** 1996. When two strands are better than one: the mediators and modulators of the cellular responses to double-stranded RNA. *Virology* **219**:339-49.
 217. **Janiak, F., B. Leber, and D. W. Andrews.** 1994. Assembly of Bcl-2 into microsomal and outer mitochondrial membranes. *J Biol Chem* **269**:9842-9.
 218. **Jenner, E.** 1798. An inquiry into the causes and effects of the variolae vaccinae, a disease discovered in some of the western countries of England, particularly Gloucestershire, and known by the name of the cow pox. S. Low, London.
 219. **Jeong, S. Y., B. Gaume, Y. J. Lee, Y. T. Hsu, S. W. Ryu, S. H. Yoon, and R. J. Youle.** 2004. Bcl-x(L) sequesters its C-terminal membrane anchor in soluble, cytosolic homodimers. *EMBO J* **23**:2146-55.
 220. **Johnston, J. B., and G. McFadden.** 2003. Poxvirus immunomodulatory strategies: current perspectives. *J Virol* **77**:6093-100.
 221. **Jost, P. J., S. Grabow, D. Gray, M. D. McKenzie, U. Nachbur, D. C. Huang, P. Bouillet, H. E. Thomas, C. Borner, J. Silke, A. Strasser, and T. Kaufmann.** 2009. XIAP discriminates between type I and type II FAS-induced apoptosis. *Nature* **460**:1035-9.
 222. **Jourdain, A., and J. C. Martinou.** 2009. Mitochondrial outer-membrane permeabilization and remodelling in apoptosis. *Int J Biochem Cell Biol* **41**:1884-9.
 223. **Jurak, I., U. Schumacher, H. Simic, S. Voigt, and W. Brune.** 2008. Murine cytomegalovirus m38.5 protein inhibits Bax-mediated cell death. *J Virol* **82**:4812-22.
 224. **Jurgensmeier, J. M., Z. Xie, Q. Deveraux, L. Ellerby, D. Bredesen, and J. C. Reed.** 1998. Bax directly induces release of cytochrome c from isolated mitochondria. *Proc Natl Acad Sci U S A* **95**:4997-5002.

225. **Katsafanas, G. C., and B. Moss.** 2007. Colocalization of transcription and translation within cytoplasmic poxvirus factories coordinates viral expression and subjugates host functions. *Cell Host Microbe* **2**:221-8.
226. **Kawaguchi, T., K. Nomura, Y. Hirayama, and T. Kitagawa.** 1987. Establishment and characterization of a chicken hepatocellular carcinoma cell line, LMH. *Cancer Res* **47**:4460-4.
227. **Kawai, T., and S. Akira.** 2006. Innate immune recognition of viral infection. *Nat Immunol* **7**:131-7.
228. **Kawanishi, M., S. Tada-Oikawa, and S. Kawanishi.** 2002. Epstein-Barr virus BHRF1 functions downstream of Bid cleavage and upstream of mitochondrial dysfunction to inhibit TRAIL-induced apoptosis in BJAB cells. *Biochem Biophys Res Commun* **297**:682-7.
229. **Ke, N., A. Godzik, and J. C. Reed.** 2001. Bcl-B, a novel Bcl-2 family member that differentially binds and regulates Bax and Bak. *J Biol Chem* **276**:12481-4.
230. **Kerr, I. M., and R. E. Brown.** 1978. pppA2'p5'A2'p5'A: an inhibitor of protein synthesis synthesized with an enzyme fraction from interferon-treated cells. *Proc Natl Acad Sci U S A* **75**:256-60.
231. **Kerr, J. F., A. H. Wyllie, and A. R. Currie.** 1972. Apoptosis: a basic biological phenomenon with wide-ranging implications in tissue kinetics. *Br J Cancer* **26**:239-57.
232. **Kettle, S., A. Alcamì, A. Khanna, R. Ehret, C. Jassoy, and G. L. Smith.** 1997. Vaccinia virus serpin B13R (SPI-2) inhibits interleukin-1 β -converting enzyme and protects virus-infected cells from TNF- and Fas-mediated apoptosis, but does not prevent IL-1 β -induced fever. *J Gen Virol* **78** (Pt 3):677-85.
233. **Khaled, A. R., K. Kim, R. Hofmeister, K. Muegge, and S. K. Durum.** 1999. Withdrawal of IL-7 induces Bax translocation from cytosol to mitochondria through a rise in intracellular pH. *Proc Natl Acad Sci U S A* **96**:14476-81.
234. **Khanim, F., C. Dawson, C. A. Meseda, J. Dawson, M. Mackett, and L. S. Young.** 1997. BHRF1, a viral homologue of the Bcl-2 oncogene, is conserved at both the sequence and functional level in different Epstein-Barr virus isolates. *J Gen Virol* **78** (Pt 11):2987-99.
235. **Kibler, K. V., T. Shors, K. B. Perkins, C. C. Zeman, M. P. Banaszak, J. Biesterfeldt, J. O. Langland, and B. L. Jacobs.** 1997. Double-stranded RNA is a trigger for apoptosis in vaccinia virus-infected cells. *J Virol* **71**:1992-2003.
236. **Kim, H., M. Rafiuddin-Shah, H. C. Tu, J. R. Jeffers, G. P. Zambetti, J. J. Hsieh, and E. H. Cheng.** 2006. Hierarchical regulation of mitochondrion-dependent apoptosis by BCL-2 subfamilies. *Nat Cell Biol.*
237. **Kim, H., H. C. Tu, D. Ren, O. Takeuchi, J. R. Jeffers, G. P. Zambetti, J. J. Hsieh, and E. H. Cheng.** 2009. Stepwise activation of BAX and BAK by tBID, BIM, and PUMA initiates mitochondrial apoptosis. *Mol Cell* **36**:487-99.
238. **Kim, H. E., F. Du, M. Fang, and X. Wang.** 2005. Formation of apoptosome is initiated by cytochrome c-induced dATP hydrolysis and subsequent nucleotide exchange on Apaf-1. *Proc Natl Acad Sci U S A* **102**:17545-50.

239. **Kim, J. Y., H. J. Ahn, J. H. Ryu, K. Suk, and J. H. Park.** 2004. BH3-only protein Noxa is a mediator of hypoxic cell death induced by hypoxia-inducible factor 1 α . *J Exp Med* **199**:113-24.
240. **Kim, P. K., M. G. Annis, P. J. Dlugosz, B. Leber, and D. W. Andrews.** 2004. During apoptosis bcl-2 changes membrane topology at both the endoplasmic reticulum and mitochondria. *Mol Cell* **14**:523-9.
241. **Kim, Y. G., K. Lowenhaupt, D. B. Oh, K. K. Kim, and A. Rich.** 2004. Evidence that vaccinia virulence factor E3L binds to Z-DNA in vivo: Implications for development of a therapy for poxvirus infection. *Proc Natl Acad Sci U S A* **101**:1514-8.
242. **Kim, Y. G., M. Muralinath, T. Brandt, M. Percy, K. Hauns, K. Lowenhaupt, B. L. Jacobs, and A. Rich.** 2003. A role for Z-DNA binding in vaccinia virus pathogenesis. *Proc Natl Acad Sci U S A* **100**:6974-9.
243. **Kitanaka, C., T. Namiki, K. Noguchi, T. Mochizuki, S. Kagaya, S. Chi, A. Hayashi, A. Asai, Y. Tsujimoto, and Y. Kuchino.** 1997. Caspase-dependent apoptosis of COS-7 cells induced by Bax overexpression: differential effects of Bcl-2 and Bcl-xL on Bax-induced caspase activation and apoptosis. *Oncogene* **15**:1763-72.
244. **Koo, G. C., and J. R. Peppard.** 1984. Establishment of monoclonal anti-Nk-1.1 antibody. *Hybridoma* **3**:301-3.
245. **Korsmeyer, S. J., J. R. Shutter, D. J. Veis, D. E. Merry, and Z. N. Oltvai.** 1993. Bcl-2/Bax: a rheostat that regulates an anti-oxidant pathway and cell death. *Semin Cancer Biol* **4**:327-32.
246. **Korsmeyer, S. J., M. C. Wei, M. Saito, S. Weiler, K. J. Oh, and P. H. Schlesinger.** 2000. Pro-apoptotic cascade activates BID, which oligomerizes BAK or BAX into pores that result in the release of cytochrome c. *Cell Death Differ* **7**:1166-73.
247. **Kozopas, K. M., T. Yang, H. L. Buchan, P. Zhou, and R. W. Craig.** 1993. MCL1, a gene expressed in programmed myeloid cell differentiation, has sequence similarity to BCL2. *Proc Natl Acad Sci U S A* **90**:3516-20.
248. **Ku, B., C. Liang, J. U. Jung, and B. H. Oh.** 2010. Evidence that inhibition of BAX activation by BCL-2 involves its tight and preferential interaction with the BH3 domain of BAX. *Cell Res*.
249. **Kuwana, T., L. Bouchier-Hayes, J. E. Chipuk, C. Bonzon, B. A. Sullivan, D. R. Green, and D. D. Newmeyer.** 2005. BH3 domains of BH3-only proteins differentially regulate Bax-mediated mitochondrial membrane permeabilization both directly and indirectly. *Mol Cell* **17**:525-35.
250. **Kuwana, T., M. R. Mackey, G. Perkins, M. H. Ellisman, M. Latterich, R. Schneider, D. R. Green, and D. D. Newmeyer.** 2002. Bid, Bax, and lipids cooperate to form supramolecular openings in the outer mitochondrial membrane. *Cell* **111**:331-42.
251. **Kvansakul, M., M. F. van Delft, E. F. Lee, J. M. Gulbis, W. D. Fairlie, D. C. Huang, and P. M. Colman.** 2007. A structural viral mimic of prosurvival bcl-2: a pivotal role for sequestering proapoptotic bax and bak. *Mol Cell* **25**:933-42.
252. **Kvansakul, M., H. Yang, W. D. Fairlie, P. E. Czabotar, S. F. Fischer, M. A. Perugini, D. C. Huang, and P. M. Colman.** 2008. Vaccinia virus anti-apoptotic F1L is a novel Bcl-2-like domain-swapped dimer that binds a

- highly selective subset of BH3-containing death ligands. *Cell Death Differ* **15**:1564-71.
253. **Kwon, J. A., and A. Rich.** 2005. Biological function of the vaccinia virus Z-DNA-binding protein E3L: gene transactivation and antiapoptotic activity in HeLa cells. *Proc Natl Acad Sci U S A* **102**:12759-64.
 254. **Lackner, C. A., and R. C. Condit.** 2000. Vaccinia virus gene A18R DNA helicase is a transcript release factor. *J Biol Chem* **275**:1485-94.
 255. **Laemmli, U. K.** 1970. Cleavage of structural proteins during the assembly of the head of bacteriophage T4. *Nature* **227**:680-5.
 256. **Lalier, L., P. F. Cartron, P. Juin, S. Nedelkina, S. Manon, B. Bechinger, and F. M. Vallette.** 2007. Bax activation and mitochondrial insertion during apoptosis. *Apoptosis* **12**:887-96.
 257. **Lallemant, C., B. Blanchard, M. Palmieri, P. Lebon, E. May, and M. G. Tovey.** 2007. Single-stranded RNA viruses inactivate the transcriptional activity of p53 but induce NOXA-dependent apoptosis via post-translational modifications of IRF-1, IRF-3 and CREB. *Oncogene* **26**:328-38.
 258. **Langland, J. O., J. C. Kash, V. Carter, M. J. Thomas, M. G. Katze, and B. L. Jacobs.** 2006. Suppression of proinflammatory signal transduction and gene expression by the dual nucleic acid binding domains of the vaccinia virus E3L proteins. *J Virol* **80**:10083-95.
 259. **Larkin, M. A., G. Blackshields, N. P. Brown, R. Chenna, P. A. McGettigan, H. McWilliam, F. Valentin, I. M. Wallace, A. Wilm, R. Lopez, J. D. Thompson, T. J. Gibson, and D. G. Higgins.** 2007. Clustal W and Clustal X version 2.0. *Bioinformatics* **23**:2947-8.
 260. **Lawen, A.** 2003. Apoptosis-an introduction. *Bioessays* **25**:888-96.
 261. **Lazarou, M., D. Stojanovski, A. E. Frazier, A. Kotevski, G. Dewson, W. J. Craigen, R. M. Kluck, D. L. Vaux, and M. T. Ryan.** 2010. Inhibition of Bak Activation by Vdac2 Is Dependent on the Bak Transmembrane Anchor. *J Biol Chem*.
 262. **Leber, B., J. Lin, and D. W. Andrews.** 2007. Embedded together: the life and death consequences of interaction of the Bcl-2 family with membranes. *Apoptosis* **12**:897-911.
 263. **Leber, B., J. Lin, and D. W. Andrews.** 2010. Still embedded together binding to membranes regulates Bcl-2 protein interactions. *Oncogene* **29**:5221-30.
 264. **Lee, E. F., P. E. Czabotar, M. F. van Delft, E. M. Michalak, M. J. Boyle, S. N. Willis, H. Puthalakath, P. Bouillet, P. M. Colman, D. C. Huang, and W. D. Fairlie.** 2008. A novel BH3 ligand that selectively targets Mcl-1 reveals that apoptosis can proceed without Mcl-1 degradation. *J Cell Biol* **180**:341-55.
 265. **Lee, S. B., R. Bablanian, and M. Esteban.** 1996. Regulated expression of the interferon-induced protein kinase p68 (PKR) by vaccinia virus recombinants inhibits the replication of vesicular stomatitis virus but not that of poliovirus. *J Interferon Cytokine Res* **16**:1073-8.
 266. **Lee, S. B., and M. Esteban.** 1994. The interferon-induced double-stranded RNA-activated protein kinase induces apoptosis. *Virology* **199**:491-6.
 267. **Lee, S. B., Z. Melkova, W. Yan, B. R. Williams, A. G. Hovanessian, and M. Esteban.** 1993. The interferon-induced double-stranded RNA-

- activated human p68 protein kinase potently inhibits protein synthesis in cultured cells. *Virology* **192**:380-5.
268. **Lee, S. B., D. Rodriguez, J. R. Rodriguez, and M. Esteban.** 1997. The apoptosis pathway triggered by the interferon-induced protein kinase PKR requires the third basic domain, initiates upstream of Bcl-2, and involves ICE-like proteases. *Virology* **231**:81-8.
 269. **Lefkowitz, E. J., C. Wang, and C. Upton.** 2006. Poxviruses: past, present and future. *Virus Res* **117**:105-18.
 270. **Lei, K., and R. J. Davis.** 2003. JNK phosphorylation of Bim-related members of the Bcl2 family induces Bax-dependent apoptosis. *Proc Natl Acad Sci U S A* **100**:2432-7.
 271. **Letai, A., M. C. Bassik, L. D. Walensky, M. D. Sorcinelli, S. Weiler, and S. J. Korsmeyer.** 2002. Distinct BH3 domains either sensitize or activate mitochondrial apoptosis, serving as prototype cancer therapeutics. *Cancer Cell* **2**:183-92.
 272. **Leu, J. I., P. Dumont, M. Hafey, M. E. Murphy, and D. L. George.** 2004. Mitochondrial p53 activates Bak and causes disruption of a Bak-Mcl1 complex. *Nat Cell Biol* **6**:443-50.
 273. **Levin, D., and I. M. London.** 1978. Regulation of protein synthesis: activation by double-stranded RNA of a protein kinase that phosphorylates eukaryotic initiation factor 2. *Proc Natl Acad Sci U S A* **75**:1121-5.
 274. **Levine, B., S. Sinha, and G. Kroemer.** 2008. Bcl-2 family members: dual regulators of apoptosis and autophagy. *Autophagy* **4**:600-6.
 275. **Li, H., H. Zhu, C. J. Xu, and J. Yuan.** 1998. Cleavage of BID by caspase 8 mediates the mitochondrial damage in the Fas pathway of apoptosis. *Cell* **94**:491-501.
 276. **Li, K., Y. Li, J. M. Shelton, J. A. Richardson, E. Spencer, Z. J. Chen, X. Wang, and R. S. Williams.** 2000. Cytochrome c deficiency causes embryonic lethality and attenuates stress-induced apoptosis. *Cell* **101**:389-99.
 277. **Li, L. Y., X. Luo, and X. Wang.** 2001. Endonuclease G is an apoptotic DNase when released from mitochondria. *Nature* **412**:95-9.
 278. **Li, P., D. Nijhawan, I. Budihardjo, S. M. Srinivasula, M. Ahmad, E. S. Alnemri, and X. Wang.** 1997. Cytochrome c and dATP-dependent formation of Apaf-1/caspase-9 complex initiates an apoptotic protease cascade. *Cell* **91**:479-89.
 279. **Lin, B., S. K. Kolluri, F. Lin, W. Liu, Y. H. Han, X. Cao, M. I. Dawson, J. C. Reed, and X. K. Zhang.** 2004. Conversion of Bcl-2 from protector to killer by interaction with nuclear orphan receptor Nur77/TR3. *Cell* **116**:527-40.
 280. **Lin, E. Y., A. Orlofsky, M. S. Berger, and M. B. Prystowsky.** 1993. Characterization of A1, a novel hemopoietic-specific early-response gene with sequence similarity to bcl-2. *J Immunol* **151**:1979-88.
 281. **Lindsay, J., M. D. Esposti, and A. P. Gilmore.** 2010. Bcl-2 proteins and mitochondria-Specificity in membrane targeting for death. *Biochim Biophys Acta*.
 282. **Lindsten, T., A. J. Ross, A. King, W. X. Zong, J. C. Rathmell, H. A. Shiels, E. Ulrich, K. G. Waymire, P. Mahar, K. Frauwirth, Y. Chen, M. Wei, V. M. Eng, D. M. Adelman, M. C. Simon, A. Ma, J. A. Golden, G. Evan, S. J. Korsmeyer, G. R. MacGregor, and C. B. Thompson.** 2000.

- The combined functions of proapoptotic Bcl-2 family members bak and bax are essential for normal development of multiple tissues. *Mol Cell* **6**:1389-99.
283. **Lithgow, T., R. van Driel, J. F. Bertram, and A. Strasser.** 1994. The protein product of the oncogene bcl-2 is a component of the nuclear envelope, the endoplasmic reticulum, and the outer mitochondrial membrane. *Cell Growth Differ* **5**:411-7.
 284. **Liu, X., C. N. Kim, J. Yang, R. Jemmerson, and X. Wang.** 1996. Induction of apoptotic program in cell-free extracts: requirement for dATP and cytochrome c. *Cell* **86**:147-57.
 285. **Liu, Y., K. C. Wolff, B. L. Jacobs, and C. E. Samuel.** 2001. Vaccinia virus E3L interferon resistance protein inhibits the interferon-induced adenosine deaminase A-to-I editing activity. *Virology* **289**:378-87.
 286. **Livak, K. J., and T. D. Schmittgen.** 2001. Analysis of relative gene expression data using real-time quantitative PCR and the 2(-Delta Delta C(T)) Method. *Methods* **25**:402-8.
 287. **Lomonosova, E., and G. Chinnadurai.** 2008. BH3-only proteins in apoptosis and beyond: an overview. *Oncogene* **27 Suppl 1**:S2-19.
 288. **Loparev, V. N., J. M. Parsons, J. C. Knight, J. F. Panus, C. A. Ray, R. M. Buller, D. J. Pickup, and J. J. Esposito.** 1998. A third distinct tumor necrosis factor receptor of orthopoxviruses. *Proc Natl Acad Sci U S A* **95**:3786-91.
 289. **Lovell, J. F., L. P. Billen, S. Bindner, A. Shamas-Din, C. Fradin, B. Leber, and D. W. Andrews.** 2008. Membrane binding by tBid initiates an ordered series of events culminating in membrane permeabilization by Bax. *Cell* **135**:1074-84.
 290. **Luo, X., I. Budihardjo, H. Zou, C. Slaughter, and X. Wang.** 1998. Bid, a Bcl2 interacting protein, mediates cytochrome c release from mitochondria in response to activation of cell surface death receptors. *Cell* **94**:481-90.
 291. **Luthi, A. U., and S. J. Martin.** 2007. The CASBAH: a searchable database of caspase substrates. *Cell Death Differ* **14**:641-50.
 292. **Macen, J. L., K. A. Graham, S. F. Lee, M. Schreiber, L. K. Boshkov, and G. McFadden.** 1996. Expression of the myxoma virus tumor necrosis factor receptor homologue and M11L genes is required to prevent virus-induced apoptosis in infected rabbit T lymphocytes. *Virology* **218**:232-7.
 293. **Majumdar, R., and U. Maitra.** 2005. Regulation of GTP hydrolysis prior to ribosomal AUG selection during eukaryotic translation initiation. *EMBO J* **24**:3737-46.
 294. **Marshall, W. L., C. Yim, E. Gustafson, T. Graf, D. R. Sage, K. Hanify, L. Williams, J. Fingerroth, and R. W. Finberg.** 1999. Epstein-Barr virus encodes a novel homolog of the bcl-2 oncogene that inhibits apoptosis and associates with Bax and Bak. *J Virol* **73**:5181-5.
 295. **Martinez-Caballero, S., L. M. Dejean, M. S. Kinnally, K. J. Oh, C. A. Mannella, and K. W. Kinnally.** 2009. Assembly of the mitochondrial apoptosis-induced channel, MAC. *J Biol Chem* **284**:12235-45.
 296. **McBride, H. M., M. Neuspiel, and S. Wasiak.** 2006. Mitochondria: more than just a powerhouse. *Curr Biol* **16**:R551-60.
 297. **McCarthy, N. J., S. A. Hazlewood, D. S. Huen, A. B. Rickinson, and G. T. Williams.** 1996. The Epstein-Barr virus gene BHRF1, a homologue of

- the cellular oncogene Bcl-2, inhibits apoptosis induced by gamma radiation and chemotherapeutic drugs. *Adv Exp Med Biol* **406**:83-97.
298. **McCormick, A. L., C. D. Meiering, G. B. Smith, and E. S. Mocarski.** 2005. Mitochondrial cell death suppressors carried by human and murine cytomegalovirus confer resistance to proteasome inhibitor-induced apoptosis. *J Virol* **79**:12205-17.
 299. **McCormick, A. L., A. Skaletskaya, P. A. Barry, E. S. Mocarski, and V. S. Goldmacher.** 2003. Differential function and expression of the viral inhibitor of caspase 8-induced apoptosis (vICA) and the viral mitochondria-localized inhibitor of apoptosis (vMIA) cell death suppressors conserved in primate and rodent cytomegaloviruses. *Virology* **316**:221-33.
 300. **McCormick, A. L., V. L. Smith, D. Chow, and E. S. Mocarski.** 2003. Disruption of mitochondrial networks by the human cytomegalovirus UL37 gene product viral mitochondrion-localized inhibitor of apoptosis. *J Virol* **77**:631-41.
 301. **McDonnell, J. M., D. Fushman, C. L. Milliman, S. J. Korsmeyer, and D. Cowburn.** 1999. Solution structure of the proapoptotic molecule BID: a structural basis for apoptotic agonists and antagonists. *Cell* **96**:625-34.
 302. **McDonnell, T. J., N. Deane, F. M. Platt, G. Nunez, U. Jaeger, J. P. McKearn, and S. J. Korsmeyer.** 1989. bcl-2-immunoglobulin transgenic mice demonstrate extended B cell survival and follicular lymphoproliferation. *Cell* **57**:79-88.
 303. **McFadden, G.** 2010. Killing a killer: what next for smallpox? *PLoS Pathog* **6**:e1000727.
 304. **McFadden, G.** 2005. Poxvirus tropism. *Nat Rev Microbiol* **3**:201-13.
 305. **McLysaght, A., P. F. Baldi, and B. S. Gaut.** 2003. Extensive gene gain associated with adaptive evolution of poxviruses. *Proc Natl Acad Sci U S A* **100**:15655-60.
 306. **Mercer, J., and A. Helenius.** 2010. Apoptotic mimicry: phosphatidylserine-mediated macropinocytosis of vaccinia virus. *Ann N Y Acad Sci* **1209**:49-55.
 307. **Mercer, J., and A. Helenius.** 2008. Vaccinia virus uses macropinocytosis and apoptotic mimicry to enter host cells. *Science* **320**:531-5.
 308. **Merino, D., M. Giam, P. D. Hughes, O. M. Siggs, K. Heger, L. A. O'Reilly, J. M. Adams, A. Strasser, E. F. Lee, W. D. Fairlie, and P. Bouillet.** 2009. The role of BH3-only protein Bim extends beyond inhibiting Bcl-2-like prosurvival proteins. *J Cell Biol* **186**:355-62.
 309. **Metivier, D., B. Dallaporta, N. Zamzami, N. Larochette, S. A. Susin, I. Marzo, and G. Kroemer.** 1998. Cytofluorometric detection of mitochondrial alterations in early CD95/Fas/APO-1-triggered apoptosis of Jurkat T lymphoma cells. Comparison of seven mitochondrion-specific fluorochromes. *Immunol Lett* **61**:157-63.
 310. **Mikhailov, V., M. Mikhailova, K. Degenhardt, M. A. Venkatachalam, E. White, and P. Saikumar.** 2003. Association of Bax and Bak homo-oligomers in mitochondria. Bax requirement for Bak reorganization and cytochrome c release. *J Biol Chem* **278**:5367-76.
 311. **Mikhailov, V., M. Mikhailova, D. J. Pulkrabek, Z. Dong, M. A. Venkatachalam, and P. Saikumar.** 2001. Bcl-2 prevents Bax oligomerization in the mitochondrial outer membrane. *J Biol Chem* **276**:18361-74.

312. **Minn, A. J., P. Velez, S. L. Schendel, H. Liang, S. W. Muchmore, S. W. Fesik, M. Fill, and C. B. Thompson.** 1997. Bcl-x(L) forms an ion channel in synthetic lipid membranes. *Nature* **385**:353-7.
313. **Moerdyk-Schauwecker, M., K. Eide, R. Bildfell, R. J. Baker, W. Black, D. Graham, K. Thompson, G. Crawshaw, G. F. Rohrmann, and L. Jin.** 2009. Characterization of Cervidpoxvirus isolates from Oregon, California, and eastern Canada. *J Vet Diagn Invest* **21**:487-92.
314. **Moldoveanu, T., Q. Liu, A. Tocilj, M. Watson, G. Shore, and K. Gehring.** 2006. The X-ray structure of a BAK homodimer reveals an inhibitory zinc binding site. *Mol Cell* **24**:677-88.
315. **Morales, A. A., D. Gutman, K. P. Lee, and L. H. Boise.** 2008. BH3-only proteins Noxa, Bmf, and Bim are necessary for arsenic trioxide-induced cell death in myeloma. *Blood* **111**:5152-62.
316. **Moss, B.** 2007. Poxviridae: The Viruses and Their Replication. *In* D. M. Knipe and P. M. Howley (ed.), *Fields Virology*, 5th ed, vol. II. Lippincott Williams & Wilkins, Philadelphia, PA.
317. **Moss, B.** 2006. Poxvirus entry and membrane fusion. *Virology* **344**:48-54.
318. **Moss, B.** 1991. Vaccinia virus: a tool for research and vaccine development. *Science* **252**:1662-7.
319. **Muchmore, S. W., M. Sattler, H. Liang, R. P. Meadows, J. E. Harlan, H. S. Yoon, D. Nettesheim, B. S. Chang, C. B. Thompson, S. L. Wong, S. L. Ng, and S. W. Fesik.** 1996. X-ray and NMR structure of human Bcl-xL, an inhibitor of programmed cell death. *Nature* **381**:335-41.
320. **Murphy, A. F., E. P. J. Gibbs, M. C. Horzinek, and M. J. Studdert.** 1999. Poxviridae, *Veterinary Virology*, 3rd ed. Academic Press, San Diego, CA.
321. **Muzio, M., B. R. Stockwell, H. R. Stennicke, G. S. Salvesen, and V. M. Dixit.** 1998. An induced proximity model for caspase-8 activation. *J Biol Chem* **273**:2926-30.
322. **Nakagawa, T., S. Shimizu, T. Watanabe, O. Yamaguchi, K. Otsu, H. Yamagata, H. Inohara, T. Kubo, and Y. Tsujimoto.** 2005. Cyclophilin D-dependent mitochondrial permeability transition regulates some necrotic but not apoptotic cell death. *Nature* **434**:652-8.
323. **Nakano, K., and K. H. Vousden.** 2001. PUMA, a novel proapoptotic gene, is induced by p53. *Mol Cell* **7**:683-94.
324. **Nechushtan, A., C. L. Smith, Y. T. Hsu, and R. J. Youle.** 1999. Conformation of the Bax C-terminus regulates subcellular location and cell death. *Embo J* **18**:2330-41.
325. **Nechushtan, A., C. L. Smith, I. Lamensdorf, S. H. Yoon, and R. J. Youle.** 2001. Bax and Bak coalesce into novel mitochondria-associated clusters during apoptosis. *J Cell Biol* **153**:1265-76.
326. **Neilan, J. G., Z. Lu, C. L. Afonso, G. F. Kutish, M. D. Sussman, and D. L. Rock.** 1993. An African swine fever virus gene with similarity to the proto-oncogene bcl-2 and the Epstein-Barr virus gene BHRF1. *J Virol* **67**:4391-4.
327. **Nguyen, M., D. G. Millar, V. W. Yong, S. J. Korsmeyer, and G. C. Shore.** 1993. Targeting of Bcl-2 to the mitochondrial outer membrane by a COOH-terminal signal anchor sequence. *J Biol Chem* **268**:25265-8.

328. **Nijhawan, D., M. Fang, E. Traer, Q. Zhong, W. Gao, F. Du, and X. Wang.** 2003. Elimination of Mcl-1 is required for the initiation of apoptosis following ultraviolet irradiation. *Genes Dev* **17**:1475-86.
329. **Nikiforov, M. A., M. Riblett, W. H. Tang, V. Gratchouck, D. Zhuang, Y. Fernandez, M. Verhaegen, S. Varambally, A. M. Chinnaiyan, A. J. Jakubowiak, and M. S. Soengas.** 2007. Tumor cell-selective regulation of NOXA by c-MYC in response to proteasome inhibition. *Proc Natl Acad Sci U S A* **104**:19488-93.
330. **Nogal, M. L., G. Gonzalez de Buitrago, C. Rodriguez, B. Cubelos, A. L. Carrascosa, M. L. Salas, and Y. Revilla.** 2001. African swine fever virus IAP homologue inhibits caspase activation and promotes cell survival in mammalian cells. *J Virol* **75**:2535-43.
331. **Norris, K. L., and R. J. Youle.** 2008. Cytomegalovirus proteins vMIA and m38.5 link mitochondrial morphogenesis to Bcl-2 family proteins. *J Virol* **82**:6232-43.
332. **Nunez, G., M. Seto, S. Seremetis, D. Ferrero, F. Grignani, S. J. Korsmeyer, and R. Dalla-Favera.** 1989. Growth- and tumor-promoting effects of deregulated BCL2 in human B-lymphoblastoid cells. *Proc Natl Acad Sci U S A* **86**:4589-93.
333. **O'Connor, L., A. Strasser, L. A. O'Reilly, G. Hausmann, J. M. Adams, S. Cory, and D. C. Huang.** 1998. Bim: a novel member of the Bcl-2 family that promotes apoptosis. *Embo J* **17**:384-95.
334. **Oda, E., R. Ohki, H. Murasawa, J. Nemoto, T. Shibue, T. Yamashita, T. Tokino, T. Taniguchi, and N. Tanaka.** 2000. Noxa, a BH3-only member of the Bcl-2 family and candidate mediator of p53-induced apoptosis. *Science* **288**:1053-8.
335. **Oh, K. J., P. Singh, K. Lee, K. Foss, S. Lee, M. Park, S. Aluvila, R. S. Kim, J. Symersky, and D. E. Walters.** 2010. Conformational changes in BAK, a pore-forming proapoptotic Bcl-2 family member, upon membrane insertion and direct evidence for the existence of BH3-BH3 contact interface in BAK homo-oligomers. *J Biol Chem* **285**:28924-37.
336. **Ojala, P. M., K. Yamamoto, E. Castanos-Velez, P. Biberfeld, S. J. Korsmeyer, and T. P. Makela.** 2000. The apoptotic v-cyclin-CDK6 complex phosphorylates and inactivates Bcl-2. *Nat Cell Biol* **2**:819-25.
337. **Oltsdorf, T., S. W. Elmore, A. R. Shoemaker, R. C. Armstrong, D. J. Augeri, B. A. Belli, M. Bruncko, T. L. Deckwerth, J. Dinges, P. J. Hajduk, M. K. Joseph, S. Kitada, S. J. Korsmeyer, A. R. Kunzer, A. Letai, C. Li, M. J. Mitten, D. G. Nettesheim, S. Ng, P. M. Nimmer, J. M. O'Connor, A. Oleksijew, A. M. Petros, J. C. Reed, W. Shen, S. K. Tahir, C. B. Thompson, K. J. Tomaselli, B. Wang, M. D. Wendt, H. Zhang, S. W. Fesik, and S. H. Rosenberg.** 2005. An inhibitor of Bcl-2 family proteins induces regression of solid tumours. *Nature* **435**:677-81.
338. **Oltvai, Z. N., C. L. Milliman, and S. J. Korsmeyer.** 1993. Bcl-2 heterodimerizes in vivo with a conserved homolog, Bax, that accelerates programmed cell death. *Cell* **74**:609-19.
339. **Opgenorth, A., K. Graham, N. Nation, D. Strayer, and G. McFadden.** 1992. Deletion analysis of two tandemly arranged virulence genes in myxoma virus, M11L and myxoma growth factor. *J Virol* **66**:4720-31.
340. **Ow, Y. P., D. R. Green, Z. Hao, and T. W. Mak.** 2008. Cytochrome c: functions beyond respiration. *Nat Rev Mol Cell Biol* **9**:532-42.

341. **Paez, E., and M. Esteban.** 1984. Nature and mode of action of vaccinia virus products that block activation of the interferon-mediated ppp(A2'p)nA-synthetase. *Virology* **134**:29-39.
342. **Paez, E., and M. Esteban.** 1984. Resistance of vaccinia virus to interferon is related to an interference phenomenon between the virus and the interferon system. *Virology* **134**:12-28.
343. **Pagliari, L. J., T. Kuwana, C. Bonzon, D. D. Newmeyer, S. Tu, H. M. Beere, and D. R. Green.** 2005. The multidomain proapoptotic molecules Bax and Bak are directly activated by heat. *Proc Natl Acad Sci U S A* **102**:17975-80.
344. **Patton, J. F., R. W. Nordhausen, L. W. Woods, and N. J. MacLachlan.** 1996. Isolation of a poxvirus from a black-tailed deer (*Odocoileus hemionus columbianus*). *J Wildl Dis* **32**:531-3.
345. **Pauleau, A. L., N. Larochette, F. Giordanetto, S. R. Scholz, D. Poncet, N. Zamzami, V. S. Goldmacher, and G. Kroemer.** 2007. Structure-function analysis of the interaction between Bax and the cytomegalovirus-encoded protein vMIA. *Oncogene* **26**:7067-80.
346. **Pavlov, E. V., M. Priault, D. Pietkiewicz, E. H. Cheng, B. Antonsson, S. Manon, S. J. Korsmeyer, C. A. Mannella, and K. W. Kinnally.** 2001. A novel, high conductance channel of mitochondria linked to apoptosis in mammalian cells and Bax expression in yeast. *J Cell Biol* **155**:725-31.
347. **Pegoraro, L., A. Palumbo, J. Erikson, M. Falda, B. Giovanazzo, B. S. Emanuel, G. Rovera, P. C. Nowell, and C. M. Croce.** 1984. A 14;18 and an 8;14 chromosome translocation in a cell line derived from an acute B-cell leukemia. *Proc Natl Acad Sci U S A* **81**:7166-70.
348. **Peixoto, P. M., S. Y. Ryu, A. Bombrun, B. Antonsson, and K. W. Kinnally.** 2009. MAC inhibitors suppress mitochondrial apoptosis. *Biochem J* **423**:381-7.
349. **Perdiguero, B., and M. Esteban.** 2009. The interferon system and vaccinia virus evasion mechanisms. *J Interferon Cytokine Res* **29**:581-98.
350. **Perez, D., and E. White.** 2000. TNF-alpha signals apoptosis through a bid-dependent conformational change in Bax that is inhibited by E1B 19K. *Mol Cell* **6**:53-63.
351. **Petros, A. M., A. Medek, D. G. Nettesheim, D. H. Kim, H. S. Yoon, K. Swift, E. D. Matayoshi, T. Oltersdorf, and S. W. Fesik.** 2001. Solution structure of the antiapoptotic protein bcl-2. *Proc Natl Acad Sci U S A* **98**:3012-7.
352. **Petros, A. M., E. T. Olejniczak, and S. W. Fesik.** 2004. Structural biology of the Bcl-2 family of proteins. *Biochim Biophys Acta* **1644**:83-94.
353. **Peyerl, F. W., S. Dai, G. A. Murphy, F. Crawford, J. White, P. Marrack, and J. W. Kappler.** 2007. Elucidation of some Bax conformational changes through crystallization of an antibody-peptide complex. *Cell Death Differ* **14**:447-52.
354. **Ploner, C., R. Kofler, and A. Villunger.** 2008. Noxa: at the tip of the balance between life and death. *Oncogene* **27 Suppl 1**:S84-92.
355. **Polster, B. M., J. Pevsner, and J. M. Hardwick.** 2004. Viral Bcl-2 homologs and their role in virus replication and associated diseases. *Biochim Biophys Acta* **1644**:211-27.
356. **Poncet, D., N. Larochette, A. L. Pauleau, P. Boya, A. A. Jalil, P. F. Cartron, F. Vallette, C. Schnebelen, L. M. Bartle, A. Skaletskaya, D. Boutolleau, J. C. Martinou, V. S. Goldmacher, G. Kroemer, and N.**

- Zamzami.** 2004. An anti-apoptotic viral protein that recruits Bax to mitochondria. *J Biol Chem* **279**:22605-14.
357. **Postigo, A., J. R. Cross, J. Downward, and M. Way.** 2006. Interaction of F1L with the BH3 domain of Bak is responsible for inhibiting vaccinia-induced apoptosis. *Cell Death Differ* **13**:1651-62.
358. **Postigo, A., M. C. Martin, M. P. Dodding, and M. Way.** 2009. Vaccinia-induced epidermal growth factor receptor-MEK signalling and the anti-apoptotic protein F1L synergize to suppress cell death during infection. *Cell Microbiol* **11**:1208-18.
359. **Puthalakath, H., A. Villunger, L. A. O'Reilly, J. G. Beaumont, L. Coultas, R. E. Cheney, D. C. Huang, and A. Strasser.** 2001. Bmf: a proapoptotic BH3-only protein regulated by interaction with the myosin V actin motor complex, activated by anoikis. *Science* **293**:1829-32.
360. **Qin, J. Z., J. Ziffra, L. Stennett, B. Bodner, B. K. Bonish, V. Chaturvedi, F. Bennett, P. M. Pollock, J. M. Trent, M. J. Hendrix, P. Rizzo, L. Miele, and B. J. Nickoloff.** 2005. Proteasome inhibitors trigger NOXA-mediated apoptosis in melanoma and myeloma cells. *Cancer Res* **65**:6282-93.
361. **Quan, L. T., A. Caputo, R. C. Bleackley, D. J. Pickup, and G. S. Salvesen.** 1995. Granzyme B is inhibited by the cowpox virus serpin cytokine response modifier A. *J Biol Chem* **270**:10377-9.
362. **Rao, L., M. Debbas, P. Sabbatini, D. Hockenbery, S. Korsmeyer, and E. White.** 1992. The adenovirus E1A proteins induce apoptosis, which is inhibited by the E1B 19-kDa and Bcl-2 proteins. *Proc Natl Acad Sci U S A* **89**:7742-6.
363. **Ray, C. A., R. A. Black, S. R. Kronheim, T. A. Greenstreet, P. R. Sleath, G. S. Salvesen, and D. J. Pickup.** 1992. Viral inhibition of inflammation: cowpox virus encodes an inhibitor of the interleukin-1 beta converting enzyme. *Cell* **69**:597-604.
364. **Reboredo, M., R. F. Greaves, and G. Hahn.** 2004. Human cytomegalovirus proteins encoded by UL37 exon 1 protect infected fibroblasts against virus-induced apoptosis and are required for efficient virus replication. *J Gen Virol* **85**:3555-67.
365. **Revilla, Y., A. Cebrian, E. Baixeras, C. Martinez, E. Vinuela, and M. L. Salas.** 1997. Inhibition of apoptosis by the African swine fever virus Bcl-2 homologue: role of the BH1 domain. *Virology* **228**:400-4.
366. **Rice, A. P., and I. M. Kerr.** 1984. Interferon-mediated, double-stranded RNA-dependent protein kinase is inhibited in extracts from vaccinia virus-infected cells. *J Virol* **50**:229-36.
367. **Rivas, C., J. Gil, Z. Melkova, M. Esteban, and M. Diaz-Guerra.** 1998. Vaccinia virus E3L protein is an inhibitor of the interferon (i.f.n.)-induced 2-5A synthetase enzyme. *Virology* **243**:406-14.
368. **Roberts, K. L., and G. L. Smith.** 2008. Vaccinia virus morphogenesis and dissemination. *Trends Microbiol* **16**:472-9.
369. **Roberts, W. K., A. Hovanessian, R. E. Brown, M. J. Clemens, and I. M. Kerr.** 1976. Interferon-mediated protein kinase and low-molecular-weight inhibitor of protein synthesis. *Nature* **264**:477-80.
370. **Rochester, S. C., and P. Traktman.** 1998. Characterization of the single-stranded DNA binding protein encoded by the vaccinia virus I3 gene. *J Virol* **72**:2917-26.

371. **Rolland, S. G., and B. Conradt.** 2010. New role of the BCL2 family of proteins in the regulation of mitochondrial dynamics. *Curr Opin Cell Biol.*
372. **Romano, P. R., F. Zhang, S. L. Tan, M. T. Garcia-Barrio, M. G. Katze, T. E. Dever, and A. G. Hinnebusch.** 1998. Inhibition of double-stranded RNA-dependent protein kinase PKR by vaccinia virus E3: role of complex formation and the E3 N-terminal domain. *Mol Cell Biol* **18**:7304-16.
373. **Roulston, A., R. C. Marcellus, and P. E. Branton.** 1999. Viruses and apoptosis. *Annu Rev Microbiol* **53**:577-628.
374. **Roumier, T., G. Szabadkai, A. M. Simoni, J. L. Perfettini, A. L. Paulau, M. Castedo, D. Metivier, A. Badley, R. Rizzuto, and G. Kroemer.** 2006. HIV-1 protease inhibitors and cytomegalovirus vMIA induce mitochondrial fragmentation without triggering apoptosis. *Cell Death Differ* **13**:348-51.
375. **Ruffolo, S. C., and G. C. Shore.** 2003. BCL-2 selectively interacts with the BID-induced open conformer of BAK, inhibiting BAK auto-oligomerization. *J Biol Chem* **278**:25039-45.
376. **Saito, M., S. J. Korsmeyer, and P. H. Schlesinger.** 2000. BAX-dependent transport of cytochrome c reconstituted in pure liposomes. *Nat Cell Biol* **2**:553-5.
377. **Sambrook, J., and D. Russel.** 2001. *Molecular Cloning: A Laboratory Manual*, 3rd ed. Cold Spring Harbor Laboratory Press, Cold Spring Harbor, NY.
378. **Sarid, R., T. Sato, R. A. Bohenzky, J. J. Russo, and Y. Chang.** 1997. Kaposi's sarcoma-associated herpesvirus encodes a functional bcl-2 homologue. *Nat Med* **3**:293-8.
379. **Sato, T., M. Hanada, S. Bodrug, S. Irie, N. Iwama, L. H. Boise, C. B. Thompson, E. Golemis, L. Fong, H. G. Wang, and et al.** 1994. Interactions among members of the Bcl-2 protein family analyzed with a yeast two-hybrid system. *Proc Natl Acad Sci U S A* **91**:9238-42.
380. **Schafer, B., J. Quispe, V. Choudhary, J. E. Chipuk, T. G. Ajero, H. Du, R. Schreiner, and T. Kuwana.** 2009. Mitochondrial outer membrane proteins assist Bid in Bax-mediated lipidic pore formation. *Mol Biol Cell* **20**:2276-85.
381. **Schendel, S. L., Z. Xie, M. O. Montal, S. Matsuyama, M. Montal, and J. C. Reed.** 1997. Channel formation by antiapoptotic protein Bcl-2. *Proc Natl Acad Sci U S A* **94**:5113-8.
382. **Schinzl, A., T. Kaufmann, and C. Borner.** 2004. Bcl-2 family members: integrators of survival and death signals in physiology and pathology [corrected]. *Biochim Biophys Acta* **1644**:95-105.
383. **Schinzl, A. C., O. Takeuchi, Z. Huang, J. K. Fisher, Z. Zhou, J. Rubens, C. Hetz, N. N. Danial, M. A. Moskowitz, and S. J. Korsmeyer.** 2005. Cyclophilin D is a component of mitochondrial permeability transition and mediates neuronal cell death after focal cerebral ischemia. *Proc Natl Acad Sci U S A* **102**:12005-10.
384. **Schlesinger, P. H., A. Gross, X. M. Yin, K. Yamamoto, M. Saito, G. Waksman, and S. J. Korsmeyer.** 1997. Comparison of the ion channel characteristics of proapoptotic BAX and antiapoptotic BCL-2. *Proc Natl Acad Sci U S A* **94**:11357-62.
385. **Schmittgen, T. D., and K. J. Livak.** 2008. Analyzing real-time PCR data by the comparative C(T) method. *Nat Protoc* **3**:1101-8.
386. **Schonborn, J., J. Oberstrass, E. Breyel, J. Tittgen, J. Schumacher, and N. Lukacs.** 1991. Monoclonal antibodies to double-stranded RNA as

- probes of RNA structure in crude nucleic acid extracts. *Nucleic Acids Res* **19**:2993-3000.
387. **Schreiber, M., L. Sedger, and G. McFadden.** 1997. Distinct domains of M-T2, the myxoma virus tumor necrosis factor (TNF) receptor homolog, mediate extracellular TNF binding and intracellular apoptosis inhibition. *J Virol* **71**:2171-81.
 388. **Schuler, M., U. Maurer, J. C. Goldstein, F. Breitenbucher, S. Hoffarth, N. J. Waterhouse, and D. R. Green.** 2003. p53 triggers apoptosis in oncogene-expressing fibroblasts by the induction of Noxa and mitochondrial Bax translocation. *Cell Death Differ* **10**:451-60.
 389. **Schwartz, T., J. Behlke, K. Lowenhaupt, U. Heinemann, and A. Rich.** 2001. Structure of the DLM-1-Z-DNA complex reveals a conserved family of Z-DNA-binding proteins. *Nat Struct Biol* **8**:761-5.
 390. **Seet, B. T., J. B. Johnston, C. R. Brunetti, J. W. Barrett, H. Everett, C. Cameron, J. Sypula, S. H. Nazarian, A. Lucas, and G. McFadden.** 2003. Poxviruses and immune evasion. *Annu Rev Immunol* **21**:377-423.
 391. **Sen, G. C., H. Taira, and P. Lengyel.** 1978. Interferon, double-stranded RNA, and protein phosphorylation. Characteristics of a double-stranded RNA-activated protein kinase system partially purified from interferon treated Ehrlich ascites tumor cells. *J Biol Chem* **253**:5915-21.
 392. **Senkevich, T. G., S. Ojeda, A. Townsley, G. E. Nelson, and B. Moss.** 2005. Poxvirus multiprotein entry-fusion complex. *Proc Natl Acad Sci U S A* **102**:18572-7.
 393. **Seo, Y. W., J. N. Shin, K. H. Ko, J. H. Cha, J. Y. Park, B. R. Lee, C. W. Yun, Y. M. Kim, D. W. Seol, D. W. Kim, X. M. Yin, and T. H. Kim.** 2003. The molecular mechanism of Noxa-induced mitochondrial dysfunction in p53-mediated cell death. *J Biol Chem* **278**:48292-9.
 394. **Seto, M., U. Jaeger, R. D. Hockett, W. Graninger, S. Bennett, P. Goldman, and S. J. Korsmeyer.** 1988. Alternative promoters and exons, somatic mutation and deregulation of the Bcl-2-Ig fusion gene in lymphoma. *EMBO J* **7**:123-31.
 395. **Sharp, T. V., F. Moonan, A. Romashko, B. Joshi, G. N. Barber, and R. Jagus.** 1998. The vaccinia virus E3L gene product interacts with both the regulatory and the substrate binding regions of PKR: implications for PKR autoregulation. *Virology* **250**:302-15.
 396. **Shibue, T., K. Takeda, E. Oda, H. Tanaka, H. Murasawa, A. Takaoka, Y. Morishita, S. Akira, T. Taniguchi, and N. Tanaka.** 2003. Integral role of Noxa in p53-mediated apoptotic response. *Genes Dev* **17**:2233-8.
 397. **Shimazu, T., K. Degenhardt, E. K. A. Nur, J. Zhang, T. Yoshida, Y. Zhang, R. Mathew, E. White, and M. Inouye.** 2007. NBK/BIK antagonizes MCL-1 and BCL-XL and activates BAK-mediated apoptosis in response to protein synthesis inhibition. *Genes Dev* **21**:929-41.
 398. **Shisler, J. L., and B. Moss.** 2001. Molluscum contagiosum virus inhibitors of apoptosis: The MC159 v-FLIP protein blocks Fas-induced activation of procaspases and degradation of the related MC160 protein. *Virology* **282**:14-25.
 399. **Skinner, M. A., S. M. Laidlaw, I. Eldaghayes, P. Kaiser, and M. G. Cottingham.** 2005. Fowlpox virus as a recombinant vaccine vector for use in mammals and poultry. *Expert Rev Vaccines* **4**:63-76.
 400. **Smith, C. A., F. Q. Hu, T. D. Smith, C. L. Richards, P. Smolak, R. G. Goodwin, and D. J. Pickup.** 1996. Cowpox virus genome encodes a

- second soluble homologue of cellular TNF receptors, distinct from CrmB, that binds TNF but not LT alpha. *Virology* **223**:132-47.
401. **Smith, E. J., I. Marie, A. Prakash, A. Garcia-Sastre, and D. E. Levy.** 2001. IRF3 and IRF7 phosphorylation in virus-infected cells does not require double-stranded RNA-dependent protein kinase R or Ikappa B kinase but is blocked by Vaccinia virus E3L protein. *J Biol Chem* **276**:8951-7.
 402. **Smith, G. L., and G. McFadden.** 2002. Smallpox: anything to declare? *Nat Rev Immunol* **2**:521-7.
 403. **Smyth, D. G., O. O. Blumenfeld, and W. Konigsberg.** 1964. Reactions of N-ethylmaleimide with peptides and amino acids. *Biochem J* **91**:589-95.
 404. **Somogyi, P., J. Frazier, and M. A. Skinner.** 1993. Fowlpox virus host range restriction: gene expression, DNA replication, and morphogenesis in nonpermissive mammalian cells. *Virology* **197**:439-44.
 405. **Song, Q., Y. Kuang, V. M. Dixit, and C. Vincenz.** 1999. Boo, a novel negative regulator of cell death, interacts with Apaf-1. *EMBO J* **18**:167-78.
 406. **Stewart, T. L., S. T. Wasilenko, and M. Barry.** 2005. Vaccinia virus F1L protein is a tail-anchored protein that functions at the mitochondria to inhibit apoptosis. *J Virol* **79**:1084-98.
 407. **Stokes, G. V.** 1976. High-voltage electron microscope study of the release of vaccinia virus from whole cells. *J Virol* **18**:636-43.
 408. **Stuart, D., K. Graham, M. Schreiber, C. Macaulay, and G. McFadden.** 1991. The target DNA sequence for resolution of poxvirus replicative intermediates is an active late promoter. *J Virol* **65**:61-70.
 409. **Su, J., G. Wang, J. W. Barrett, T. S. Irvine, X. Gao, and G. McFadden.** 2006. Myxoma virus M11L blocks apoptosis through inhibition of conformational activation of Bax at the mitochondria. *J Virol* **80**:1140-51.
 410. **Subramanian, T., B. Tarodi, and G. Chinnadurai.** 1995. p53-independent apoptotic and necrotic cell deaths induced by adenovirus infection: suppression by E1B 19K and Bcl-2 proteins. *Cell Growth Differ* **6**:131-7.
 411. **Subramanian, T., S. Vijayalingam, E. Lomonosova, L. J. Zhao, and G. Chinnadurai.** 2007. Evidence for involvement of BH3-only proapoptotic members in adenovirus-induced apoptosis. *J Virol* **81**:10486-95.
 412. **Sudhakar, A., A. Ramachandran, S. Ghosh, S. E. Hasnain, R. J. Kaufman, and K. V. Ramaiah.** 2000. Phosphorylation of serine 51 in initiation factor 2 alpha (eIF2 alpha) promotes complex formation between eIF2 alpha(P) and eIF2B and causes inhibition in the guanine nucleotide exchange activity of eIF2B. *Biochemistry* **39**:12929-38.
 413. **Sun, Y., and D. W. Leaman.** 2005. Involvement of Noxa in cellular apoptotic responses to interferon, double-stranded RNA, and virus infection. *J Biol Chem* **280**:15561-8.
 414. **Sundararajan, R., and E. White.** 2001. E1B 19K blocks Bax oligomerization and tumor necrosis factor alpha-mediated apoptosis. *J Virol* **75**:7506-16.
 415. **Susin, S. A., H. K. Lorenzo, N. Zamzami, I. Marzo, B. E. Snow, G. M. Brothers, J. Mangion, E. Jacotot, P. Costantini, M. Loeffler, N. Larochette, D. R. Goodlett, R. Aebersold, D. P. Siderovski, J. M. Penninger, and G. Kroemer.** 1999. Molecular characterization of mitochondrial apoptosis-inducing factor. *Nature* **397**:441-6.

416. **Suzuki, M., R. J. Youle, and N. Tjandra.** 2000. Structure of Bax: coregulation of dimer formation and intracellular localization. *Cell* **103**:645-54.
417. **Suzuki, Y., Y. Imai, H. Nakayama, K. Takahashi, K. Takio, and R. Takahashi.** 2001. A serine protease, HtrA2, is released from the mitochondria and interacts with XIAP, inducing cell death. *Mol Cell* **8**:613-21.
418. **Tait, S. W., and D. R. Green.** 2010. Mitochondria and cell death: outer membrane permeabilization and beyond. *Nat Rev Mol Cell Biol* **11**:621-32.
419. **Tamaoki, T., H. Nomoto, I. Takahashi, Y. Kato, M. Morimoto, and F. Tomita.** 1986. Staurosporine, a potent inhibitor of phospholipid/Ca⁺⁺dependent protein kinase. *Biochem Biophys Res Commun* **135**:397-402.
420. **Tan, C., P. J. Dlugosz, J. Peng, Z. Zhang, S. M. Lapolla, S. M. Plafker, D. W. Andrews, and J. Lin.** 2006. Auto-activation of the apoptosis protein Bax increases mitochondrial membrane permeability and is inhibited by Bcl-2. *J Biol Chem* **281**:14764-75.
421. **Tan, K. O., N. Y. Fu, S. K. Sukumaran, S. L. Chan, J. H. Kang, K. L. Poon, B. S. Chen, and V. C. Yu.** 2005. MAP-1 is a mitochondrial effector of Bax. *Proc Natl Acad Sci U S A* **102**:14623-8.
422. **Tan, K. O., K. M. Tan, S. L. Chan, K. S. Yee, M. Bevort, K. C. Ang, and V. C. Yu.** 2001. MAP-1, a novel proapoptotic protein containing a BH3-like motif that associates with Bax through its Bcl-2 homology domains. *J Biol Chem* **276**:2802-7.
423. **Tao, W., C. Kurschner, and J. I. Morgan.** 1997. Modulation of cell death in yeast by the Bcl-2 family of proteins. *J Biol Chem* **272**:15547-52.
424. **Tarodi, B., T. Subramanian, and G. Chinnadurai.** 1994. Epstein-Barr virus BHRF1 protein protects against cell death induced by DNA-damaging agents and heterologous viral infection. *Virology* **201**:404-7.
425. **Taylor, J. M., and M. Barry.** 2006. Near death experiences: poxvirus regulation of apoptotic death. *Virology* **344**:139-50.
426. **Taylor, J. M., D. Quilty, L. Banadyga, and M. Barry.** 2006. The vaccinia virus protein F1L interacts with Bim and inhibits activation of the pro-apoptotic protein Bax. *J Biol Chem* **281**:39728-39.
427. **Taylor, R. C., S. P. Cullen, and S. J. Martin.** 2008. Apoptosis: controlled demolition at the cellular level. *Nat Rev Mol Cell Biol* **9**:231-41.
428. **Terrones, O., B. Antonsson, H. Yamaguchi, H. G. Wang, J. Liu, R. M. Lee, A. Herrmann, and G. Basanez.** 2004. Lipidic pore formation by the concerted action of proapoptotic BAX and tBID. *J Biol Chem* **279**:30081-91.
429. **Tewari, M., L. T. Quan, K. O'Rourke, S. Desnoyers, Z. Zeng, D. R. Beidler, G. G. Poirier, G. S. Salvesen, and V. M. Dixit.** 1995. Yama/CPP32 beta, a mammalian homolog of CED-3, is a CrmA-inhibitable protease that cleaves the death substrate poly(ADP-ribose) polymerase. *Cell* **81**:801-9.
430. **Theodorakis, P., C. D'Sa-Eipper, T. Subramanian, and G. Chinnadurai.** 1996. Unmasking of a proliferation-restraining activity of the anti-apoptosis protein EBV BHRF1. *Oncogene* **12**:1707-13.
431. **Thome, M., P. Schneider, K. Hofmann, H. Fickenscher, E. Meinl, F. Neipel, C. Mattmann, K. Burns, J. L. Bodmer, M. Schroter, C. Scaffidi,**

- P. H. Krammer, M. E. Peter, and J. Tschopp.** 1997. Viral FLICE-inhibitory proteins (FLIPs) prevent apoptosis induced by death receptors. *Nature* **386**:517-21.
432. **Thornberry, N. A., T. A. Rano, E. P. Peterson, D. M. Rasper, T. Timkey, M. Garcia-Calvo, V. M. Houtzager, P. A. Nordstrom, S. Roy, J. P. Vaillancourt, K. T. Chapman, and D. W. Nicholson.** 1997. A combinatorial approach defines specificities of members of the caspase family and granzyme B. Functional relationships established for key mediators of apoptosis. *J Biol Chem* **272**:17907-11.
433. **Tortorella, D., B. E. Gewurz, M. H. Furman, D. J. Schust, and H. L. Ploegh.** 2000. Viral subversion of the immune system. *Annu Rev Immunol* **18**:861-926.
434. **Tripathy, D. N., and L. E. Hanson.** 1978. Pathogenesis of fowlpox in laying hens. *Avian Dis* **22**:259-65.
435. **Tripathy, D. N., and W. M. Reed.** 2008. Pox. In Y. M. Saif (ed.), *Diseases of Poultry*, 12th ed. Blackwell Publishing Ltd., Oxford, UK.
436. **Tsujimoto, Y., J. Cossman, E. Jaffe, and C. M. Croce.** 1985. Involvement of the bcl-2 gene in human follicular lymphoma. *Science* **228**:1440-3.
437. **Tsujimoto, Y., J. Gorham, J. Cossman, E. Jaffe, and C. M. Croce.** 1985. The t(14;18) chromosome translocations involved in B-cell neoplasms result from mistakes in VDJ joining. *Science* **229**:1390-3.
438. **Tulman, E. R., C. L. Afonso, Z. Lu, L. Zsak, G. F. Kutish, and D. L. Rock.** 2004. The genome of canarypox virus. *J Virol* **78**:353-66.
439. **Upton, C., S. Slack, A. L. Hunter, A. Ehlers, and R. L. Roper.** 2003. Poxvirus orthologous clusters: toward defining the minimum essential poxvirus genome. *J Virol* **77**:7590-600.
440. **Upton, J. P., A. J. Valentijn, L. Zhang, and A. P. Gilmore.** 2007. The N-terminal conformation of Bax regulates cell commitment to apoptosis. *Cell Death Differ* **14**:932-42.
441. **Uren, R. T., G. Dewson, L. Chen, S. C. Coyne, D. C. Huang, J. M. Adams, and R. M. Kluck.** 2007. Mitochondrial permeabilization relies on BH3 ligands engaging multiple prosurvival Bcl-2 relatives, not Bak. *J Cell Biol* **177**:277-87.
442. **Van Antwerp, D. J., S. J. Martin, T. Kafri, D. R. Green, and I. M. Verma.** 1996. Suppression of TNF-alpha-induced apoptosis by NF-kappaB. *Science* **274**:787-9.
443. **van Buuren, N., B. Couturier, Y. Xiong, and M. Barry.** 2008. Ectromelia virus encodes a novel family of F-box proteins that interact with the SCF complex. *J Virol* **82**:9917-27.
444. **van Delft, M. F., A. H. Wei, K. D. Mason, C. J. Vandenberg, L. Chen, P. E. Czabotar, S. N. Willis, C. L. Scott, C. L. Day, S. Cory, J. M. Adams, A. W. Roberts, and D. C. Huang.** 2006. The BH3 mimetic ABT-737 targets selective Bcl-2 proteins and efficiently induces apoptosis via Bak/Bax if Mcl-1 is neutralized. *Cancer Cell* **10**:389-99.
445. **Varfolomeev, E. E., M. P. Boldin, T. M. Goncharov, and D. Wallach.** 1996. A potential mechanism of "cross-talk" between the p55 tumor necrosis factor receptor and Fas/APO1: proteins binding to the death domains of the two receptors also bind to each other. *J Exp Med* **183**:1271-5.

446. **Vaux, D. L., S. Cory, and J. M. Adams.** 1988. Bcl-2 gene promotes haemopoietic cell survival and cooperates with c-myc to immortalize pre-B cells. *Nature* **335**:440-2.
447. **Vayssiere, J. L., P. X. Petit, Y. Risler, and B. Mignotte.** 1994. Commitment to apoptosis is associated with changes in mitochondrial biogenesis and activity in cell lines conditionally immortalized with simian virus 40. *Proc Natl Acad Sci U S A* **91**:11752-6.
448. **Verhagen, A. M., P. G. Ekert, M. Pakusch, J. Silke, L. M. Connolly, G. E. Reid, R. L. Moritz, R. J. Simpson, and D. L. Vaux.** 2000. Identification of DIABLO, a mammalian protein that promotes apoptosis by binding to and antagonizing IAP proteins. *Cell* **102**:43-53.
449. **Walensky, L. D., K. Pitter, J. Morash, K. J. Oh, S. Barbuto, J. Fisher, E. Smith, G. L. Verdine, and S. J. Korsmeyer.** 2006. A stapled BID BH3 helix directly binds and activates BAX. *Mol Cell* **24**:199-210.
450. **Wang, G., J. W. Barrett, S. H. Nazarian, H. Everett, X. Gao, C. Bleackley, K. Colwill, M. F. Moran, and G. McFadden.** 2004. Myxoma virus M11L prevents apoptosis through constitutive interaction with Bak. *J Virol* **78**:7097-111.
451. **Wang, G. Q., E. Wieckowski, L. A. Goldstein, B. R. Gastman, A. Rabinovitz, A. Gambotto, S. Li, B. Fang, X. M. Yin, and H. Rabinowich.** 2001. Resistance to granzyme B-mediated cytochrome c release in Bak-deficient cells. *J Exp Med* **194**:1325-37.
452. **Wang, K., X. M. Yin, D. T. Chao, C. L. Millman, and S. J. Korsmeyer.** 1996. BID: a novel BH3 domain-only death agonist. *Genes Dev* **10**:2859-69.
453. **Wasilenko, S. T., L. Banadyga, D. Bond, and M. Barry.** 2005. The vaccinia virus F1L protein interacts with the proapoptotic protein Bak and inhibits Bak activation. *J Virol* **79**:14031-43.
454. **Wasilenko, S. T., A. F. Meyers, K. Vander Helm, and M. Barry.** 2001. Vaccinia virus infection disarms the mitochondrion-mediated pathway of the apoptotic cascade by modulating the permeability transition pore. *J Virol* **75**:11437-48.
455. **Wasilenko, S. T., T. L. Stewart, A. F. Meyers, and M. Barry.** 2003. Vaccinia virus encodes a previously uncharacterized mitochondrial-associated inhibitor of apoptosis. *Proc Natl Acad Sci U S A* **100**:14345-50.
456. **Watson, J. C., H. W. Chang, and B. L. Jacobs.** 1991. Characterization of a vaccinia virus-encoded double-stranded RNA-binding protein that may be involved in inhibition of the double-stranded RNA-dependent protein kinase. *Virology* **185**:206-16.
457. **Weaver, J. R., M. Shamim, E. Alexander, D. H. Davies, P. L. Felgner, and S. N. Isaacs.** 2007. The identification and characterization of a monoclonal antibody to the vaccinia virus E3 protein. *Virus Res* **130**:269-74.
458. **Wei, M. C., T. Lindsten, V. K. Mootha, S. Weiler, A. Gross, M. Ashiya, C. B. Thompson, and S. J. Korsmeyer.** 2000. tBID, a membrane-targeted death ligand, oligomerizes BAK to release cytochrome c. *Genes Dev* **14**:2060-71.
459. **Wei, M. C., W. X. Zong, E. H. Cheng, T. Lindsten, V. Panoutsakopoulou, A. J. Ross, K. A. Roth, G. R. MacGregor, C. B. Thompson, and S. J. Korsmeyer.** 2001. Proapoptotic BAX and BAK: a

- requisite gateway to mitochondrial dysfunction and death. *Science* **292**:727-30.
460. **Westphal, D., E. C. Ledgerwood, M. H. Hibma, S. B. Fleming, E. M. Whelan, and A. A. Mercer.** 2007. A novel Bcl-2-like inhibitor of apoptosis is encoded by the parapoxvirus ORF virus. *J Virol* **81**:7178-88.
 461. **Westphal, D., E. C. Ledgerwood, J. D. Tyndall, M. H. Hibma, N. Ueda, S. B. Fleming, and A. A. Mercer.** 2009. The orf virus inhibitor of apoptosis functions in a Bcl-2-like manner, binding and neutralizing a set of BH3-only proteins and active Bax. *Apoptosis* **14**:1317-30.
 462. **Whitaker-Dowling, P., and J. S. Youngner.** 1984. Characterization of a specific kinase inhibitory factor produced by vaccinia virus which inhibits the interferon-induced protein kinase. *Virology* **137**:171-81.
 463. **White, E., P. Sabbatini, M. Debbas, W. S. Wold, D. I. Kusher, and L. R. Gooding.** 1992. The 19-kilodalton adenovirus E1B transforming protein inhibits programmed cell death and prevents cytolysis by tumor necrosis factor alpha. *Mol Cell Biol* **12**:2570-80.
 464. **Wiens, M., A. Krasko, C. I. Muller, and W. E. Muller.** 2000. Molecular evolution of apoptotic pathways: cloning of key domains from sponges (Bcl-2 homology domains and death domains) and their phylogenetic relationships. *J Mol Evol* **50**:520-31.
 465. **Wilkins, C., and M. Gale, Jr.** 2010. Recognition of viruses by cytoplasmic sensors. *Curr Opin Immunol* **22**:41-7.
 466. **Williams, B. R., R. R. Golgher, and I. M. Kerr.** 1979. Activation of a nuclease by pppA2'p5'A2'p5'A in intact cells. *FEBS Lett* **105**:47-52.
 467. **Williams, E. S., V. M. Becerra, E. T. Thorne, T. J. Graham, M. J. Owens, and C. E. Nunamaker.** 1985. Spontaneous poxviral dermatitis and keratoconjunctivitis in free-ranging mule deer (*Odocoileus hemionus*) in Wyoming. *J Wildl Dis* **21**:430-3.
 468. **Williams, T., D. Sale, and S. A. Hazlewood.** 2001. BHRF1 is highly conserved in primate virus analogues of Epstein-Barr virus. *Intervirology* **44**:55-8.
 469. **Willis, S. N., and J. M. Adams.** 2005. Life in the balance: how BH3-only proteins induce apoptosis. *Curr Opin Cell Biol* **17**:617-25.
 470. **Willis, S. N., L. Chen, G. Dewson, A. Wei, E. Naik, J. I. Fletcher, J. M. Adams, and D. C. Huang.** 2005. Proapoptotic Bak is sequestered by Mcl-1 and Bcl-xL, but not Bcl-2, until displaced by BH3-only proteins. *Genes Dev* **19**:1294-305.
 471. **Willis, S. N., J. I. Fletcher, T. Kaufmann, M. F. van Delft, L. Chen, P. E. Czabotar, H. Ierino, E. F. Lee, W. D. Fairlie, P. Bouillet, A. Strasser, R. M. Kluck, J. M. Adams, and D. C. Huang.** 2007. Apoptosis initiated when BH3 ligands engage multiple Bcl-2 homologs, not Bax or Bak. *Science* **315**:856-9.
 472. **Wilson, N. S., V. Dixit, and A. Ashkenazi.** 2009. Death receptor signal transducers: nodes of coordination in immune signaling networks. *Nat Immunol* **10**:348-55.
 473. **Wilson-Annan, J., L. A. O'Reilly, S. A. Crawford, G. Hausmann, J. G. Beaumont, L. P. Parma, L. Chen, M. Lackmann, T. Lithgow, M. G. Hinds, C. L. Day, J. M. Adams, and D. C. Huang.** 2003. Proapoptotic BH3-only proteins trigger membrane integration of prosurvival Bcl-w and neutralize its activity. *J Cell Biol* **162**:877-87.

474. **Wolter, K. G., Y. T. Hsu, C. L. Smith, A. Nechushtan, X. G. Xi, and R. J. Youle.** 1997. Movement of Bax from the cytosol to mitochondria during apoptosis. *J Cell Biol* **139**:1281-92.
475. **Xiang, J., D. T. Chao, and S. J. Korsmeyer.** 1996. BAX-induced cell death may not require interleukin 1 beta-converting enzyme-like proteases. *Proc Natl Acad Sci U S A* **93**:14559-63.
476. **Xiang, Y., R. C. Condit, S. Vijaysri, B. Jacobs, B. R. Williams, and R. H. Silverman.** 2002. Blockade of interferon induction and action by the E3L double-stranded RNA binding proteins of vaccinia virus. *J Virol* **76**:5251-9.
477. **Xiang, Y., D. A. Simpson, J. Spiegel, A. Zhou, R. H. Silverman, and R. C. Condit.** 1998. The vaccinia virus A18R DNA helicase is a postreplicative negative transcription elongation factor. *J Virol* **72**:7012-23.
478. **Yamamoto, K., H. Ichijo, and S. J. Korsmeyer.** 1999. BCL-2 is phosphorylated and inactivated by an ASK1/Jun N-terminal protein kinase pathway normally activated at G(2)/M. *Mol Cell Biol* **19**:8469-78.
479. **Yang, E., J. Zha, J. Jockel, L. H. Boise, C. B. Thompson, and S. J. Korsmeyer.** 1995. Bad, a heterodimeric partner for Bcl-XL and Bcl-2, displaces Bax and promotes cell death. *Cell* **80**:285-91.
480. **Yang, T., K. M. Kozopas, and R. W. Craig.** 1995. The intracellular distribution and pattern of expression of Mcl-1 overlap with, but are not identical to, those of Bcl-2. *J Cell Biol* **128**:1173-84.
481. **Yethon, J. A., R. F. Epand, B. Leber, R. M. Epand, and D. W. Andrews.** 2003. Interaction with a membrane surface triggers a reversible conformational change in Bax normally associated with induction of apoptosis. *J Biol Chem* **278**:48935-41.
482. **Yin, X. M., Z. N. Oltvai, and S. J. Korsmeyer.** 1994. BH1 and BH2 domains of Bcl-2 are required for inhibition of apoptosis and heterodimerization with Bax. *Nature* **369**:321-3.
483. **Youle, R. J., and A. Strasser.** 2008. The BCL-2 protein family: opposing activities that mediate cell death. *Nat Rev Mol Cell Biol* **9**:47-59.
484. **Yu, J., L. Zhang, P. M. Hwang, K. W. Kinzler, and B. Vogelstein.** 2001. PUMA induces the rapid apoptosis of colorectal cancer cells. *Mol Cell* **7**:673-82.
485. **Yuwen, H., J. H. Cox, J. W. Yewdell, J. R. Bennink, and B. Moss.** 1993. Nuclear localization of a double-stranded RNA-binding protein encoded by the vaccinia virus E3L gene. *Virology* **195**:732-44.
486. **Zamzami, N., P. Marchetti, M. Castedo, D. Decaudin, A. Macho, T. Hirsch, S. A. Susin, P. X. Petit, B. Mignotte, and G. Kroemer.** 1995. Sequential reduction of mitochondrial transmembrane potential and generation of reactive oxygen species in early programmed cell death. *J Exp Med* **182**:367-77.
487. **Zamzami, N., P. Marchetti, M. Castedo, C. Zanin, J. L. Vayssiere, P. X. Petit, and G. Kroemer.** 1995. Reduction in mitochondrial potential constitutes an early irreversible step of programmed lymphocyte death in vivo. *J Exp Med* **181**:1661-72.
488. **Zha, H., C. Aime-Sempe, T. Sato, and J. C. Reed.** 1996. Proapoptotic protein Bax heterodimerizes with Bcl-2 and homodimerizes with Bax via a novel domain (BH3) distinct from BH1 and BH2. *J Biol Chem* **271**:7440-4.

489. **Zha, H., H. A. Fisk, M. P. Yaffe, N. Mahajan, B. Herman, and J. C. Reed.** 1996. Structure-function comparisons of the proapoptotic protein Bax in yeast and mammalian cells. *Mol Cell Biol* **16**:6494-508.
490. **Zha, J., H. Harada, E. Yang, J. Jockel, and S. J. Korsmeyer.** 1996. Serine phosphorylation of death agonist BAD in response to survival factor results in binding to 14-3-3 not BCL-X(L). *Cell* **87**:619-28.
491. **Zha, J., S. Weiler, K. J. Oh, M. C. Wei, and S. J. Korsmeyer.** 2000. Posttranslational N-myristoylation of BID as a molecular switch for targeting mitochondria and apoptosis. *Science* **290**:1761-5.
492. **Zhai, D., E. Yu, C. Jin, K. Welsh, C. W. Shiau, L. Chen, G. S. Salvesen, R. Liddington, and J. C. Reed.** 2010. Vaccinia virus protein F1L is a caspase-9 inhibitor. *J Biol Chem* **285**:5569-80.
493. **Zhang, F., P. R. Romano, T. Nagamura-Inoue, B. Tian, T. E. Dever, M. B. Mathews, K. Ozato, and A. G. Hinnebusch.** 2001. Binding of double-stranded RNA to protein kinase PKR is required for dimerization and promotes critical autophosphorylation events in the activation loop. *J Biol Chem* **276**:24946-58.
494. **Zhang, P., B. L. Jacobs, and C. E. Samuel.** 2008. Loss of protein kinase PKR expression in human HeLa cells complements the vaccinia virus E3L deletion mutant phenotype by restoration of viral protein synthesis. *J Virol* **82**:840-8.
495. **Zhang, P., and C. E. Samuel.** 2008. Induction of protein kinase PKR-dependent activation of interferon regulatory factor 3 by vaccinia virus occurs through adapter IPS-1 signaling. *J Biol Chem* **283**:34580-7.
496. **Zhang, Z., S. M. Lapolla, M. G. Annis, M. Truscott, G. J. Roberts, Y. Miao, Y. Shao, C. Tan, J. Peng, A. E. Johnson, X. C. Zhang, D. W. Andrews, and J. Lin.** 2004. Bcl-2 homodimerization involves two distinct binding surfaces, a topographic arrangement that provides an effective mechanism for Bcl-2 to capture activated Bax. *J Biol Chem* **279**:43920-8.
497. **Zhang, Z., W. Zhu, S. M. Lapolla, Y. Miao, Y. Shao, M. Falcone, D. Boreham, N. McFarlane, J. Ding, A. E. Johnson, X. C. Zhang, D. W. Andrews, and J. Lin.** 2010. Bax forms an oligomer via separate, yet interdependent, surfaces. *J Biol Chem* **285**:17614-27.
498. **Zhong, Q., W. Gao, F. Du, and X. Wang.** 2005. Mule/ARF-BP1, a BH3-only E3 ubiquitin ligase, catalyzes the polyubiquitination of Mcl-1 and regulates apoptosis. *Cell* **121**:1085-95.
499. **Zhou, L., and D. C. Chang.** 2008. Dynamics and structure of the Bax-Bak complex responsible for releasing mitochondrial proteins during apoptosis. *J Cell Sci* **121**:2186-96.
500. **Zhou, Q., S. Snipas, K. Orth, M. Muzio, V. M. Dixit, and G. S. Salvesen.** 1997. Target protease specificity of the viral serpin CrmA. Analysis of five caspases. *J Biol Chem* **272**:7797-800.
501. **Zhu, H., Y. Shen, and T. Shenk.** 1995. Human cytomegalovirus IE1 and IE2 proteins block apoptosis. *J Virol* **69**:7960-70.
502. **Zong, W. X., T. Lindsten, A. J. Ross, G. R. MacGregor, and C. B. Thompson.** 2001. BH3-only proteins that bind pro-survival Bcl-2 family members fail to induce apoptosis in the absence of Bax and Bak. *Genes Dev* **15**:1481-6.

APPENDIX A

A UNIFIED MODEL OF BAK/BAX ACTIVATION

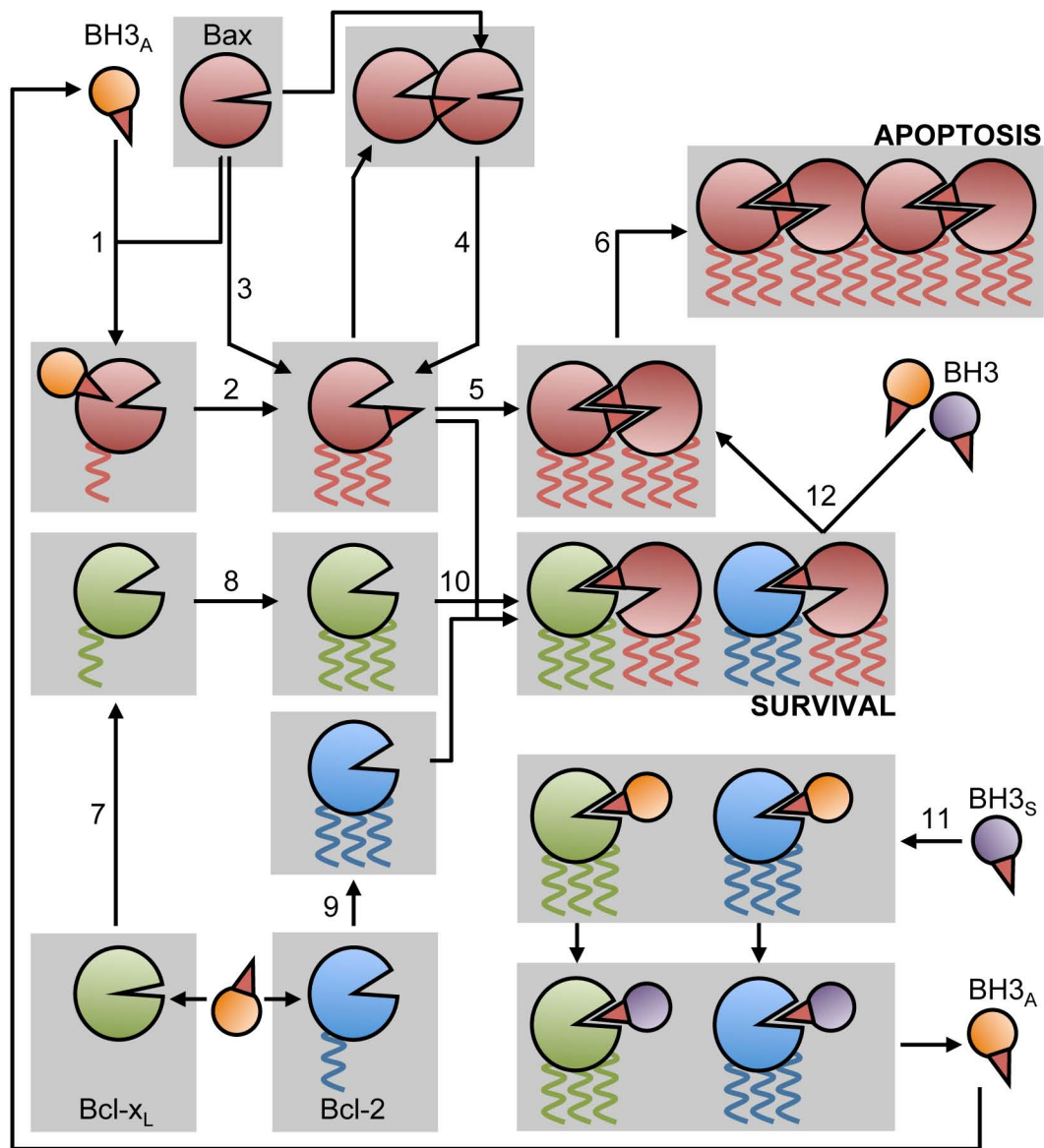


Figure A.1. A unified model of Bak/Bax activation. In healthy cells Bax resides in the cytoplasm as an inactive monomer. Upon receipt of an apoptotic stimulus, activator BH3-only proteins (BH3_A) interact with Bax at the rear interface, resulting in Bax translocation to the mitochondria and insertion of the transmembrane domain (helix 9) into the MOM (1). Additional conformational changes result in the insertion of helices 5 and 6 and complete the activation of Bax into a “multi-spanning monomer” (2). In some cases, Bax may be activated spontaneously or by non-Bcl-2 protein factors (3). Active Bax may also recruit and activate Bax monomers in a process termed auto-activation (4). Active Bax forms symmetric dimers (5) via the front interface that then interact with other dimers via the rear interface to nucleate the formation of Bax oligomers (6), leading to MOMP and apoptosis. The process is similar for Bak, except that Bak constitutively resides at the MOM with helix 9 inserted. In healthy cells, Bcl-x_L resides inactive in the cytoplasm. BH3-only proteins are proposed to activate Bcl-x_L to translocate to the MOM and insert helix 9 (7), followed by insertion of helices 5 and 6 to form a multi-spanning monomer (8). Similarly, Bcl-2, which is constitutively associated with the MOM, is activated by BH3-only proteins to undergo conformational changes that result in the insertion of helices 5 and 6 into the MOM (9). Activated Bcl-2 and Bcl-x_L then interact with active Bak/Bax to form oligomerisation-incompetent hetero-dimers or trimers, promoting cell survival. Sensitizer BH3-only proteins (BH3_S) can bind anti-apoptotic Bcl-2 proteins to release activator BH3-only proteins (11), which are then able to activate Bak/Bax. Additionally, BH3-only proteins may bind anti-apoptotic Bcl-2 proteins to release Bak/Bax from repression and allow their homo-oligomerisation and apoptosis (12). The ability of anti-apoptotic Bcl-2 proteins to inactivate Bak/Bax depends largely on their sequestration of activator BH3-only proteins and active Bak/Bax. Mcl-1, Bcl-w, and Bcl-2A1 are omitted for simplicity’s sake but may function similarly to either Bcl-x_L or Bcl-2.